Assessing Human Heat Stress Risk During Outdoor Summer Sports

A thesis submitted to the University of Sydney

In the fulfilment of the requirement for the degree of

Doctor of Philosophy (Medicine and Health)

June 2024

Mr Lindsey Hunt

BAppSc(Ex&SpSc), The University of Sydney 2016

MApplSc, The University of Sydney 2020

Thermal Ergonomics Laboratory, Heat and Health Research Impact Centre

Sydney School of Health Sciences

Faculty of Medicine and Health, The University of Sydney

Acknowledgements

I would like to thank my lead supervisor, Professor Ollie Jay for your support which started initially with my MSc and continued throughout my PhD. I have been fortunate to be able to work with you and learn from you as one of the leading minds in thermal physiology, which has benefitted me as a researcher in a wider context than just the field. Thank you to my first co-supervisor, Dr James Smallcombe, your guidance and expertise have been imperative throughout all aspects of the PhD, but particularly from study design, participant recruitment, data analysis and academic writing perspectives. To my second co-supervisor Dr Federico Tartarini, thank you for the encouragement surrounding data analysis and presentation with Python, which enabled me to learn new skills that will be forever helpful and help in my future endeavours, I am sure.

I have been with the Thermal Ergonomics Laboratory (TEL) in some capacity for a significant period since joining as a MSc student in 2017 and I have been fortunate to work with many inspiring individuals who are now scattered across the globe in various roles. At the risk of missing anyone out, thank you to everyone who has been a part of my TEL experience since 2017. These are people who have made the processes of completing the MSc and now PhD even more worth it. I would also like to thank the many participants who took time out of their busy lives and donated their time (and sweat, a lot of sweat) to the experimental studies within this thesis.

I would also like to thank the now former technical support staff John Eisenhuth and Timothy Turner from the University of Sydney for their technical expertise and guidance. Both Tim and John helped enable data collection by building various data collection tools such as the EMU, without which, this thesis would not have been possible. I would additionally like to acknowledge the helpful staff from the Sydney Knowledge Hub, in particular, Stanislaus who assisted me with novel analysis techniques used within this work.

Throughout my candidature, I was supported by the Australian Government Research Training Program (RTP) Scholarship and the Fee Offset program, without which I would very likely not have been able to complete my thesis.

Last but certainly not least I would like to thank my partner, Eliza Wunsch. You have supported me throughout almost every day of the PhD journey and dealt with all the ups and downs of long travel days and the chaos that can occur with research and fieldwork, which this thesis has required. I love you and I am very much looking forward to the next adventures together, wherever they may take us.

Dissemination of Results

Results culminating from the study of this thesis which have been published, submitted for publication and/or presented at a scientific conference.

Conference Presentations

Hunt, L, Smallcombe, J, Jay, O. (2023). The association between the evaporative requirements for heat balance (E_{req}) and Whole-body Sweat Rate (WBSR) while cycling in an outdoor environment. Presented at: *The American College of Sports Medicine (ACSM) Annual Conference*, May 30th-2nd, 2023, Denver, Colorado.

10.1249/01.mss.0000980796.30478.af *poster session*

Published works that have been published during my candidature, however, do not form a part of this thesis.

Moyen, NE, Bapat, RC, Tan, B, **Hunt, L**, Jay, O, Mündel, T. (2021). Accuracy of Algorithm to Non-Invasively Predict Core Body Temperature Using the Kenzen Wearable Device. *International Journal of Environmental Research and Public Health*, *18*, 13126. https://doi.org/10.3390/ijerph182413126

Jay O, Périard JD, Clark B, **Hunt L**, Ren H, Suh H, Gonzalez RR & Sawka MN. (2024). Whole-Body Sweat Rate Prediction: Outdoor Running and Cycling Exercise. *Journal of Applied Physiology* **0:**. https://doi.org/10.1152/japplphysiol.00831.2023

Table of Contents

Candidate's Certificate

This is to certify that to the best of my knowledge, the content of this thesis is my own work. This thesis has not been submitted for any degree or other purposes.

I certify that the intellectual content of this thesis is the product of my own work and that all the assistance received in preparing this thesis and sources have been acknowledged.

Lindsey Hunt

Sydney School of Health Sciences

Faculty of Medicine and Health

The University of Sydney

24 June 2024

List of Figures and Tables

Chapter IV: Experimental Study Two

Chapter V: Experimental Study Three

Abbreviations

Term	Abbreviation	Term	Abbreviation
Ambient vapour pressure	P_a	Mean arterial pressure	MAP
American college of sports medicine	ACSM	Mean body temperature	T_b
Area weighted emissivity of clothing on the body surface	ε	Mean radiant temperature	T_r
Barometric pressure	P_b	Mean skin temperature	T_{sk}
Black globe temperature	T_g	Mechanical efficiency	η
Body mass	m_b	Metabolic energy equivalent	MEE
Body surface area	A_d	Metabolic rate	$\dot{M}$
Body tissue thermal resistance	r_t	Metabolic heat production	H_{prod}
Boundary layer thermal resistance	r_a	Pedalling frequency (cadence)	f_{ped}
Central nervous system	CNS	Percent oxygen consumption	$\%\dot{V}O_{2max}$
Circumference	c	Phosphocreatine	Pcr
Cold water immersion	CWI	Prandtl number	Pr
Conductive heat transfer	K	Radiative heat transfer	R
Convective heat transfer	C	Radius	r
Convective heat transfer coefficient	h_c	Rating of perceived exertion	RPE
Body core temperature	T_c	Ratio of clothed BSA to nude BSA	f_{cl}
Cricket Australia	CA	Rectal temperature	T_{rec}
Degrees Celsius	°C	Relative humidity	RH
Degrees Kelvin	°K	Respiratory convective heat exchange	C_{resp}
Diameter	d	Respiratory evaporative heat exchange	E_{resp}
Dry heat transfer	Dry	Respiratory exchange ratio	RER
Dry-bulb temperature	T_{db}	Respiratory heat loss	H_{resp}
Dynamic clothing resistance	r_{co}	Resting metabolic rate	RMR
Effective area for radiant heat exchange	A_r/A_D	Reynolds number	Re
Environmental monitoring unit	EMU	Saturated water vapour pressure at the skin surface	$P_{sat,sk}$
Evaporative heat transfer coefficient	h_e	Seconds	s
Evaporative requirement for heat balance	E_{req}	Self generated air velocity	v_{self}
Evaporative resistance of clothing	$R_{e,cl}$	Skin blood flow	SKBF
Excess post-exercise oxygen consumption	EPOC	Skin wettedness required to attain heat balance	ω_{req}
Exertional heat stroke	EHS	Standard deviation	SD
External work	W	Static clothing resistance	r_c
Extreme heat policy	EHP	Steady state core temperature	T_{ceq}

Gastrointestinal temperature	T_{gi}	Stefan-Boltzmann constant	σ
Heart rate	HR	Sweat rate required to maintain heat balance	S_{req}
Heat exhaustion	HE	Sweating efficiency	S_{eff}
Heat loss	H_{loss}	Temperature of clothing	T_{cl}
Heat stored within the body	S	Thermal diffusivity of air	k
Heat Stress Risk Index	HSRI	Volume of carbon dioxide production	$\dot{V}CO_2$
Hours	h	Volume of oxygen consumption	$\dot{V}O_2$
Insulative properties of clothing	I_{cl}	Watts	W
Intrinsic thermal resistance (insulation) of the clothing	R_{cl}	Watts per square meter	$W \cdot m^{-2}$
Local sweat rate	LSR	Whole-body sweat loss	WBSL
Maximum evaporative capacity of the environment	E_{max}	Whole-body sweat rate	WBSR
Maximum oxygen consumption	$\dot{V}O_{2max}$	Years old	yrs.

Thesis Abstract

Exposure to extreme thermal environmental conditions for people engaging in outdoor sports and physical activity is projected to increase as global conditions worsen in the face of climate change. The broad objective of this thesis was to quantify both the personal and thermal environment to enhance biophysical modelling and reduce the risk of heat illnesses. Chapter III assessed the agreement in heat stress between nearby Bureau of Meteorology (BoM) stations and the playing surface of Cricket stadiums across Australia. The findings suggest that on-site monitoring reduces the frequency of misclassifying the heat stress risk, particularly at Major sporting venues where the inaccurate assessment of heat stress risk with BoM data is more frequent. Chapter IV examined the association between the evaporative requirement for heat balance (E_{req}) and whole-body sweat rate (WBSR) in an outdoor environment; where our ability to calculate E_{req} is challenged predominantly by the need to estimate key variables for calculating E_{req}, without access to standard laboratory procedures and equipment. We observed a weaker association between E_{req} and WBSR than previously seen indoors, with further evidence suggesting that the highest source of error in our calculation of E_{req} outdoors, comes from uncertainties when estimating metabolic rate. Finally, chapter V compares the accuracy of available prediction equations for mean skin temperature (T_{sk}) during physical activity with measured T_{sk} data and develops a novel T_{sk} prediction equation that is suitable for use in high airflow environments ($< 4.0\ m \cdot s^{-1}$), with high metabolic rates. Together, the findings from this thesis help to enhance extreme heat stress risk assessment by confirming the importance of on-site monitoring of thermal environmental conditions and through enhanced biophysical modelling during high-intensity physical activity in high airflow environments.

CHAPTER I

Introduction

1.0 Introduction

The management of heat stress risk in sports is a challenge being brought to the front of mind for sporting participants, officials and organisations due to the increasing prevalence, duration, and intensity of extreme heat stress conditions across the globe due to climate change (Coris, Ramirez & Van Durme, 2004; Armstrong *et al.*, 2007; Barros *et al.*, 2012; Perkins-Kirkpatrick & Gibson, 2017). Climate projections indicate that mean and peak dry-bulb temperatures will continue to increase throughout this century, particularly if greenhouse gas emissions are not meaningfully reduced as mean global temperatures exceed 1.5 ºC above pre-industrial averages by the early 2030s (IPCC, 2023). Extreme heat is currently estimated to cost the Australian and global economies USD$6.2 billion (Zander *et al.*, 2015) and USD$311 billion, respectively, due to productivity losses. These values are projected to increase as extreme climactic conditions worsen in the coming decades. People who engage in sports or physical activity, especially in an outdoor environment during times of extreme heat experience a higher likelihood of developing hyperthermia and associated exertional heat-related illness (Coris, Ramirez & Van Durme, 2004; Cooper Jr, Ferrara & Broglio, 2006; Kakamu *et al.*, 2017) that can lead to reductions in physical performance at best and mortality at worst.

In 2019, approximately 80% of men and women in Australia, across all ages, participated in some form of physical activity at least once per week (AusSport, 2020). As a popular outdoor summer sport, 627,693 registered players participated in cricket over the 2022/2023 summer (Cricket Australia, 2023). Another defining characteristic of Australian life is the occurrence of extreme summer heat. Consequently, playing cricket is associated with high rates of physical activity induced, heat-related hospitalisations across Australia, which accounts for 10% of all sports-related heat-illness cases (Driscoll, Cripps & Brotherhood, 2008). As these data capture hospitalisations only, it is probable that many less severe instances of heat illness occur but are not captured by healthcare statistics both due to the difficulties in categorising heat illnesses in our healthcare system (Garcia *et al.*, 2022) and less serious cases being treated at home or on the sidelines, thus going under- and unreported. The relatively high rates of heat-related hospitalisations observed with cricket are likely due to the long match times (2-6 hrs), regular intense bouts of running, and the requirement to wear insulating, protective clothing and equipment which increase metabolic heat production and impair heat loss.

Extreme heat stress risk management in sports requires an understanding of the human response to their environment (Chalmers, Anderson & Jay, 2020). That is, where the relevant environmental conditions must be assessed appropriately (dry-bulb temperature and its associated relative humidity, wind velocity, and mean radiant temperature), and we must understand the personal factors that also govern the overall heat stress risk (metabolic heat production, body morphology [e.g., body surface area, height, weight], and clothing) (Parsons, 2014). Extreme heat policies aim to ensure player safety and are considered an essential component of the sports industry (Larsen *et al.*, 2007; Nichols, 2014; Chalmers & Jay, 2018). Many extreme heat policies across Australian sports rely on climate data from nearby Bureau of Meteorology (BoM) weather sites (Australian Football League, 2013; Cricket Australia, 2020; Cycling Australia, 2021; Jay, Broderick & Smallcombe, 2021; Lawn Tennis Association, 2022). These BoM sites are generally accepted as the most accessible method to assess most of the relevant thermal environment data to inform whether play is continued or suspended, and at which point cooling interventions such as extended breaks or active cooling methods are recommended. However, the data reported by these organisations (e.g. BoM) may not be representative of the conditions at the sporting venue (Cheuvront *et al.*, 2015; Pryor *et al.*, 2017; Chalmers *et al.*, 2020; Guyer *et al.*, 2021). Variability between the thermal environments of nearby BoM stations and sporting venues may result from the complex interactions between the unique topographical, geographical, and built/natural environments surrounding each BoM station and sporting venue. Differences in the surrounding natural and built environment (e.g., rivers, lakes, parks, grandstands, and building/building density) between sites could lead to local microenvironments in which the thermal environment can vary considerably (Grundstein & Cooper, 2020; Liu & Jim, 2021). For example, in a large cricket venue with built-up seating areas, the overall level of heat stress experienced could be higher than outside the stadium or at a nearby BoM site, due to lower natural ventilation and increased reflected radiation from the artificial grandstands. Consequently, it is of utmost importance that sports stadia are assessed and characterised on an individual basis, to ensure an accurate quantification of the thermal environment to reduce the risk of exertional heat illness in sports and allow for sport to be played safely, without prematurely cancelling matches.

To assess extreme heat stress risk, we must also be able to accurately characterize the expected level of heat stress via understanding the personal factors that affect heat production and heat exchange between the human and their environment. During physical activity such as cycling and running humans secrete sweat to lose heat to the environment by the evaporation of latent heat in sweat, to limit rises in body core temperature and maintain a steady-state thermal condition (Parsons, 2014; Ravanelli, Imbeault & Jay, 2020). If this secreted sweat is not sufficiently replaced with fluids (particularly during extended exercise bouts in warm environments) larger increases in body core temperature (T_c), thermal and cardiovascular strain and exertional heat illnesses can ensue. In outdoor sports such as professional and recreational cycling, the racing season is typically in the summertime. An extreme example is the Tour de France, where riders are often required to compete day after day, in stages that last typically ~3-4 hours, where dry-bulb temperatures are commonly over 30 ºC with high solar loads (Mustapha, 2022). It has been suggested that holding the Tour de

France in July may be untenable soon due to climate change (Orr, 2022). However, an accurate assessment of the expected level of heat stress for a given situation (e.g., running, cycling) through appropriate biophysical modelling may allow sport to continue for longer, without the need for arbitrary, non-sport-specific dry-bulb and/or wet-bulb globe temperature (WBGT) cut-offs that are adopted within sporting organisations.

Since the 1930's, scientists have been aware of a relationship between the evaporative requirement for heat balance (E_{req}) and whole-body sweat rate (WBSR) (Nielsen, 1938). Based on heat balance theory where the human body aims to maintain homeostasis at all times (i.e., not actively cooling itself, but responding to the requirement to maintain heat balance), E_{req} is the theoretical requirement for evaporative heat loss at rest or during steady-state physical activity for a given metabolic heat production and morphological characteristics (mainly body surface area) in a given or variable set of thermal environmental conditions (Parsons, 2014). Contemporary research has confirmed that E_{req} describes ~95% of the variability in WBSR in perfect laboratory conditions (Gagnon, Jay & Kenny, 2013) and in a more realistic laboratory setting, the authors observed that E_{req} explained ~78% of the variability in WBSR (Hospers *et al.*, 2020). During steady-state endurance exercise outside perfect laboratory conditions, where sweating efficiency (S_{eff}) is not significantly reduced, E_{req} could potentially be utilised in a biophysical model nested within extreme heat policies to help determine the level of expected heat stress and associated hydration requirements for athletes competing in temperate-hot environments.

The following challenge is then how to translate the E_{req} model from perfect laboratory conditions to an outdoor environment. Compared to ideal laboratory conditions which permit free and rapid evaporation of sweat (low levels of clothing, low ambient humidity, high dry-bulb temperature and high air velocity), in an outdoor free-living environment, there is increased uncertainty regarding the influence of wind in terms of both its varying speed and varying skin surface coverage during outdoor activities, metabolic rate, challenges to S_{eff}, and increased measurement uncertainty due to less accurate equipment and the potential need to rely on prediction equations for key variables such as skin temperature, metabolic rate where mobile measures are may be unavailable or impractical. The main challenge to the association between E_{req} and WBSR in an outdoor environment will be reducing the impact of reduced S_{eff} due to clothing (Havenith *et al.*, 2008; Havenith *et al.*, 2013) and conditions where the maximum evaporative capacity of the environment (E_{max}) is low (Cramer & Jay, 2019). E_{max} can be reduced by both personal and environmental factors such as low airflow, high levels of clothing, high ambient vapour pressures and through the modification to maximum skin wettedness (ω_{max}), training/acclimation/acclimatisation status (see Eq. 24) (Ravanelli, 2018). Therefore, evaluating the E_{req} model outdoors may be most suitable and initially relevant to sports and environmental conditions where there are limited impacts to S_{eff} such as road cycling (Parsons, 2014).

Calculating E_{req} requires various measures of human heat production and dry heat exchange with the surrounding environment, which is moderated by clothing (Parsons, 2014). One of these key measures is mean skin temperature, which, together with dry-bulb temperature and mean radiant temperature governs heat exchange between the skin and the air. Existing regression-based mean skin temperature prediction equations have been developed for various occupational and exercise settings, which have been codified for widespread use in the ISO standard 7933 (Mehnert *et al.*, 2000; ISO, 7933, 2004), and one study has developed an empirical prediction equation to calculate mean skin temperature during outdoor stationary cycling (Vanos *et al.*, 2012). However, none of these equations have been developed for use at > 4.0 $m \cdot s^{-1}$ air velocities, potentially limiting their utility when estimating mean skin temperature in high airflow environments such as recreational and professional road cycling.

1.1 Objectives and Hypotheses

Experimental Chapter 3 focusses on understanding the external environmental factors that contribute to heat stress risk (dry-bulb temperature, humidity, mean radiant temperature and wind speed). Chapters 4 and 5 deals with the individual, personal factors that influence extreme heat stress risk (i.e., the ability to dissipate heat through sweat and dry heat transfer in outdoor environments).

Objective one: To assess the agreement between nearby meteorological (BoM) station data and environmental conditions measured at the site of play using the Cricket Australia (CA) Heat Stress Risk Index (HSRI) at cricket venues across Australia.

Hypothesis one: On-site extreme heat stress risk will be higher within sporting stadia due to likely lower ambient air velocities on-site versus reported by the BoM sites and the reduction in wind speed at venues will be exacerbated at larger venues due to the local built environment.

Objective two: (1) To assess the relation between E_{req} and WBSR during outdoor cycling and (2) to determine the optimal methods for calculating E_{req} using different methods for estimating metabolic energy expenditure, the convective heat transfer coefficient, and mean skin temperature.

Hypothesis two: E_{req} will remain a strong predictor of WBSR in an outdoor environment, however, the strength of the relation would be lower than previously reported indoors due to uncontrolled environmental conditions, increased measurement uncertainty with field equipment (e.g., power meters) and the reliance on predictive equations for key variables such as metabolic rate and mean skin temperature.

Objective three: (1) To evaluate current mean skin temperature prediction models against empirical data during outdoor cycling, (2) if available models are not appropriate, develop a prediction equation for mean skin temperature for use in high airflow scenarios such as road cycling to allow for improved biophysical modelling.

Hypothesis three: Current prediction equations may overestimate mean skin temperature, particularly at lower air temperatures given the high self-generated air velocities experienced while road cycling.

1.2 References

AusSport. (2020). AusPlay Survey, ed. Australia S. https://www.clearinghouseforsport.gov.au/research/smi/ausplay/results/national.

Australian Football League. (2013). National Extreme Weather Policy.

Chalmers S, Anderson G & Jay O. (2020). Considerations for the development of extreme heat policies in sport and exercise. *BMJ Open Sport & Exercise Medicine* **6,** e000774.

Chalmers S & Jay O. (2018). Australian community sport extreme heat policies: Limitations and opportunities for improvement. *Journal of Science and Medicine in Sport* **21,** 544-548.

Cheuvront SN, Caruso EM, Heavens KR, Karis AJ, Santee WR, Troyanos C & D'Hemecourt P. (2015). Effect of WBGT Index Measurement Location on Heat Stress Category Classification. *Med Sci Sports Exerc* **47,** 1958-1964.

Cooper Jr ER, Ferrara MS & Broglio SP. (2006). Exertional heat illness and environmental conditions during a single football season in the southeast. *Journal of Athletic Training* **41,** 332.

Coris EE, Ramirez AM & Van Durme DJ. (2004). Heat illness in athletes: the dangerous combination of heat, humidity and exercise. *Sports Medicine* **34,** 9-16.

Cramer MN & Jay O. (2019). Partitional calorimetry. *Journal of Applied Physiology* **126,** 267-277.

Cricket Australia. (2020). Australian Cricket Heat Policy, 3 edn.

Cricket Australia. (2023). Australian Cricket Census.

Cycling Australia. (2021). Extreme Weather Policy, 2 edn, pp. 21.

Driscoll TR, Cripps R & Brotherhood JR. (2008). Heat-related injuries resulting in hospitalisation in Australian sport. *Journal of Science and Medicine in Sport* **11,** 40-47.

Gagnon D, Jay O & Kenny GP. (2013). The evaporative requirement for heat balance determines whole-body sweat rate during exercise under conditions permitting full evaporation. *The Journal of Physiology* **591,** 2925-2935.

Garcia CK, Renteria LI, Leite-Santos G, Leon LR & Laitano O. (2022). Exertional heat stroke: pathophysiology and risk factors. *BMJ Medicine* **1,** e000239.

Grundstein A & Cooper E. (2020). Comparison of WBGTs over Different Surfaces within an Athletic Complex. In *Medicina*.

Guyer H, Georgescu M, Hondula DM, Wardenaar F & Vanos J. (2021). Identifying the need for locally-observed wet bulb globe temperature across outdoor athletic venues for current and future climates in a desert environment. *Environmental Research Letters* **16,** 124042.

Havenith G, Bröde P, Hartog Ed, Kuklane K, Holmer I, Rossi RM, Richards M, Farnworth B & Wang X. (2013). Evaporative cooling: effective latent heat of evaporation in relation to evaporation distance from the skin. *Journal of Applied Physiology* **114,** 778-785.

Havenith G, Richards MG, Wang X, Brode P, Candas V, den Hartog E, Holmer I, Kuklane K, Meinander H & Nocker W. (2008). Apparent latent heat of evaporation from clothing: attenuation and “heat pipe” effects. *Journal of Applied Physiology* **104,** 142-149.

Introduction

IPCC. (2023). Climate Change 2023. In *Contribution of Working Groups I, II and III to the Sixth Assessment Report*

of the Intergovernmental Panel on Climate Change [Core Writing Team, H Lee and J Romero (eds)], pp. 186. Geneva, Switzerland.

ISO. (7933, 2004). Ergonomics of the thermal environment — Analytical determination and interpretation of heat stress using calculation of the predicted heat strain.

Jay O, Broderick C & Smallcombe JW. (2021). Extreme Heat Policy, ed. Australia SM, pp. 12. Sports Medicine Australia.

Kakamu T, Wada K, Smith DR, Endo S & Fukushima T. (2017). Preventing heat illness in the anticipated hot climate of the Tokyo 2020 Summer Olympic Games. *Environmental Health and Preventive Medicine* **22,** 1-6.

Larsen T, Kumar S, Grimmer K, Potter A, Farquharson T & Sharpe P. (2007). A systematic review of guidelines for the prevention of heat illness in community-based sports participants and officials. *Journal of Science and Medicine in Sport* **10,** 11-26.

Lawn Tennis Association. (2022). Extreme Heat Policy LTA Competition Regulations.

Liu Z & Jim CY. (2021). Playing on natural or artificial turf sports field? Assessing heat stress of children, young athletes, and adults in Hong Kong. *Sustainable Cities and Society* **75,** 103271.

Mehnert P, Malchaire J, Kampmann B, Piette A, Griefahn B & Gebhardt H. (2000). Prediction of the average skin temperature in warm and hot environments. *Eur J Appl Physiol* **82,** 52-60.

Mustapha I. (2022). TOUR DE FRANCE: 'CRAZY HOT!' - ROMAIN BARDET SAYS THE HEAT IS 'UNCOMFORTABLE' THIS YEAR AFTER TEMPERATURES HIT HIGH 30S. In *Eurosport*. Eurosport, Eurosport.

Nichols AW. (2014). Heat-related illness in sports and exercise. *Current Reviews in Musculoskeletal Medicine* **7,** 355-365.

Nielsen M. (1938). Die Regulation der Körpertemperatur bei Muskelarbeit1. *Skandinavisches Archiv Für Physiologie* **79,** 193-230.

Orr M. (2022). Tour de France: future heatwaves may make it untenable to hold the race in July. In *The Conversation*. The Conversation, The Conversation.

Parsons K. (2014). *Human thermal environments: the effects of hot, moderate, and cold environments on human health, comfort, and performance*. CRC press.

Pryor JL, Pryor RR, Grundstein A & Casa DJ. (2017). The Heat Strain of Various Athletic Surfaces: A Comparison Between Observed and Modeled Wet-Bulb Globe Temperatures. *Journal of Athletic Training* **52,** 1056-1064.

Ravanelli, N, Coombs, G, Imbeault, P. &O. Jay. (2018). Maximum Skin Wettedness after Aerobic Training with and without Heat Acclimation. *Medicine & Science in Sports & Exercise* **50** 2, 299-307.

Ravanelli N, Imbeault P & Jay O. (2020). Steady-state sweating during exercise is determined by the evaporative requirement for heat balance independently of absolute core and skin temperatures. *J Physiol* **598,** 2607-2619.

Vanos JK, Warland JS, Gillespie TJ & Kenny NA. (2012). Thermal comfort modelling of body temperature and psychological variations of a human exercising in an outdoor environment. *International Journal of Biometeorology* **56,** 21-32.

Zander KK, Botzen WJW, Oppermann E, Kjellstrom T & Garnett ST. (2015). Heat stress causes substantial labour productivity loss in Australia. *Nature Climate Change* **5,** 647-651.

CHAPTER II

Literature Review

2.0 Extreme heat in the sporting context

Participation in outdoor sports is a popular method across the globe for keeping active, healthy and engaged in society (Heinemann, 2005). Sport participation as a child (at age 10) is associated with increased physical activity later in life (at age 42) (Smith *et al.*, 2015). Participation in sports is associated with a myriad of potential benefits to mental and physical well-being across the lifespan including academic progression (Burns, Bai & Brusseau, 2020), body appreciation, life satisfaction (Riddervold, Haug & Kristensen, 2023), long-term mental health outcomes (Easterlin *et al.*, 2019), self-efficacy and self-esteem (Ouyang *et al.*, 2020), social competence (Bedard, Hanna & Cairney, 2020) and happiness as we age (Kim *et al.*, 2021). Across Australia, between 2020-21 over 18.8 million adults (89% of the adult population) participated in outdoor sport and physical activities across the year (AusSport, 2020). Four out of the top five most popular physical activities (walking [1st], running [3rd], swimming [4th], cycling [5th]) and three of the top five team sports (soccer [1st], Australian Rules Football (AFL) [3rd], and cricket [5th]) are typically conducted in an outdoor environment. In the United States of America, outdoor recreation participation increased from 50% of the adult population (~143 million) in 2011 to 54% (~167 million) in 2022 (Outdoor Foundation, 2022).

With the likelihood of extreme heat exposure increasing in the coming decades due to anthropogenic climate change (Meehl & Tebaldi, 2004; Perkins, Alexander & Nairn, 2012; Brown, 2020), it will be increasingly important for governments and sporting organisations around the world to facilitate continued participation in outdoor sports and physical activities to maintain the health and well-being of their people. Currently, physical inactivity rates are increasing (Wang *et al.*, 2020) as are rates of physiological and psychological morbidity (Cunningham *et al.*, 2020). Many cases of morbidity and mortality are encouragingly, preventable and treatable with adequate physical activity and diet modifications (Rodríguez-

Monforte, Sánchez & Barrio, 2017; Rico-Campà *et al.*, 2019; Schnabel *et al.*, 2019; Lane *et al.*, 2024). Therefore, appropriate extreme heat policies that enable continued and safe access to outdoor sports in the face of more extreme weather conditions, without limiting playing opportunities and exposing athletes to unnecessarily extreme playing conditions will contribute to facilitating a healthier population and reducing unnecessary disruptions to elite sports.

Sports administrators and sports medicine personnel take an interest in heat stress risk because of the increased risk of heat casualties when sport occurs in warm and/or humid environmental conditions (Armstrong *et al.*, 2007). Both professional and community sports, particularly in already warm parts of the globe will become increasingly at risk unless appropriate, evidence-based heat policies that include appropriate recommendations for the modification to play (such as extended half-time breaks and additional breaks in play to apply cooling strategies (Bongers *et al.*, 2015; Chalmers, 2017; Lynch *et al.*, 2018; Chalmers *et al.*, 2019)), the local environment (e.g., increased shade, airflow) and local environmental monitoring (Racinais *et al.*, 2023) are implemented. From an organisational perspective, if a sporting or physical activity event is run when the risk of heat illness exceeds a safe threshold, undue risk is placed on the participants of that event. If such risk thresholds are too conservative, then events may be needlessly cancelled, leading to reductions in important physical activity opportunities (for community sports) as well as impacting the financial outcomes of professional sporting events. The risk thresholds for cancelling/postponing events must therefore be individualised appropriately based on the activity level, clothing of the participants and the environment in which the activity occurs.

2.1 Risk and consequences of extreme heat stress

Running a community or professional sporting event in thermally challenging environmental conditions can risk the health of athletes, spectators and officials. The health consequences of exertional heat stress reside along a physiological continuum of severity, from mild-moderate-severe-fatal (Adams & Jardine, 2020). Exertional heat illnesses (EHIs) include exercise-associated muscle cramps, heat syncope, heat exhaustion, and exertional heat stroke (EHS). EHS is the most severe and is most likely to occur during uncompensable conditions. For EHS to be diagnosed, CNS dysfunction and severe hyperthermia must be present (body core temperature, T_c >40.5 °C) (Casa *et al.*, 2015; Cramer & Jay, 2016; Cottle *et al.*, 2022) as some well trained (and likely acclimatised/acclimated) athletes can handle T_c >40.5 ºC without CNS dysfunction (Racinais *et al.*, 2019). Uncompensable conditions are a set of thermal environmental conditions, metabolic rate and level of clothing (E_{req}) which exceeds the maximum capacity of the environment for evaporation (E_{max}), which is marked by an uncontrolled, continual rise in body core temperature. Exertional heat stroke (EHS) is a life-threatening condition for professional athletes; however, with the correct EHPs and available medical treatment, it is preventable and treatable (Casa & Stearns, 2016). A body core temperature of ~40.5 ºC is a commonly used threshold for EHS, however, there have been cases documented where body core temperatures of up to 41.9 ºC have been well tolerated in highly trained (and likely acclimated/acclimatised) populations (Maron, Wagner & Horvath, 1977; Racinais *et al.*, 2019; Stevens *et al.*, 2020). It is important to note that an elevated core temperature above 40.5 ºC, particularly in an untrained individual, is requisite for EHS to be declared, however, it is not the only criteria used to determine the incidence of EHS (additional CNS symptoms must be present). It is clear, however, that thermal injuries occur above these temperatures as proteins unfold at temperatures beyond ~42 ºC (Burger & Fuhrman, 1964; Bynum *et al.*, 1978). Cases of EHS can result in central nervous system dysfunction, organ damage, organ failure and morbidity (Costrini *et al.*, 1979).

The risks for an individual to experience an EHI are dependent on personal and external factors including recent history of upper respiratory tract illness (e.g., cold/flu), organisational (e.g., access to water, breaks in work etc), the environmental conditions, and individual medication and drug use, and behavioural responses (Westwood *et al.*, 2021). Some risk factors are modifiable by the individual, for example: acclimation/acclimatisation status (Kerr *et al.*, 2019), recent (<2 years) prior EHS (Stearns *et al.*, 2020), recent illness (Abriat *et al.*, 2014; Stacey *et al.*, 2015), poor physical fitness (Armstrong & Pandolf, 1988; Gardner *et al.*, 1996), dehydration (Bouchama & Knochel, 2002; Breslow *et al.*, 2019), drugs (e.g., cocaine (Crandall, Vongpatanasin & Victor, 2002)), alcohol intake(Hobson & Maughan, 2010), and age (Breslow *et al.*, 2021); and others such as activity-specific clothing and/or exercise demands (including exercise intensity and duration) (Montain *et al.*, 1994; Armstrong *et al.*, 2010), environmental conditions (e.g., dry-bulb temperature, relative humidity, mean radiant temperature and wind velocity) (Wallace *et al.*, 2006; Grundstein, Hosokawa & Casa, 2018) are non-modifiable. However, some strategies are available to modify environmental conditions outdoors and indoors, for example, adding shade and/or increasing green spaces in outdoor areas to reduce mean radiant temperature (Kim *et al.*, 2023), and building design to ensure cross ventilation workspaces such as manufacturing facilities and warehouses. These strategies can be a useful tool, particularly in the occupational setting to reduce the severity of the surrounding thermal environment (Roy *et al.*, 2022). Given the severe consequences of extreme body core temperatures and symptoms associated with exertional heat illnesses, it is imperative to develop our understanding of best practices for monitoring the thermal environment and the factors affecting human heat balance during outdoor exercise to reduce the chances of exertional heat stress cases.

2.2 Human heat balance

Human body core temperature typically rests in a range around ~37 ºC. However, normal resting body core temperature sits along a spectrum, and this variability is based on a variety of factors including individual variability, time of day (Waterhouse *et al.*, 2005), heat acclimation/acclimatisation status (Périard, Racinais & Sawka, 2015), and menopause status (Neff *et al.*, 2016); pre-menopausal women may have a higher resting core temperature (~0.3-0.7 ºC) in the luteal phase compared to the follicular phase of the ovulatory menstrual cycle (Marshall, 1968) due to fluctuations in progesterone and oestrogen (Marsh & Jenkins, 2002; Baker, Siboza & Fuller, 2020).

Notwithstanding these small and normal variations in resting body temperature, it is critical to maintain body core temperature within a relatively narrow range to sustain health. According to heat balance theory, two personal and four environmental factors determine how much body core temperature can change at rest and during physical activity in any given environment (Parsons, 2014). The personal factors are metabolic heat production (H_{prod}), which is calculated with metabolic energy expenditure (M, W) and external work (Wk, W) (see **Eq. 1**). Metabolic energy expenditure is defined as the total amount of energy required to sustain metabolic processes, in addition to the energy requirement of any involuntary or voluntary locomotion. Metabolic heat production (H_{prod}, W) can be calculated from M and Wk the following equation:

$$H_{prod} = M - Wk \qquad \text{[W] [1]}$$

The second personal factor is clothing, which can be split into two factors of evaporative resistance of clothing ($R_{e,cl}$, $m^2 \cdot kPa \cdot W^{-1}$), and dry insulation ($I_{cl}$, clo) (Parsons, 2014) which permit or restrict certain amounts of evaporative heat loss and dry heat exchange depending on the extent of clothing coverage, material type and thickness of the material. The four environmental factors that affect human heat balance are dry-bulb temperature (T_{db}, °C), ambient vapour pressure (P_a, kPa), mean radiant temperature (T_r, °C) and air velocity (ν, $m \cdot s^{-1}$). These factors can be combined to form the basis of the human heat balance equation below:

$$M - Wk = E \pm R \pm C \pm K \pm S \qquad \text{[W] [2]}$$

Where: E is evaporative heat loss, R is radiative heat exchange, C is convective heat exchange, K is conductive heat exchange, and S is heat storage or loss.

During prolonged steady-state exercise (>30 mins) in compensable environmental conditions (Jay, Imbeault & Ravanelli, 2018; Ravanelli *et al.*, 2019b), it can be assumed that the rate of heat storage approaches (S = 0). The conceptual heat balance equation [**Eq. 2**] can therefore be rearranged to solve for the evaporative requirement for heat balance (E_{req}) and the resultant equation is given by:

$$E_{req} = H_{prod} - (\pm C \pm K \pm R) - (\pm C_{res} \pm E_{res}) \qquad \text{[W] [3]}$$

Where: metabolic heat production (H_{prod}) is equal to M-Wk, which is given by subtracting external work (Wk) from metabolic energy expenditure (M), dry heat exchange (convection (C), conduction (K), and radiation (R)) from the skin surface and convective and evaporative heat exchange pathways via the respiratory tract (through convection [C_{res}] and evaporation [E_{res}]).

2.2.1 Factors affecting metabolic heat production

According to heat balance theory, two factors affect metabolic heat production (H_{prod}). The first is the rate of metabolic energy expenditure (M, W) as a result of all the metabolic processes associated with resting and active metabolism, and the second is external workload (Wk, W).

2.2.2 Rate of metabolic energy expenditure

The rate of metabolic energy expenditure in humans occurs predominantly through the oxidation of substrates (namely carbohydrates and fats) to synthesise adenosine triphosphate (ATP) in mitochondria. Laboratory approaches utilise indirect calorimetry (i.e., the ratio of $\dot{V}CO_2$:$\dot{V}O_2$ expired and absolute O_2 consumption) for the estimation of metabolic rate (Cramer & Jay, 2019). At the onset of exercise or a change in intensity, there is a delay in oxygen consumption to reach a metabolic steady-state, which in the domain of oxygen uptake kinetics is known as phase II, which reflects the system's ability to transport oxygen to the working muscles, where increased physical fitness appears to reduce to the time to reach phase II (Poole & Jones, 2012). As exercise begins or intensity increases, any difference between required and consumed oxygen will present as a deficit, and energy needs to be sourced from other energy systems.

There are three mechanisms of metabolism with different metabolic time courses (i.e., kinetics) to match the demands of physical activity from short (<30s) to prolonged durations such as for ultra-endurance events (>4 hours). The first is the rapid Phosphocreatine (PCr) system, also known as alactic oxygen debt which lasts for ~30 seconds of maximal effort. The second is the lactic oxygen debt, which is produced via glycolysis, which as an energy system, lasts much longer (~15 mins) (Gastin, 2001). Together, these first two components of metabolism have been described as an oxygen debt (OD) that needs to be repaid by increased oxygen consumption, which can occur during and/or post-exercise (Excess post-exercise oxygen consumption - EPOC) (Margaria, Edwards & Dill, 1933). During heavy constant load and intermittent high-intensity exercise, metabolic energy expenditure *may* be underestimated using solely oxygen consumption data, as additional energy contributions through glycolytic and/or PCr metabolism, which may go unaccounted for with standard indirect calorimetry (Scott, 2005) and further research must be conducted to account for the heat produced by additional glycolytic energy contributions to exercise.

Currently, there is no accepted method to account for any additional metabolic heat produced through glycolysis. One method has been proposed to account for this glycolytic contribution to whole-body thermogenesis (di Prampero & Ferretti, 1999). This method suggests that for every 1 mmol/L of blood lactate above resting levels, there is an equivalent rise in energy expenditure of 3 mL of oxygen uptake per kilogram of body weight. Using the change in lactate concentration in the blood is a novel method for estimating the glycolytic contribution to metabolic heat production however, it needs to be examined further, with reference to potential contributions to the $\dot{V}O_2$ slow component (Colosio *et al.*, 2020). However, during prolonged exercise (>30 minutes), the relative contribution of anaerobic metabolism to the total metabolic rate is likely <2% for elites (Sandford & Stellingwerff, 2019) and presumably lower for lower calibre athletes (as less capable athletes typically have a lower sustainable fractional utilisation of $\dot{V}O_{2max}$) (Maughan & Leiper, 1983), especially at intensities well below the second lactate turn point (LT2). Therefore, for prolonged endurance activities, it is unlikely that any significant underestimation of the total metabolic rate occurs as the total contribution of anaerobic metabolism is limited (<2%), particularly at sub-maximal workloads (see **Fig. 1**).

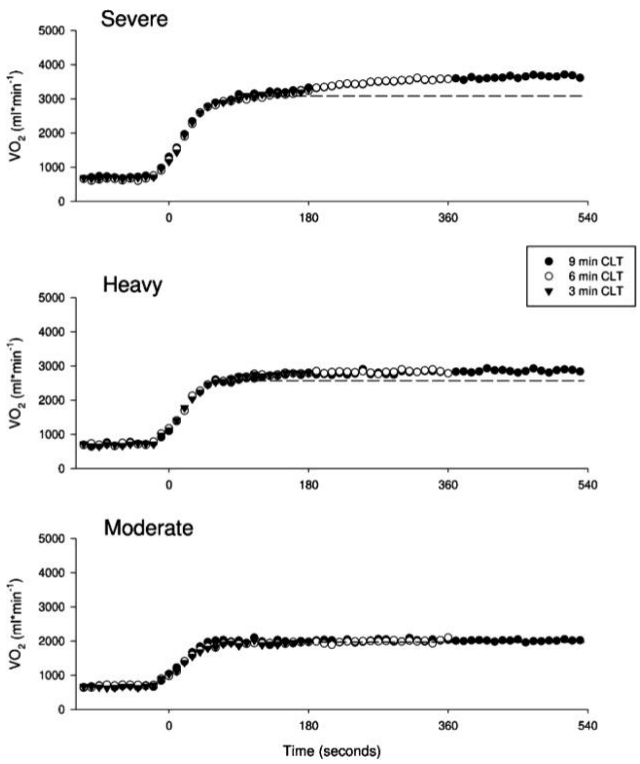

Figure 1 Colosio, A (2019) VO2 slow component during constant load cycling. Retrieved from https://doi.org/10.1007/s00424-020-02437-7 Licensed under CC BY 4.0.

The $\dot{V}O_2$ slow component is described as an increase in oxygen consumption during constant load exercise due to loss of efficiency in locomotion, but possibly other factors such as increased oxidative processing of glycolytic ‘waste products’ (e.g., lactate shuttling) (Rabinowitz & Enerbäck, 2020), which can also be described as a reduction in gross efficiency (η). A reduced or lower η means that there is increased oxygen cost associated with a given constant workload, as the metabolic cost for producing a given amount of power at intensities increases above the moderate-heavy zones (see **Fig. 1**). However, the root cause/s for that reduction in η is still of a key area of research. Some research suggests it is due to increases in blood lactate levels, increases in plasma epinephrine, increased ventilatory work, elevation of body core temperature, and increased recruitment of type IIb muscle fibres (Xu & Rhodes, 1999). However, taking recent findings together, it seems plausible that the increased oxygen consumption during intense and severe intensity constant load exercise may be a result of the increased oxygen cost potentially associated with replenishing PCr and glycolytic energy stores (via mainly lactate recycling through gluconeogenesis in the liver) within that exercise bout (Bergman *et al.*, 2000; Jeukendrup & Wallis, 2005; Brooks *et al.*, 2022).

The rate of metabolic energy expenditure during physical activity is determined by two components of metabolism, resting metabolic rate (RMR) and active metabolic rate (AMR). At rest, metabolic rate (RMR) is largely driven by skeletal muscle mass (Ravussin *et al.*, 1986). During physical activity below the severe intensity domain (<100% $\dot{V}O_{2max}$) metabolic energy expenditure can be measured via indirect calorimetry, using oxygen uptake ($\dot{V}O_2$), and carbon dioxide ($\dot{V}CO_2$) data, however, this metabolic cart data gathered beyond 75% $\dot{V}O_{2max}$ must be treated with caution if the primary outcome variable is substrate utilisation, due to the increased error in $\dot{V}CO_2$ as intensity increases(Jeukendrup & Wallis, 2005). The stoichiometric ratio of $\dot{V}CO_2$:$\dot{V}O_2$ measured from the mouth is known as the non-protein respiratory exchange ratio (RER) as a surrogate for the interpretation of substrate utilization at the cellular level (e.g., respiratory quotient, RQ).

Measuring metabolic rate inside the laboratory using gas analysis with traditional Douglas bags or the newer Cosmed style mask system are well-established processes. However, measuring metabolic outside the laboratory becomes problematic with variable environmental conditions potentially affecting readings, and high air flows across the measurement device (during outdoor cycling), which may introduce measurement error in RER and minute ventilation (V_E) (Salier Eriksson, Rosdahl & Schantz, 2012). Some companies have produced portable metabolic carts that measure metabolic variables traditionally monitored via laboratory indirect calorimetry (e.g., Cosmed K5, VO2 Master). However, the cost of these devices may be practically limiting for unfunded research projects and laboratories without access to a portable metabolic cart such as the Cosmed K5, which costs ~AUD$60,000. Other, more cost-effective devices have slowly hit the market (VO2 Master, Vernon, British Columbia), however the validity of these newer devices from companies with less experience with metabolic measurement remains to be verified. For instance, the VO2 Master seems to underestimate oxygen consumption at absolute workloads below 200W and overestimate oxygen consumption above 200W, compared to a classic laboratory based Parvomedics system (Montoye, Vondrasek & Hancock, 2020). The test of the VO2 Master system was indeed in the laboratory, with no challenges to the environmental variability which can be quite important when measuring expired gases. Recent data suggests the more cost-effective portable metabolic unit (VO2 Master system) may significantly underestimate $\dot{V}O_2$, tidal volume and ventilation compared to the more robust Cosmed K5 unit during track running in an outdoor environment (Toulouse *et al.*, 2022). Nevertheless, these devices for portable metabolic rate do open the door for a potentially better estimate of true metabolic rate in a free-living outdoor environment than can be achieved with estimations from external workload data.

To estimate metabolic rate consumption during physical activity, multiple methods have been explored by researchers both in and outside the laboratory. In the laboratory (or when gas analysis is available), metabolic rate is best derived from stoichiometric principles which use metabolic gas exchange analysis which accounts for the caloric equivalents of carbohydrates and fats and oxygen consumption, and ignores any protein/amino acid oxidation (see Eq. 4) (Cramer and Jay, 2019).

$$\mathrm{M} = \mathrm{VO}_2 \cdot \frac{\left\{\left[\left(\frac{RER-0.7}{0.3}\right)\cdot 21.13\right]+\left[\left(\frac{1.0-RER}{0.3}\right)\cdot 19.62\right]\right\}}{60} \cdot 1{,}000 \qquad \text{[W] [4]}$$

Where: $\dot{V}O_2$ is the rate of oxygen consumption ($L \cdot min^{-1}$), and RER the respiratory exchange ratio.

Outside the laboratory (or without the availability of gas exchange data), through a series of experimental studies, the American College of Sport Medicine (ACSM) published regression equations that (for cycle ergometry) utilise external workload (Wk) and body mass (m_b) to predict O_2 consumption for a given external workload and body mass (Liguori *et al.*, 2022). This first potential method for estimating metabolic energy expenditure (M_{acsm}): assumes rates of oxygen consumption calculated using **Eq. 5** (Liguori *et al.*, 2022) then converted to an estimated metabolic energy expenditure using **Eq. 6** assuming a metabolic energy equivalent (MEE) of 20.7 for low-moderate intensity sessions (session rating of perceived exertion [RPE] <4) and 21.1 for high-intensity sessions (session RPE >4) (in $kj \cdot LO_2^{-1}$) (Peronnet & Massicotte, 1991): The rate of oxygen consumption is given by:

$$\dot{V}O_2 = \left[\frac{(10.8 \times \mathrm{Wk})}{m_b}\right] + 7 \qquad [mL \cdot kg^{-1} \cdot min^{-1}]\ [5]$$

Where: $\dot{V}O_2$ is the rate of oxygen consumption ($mL \cdot kg^{-1} \cdot min^{-1}$) estimated with **Eq. 1**, Wk is external workload and m_b is total body mass (kg). Metabolic energy expenditure (M_{acsm}) is then given by:

$$M_{acsm} = \frac{(\dot{V}O_2 \times m_b) \cdot \mathrm{MEE} \cdot 1000}{60} \qquad [W]\ [6]$$

Where: $\dot{V}O_2$ is the rate of oxygen consumption ($mL \cdot kg^{-1} \cdot min^{-1}$), m_b is total body mass (kg) and MEE is the relevant metabolic energy equivalent given above (e.g., high: 21.1; low: 20.7, $kj \cdot LO_2^{-1}$).

The second method (M_{ett}) for estimating metabolic rate from external workload uses external workload and cycling cadence to estimate metabolic rate based on previous data (Ettema & Lorås, 2009). The regression equation to estimate metabolic rate from cycling power output and cadence is as follows:

$$M_{ett} = 39.7 + (28.4 \cdot f_{ped}) + (3.73 \cdot \mathrm{Wk}) \qquad [W]\ [7]$$

Where: f_{ped} is cycling cadence (revolutions·min^{-1}) and Wk is external workload (W).

A potentially suitable third approach (M_{ge}) is to assume a certain gross mechanical efficiency (η) from previous data (Moseley *et al.*, 2004). The authors explored the relationship between Wk and η in 69 trained cyclists ($\dot{V}O_{2peak}$: 62.3 ± 7.0 mL/kg/min) and stratified participants into 3 groups of fitness levels (High: > 70 mL·kg^{-1}·min^{-1}, Med: 60-70 mL·kg^{-1}·min^{-1}and Low: <60 mL·kg^{-1}·min^{-1}). The authors reported no differences in gross cycling efficiency across each of the fitness groups, indicating that $\dot{V}O_{2peak}$ does not describe the variability in cycling efficiency. The data provided by the authors (see **Fig. 2**) allowed for the generation of an estimated second-order polynomial to estimate η across a range of external workloads (~95-340 W, **Eq. 8**). The polynomial can be replicated with the following equation:

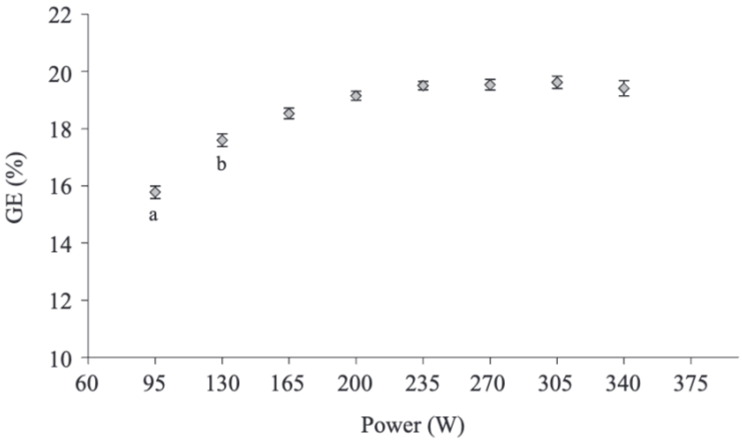

Figure 2. Moseley. L (2004). No differences in cycling efficiency between world-class and recreational cyclists. Retrieved from https://doi.org/10.1055/s-2004-815848. Licensed under CC BY 4.0.

$$\eta = \frac{-0.0001 \cdot Wk^2 + 0.0579 \cdot Wk + 11.605}{100} \qquad [\%]\ [8]$$

Where: Wk is mean power output (W) and η is gross mechanical efficiency.

Therefore, to estimate metabolic rate from external workload and an estimated gross mechanical efficiency (M_{ge}) the following equation could be used:

$$M_{ge} = \frac{Wk}{\eta} \qquad [W]\ [9]$$

Where: Wk is external workload (W) and η is estimated mechanical efficiency.

2.2.3 Mechanical work

Mechanical work (Wk) is a measure of power output or external workload and for cycling related applications it is usually measured in Watts. External work or 'Wk' is given by the formula:

$$Wk = f \times d \times f_{ped} \qquad \text{[W] [10]}$$

Where: *f* is the force exerted through the pedals (Nm), *d* is the distance travelled by the pedals given by the crank length (meters, *m*) and f_{ped} is the cycling cadence (revolutions·min^{-1}). For example, for a cyclist producing 2 newton meters (Nm) of force at the pedals, cycling on a bike with a crank length of 170 mm, at a cadence of 80 revolution per minute (rpm), we would expect a power output of 171 W. Distance (*d*) is calculated from the crank length (radius of the circle, *r*) and circumference (*c*) (distance the pedals will travel each revolution) by the following equation:

$$c = 2\pi r \qquad \text{[m] [11]}$$

External work during cycling is commonly referred to as power output or simply 'power'. External work on bikes is typically measured using resonant string gauges or strain gauge(s) that are mostly located at the crank or the pedals, however other locations and methods are available (Bouillod *et al.*, 2022). Measuring power for racing and training has become increasingly popular over the past two decades (Sparks *et al.*, 2015). Typically, most power meters report an accuracy of ±1-2%, however, the veracity of these claims made by manufacturers is constantly under review by researchers around the globe (Lanferdini *et al.*, 2020; Rodríguez-Rielves *et al.*, 2021; Bouillod *et al.*, 2022).

2.2.4 Mechanical (cycling) efficiency

Mechanical efficiency can be defined in multiple ways. There are three main variations for defining mechanical efficiency: gross efficiency (η), delta efficiency, and net efficiency (Ettema & Lorås, 2009). Gross efficiency is the ratio of work output to input and is the most important variation to consider here as a higher η for a given amount of Wk would result in a lower H_{prod} (see **Eq. 1** **and 12**). Gross efficiency can be defined by the following equation:

$$\eta = Wk \times \frac{100}{M} \qquad [12]\ [\%]$$

Where: η is gross mechanical efficiency, Wk is external workload, and M is the metabolic rate required to produce a given external workload.

There has been much debate regarding the trainability of cycling efficiency across time, where methodological issues relating to different equipment (metabolic carts and ergometers) between tests and individual studies being underpowered to demonstrate statistical differences have dogged the research (Hopker *et al.*, 2009). Potential mechanisms for longitudinal improvements in cycling efficiency due to training are suggested to be driven by muscle fibre type transformation (type IIB -> IIA -> I) changes to muscle fibre type shortening velocities (Horowitz, Sidossis & Coyle, 1994; Hopker *et al.*, 2013). Current evidence suggests that η is often different between individuals, is marginally trainable (Hopker *et al.*, 2009), and tends to follow a similar trend across the power output range (Moseley *et al.*, 2004) (see **Fig. 3**).

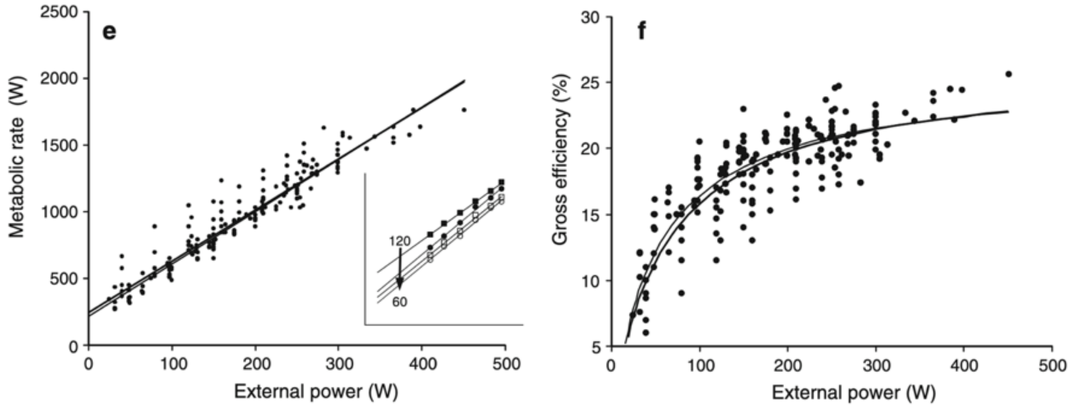

Figure 3 Ettema G & Lorås HW. (2009) Relationship between external power metabolic rate and gross efficiency during cycling. Retrieved from 10.1007/s00421-009-1008-7 CC BY 4.0.

The relationship between gross efficiency and absolute power output appears to be non-linear (see **Fig. 2, f**), owing to the lower relative contribution of resting metabolic rate to total metabolic rate as metabolic rate increases, and the subsequent physiological and biomechanical inefficiencies that occur beyond maximal intensities as multifactorial fatigue ensues (Abbiss & Laursen, 2005). Cycling at a higher cadence for a given power output leads to a slightly increased metabolic rate (Ettema & Lorås, 2009). Around 91% of the variability in metabolic rate while cycling can be attributed to external workload, whereas about 10% is explained by cadence (Ettema & Lorås, 2009). A ~24% higher percentage of Type I to II muscle fibres (72±3% Type I vs. 48±2% Type I fibres n=14) was shown to increase external work capacity by ~9% (high 342±9 vs. normal 315±11 watts) within experienced cyclists. Individuals with a higher ratio of Type I to Type II muscle fibres may have a higher gross mechanical efficiency (Type I high: 21.9±0.3% vs. Type II normal: 20.4±0.3%; $p < 0.001$) for a given rate metabolic energy expenditure (Coyle *et al.*, 1992). It has been suggested that cycling efficiency changes as a function of ability/training status (Coyle, 2005), however, this example has been thoroughly questioned due to potential methodological challenges associated with longitudinal cycling efficiency tests (e.g., different ergometers, and accuracy and reliability of efficiency tests) (Martin, Quod & Gore, 2005) and now we understand the potential impacts of systematic and long-term doping by the athlete in question (Lance Armstrong). More robust evidence suggests that cycling efficiency is not determined by one's $\dot{V}O_{2max}$, where 69 male recreational to world-class cyclists were recruited to study their gross efficiency, the authors found no differences between the low (<60 mL·kg^{-1}·min, n=26), Medium (60-70 mL·kg^{-1}·min, n=27) and High (>70 mL·kg^{-1}·min, n=16) groups (Moseley *et al.*, 2004) across 50-300W of external workload (see **Fig 2**). Although Moseley and colleagues (2004) observed a tight spread between their participants with fitness levels, gross mechanical efficiency has been reported to be substantially higher in elite (24.4 ± 2%) and professional world tour men (25.6 ± 2.6%) (Sallet *et al.*, 2006) than reported by the well-trained cyclists from Moseley *et al.*, (2004). This means that differences between the lowest and highest mechanical efficiency for recreational and professional, elite cyclists at the same external workloads could be up to 6-7%.

When estimating gross cycling efficiency across time, the potential for fatigue and reduced exercise efficiency should be considered. A recent study found that gross efficiency remains relatively stable from ~6 minutes onwards and presumably the rate at which steady-state metabolic rate occurs largely depends on the individual's $\dot{V}O_{2max}$, age, and oxidative enzyme inertia (Poole *et al.*, 2005). Gross efficiency can decline as exercise progresses and fatigue sets in, ostensibly due to mitochondrial oxygen consumption increases (or a reduction in mitochondrial efficiency) (Hopker, O'Grady & Pageaux, 2017) and the $\dot{V}O_2$ slow component if exercise is conducted close to and/or above the second lactate turn point (LT2) (Poole *et al.*, 1991; Lucía, Hoyos & Chicharro, 2000; Jones *et al.*, 2011). For example, in 14 well-trained cyclists, gross efficiency reduced slightly from the most efficient at ~6 minutes into constant load cycling (at ~60% of their power at $\dot{V}O_{2max}$) but remained relatively stable from 30-120 minutes of cycling (Hopker *et al.*, 2017). Therefore, to estimate gross cycling efficiency and metabolic rate across submaximal steady-state exercise intensities we will assume relative metabolic steady-state across each trial for all individuals and have participants exercise have submaximal intensities to reduce fatigue.

2.2.5 Factors governing heat exchange

Heat moves along temperature gradients, from hot areas to cool areas, and this process is driven by temperature differences between objects/environments. This form of heat exchange is known as sensible or 'dry' heat exchange. Particularly relevant to humans in warm environments is another method of heat exchange, evaporative heat exchange. Evaporative heat exchange occurs through a phase change of an object from a liquid to a gas (for humans this is typically sweat or in some cases can be exogenous fluid/water), which is known as latent heat. Heat is exchanged between the body and the environment through all these methods; however, latent heat loss is critical while exposed to high dry-bulb temperatures that exceed mean skin temperature (>~36 ºC, depending on the thermal environment, clothing and metabolic rate) (Parsons, 2003). This section covers the various avenues for both dry heat exchange and evaporative heat loss particularly during outdoor physical activity.

2.2.5.1 Radiative heat exchange

Radiative heat exchange (R) is the process of electromagnetic energy flux between the skin/body tissues and other objects that emit or absorb radiation nearby. In the context of outdoor sport, substantial amounts of radiative heat exchange can occur when in direct sunlight from solar radiation. Radiative heat exchange is expressed by the following equation:

$$R = h_r \cdot (T_{sk} - T_r) \qquad [\mathrm{W \cdot m^{-2}}]\ [12]$$

Where: h_r is the radiative heat transfer coefficient (in $\mathrm{W \cdot m^{-2} \cdot K}$) [see **Eq. 14**], T_{sk} is mean skin temperature and T_r is mean radiant temperature. Mean radiant temperature can be calculated from measures of T_g, T_{db} and wind velocity (*v*) data using the following calculation when air velocity is $\geq 0.15\ \mathrm{m \cdot s^{-1}}$ (Parsons, 2003):

$$T_r = \left[(T_g + 273.15)^4 + \frac{(1.1 \times 10^8 \times v^{0.6})}{\varepsilon \times d^{0.4}}(T_g - T_{db})\right]^{0.25} - 273.15 \qquad [^{\circ}\mathrm{C}]\ [13]$$

Where v is air velocity in $\mathrm{m \cdot s^{-1}}$, ε is the emissivity of the black copper globe - assumed to be 0.97 (Parsons, 2003), T_{db} is dry-bulb temperature, T_g is black globe temperature, and *d* is the diameter of the black globe in meters (in this case - 0.15 m). Similar to convective heat exchange [see section 2.2.5.2], radiant heat exchange is driven primarily by temperature gradients between the body and the environment whereby heat energy moves from high to low temperature objects, which is augmented by a heat transfer coefficient, in this case, the radiant heat transfer coefficient (h_r). The h_r can be changed by increasing or reducing the surface area of skin exposed to the environment (i.e., increasing or decreasing available skin surface area) or changing T_{sk} or/or T_r. The h_r can be calculated as follows:

$$h_r = \left(4 \cdot \varepsilon \cdot \sigma \cdot f_{eff} \cdot \frac{273.15 \cdot (T_{sk} + T_r)}{2}\right)^3 \qquad [\mathrm{W \cdot m^{-2} \cdot K}]\ [14]$$

Where: ε is the emissivity of a clothed human (assumed to be 0.97), σ is the Stefan-Boltzmann constant (5.67×10^{-8} $\mathrm{W/m^{-2} \cdot K^{-4}}$), f_{eff} is effective radiation area factor (assumed to be 0.73 for cycling), T_{sk} is mean skin temperature (ºC) and T_r is mean radiant temperature (ºC).

2.2.5.2 Convective heat exchange

Convective heat exchange occurs through liquids such as air and sometimes water (for the case of swimming) and the flow of heat energy is transferred across a temperature gradient from a higher to lower temperature (Parsons, 2014). Convection is an important factor that affects both convective and evaporative heat exchange in humans both in and outside the laboratory. For example, in temperate environments, convection is the predominant method of cooling, which results in lowered sweating requirements (see **Fig 5**). Convective heat exchange (C) is determined primarily via the skin-to-dry-bulb-temperature (T_{sk}-T_{db}) and the convective heat transfer coefficient (h_c). Both convective and radiative heat exchange can be summarised with the operative temperature (T_o) (see section 2.3.4) in an outdoor environment. Calculating dry heat exchange with T_o or separately as convective and radiative heat exchange must be utilised when there are significant additional sources of radiation present, given the likely significant effect of solar radiation (when present) influencing the thermal environment (see section 2.3.3) (Cramer & Jay, 2019).

Convective heat exchange (C) can be expressed by the following equation:

$$C = \frac{(T_{sk} - T_{db})}{\left(R_{cl} + \frac{1}{h_c \cdot f_{cl}}\right)} \cdot A_D \qquad [\mathrm{W}]\ [15]$$

Where: h_c is the convective heat transfer coefficient ($W \cdot m^{-2} \cdot {}^{\circ}C^{-1}$), f_{cl} is clothing area factor, R_{cl} is the dry heat transfer resistance of clothing ($m^2 \cdot {}^{\circ}C \cdot W^{-1}$) which can be estimated from standard tables (McCullough, Jones & Huck, 1985), A_D is body surface area, and T_{sk} is mean skin temperature (ºC) and T_{db} is dry-bulb temperature (ºC) (Parsons, 2003). Importantly, when $T_{db} > T_{sk}$ then dry heat loss turns to dry heat gain and all metabolic heat including heat gained from the environment must be lost via evaporative mechanisms.

The only potential physiological control mechanism humans possess to affect convective heat exchange directly is the modification of skin blood flow which occurs mainly via adjustments in blood vessel diameter (vasomotor control) and the rate of blood flow delivery to the skin through changes in cardiac output and small blood vessel diameter. Skin temperature can be reduced by the evaporation of sweat which can indirectly reduce (in an environment where $T_{sk} < T_o$) convective heat exchange through the reduction in T_{sk}, since the evaporation of sweat liberates heat. Skin blood flow is thought to augment heat loss via increases (vasodilation) or decreases (vasoconstriction) in skin temperature which modifies the skin-to-air temperature gradient. However, recent evidence suggests that even with 20% reductions in skin blood flow does not affect T_{sk} and subsequent dry heat exchange, whole body sweat rate, and core temperature at rest (Cramer *et al.*, 2017). Because of the greater heat exchange which occurs during exercise, further research is needed to determine if such a large reduction in SkBF during exercise also does not reduce heat loss. Mean skin temperature is a component of E_{req} and affects E_{req} directly, through augmenting dry heat exchange, however, T_{sk} appears to describe no additional variability in WBSR outside of E_{req} (Hospers *et al.*, 2020; Guyer, 2021). Thus, small differences in the skin-to-air temperature gradient do affect heat exchange via the E_{req} model, although a higher T_{sk} does not result in higher sweat rates for matched conditions. Indeed, for the same dry-bulb temperature in the shade, a higher T_{sk} would result in a larger skin-air-temperature gradient and theoretically allow for a greater dry heat loss, thereby increasing E_{max}, reducing E_{req} and associated sweat losses.

The convective heat transfer coefficient (h_c) is influenced predominantly by wind velocity, posture (seated vs. standing vs. cycling), barometric pressure and clothing, which has been studied extensively in the context of clothing and textile manufacturing for thermal comfort and physical work capacities at modest air speeds (0.2-4.0 $m \cdot s^{-1}$) (Nishi & Gagge, 1970; Holmér *et al.*, 1999; Xu *et al.*, 2021b, a). There has been very limited research on h_c at outdoor cycling relevant airspeeds (>4.0 $m \cdot s^{-1}$), with only one study assessing the h_c with a thermal manikin up to 10 $m \cdot s^{-1}$, which is the most relevant to typical speeds for recreational road cyclists (Oliveira *et al.*, 2014). One research group has used computational fluid dynamics modelling to predict the h_c of a cyclist in 3 riding positions: upright, aerodynamic and in the time-trial position, with the upright position being the most common for most cyclists (Defraeye *et al.*, 2011). However, in contrast to the non-linear model put forward by Oliveira et al. (2014), Defraeye and colleagues (2011) suggest that the h_c responds almost linearly as air velocity increases. Models of the convective heat transfer coefficient depict a non-linear coefficient at air velocities between 0-1 $m \cdot s^{-1}$, which appears to turn linear at air velocities >1 m·s^{-1} (see **Fig. 4**)(Nishi & Gagge, 1970).

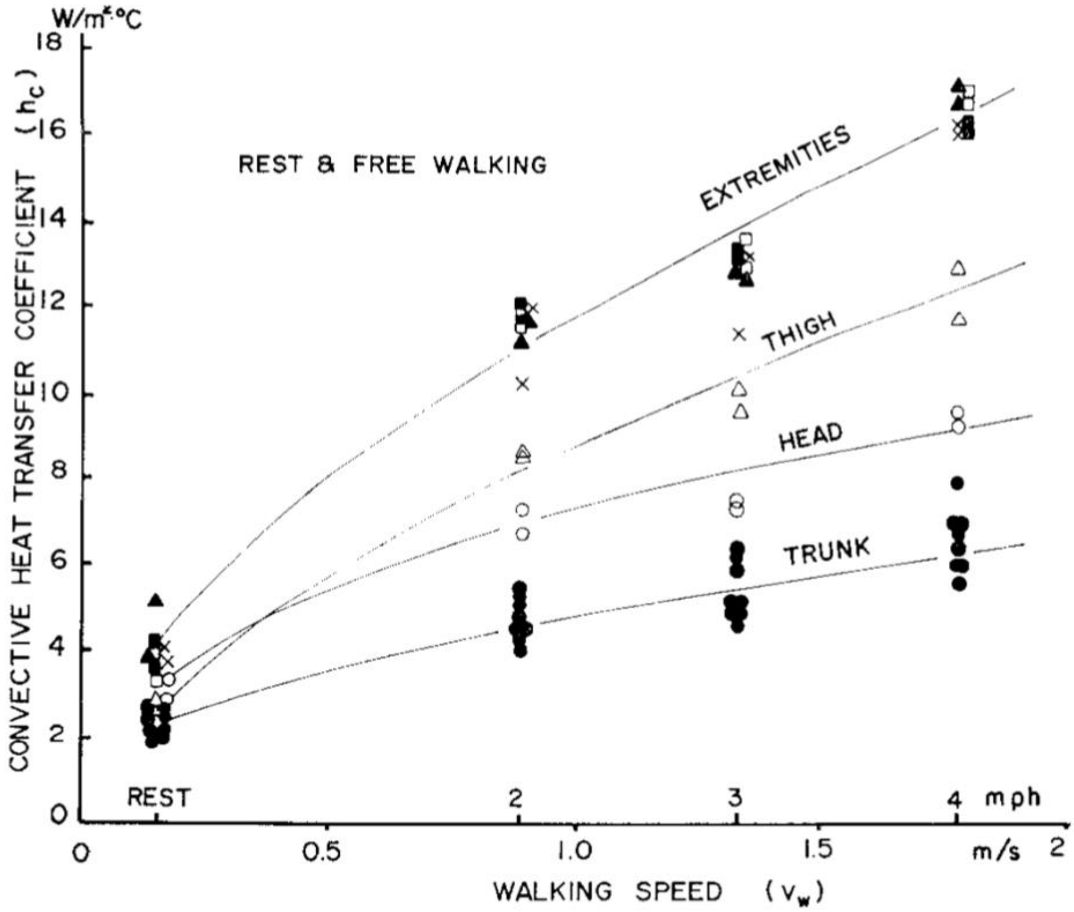

Figure 4 Nishi and Gagge (1970). Regional variation in the convective heat transfer for rest and free walking. Retrieved from [*https://doi.org/10.1152/jappl.1970.29.6.830*](https://doi.org/10.1152/jappl.1970.29.6.830) *CC BY 4.0.*

For this thesis and to determine the most appropriate model of the convective heat transfer coefficient (h_c) while cycling outdoors, we will assess multiple methods to estimate h_c. The first method (h_{c1}) was developed specifically for stationary cycle ergometry, which takes cycling cadence into account, albeit in an indoor environment with forced convection, h_{c1} (Lotens & Havenith, 1991). We will assess multiple models that have reported h_c at both at (h_{c1}) and below outdoor cycling relevant air speeds: h_{c2}, h_{c3}. The 2nd and 3rd methods for estimating h_c (h_{c2}, h_{c3}) have been derived for use indoors with minimal clothing with low forced convection (Nishi & Gagge, 1970; Xu *et al.*, 2021a) except for Lotens and Havenith, 1991 (Lotens & Havenith, 1991) who describe the first method (h_{c1}) which is theoretically appropriate for higher air velocities (> 2.5 m·s^{-1}) commonly experienced by recreational and professional road cyclists (Clarry, Faghih Imani & Miller, 2019; VAN Erp *et al.*, 2020). This empirically derived estimate of h_c, is in relative agreement with computational fluid dynamics modelling in cycling (Defraeye *et al.*, 2011) at higher air velocities, despite h_{c1} only being validated for use with air velocities up to 4 m·s^{-1}. More research is needed to confirm the convective heat transfer coefficient at relevant air speeds for recreational and professional cycling. Here we will evaluate the best available methods for estimating h_c which are detailed below:

$$h_{c1} = 8.3 \cdot \left(0.07 + 0.0043 \cdot f_{ped} + v_{self}\right)^{0.86} \qquad [\mathrm{W \cdot m^{-2} \cdot {}^{\circ}C^{-1}}]\ [16]$$

$$h_{c2} = 8.3 \cdot \left(v_{self}\right)^{0.86} \qquad [\mathrm{W \cdot m^{-2} \cdot {}^{\circ}C^{-1}}]\ [17]$$

$$h_{c3} = 5.5 + 1.96 \cdot \left(v_{self}\right)^{0.86} \qquad [\mathrm{W \cdot m^{-2} \cdot {}^{\circ}C^{-1}}]\ [18]$$

Where: v_{self} is self-generated air velocity (i.e., average cycling velocity) in m·s^{-1}, and mean skin temperature (T_{sk}, ºC).

2.2.5.3 Evaporative heat exchange

Evaporative heat loss is driven by the difference between the vapour pressure at the skin surface ($P_{sk,sat}$), assumed to be saturated with sweat, and ambient water vapour pressure (P_a) [kPa] (Parsons, 2014). As the $P_{sk,sat}$ -P_a gradient reduces, the evaporative potential is reduced, and the risk for thermal and cardiovascular strain, particularly during exercise increases. The water vapour pressure gradient between the skin and the environment governs the rate of evaporation from the skin surface, which is modified by the evaporative heat transfer coefficient (h_e). Evaporative heat loss can be calculated as follows:

$$\mathrm{E} = h_e \cdot (\mathrm{P}_{sk\_sat} - \mathrm{P}_a) \qquad [\mathrm{W \cdot m^{-2}}]\ [19]$$

Where: E is the rate of evaporative heat loss, h_e is the evaporative heat transfer coefficient (W·m^{-2}·kPa^{-1}), P_{sk_sat} is the saturated water vapour pressure at the skin surface (kPa), and P_a is the ambient water vapour pressure (kPa). Changes in the h_e are primarily driven by changes in the h_c, in combination with changes in barometric pressure (P_b). The h_e can be calculated as:

$$h_e = \mathrm{LR} \cdot h_c \cdot (760 - \mathrm{P}_b) \qquad [\mathrm{W \cdot m^{-2} \cdot kPa^{-1}}]\ [20]$$

Where: LR is the Lewis Relation which is a constant assumed to be 16.5 (AU) (Parsons, 2003), h_c is the convective heat transfer coefficient ($\mathrm{W \cdot m^{-2} \cdot {}^{o}K^{-1}}$) appropriate for the activity level and clothing [see **Eq. 16-18**].

During exercise in warm environments, the predominant method for cooling the body is through the evaporation of secreted sweat. Therefore, the evaporation of sweat is vital to minimise heat storage and protect against exertional heat illness (EHI), particularly when stressful thermal environmental conditions, high metabolic rates and/or high levels of clothing are present. As sweat is secreted onto the skin surface, evaporation occurs as the sweat transforms from a liquid to a gas which transfers heat energy (2430 J/g of sweat (PW & Charmchi, 1997)) from the skin surface to the surrounding environment. However, the exact value for the latent heat of evaporation (λ) of human sweat has been debated and is modified by certain factors. The value for λ decreases with increasing temperature of the skin surface (Monteith, 1972) and decreases with increasing distance from the skin surface (Havenith *et al.*, 2013). However, the magnitude of the difference in the value across physiologically relevant temperatures and electrolyte content for λ is relatively small (±30 J/g) so the impact of any miscalculation will be ultimately minor. If sweat or fluid evaporates from clothing, the greater distance of evaporation location, the lower amount of latent heat is released from the skin surface, which could lead to higher skin temperatures and thermal strain. For some clothing types, there is also a complication (potentially beneficial) when estimating evaporation rates, where sweat evaporates from the skin surface and it may then condense back onto clothing/garments, which then evaporates again from the garment (Havenith *et al.*, 2008), serving to potentially increase S_{eff} through this cyclical effect. Garments such as form fitting, sweat wicking fabrics mostly absorb sweat immediately which then evaporates from the garment rather than the skin (e.g. underwear [11% reduction] vs outer clothing layer [28%]), which is known as the effective latent heat evaporation (λ_{eff}) (Havenith *et al.*, 2013).

2.2.5.4 Respiratory heat exchange during physical activity

During rest and physical activity, heat can be exchanged in the respiratory system through both convective and evaporative mechanisms. As inhaled air is humidified and heated to body temperature within the respiratory tract, relatively small but important amounts of heat are lost to the environment (Nishi, 1981). As ventilation increases, air temperature and atmospheric humidity decrease larger amounts of heat will be lost via respiratory means. Therefore: respiratory heat exchange (H_{res}) can be estimated by combining estimated respiratory heat loss via convection (C_{res}) and evaporation (E_{res}) from the respiratory tract (Parsons, 2003):

$$C_{res} = 0.001516 \cdot M(28.56 + 0.641 \cdot \mathrm{P}_a - 0.641 \ \cdot \mathrm{T}_{db}) \quad \text{[W] [21]}$$

$$E_{res} = 0.00127 \cdot M(59.34 + 0.53 \cdot \mathrm{T}_{db} - 11.63 - \ P_a) \quad \text{[W] [22]}$$

$$H_{res} = C_{res} + E_{res} \quad \text{[W] [23]}$$

Where: M is metabolic rate [W], T_{db} is the temperature of the inspired air [ºC], assumed to be equal to the dry-bulb temperature, and P_a is the ambient vapour pressure [kPa].

2.2.5.5 The evaporative requirement for heat balance

Since the late 1930's, in accordance with heat balance theory, there has been evidence that whole-body sweat rate (WBSR) is directly determined from the evaporative requirement for heat balance (E_{req}) (Nielsen, 1938). As methods for measuring various components of E_{req} have improved over the years, many recent laboratory studies have shown exactly how well (r > 0.8-0.9) the evaporative requirement for heat balance determines whole-body sweat rate during steady-state exercise (Gagnon, Jay & Kenny, 2013; Cramer & Jay, 2019; Hospers *et al.*, 2020). However, in situations where full evaporation of sweat is restricted, S_{eff} is reduced and the association between E_{req} and WBSR will fall. During steady-state exercise heat storage can be assumed to be zero (S=0). Therefore, the conceptual heat balance equation can be rearranged to give the evaporative requirement for heat balance (Nishi, 1981).

$$E_{req} = H_{prod} - (\pm C \pm K \pm R) - (\pm C_{res} \pm E_{res}) \qquad [W] [24]$$

Where: H_{prod} is metabolic heat production. Dry heat transfer avenues are given by convection (C), conduction (K), and radiation (R)) from the skin surface and heat exchange avenues from the respiratory tract are given by convection [C_{res}] and evaporation [E_{res}]).

$$E_{max} = \omega_{max} \cdot \frac{(P_{sk,sat} - P_a)}{\left(R_{e,cl} + \frac{1}{h_e \cdot f_{cl}}\right)} \qquad [W \cdot m^{-2}] [25]$$

Where: E_{max} is the maximum capacity of the environment for evaporation, ω_{max} is maximum skin wettedness (ND), h_e is evaporative heat transfer coefficient, $P_{sk,sat}$ is the saturated water vapour pressure at skin temperature, and P_a is ambient water vapour pressure, (both in kPa) and $R_{e,cl}$ is the evaporative resistance of clothing (in $m^2 \cdot kPa \cdot W^{-1}$) and f_{cl} is clothing area factor (Parsons, 2014; Cramer & Jay, 2019). $P_{sk,sat}$ values can be calculated using Antoine's equation (Osborne & Meyers, 1934) at 100% relative humidity at mean skin temperature. Clothing area factor can be estimated by the following equation (McCullough *et al.*, 1985):

$$f_{cl} = 1 + (2 \times R_{cl}) \qquad [W \cdot m^{-2}] [25]$$

Where R_{cl} is the intrinsic thermal resistance (insulation) of the clothing.

A higher maximum skin wettedness (ω_{max}) helps by increasing the surface area of the skin that is available to evaporate sweat (i.e., a more even distribution of sweat across the skin surface) which reduces the chances for sweat to pool and drip off the body, unevaporated resulting in losses to S_{eff}. Fortunately, there are two methods to increase the upper limit of ω_{max}; heat acclimation/acclimatisation and general fitness improvements through cardiovascular and resistance exercise (Ravanelli *et al.*, 2018; Ravanelli, Bongers &

Jay, 2019a; Ravanelli *et al.*, 2019b). With general physical activity (cardiovascular and endurance exercise) ω_{max} can be improved from 0.72 (untrained and unacclimated) to ~0.84 (ND), which allows for a greater proportion of the skin surface to be saturated with sweat, however, a series of dedicated active heat exposures are required to achieve a ω_{max} nearing 1.0 (ND) (Ravanelli *et al.*, 2018).

A person's perception of their sweat rate is highly individualised and often unreliable. While there is considerable variability in observed sweat rates between individuals (Baker, 2017), recent evidence has confirmed earlier work (Nielsen, 1938) and suggested that the calculation of exactly what those differences are between individuals (body morphology and clothing) through heat balance modelling (Cramer & Jay, 2019) is possible (Gagnon *et al.*, 2013). This research provides strong evidence to suggest that the observed interindividual differences in sweat rates are likely not a result of unexplained factors such as genetics, but rather calculatable differences in the complex biophysical interactions that occur between humans and their environment during rest and exercise. The evaporative requirement for heat balance (E_{req}) is a biophysical model which has been shown to almost entirely (~95%) determine WBSR during steady-state exercise in compensable conditions (Gagnon *et al.*, 2013). In this study, the authors collected data in well-designed and intently perfect laboratory conditions for E_{req} to agree with WBSR whereby, participants were inside a whole-room direct calorimeter, with a range of high dry-bulb temperatures (30, 35, 40, 45 ºC), low ambient vapour pressures, low levels of clothing and high levels of airflow. All these factors together reduced the chance for sweat to evaporate away from the skin surface or drip from the skin which would ultimately lead to a reduced sweating efficiency (Havenith *et al.*, 2008; Havenith *et al.*, 2013) and likely less agreement between E_{req} and WBSR.

Most physical activity, however, does not occur in such perfect conditions. If we are to translate these findings into a useful model to help inform heat balance modelling and extreme heat policies in sport, then we must do so in an outdoor environment where most community and professional sports occur when exposed to warm conditions. There is much greater variability in free living in outdoor settings (natural fluctuations in dry-bulb temperature, air velocity, solar radiation and metabolic rate) compared to the controlled laboratory environment, which may reduce the association between E_{req} and WBSR. When selecting a modality of exercise that could elicit the extrapolation of the E_{req} model to the outdoor environment, many factors had to be considered. Within the E_{req} model (described above in section 2.2), metabolic rate, skin temperature, and dry and respiratory heat exchange all need to be either measured or estimated. The popular sport of cycling was therefore chosen, as metabolic rates can be estimated from power meters (Lanferdini *et al.*, 2020; Dickinson & Wright, 2021; Rodríguez-Rielves *et al.*, 2021; Liguori *et al.*, 2022) and concomitant high convective and evaporative heat transfer coefficients [sections. 2.2.5.2-3] from high self-generated air velocities (Clarry *et al.*, 2019; VAN Erp *et al.*, 2020) mean that is only minor reductions in S_{eff}, which would impact the relationship between E_{req} and WBSR [section 2.2.6], so that the result could applied to many.

Evidence suggests that endurance performance decreases and the health risks of dehydration increases at levels of dehydration beyond a ~2% reduction in body mass due to sweat loss (James *et al.*, 2019). The impacts to performance and health are due to multifactorial system changes where blood volume is reduced, extracellular osmolality is increased and cardiovascular strain is increased (Cheuvront & Kenefick, 2014). Developing our understanding and ability to calculate E_{req} well in a range of environments should allow for the development of refined sweat rate prediction models to inform hydration guidelines for many sports, across various environmental conditions and combinations of clothing/equipment and metabolic rates/individual body morphology. General guidelines for whole-body sweat rates (WBSR) across sports (endurance exercise, football, American football, baseball, basketball, skiing and motorsport) and various populations (men vs women, recreationally vs professionally trained, adolescents vs adults) have recently been published (Barnes *et al.*, 2019). However, without assessing the heat balance factors at an individual level (metabolic heat production [H_{prod}, W], clothing [clo, AU], and dry heat transfer between the body and environment [H_{dry}, W]) the translation of the guidelines into accurate, non-personalised recommendations is problematic. Using generalised, normative sweat rate data to guide individual hydration plans may increase the risks of hyponatremia when athletes ingest too much fluid or dehydration when they ingest too little fluid, particularly for individuals whose morphological and physiological characteristics (height, weight and achievable metabolic rate) and clothing differs significantly from the original tests subjects.

For situations where an individual's maximum WBSR is less than E_{req}, the limit of compensability has likely been reached and the individual will experience a continual rise in body core temperature until the demands of the activity or the environment change. E_{req} is determined by biophysical interactions between the skin surface and the environment, as such individuals with different body shapes, sizes and metabolic heat production as well as different levels of clothing can have a different E_{req} in the same environment. Further, individuals can have different maximum whole-body sweat rates which are more of a physiological limitation. From a physiological perspective, the limit of compensability can be improved for an individual through aerobic training and heat acclimation/acclimatization, which help to improve sweating efficiency through improvements to maximum skin wettedness and increased maximum sweat rates (Racinais *et al.* 2015*;* Ravanelli *et al.*, 2018).

2.2.6 Sweating efficiency

Sweating efficiency (S_{eff}) is defined as the fraction of secreted sweat that evaporates from the skin surface. Sweating efficiency is determined by both environmental factors such as ambient humidity, dry-bulb temperature, prevailing air velocity, and individual physiology and morphology (e.g., acclimatization status, skin surface area) (Candas, Libert & Vogt, 1979a, b), and is primarily driven by the ratio of the evaporative requirement for heat balance (E_{req}) to the maximum evaporative capacity of the environment (E_{max}), which can be expressed the skin wettedness required to maintain heat balance (ω_{req}) (Gagge, 1937).

$$\omega_{req} = \frac{E_{req}}{E_{max}} \quad \text{[ND] [26]}$$

Where: ω_{req} is the proportion of the skin surface required to be saturated with fluid (e.g., sweat) to maintain heat balance (ND), E_{req} is the evaporative requirement to maintain heat balance (W), E_{max} is the maximum evaporative capacity of the environment (W).

High absolute rates of metabolic heat production, high ambient vapour pressure (humidity), low air flows, and high levels of impermeable clothing all reduce S_{eff} by either increasing E_{req} or decreasing E_{max}. S_{eff} can be estimated using (Vogt *et al.*, 1981):

$$S_{eff} = 1 - \frac{\omega^2 req}{2} \quad \text{[ND] [27]}$$

Where: ω_{req} is the proportion of the skin surface required to be saturated with fluid (e.g., sweat) to maintain heat balance (ND).

2.2.7 Physiological control of heat exchange

Humans are in a constant state of bi-directional heat exchange with the environment, both losing and gaining heat via convection, radiation, evaporation, and conduction. Humans have two physiological control mechanisms that enable us to survive in a wide range of environmental temperatures. The first and most important during exercise and warm environments is the secretion of sweat and importantly the subsequent evaporation of that sweat (Gisolfi & Wenger, 1984). The second is via changes in skin blood flow [SkBF] (through vasodilation and vasoconstriction) which subsequently affects skin temperature and therefore dry heat exchange.

2.2.7.1 Sweat rate and dehydration

Classic work in thermal physiology has demonstrated that the forcing function for thermoeffector responses (on-set and thermosensitivity [the rate of increase – slope of the line] of both sweat rate and SkBF) can be quantified using the change in mean body temperature (T_b) where T_b is a weighted average of T_c (0.9) and T_{sk} (0.1) (Nadel *et al.*, 1971; Gisolfi & Wenger, 1984; Simon, Pierau & Taylor, 1986). The effect therefore on thermoeffector responses is for a greater change in T_b, there will be a faster onset of sweating, and/or a faster rate of sweat increase (thermosensitivity) to the individual's limit. However, the forcing function for steady state-sweat rate during exercise has been less clear. By the very nature of differences in body shapes and sizes, metabolic heat productions, clothing levels and environmental conditions across people, it has been commonly thought that there is considerable individual variability in sweat rates (Baker, 2017) and individualised sweat rate profiles have been recommended (Sawka *et al.*, 2007; McDermott *et al.*, 2017). While considerable variability in sweat rates does occur, the cause of this variability has been observed to be due to known factors as such height, weight, metabolic heat production, clothing (both insulation and evaporative resistance) and environmental conditions, which collectively can be described by E_{req} (see **Eq. 3**), with one study reporting that individual differences and/or inherent measurement error only explained the remaining ~5-24% (E_{req} explained 76-95%) of unexplained variance in WBSR (Gagnon *et al.*, 2013; Ravanelli, Imbueault, & Jay 2020; Hospers *et al.*, 2020). While it is certainly important and potentially helpful for recreational and professional athletes to characterise their sweat rate for their unique circumstances (clothing level, exercise duration, intensity environment), this can be resource intensive (Baker, 2016), prone to error with poor accuracy balances (and not accounting for food/fluid intake, and urine/faecal loss), and can interrupt or reduce training quality. Indeed, this also only provides insight into the sweat rate for that given set of personal and environmental conditions and the translation of that observed sweat rate may be limited.

One of the main factors limiting our ability to continue exercising is the volume of sweat that comes from the blood to cool ourselves down. While this function is crucial in maintaining body temperature across a wide array of activity levels and environments, even mild-moderate dehydration can negatively impact thermoregulation through a poorer distribution of heat content inside the body and reduced sweat rate which results in a faster rise in body core temperature (Graham *et al.*, 2020). Combined, these factors mostly affect performance through an increased heart rate and increased relative intensity (%VO_{2max}) (James *et al.*, 2019; Sawka *et al.*, 2007). During prolonged work, exercise or simply being exposed to hot environments for long periods, the appropriate replenishment of fluids lost through sweat is an important factor to maintain health and performance. Current evidence suggests that appropriate fluid replacement for most endurance activities means maintaining a body mass loss during exercise of less than 2% of starting body mass. (James *et al.*, 2019; Sawka *et al.*, 2007).

2.2.7.2 Skin blood flow

Skin blood flow (SkBF) is controlled through two branches of the sympathetic nervous system, the active vasodilator and the adrenergic vasoconstrictor systems (Charkoudian, 2010). With vasodilation in the cutaneous vascular system, more blood flow is distributed towards the skin and skin temperatures begin to rise, conversely, as vasoconstriction occurs in response to cold stimuli, SkBF lowers, and skin temperatures are further reduced. These physiological effects (of vasodilation and vasoconstriction) result in small physiological changes to T_{sk} in stable environments, which subsequently augments dry heat exchange with the environment by theoretically altering the skin-to-air gradient. However, this presumption was challenged recently as it was observed that the skin-air temperature gradient was unaffected even with a ~20% reduction in SkBF (Cramer *et al.*, 2017). This ~20% reduction in SkBF not only did not affect dry heat transfer, but also did not reduce the critical ambient vapour pressure (P_{crit}), which is the ambient vapour pressure point at which E_{req} exceeds E_{max}. Firstly, these findings indicate that changes in SkBF itself may not meaningfully (at least when considering SkBF in the context of the skin-air temperature gradient) affect T_{sk}, and secondly that T_{sk} is driven primarily by other factors, such as the rate of sweat evaporation and environmental conditions such as dry-bulb temperature. These data were collected in a hot environment; where T_{db} (41 ºC) > T_{sk}, however, more data need to be collected in an environment where T_{db} is below T_{sk} to confirm these findings across different conditions.

2.2.8 Skin temperature

Skin temperature is an important physiological factor that not only affects dry heat transfer with the surrounding environment via augmenting the skin-air temperature gradient (see section 2.2.5.2), but also plays a role in affecting endurance performance and reducing thermal comfort (Frank *et al.*, 1999; Stevens *et al.*, 2018; Bright *et al.*, 2023). High skin temperatures often result in higher levels of discomfort, particularly as the level of dehydration progresses (Kenefick *et al.*, 2010). Skin temperature is an interface temperature between what is occurring within the body, and the biophysical interactions occurring at the skin surface (e.g., evaporation of sweat cooling the skin, heat transferred from the core to the skin via blood flow and heat being exchanged via evaporation, conduction, convection and radiation at the skin surface). Skin temperature is typically measured using multiple local skin temperatures and corresponding weighting factors to determine the relative contribution of each body segment which corresponds to the approximate surface area of the body part to mean skin temperature. As such there have been many measurement sites and associated weightings proposed to capture an accurate mean skin temperature, which range from as little as 3 sites to as many as 17 sites across the body (Liu *et al.*, 2011). When measuring T_{sk} in or outside the laboratory researchers must be aware of the environmental conditions when selecting the number of sites to measure as the variance in skin temperature across body parts widens with reductions in dry-bulb temperatures (and skin temperatures) (Livingstone *et al.*, 1987). Researchers must also consider the practicalities of their studies and the number of sites to measure. Evidence suggests that a minimum of 7 sites is required to adequately capture mean skin temperature across variable environmental conditions (Livingstone *et al.*, 1987). Therefore, in the studies presented in this thesis, skin temperature will be measured at 8 sites as recommended by the ISO standard for evaluating thermal strain (ISO, 9886, 2004).

There are current models which estimate T_{sk} that have been developed for both rest and exercise, across a range of environmental conditions and with a range of clothing levels (Mairiaux, Malchaire & Candas, 1987; Mehnert *et al.*, 2000; Vanos *et al.*, 2012; ISO, 7933, 2004). Data have been collected mostly within laboratories but also in some outdoor settings to account for the effects of solar radiation (through increases in mean radiant temperature) on T_{sk}. All current estimation models for T_{sk} have been developed at air velocities of < 4.0 $m \cdot s^{-1}$ with most trials being conducted at much lower air velocities (0-2 $m \cdot s^{-1}$). As such the performance of these models could be expected to reduce outside during outdoor cycling, where radiative heat load (solar radiation) is present and metabolic rate and particularly self-generated air velocities are much higher than the models were developed for.

The following methods for estimating mean skin temperature could be relevant for road cycling despite the potential limitations regarding metabolic rates and air velocities, $T_{sk\_mehnert}$ (Mehnert *et al.*, 2000), T_{sk_ISO} (ISO, 7933, 2004) and T_{sk_COMFA} (Brown & Gillespie, 1986; Vanos *et al.*, 2012):

$$T_{sk\_menhert} = 12.17 + 0.02T_a + 0.044T_r - 0.253v_{self} + 0.194P_a + 0.0029M + 0.51346T_{c_{eq}} \text{ [°C] [28]}$$

The ISO standard (7933) gives two equations for scenarios where clothing is > 0.6 clo (T_{sk_cl}), and < 0.2 clo clothing (T_{sk_nu}). For situations where clothing falls between 0.2-0.6 clo, the equation T_{sk_ISO} is given which is a combination of T_{sk_cl} and T_{sk_nu}. A clothing level during cycling in temperate ambient conditions (shoes, socks, jersey, bibs and helmet [and a sports bra for women]) could be estimated to be 0.3 [0.31 for women] (Zuo & McCullough, 2004). Therefore, it is likely that the additional variable for I_{cl} in the T_{sk_ISO} model will thus improve its performance relative to the $T_{sk\_mehnert}$ model. T_{sk_cl} is equal to $T_{sk\_mehnert}$ (ISO, 7933, 2004).

$$T_{sk\_nu} = 7.19 + 0.064T_a + 0.061T_r - 0.348v_{self} + 0.198P_a + 0.616T_{c_{eq}} \qquad [^\circ C]\ [29]$$

$$T_{sk\_ISO} = T_{sk\_nu} + 2.5\left(T_{sk\_menhert} - T_{sk\_nu}\right) \times (I_{cl} - 0.2) \qquad [^\circ C]\ [30]$$

$$T_{sk\_COMFA} = \left(\frac{T_{c_{eq}} - T_{db}}{r_t + r_c + r_a}\right)(r_a + r_c) + T_{db} \qquad [^\circ C]\ [31]$$

Where: T_{db} is ambient temperature (in ˚C), T_r is mean radiant temperature (in ˚C), P_a is absolute humidity (in kPa); M is metabolic rate (in W·m^{-2}), and $T_{c_{eq}}$ is steady-state body core temperature [estimated with **Eq. 36**]. Tissue (r_t), clothing (r_c) and aerodynamic (r_a) resistances (s·m^{-1}) were calculated according to Brown and Gillespie (1986) (Brown & Gillespie, 1986). I_{cl} is the insulative resistance of the clothing ensemble assumed to be (0.3 clo) (Zuo & McCullough, 2004). Clo is an arbitrary unit of clothing insulation (1 clo = 186.6, s·m^{-1} = 0.1555 m^2·°C^{-1}·W^{-1}).

Body tissue thermal resistance (r_t) decreases with metabolic rate (W·m^{-2}) and was calculated as (Brown & Gillespie, 1986):

$$r_t = (-0.1\,M) + 65 \qquad [s \cdot m^{-1}]\ [32]$$

Static and dynamic clothing thermal resistance (r_{co}, r_c) were calculated respectively as: (Brown & Gillespie, 1986)

$$r_{co} = clo \times 186.61 \qquad [s \cdot m^{-1}]\ [33]$$

$$r_c = r_{co} \times \left(-0.37\left(1 - exp^{\frac{-v_{self}}{0.72}}\right) + 1\right) \qquad [\text{s}\cdot\text{m}^{-1}]\ [34]$$

Where: v_{self} is cycling velocity (m·s^{-1}), clo is equal to I_{cl} and r_{co} is static clothing thermal resistance given by **Eq. 33**.

Boundary layer thermal resistance (r_a) was calculated as (Brown & Gillespie, 1986):

$$r_a = \frac{(0.17)}{(ARe^n Pr^{0.33} k)} \qquad [\text{W}\cdot\text{m}^{-2}]\ [35]$$

Where: Re is the Reynolds number $\left(\frac{0.17 v_{self}}{v}\right)$, where v_{self} is free stream air velocity (cycling velocity, m·s^{-1}), v is the kinematic viscosity of air (~1.5×10^{-5} m^{-2}·s^{-1}). A and n are empirical constants. When Re is > 40,000, A=0.0266 and n=0.805 (Kreith & Black, 1980). Pr is the Prandtl number assumed to be 0.7296 (Kreith & Black, 1980), k is the thermal diffusivity of air assumed to be 2.14×10^{-5} m^2·s^{-1} at 25 °C (Y. S. Touloukian, 1970).

2.2.9 Clothing (resistance to heat exchange)

Clothing augments heat gain and heat loss from the surrounding environment via two methods. Clothing acts as a thermal barrier, influencing the rate of heat transfer from the body to the environment. The insulative properties of clothing are largely determined by the thickness, material, and construction of the fabric (Havenith, 2003). Materials with high thermal resistance reduce heat loss in cold environments and impede heat dissipation in hot environments. The ability of clothing to allow moisture (typically sweat, but also exogenous fluids [e.g., water] to facilitate cooling and reduce hydration requirements) to pass through it, known as moisture permeability, significantly impacts evaporative heat loss. Clothing that allows moisture to permeate and evaporate through the material and away from the skin can impact evaporative cooling less than a less permeable material (Pascoe, Shanley & Smith, 1994). Conversely, clothing with poor moisture permeability can lead to sweat accumulation, reducing S_{eff}, thereby reducing evaporative cooling and increasing sweat losses.

Importantly, clothing manufacturers have been pushing the idea of sweat wicking materials and fabrics (Mokha *et al.*, 2011; Di Domenico, Hoffmann & Collins, 2022) that may increase perceived cooling functionality, reducing the wetness perception of the clothing worn (Ioannou *et al.*, 2024). However, this is potentially at the cost of thermoregulation by reducing sweating efficiency. Sweat wicking fabrics absorb fluid from the skin surface quickly and then allow evaporation from the fabric itself to reduce wetness perception. However, the utility of this from a heat safety and thermoregulatory perspective is potentially low. Evidence suggests that the latent heat vaporisation of sweat (λ) is highest when the fluid evaporates from the skin surface, and that the effective latent heat vaporisation of water (λ_{eff}) reduces proportionally as the evaporation distance from the skin surface increases (Havenith *et al.*, 2013). The practical implication of this effect is that sweat wicking clothing may counter initiatively increase fluid requirements during physical activity by decreasing λ_{eff}, thereby reducing evaporative cooling efficiency.

2.2.10 Heat Storage (S)

The human thermoregulatory system aims to maintain heat balance, that is, where heat loss matches heat production. Heat storage occurs when there is a mismatch between heat produced within the body (H_{prod}) and dry and evaporative heat exchange pathways (H_{loss}). At rest in a temperate environment, homeostasis is readily achieved where heat storage (S) = 0. An imbalance between H_{prod} and H_{loss} typically occurs at the outset of physical activity as thermoeffector responses (sweat rate and skin blood flow) typically take 5-15 minutes to reach parity with H_{prod} at the onset of exercise in a warm environment (Ravanelli *et al.*, 2019a), which results in a rise in body core temperature (T_c). And secondly, an imbalance can occur in uncompensable environments, where the evaporative requirement for heat balance (E_{req}) exceeds the maximum evaporative capacity of the environment (E_{max}) (Cramer & Jay, 2016). During physical activity in an uncompensable environment, heat storage persists, resulting in a continual rise in core temperature (Ravanelli *et al.*, 2019b). Extreme heat policies may then naturally define the upper tolerance for play for their sport at the limit of compensability for the level of activity (metabolic rate), clothing (clo), activity duration and combined thermal environmental conditions.

2.2.10.1 Body core temperature estimation

Estimating body core temperature (T_c) has been a key area of research at rest (Myny *et al.*, 2005), during physical activity (Buller *et al.*, 2013) and in occupational settings (Kampmann & Piekarski, 2000; Malchaire *et al.*, 2000; Buller *et al.*, 2015; Falcone *et al.*, 2021), mostly as a means for characterising both passive and exertional heat stress risk, without the need for high quality but expensive or invasive measures of T_c (e.g., telemetric gastrointestinal pill, esophageal, rectal temperature measurement). Body core temperature does not factor into the calculation of E_{req} directly, however, T_c is a factor when calculating mean skin temperature using available prediction methods (see section 2.2.7 **Eq. [28-31]**) (Mehnert *et al.*, 2000; Vanos *et al.*, 2012; ISO, 7933, 2004). To that end, a potentially useful and accessible option to estimate steady-state body core temperature (T_{ceq}) has been described by Malchaire *et al.*, (2000) with the following equation:

$$T_{ceq} = 36.6 + 0.002 \cdot M \qquad [^\circ C]\ [36]$$

Where: M is metabolic rate ($W \cdot m^{-2}$) and T_{ceq} is estimated steady-state body core temperature (ºC). This equation was originally proposed to describe T_{ceq}, during physical activity and occupational settings, where any activity is conducted at neutral environmental conditions. Given this equation [35] does not include any indication of clothing, or the environmental conditions it is likely that T_{ceq} may underestimate the true steady body core temperature where environmental conditions exceed ~25 ºC, given potentially greater and extended mismatch between E_{req} and E_{max} and the equation [**Eq. 36**] was developed for temperate environments (Saltin & Hermansen, 1966). In the context of estimated sweat rates during physical activity, however, there is evidence to suggest that T_c does not independently influence whole body sweat rate (WBSR) (Ravanelli, Imbeault & Jay, 2020). Therefore, any small errors between estimated and actual T_c wouldn't directly affect WBSR but may affect the accuracy of the skin temperature prediction equations, thereby impacting the association between E_{req} and WBSR when using different skin temperature prediction equations.

To address the identified gaps in the outdoor heat stress research literature, this thesis will focus on:

1. The agreement in thermal environmental conditions between nearby BoM sites and playing surfaces at professional and community oval/cricket sporting venues across Australia. It is unclear how different conditions are and such a determination is necessary to determine how useful nearby BoM sites are to inform extreme heat policies in professional and community cricket.
2. The most appropriate methods to calculate E_{req} in an outdoor environment during recreational road cycling given the important relationship of E_{req} to WBSR and the potential to improve the assessment of heat stress risk in sports where high sweat rates and extreme heat stress risk are probable.
3. Understanding the accuracy and applicability of existing prediction equations for the prediction of mean skin temperature outside their original intended use (i.e., high airflow environments), and if appropriate, develop a novel method for the prediction of mean skin temperature in high airflow environments to better inform extreme heat policies through enhanced biophysical modelling.

2.3 Outdoor thermal environment

As discussed in section 2.2, heat exchange between humans and their environment is determined by personal and environmental factors. The following section will discuss the relevant environmental factors that interact with humans to augment heat transfer between the skin surface and the outdoor environment. All studies within this thesis have utilised a custom-designed and built Environmental Monitoring Unit (EMU) (see **Fig. 4**) to measure and log all environmental variables that affect human heat balance in an outdoor environment (dry-bulb temperature, humidity, mean radiant temperature [via black globe temperature], wind speed). The specifications for the EMU are presented in the methods of the experimental chapters below (see section 3.2).

Figure 5. Two EMUs on location at Optus Stadium in Perth, WA

2.3.1 Dry-bulb temperature

Dry-bulb temperature affects heat exchange through modifications to the skin-to-dry-bulb temperature gradient ($T_{sk} – T_{db}$). In environments where T_{db} is below T_{sk}, dry heat loss occurs and vice versa. As the difference between T_{sk} and T_{db} reduces, the amount of dry heat loss approaches 0 and heat loss flips to heat gain from the environment ($T_{sk} < T_{db}$) (Parsons, 2014). At this point, the additional heat from the environment, including all metabolic heat production (from resting and active metabolism) must be offset by evaporative heat loss (sweat loss) to prevent extreme rises in core temperature (see **Fig. 6**).

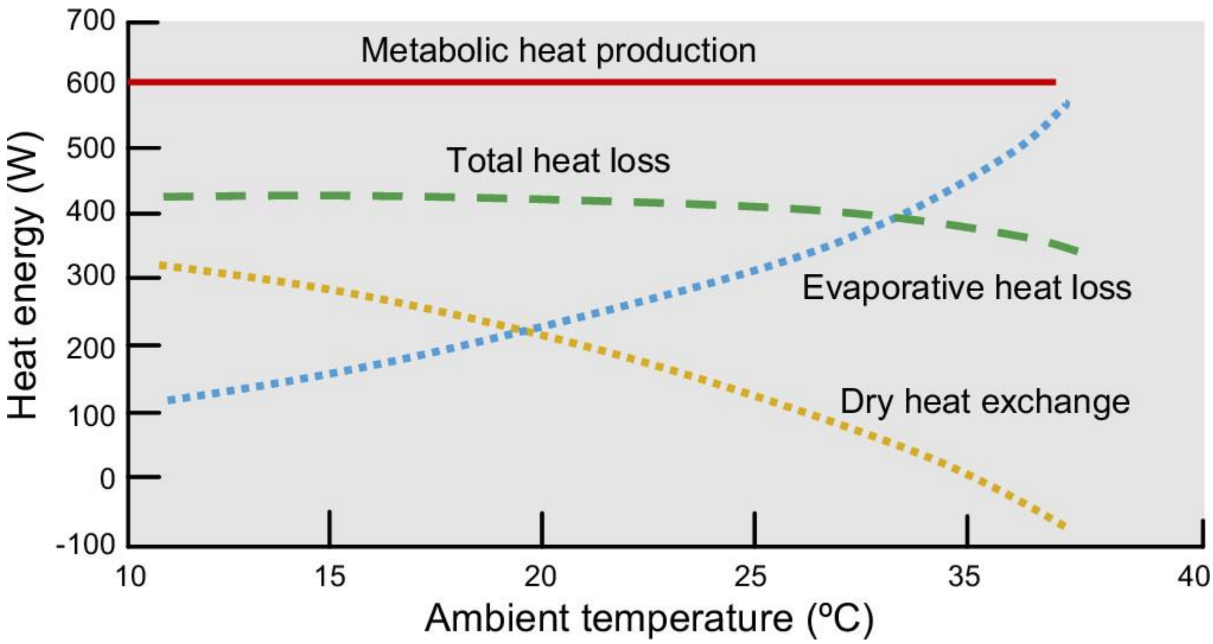

Figure 6 Périard JD, Eijsvogels TMH & Daanen HAM (2021) Exercise under heat stress: thermoregulation, hydration, performance implications, and mitigation strategies. Where: ambient temperature = dry-bulb temperature. Adapted from Neilsen (1937). Retrieved from https://doi.org/10.1152/physrev.00038.2020 CC BY 4.0.

Assessing the effects of one environmental variable on performance methodically can be challenging due to the interplay between environmental and physiological variables (i.e., as T_{db} increases so does T_{sk} which may increase E_{max}, see section 2.2.5.5). However, T_{db} is consistently shown to impact thermal and cardiovascular outcomes during physical activity given its influence on heat exchange. For example, a recent study fixed ambient vapour pressure across 29 ºC and 35 ºC trials to elucidate any potential effects of a 6 ºC difference in dry-bulb temperature on 30-min cycling time trial performance and found similar results between the warm (~206W) and hot (~205W) trials (Lei *et al.*, 2020). However, in the hot trial, participants had a ~1.8 ºC higher T_{sk}. The maximum potential for evaporation (E_{max}) increases as skin temperature rises, therefore resulting in a higher E_{max}, which may have allowed the maintenance of a similar power output between warm and hot trials, as participants were likely able to evaporate sweat more freely in the hotter condition due to a higher T_{sk} and E_{max}. A more recent study has investigated the independent effects of dry-bulb temperature on 30-km cycling time trial performance across a wide range of dry-bulb temperatures (13 ºC, 20 ºC, 28 ºC, 36 ºC), while fixing the skin-to-air pressure gradient ($P_{sk,sat} - P_a$) (Bright *et al.*, 2021). In this study, mean power output across the 30-km time trial was maintained between the 13 ºC and 20 ºC trials (~275W and ~272W respectively) but dropped at 28 ºC (262W) and 36 ºC (~228W), owing to the increased cardiovascular strain experienced at 36 ºC mainly due to the reduced dry heat loss in the warm (28 ºC) and hot (36 ºC) conditions.

2.3.2 Atmospheric humidity

Atmospheric humidity is a measure of the total water vapour content of air. Typically, humidity is reported as relative humidity (RH), which is the ratio between the partial ambient vapour pressure (P_a, kPa) and the saturated ambient vapour pressure (P_{sa}, kPa). The total amount of water vapour content air can hold, increases with increasing dry-bulb temperature. Therefore, warm air can have the same relative humidity as colder air yet hold a vastly greater amount of water vapour (P_a) (see **Fig. 7**).

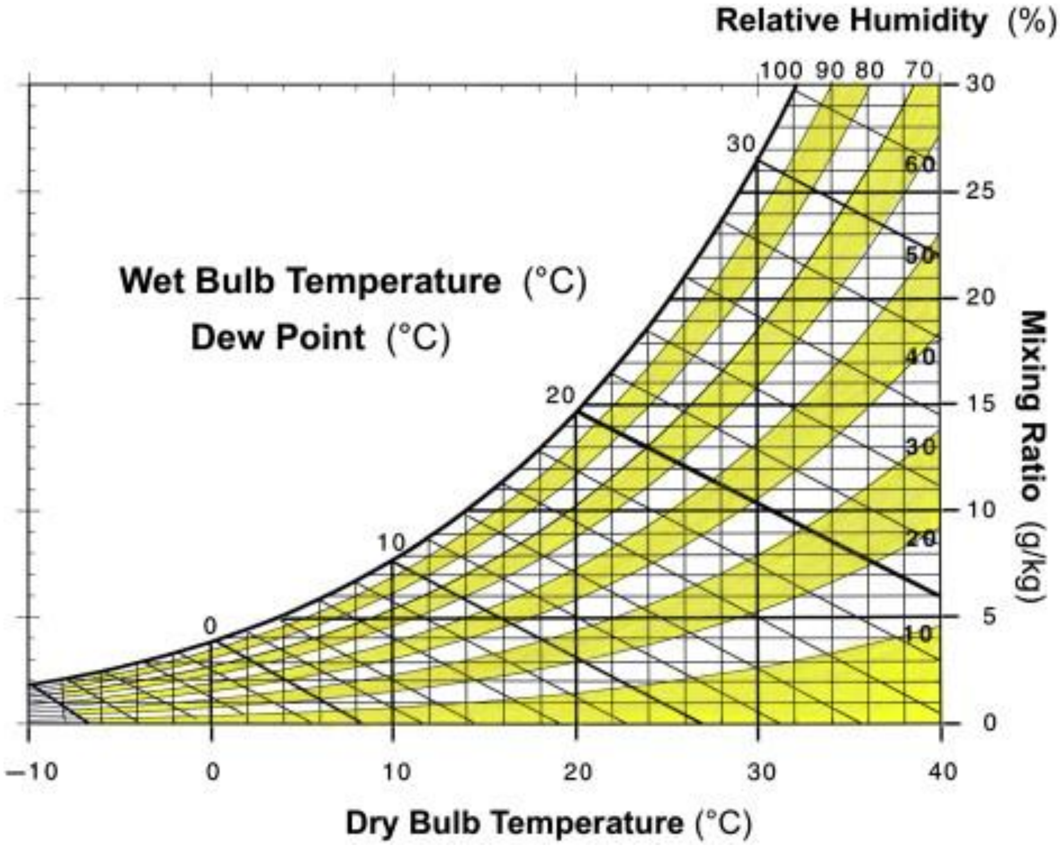

Figure 7 Camuffo (2014) Psychrometric chart for dry-bulb temperature, mixing ratio (or absolute humidity), and relative humidity. Adapted from https://doi.org/10.1016/B978-0-444-63296-8.00002-0 CC BY 4.0

Evaporative heat loss (E) is driven by the difference between the vapour pressure gradient at the skin surface ($P_{sk,sat}$), assumed to be saturated with sweat, and ambient water vapour pressure (P_a) [kPa] (Parsons, 2014). Therefore, changes in P_a and not RH augment evaporative potential. As the $P_{sk,sat}$ -P_a gradient approaches zero, the evaporative potential is reduced, and the risk for thermal and cardiovascular strain, particularly during exercise, increases.

2.3.3 Mean radiant temperature

Similar to other forms of heat energy, radiant heat moves along temperature gradients, from hot to cold. Radiant energy moves via electromagnetic infrared waves typically from the environment (solar radiation) to the body when outdoors. The body can absorb solar radiation directly (when standing in direct sunlight) or indirectly when the surrounding environment (such as buildings, sidewalks, and roads) absorbs, reflects and re-emits radiant heat energy from the sun (Parsons, 2014).

To determine the amount of radiant heat that moves between two masses (~air-to-body) the difference in temperatures between masses can be multiplied by the mass's ability to absorb and emit radiative heat energy, known as emissivity (ε) (Campbell, 1977). Mean radiant temperature (T_r) is a calculated metric that includes T_{db}, T_g, and air velocity. A prevailing breeze across the black globe thermometer (T_g) will provide convective cooling and reduce or keep T_g in check. Similarly, if there is no breeze but a high solar radiant load, then the difference between T_{db} and T_g will widen, thereby increasing T_r (Parsons, 2014). To determine the amount of heat transfer between the environment and humans, T_r can be calculated using the following equation at velocities ≥ 0.15 m·s^{-1} (ISO, 7726, 1998):

$$T_r = \left[(T_g + 273.15)^4 + \frac{(1.1 \times 10^8 \times v^{0.6})}{\varepsilon \times d^{0.4}}(T_g - T_a)\right]^{0.25} - 273.15 \qquad \text{[ºC] [37]}$$

Where ν is air velocity in m·s^{-1}, ε is the emissivity of the black copper globe, assumed to be 0.97 (Parsons, 2003), and *d* is the diameter of the globe in meters (0.15 m).

2.3.4 Operative temperature

The operative temperature (T_o) is a combined model of T_a and T_r and their respective heat transfer coefficients that can be conveniently used to calculate both convective and radiative heat exchange where $T_r > T_a$, which is usually the case in outdoor environments (namely caused by solar radiation). T_o can be calculated as follows:

$$T_o = \frac{(h_r T_r + h_c T_a)}{(h_r + h_c)} \quad [°C]\ [38]$$

The greatest sources of variation within T_o come from differences in h_c, T_a, and T_r, as h_r remains relatively stable in most indoor and outdoor environments, noted by the fact in most indoor environments h_r can be estimated at 4.7 W·m^{-2}·K^{-1} (ASHRAE, 2009), however, a more accurate calculation for h_r can be conducted with Eq. 14 when outdoors.

2.3.5 Air velocity

During outdoor recreation, airflow over the skin surface can be a critical facilitator of heat loss. Natural air movement occurs due to pressure fluctuations in the atmosphere, whereby air moves from high to low pressure areas which result from atmospheric temperature differences which may be modified by water vapour condensation (Makarieva *et al.*, 2013). Air velocity serves to increase any given heat transfer via increases to h_c and by indirectly increasing h_e as well as directly reducing environmental conditions by reducing T_r (as increased airflow over the black globe keep T_g closer to T_{db}). In environments where the air is still, h_c is low, as v increases, so does h_c. Increases to h_c mean that even at small temperature gradients between the skin and the environment, there can still be considerable dry heat loss which is partly why using a fan to move the air across the skin surface can feel so cool.

During physical activity air velocity from both self-generated convection (e.g., cycling, running) and forced convection (indoors during treadmill running, ergometer cycling etc.) is important for the maintenance of thermal comfort and performance (Bright *et al.*, 2023). Bright *et al.* (2023) recently demonstrated there are diminishing returns on endurance exercise performance with increases in forced convection (i.e., forced airflow with fans) passed over the skin during a self-paced indoor cycling time trial in laboratory conditions at ~32 °C and ~40% RH. They observed that cycling time trial performance was the lowest in still air, versus 16, 30, and 44 km·h^{-1} air velocities. Performance did not differ between the conditions until the final stages of the time trial, yet T_{sk} and thermal comfort were largely increased and reduced, respectively, during the still condition. Increasing wind speed from 16 to 30 to 44 km·h^{-1} did not appear to have a large effect on T_{sk}, despite the large reduction in T_{sk} from still air to the 16 km·h^{-1} condition, perhaps due to the high dry-bulb temperature (32 ºC) resulting in a higher floor for T_{sk}. Had this study been conducted in cooler conditions, it stands to reason that increasing airspeeds from 16 to 44 km·h^{-1} may provide additional T_{sk} cooling. Interestingly, individuals in this study appeared to have a lower WBSR in the 44 km·h^{-1} condition (1.88 L·h^{-1}) compared to the still air condition (1.95 L·h^{-1}), despite producing more power (and therefore producing more metabolic heat). This did not reach statistical significance as WBSR was not a primary outcome and so the authors did not power their study to observe these differences.

The relationship between air velocity and human heat exchange is not without nuance. For example, when calculating E_{req} in an environment where $T_{db} < T_{sk}$ there will be dry heat loss to the environment, but if air velocity increases via forced or natural convection, T_{sk} will reduce thereby reducing the skin-to-air temperature gradient and concomitant dry heat loss. How this affects E_{req} is that if all other conditions remain the same, a reduced T_{sk} would result in a lower dry heat transfer and potentially a higher E_{req}. This relationship between air velocity, T_{db} and T_{sk}, will presumably only grow stronger as air velocity increases due to the higher mass airflow across the skin.

2.4 Extreme heat policies in outdoor sport

Effective extreme heat policies in sport are necessary to maintain player safety while facilitating as much professional and community sport as possible, even when stressful thermal environmental conditions are present. Many sporting organisations have historically deferred to a sport agnostic general extreme heat policy and/or relied upon fixed dry bulb temperature cut-offs for play (Chalmers & Jay, 2018; Gamage, Finch & Fortington, 2020), without the consideration for sport specific metabolic rate or clothing and other environmental parameters (wind velocity, ambient humidity, mean radiant temperature). The move to biophysical models that integrate the expected metabolic rates of athletes and sport specific clothing with environmental conditions has been recommended (Jay, Broderick & Smallcombe, 2021; Racinais *et al.*, 2023), however, many sports – except for Cricket Australia (Cricket Australia, 2020) - persist with environmental limits for wet-bulb globe temperature (WBGT), or T_{db} and/or RH fixed environmental cuts offs (Union Cycliste Internationale, 2024), which don't adequately account for solar radiation or the personal factors (metabolic rate, body shape and size, and clothing level) of the athletes. Often, these policies could be economically improved by including on-site measurements of basic local environmental conditions (T_{db}, RH and v) (Pryor *et al.*, 2017; Tripp *et al.*, 2020; Guyer *et al.*, 2021), and in the best-case scenario, including the measurement of T_g to provide information about the radiative thermal environment, rather than rely on problematic estimations of T_g.

Extreme heat policies require a multi-pronged approach to mitigate the risks to players and spectators at sporting events in hot conditions. They require the evaluation and implementation of strategies from prevention, monitoring, to treatment. A recent International Olympic Committee (IOC) report includes appropriate environmental monitoring as step #1 in their guidelines for extreme heat policy development (Racinais *et al.*, 2023). For example, the IOC recommends the following key aspects to be considered during extreme heat policy development: appropriate environmental monitoring (dry-bulb temperature, mean radiant temperature, air velocity and ambient humidity) (monitoring), heat acclimation/heat training (prevention), on-site/field of play, ice supply (cooling strategies - personal), misting fans to the (cooling strategies – personal/environmental), increased shade in preparation (prevention), recovery and post event (cooling strategies – environmental), medically supervised ice-baths facilities for the treatment of EHIs (treatment), hydration recommendations to limit the level of dehydration and not fully replace sweat losses during competition (prevention/treatment), electrolytes and carbohydrates for recovery, appropriate clothing for athletes (clothing that does not impair direct evaporation from the skin surface (Havenith *et al.*, 2013)) and officials (light, loose fitting sun protective) (prevention), athlete monitoring (prevention/monitoring), field of play medical supervision (monitoring), finish area medical care and pre-triage (treatment).

Part of this thesis focuses on the first important aspect of extreme heat policy development and implementation, which deals with the appropriate and accurate monitoring of environmental conditions at the playing surface. Extreme heat policies typically categorise the prevailing heat stress risk using a thermal index or perhaps more appropriately, a biophysical thermal index, which combines the environmental factors that affect human heat balance, with personal (metabolic rate, height, weight) and clothing factors. These heat stress risk categories describe an increasing level of heat stress risk if the event/match continues and will usually provide guidance on the modification to play, postponing the event, and/or cooling strategies for the athletes (Armstrong *et al.*, 2007; Casa *et al.*, 2015; Jay *et al.*, 2021). To appropriately categorise the heat stress risk where competition is occurring, accurate environmental data are required. If appropriate environmental data are not available competition officials are at an increased risk of being overly conservative and calling competition off unnecessarily and alternatively not calling off play fast enough to protect athletes from undue risk of exertional heat illness.

Many sporting organisations across Australia such as Softball Australia (Softball Australia, 2022), the Australia Football League (Australian Football League, 2013), Lawn Tennis Association (Lawn Tennis Association, 2022), Cricket Australia (Cricket Australia, 2020), Cycling Australia (Cycling Australia, 2021) and Sports Medicine Australia (Jay *et al.*, 2021) rely on using nearby meteorological weather site data (typically from the Bureau of

Meteorology [BoM] in Australia) to provide an indication of the thermal environment in which the athletes are participating in sport. How applicable these data from 'nearby' BoM sites are for these sporting venues is questionable (Pryor *et al.*, 2017), given the likely differences between the natural and built environments surrounding the competition area and the natural and built environments surrounding the BoM or meteorological site. The use of on-site environmental monitoring is therefore optimal for the implementation of extreme heat policies in sports, as it may account for within-venue microclimates (Pryor *et al.*, 2017), and differences between the meteorological site and playing surface (Cheuvront *et al.*, 2015; Guyer *et al.*, 2021) which causes additional error between nearby meteorological sites and the venue.

2.5 Sporting venues and extreme heat stress risk assessment

Individuals participate in sports across many different surface types, exposed to many different types of environmental conditions, from extreme heat and humidity to extreme cold and wind. A common issue when characterising the prevailing level of heat stress risk is the correct assessment of the thermal environment within a particular sporting venue. As there are four environmental parameters that affect human heat balance and therefore heat stress risk, an organisation must consider how they will categorise the heat stress risk as simple T_{db} and/or RH cut-offs (using a climatic index such as WBGT or the apparent temperature [AT] which characterise the thermal environment into one variable, is quite common yet usually inadequate and quite problematic (Racinais *et al.*, 2023)). In addition to a suitable assessment of the thermal environmental conditions, it is important to understand how representative to the areas which athletes are competing (i.e., within sporting venues [Football, Rugby, Cricket], or across large distances and varied topographical features [Road Cycling, Ultra-Running) those reported environmental conditions are. Some sports like road cycling take competitors across an array of environments (valleys to mountain tops in one day) but many others such as Cricket, Football, and Tennis compete in a fixed location such as a stadium. Characterising the heat stress risk along the course across a ~160 km Tour de France stage may prove quite challenging, and this problem is yet to be solved, however, characterising the level of heat stress risk for sports held in large sporting venues is not without its challenges. Different competition surfaces and surface types surrounding the competition areas can produce different environmental readings (Kosaka *et al.*, 2018; Grundstein & Cooper, 2020) that differ from nearby meteorological weather sites (Pryor *et al.*, 2017). As more sports require extreme heat stress policies, more focus will be on the details of if they are measuring the heat stress (local or nearby environmental measures), how they are measuring the heat stress (independent T_{db}, RH, T_g, and wind speed, or other variables such as calculated or estimated WBGT), and where in relation to the athletes heat stress is monitored (e.g., along the potentially most risky section such as climb in a road cycling event during the European summer where metabolic heat production and temperatures are high, and self-generated air velocities and associated heat losses are lowered).

It is recommended that sporting organisations use field-of-play measures of the environmental conditions with appropriate thermal environmental monitoring equipment (Racinais *et al.*, 2023) however, some barriers to best practice exist. Firstly, throughout Australia and across the developed world there is easy access to meteorological information from sources such as the Australian Bureau of Meteorology (BoM), which provides almost the complete suite of environmental conditions required within an effective heat policy (except for an indication of radiation through T_g). BoM sites provide environmental data for T_{db}, relative humidity, and wind velocity from many relatively nearby locations across Australia. The BoM also provides an estimated outdoor WBGT using an estimated solar load, which is equivalent to a 'moderately sunny day' and fixed 'light' wind speed. However, this is always prone to error but particularly so when solar radiation is reduced due to cloud cover or other obstructions (e.g., buildings) (Grundstein & Cooper, 2018; Tripp *et al.*, 2020). While common thermal environmental variables such as T_{db} and RH are reported and widely available, the applicability of those data to sporting venues are limited due to differing surface types and the potential for microclimate development due to differing local built and environments (e.g., grandstands, natural surfaces, built surfaces), potentially inappropriate reported wind speeds, and the lack of true solar load which indicates the intensity of the radiant environment.

Sporting venues across Australia can be unique in their design and location within a city or area. For example, major sporting venues for elite, professional sports such as the SCG (Sydney, NSW) and Optus Stadium (Perth, WA) are near the city centre due to the proximity to other infrastructure (e.g., transport, nightlife, restaurants) to facilitate ease of amenity. These venues are also located immediately within and surrounded by natural environments such as Centennial and Moore Park (for the SCG), Chevron Parkland and the Swan River for Optus Stadium but may yet experience local heating due to the Urban Heat Island (UHI) effect due to being in such large and dense urban environments such as Sydney and Perth. However, more community sporting venues such as Howell Oval (Penrith, NSW) and Blacktown International Sports Park (Blacktown, NSW) are on the outskirts of Sydney (NSW) and may experience less of an impact due to any urban heat islands due to the surrounding built environment.

2.6 Effects on the urban landscape on the thermal environment

More than half the world's population lives within cities and urban areas, which is only projected to increase to 68% in 2050 (United Nations, 2018). Land use change from natural to built occurs with urbanisation which impacts the local thermal environment (Foley *et al.*, 2005; Grimm *et al.*, 2008). Global urbanisation has impacted local thermal environments by increasing dry-bulb temperatures within cities and reducing evapotranspiration (Mazrooei *et al.*, 2021) through land use changes reducing natural vegetation and increasing built structures (e.g., houses, office buildings).

Practically, meteorological weather sites cannot be in that many locations within cities, so if sporting organisations rely on these sites for their thermal environmental data, they must be aware of how the thermal environment varies within cities due to factors such as green spaces, waterways and the built environment. Reducing green spaces such as parks and wetlands through urbanisation tends to increase dry-bulb temperatures as green spaces facilitate convective and evaporative cooling (Hao *et al.*, 2023), and built environments tend to lower air movement (Coutts, Beringer & Tapper, 2007) and reduce shade, which increases mean radiant temperature (Tan, Wong & Jusuf, 2014). The UHI effect has been studied with detail (Zhao *et al.*, 2014; Li *et al.*, 2019), however, how the local thermal environment varies within cities has been much less studied. The natural and built environments that surround meteorological sites and playing surfaces may determine the quality of their agreement, as evidence suggests that green infrastructure is a key way urban heat can be mitigated (Li *et al.*, 2019) and that variability in the local thermal environment is increased within native ecosystems compared to residential landscapes (Hall *et al.*, 2016).

To address the identified gaps in the research literature, this thesis will focus on:

- Determine if thermal environmental conditions at professional and community sporting venues matches the conditions which are reported by nearby meteorological organisations (e.g., BoM).
- Evaluate the E_{req} model and understand how it associates with WBSR in an outdoor environment during recreational road cycling.
- Evaluate the available skin temperature prediction models for high airflow scenarios such as during recreational outdoor cycling and develop a new method of mean skin temperature prediction if required.

2.7 References

Abbiss CR & Laursen PB. (2005). Models to explain fatigue during prolonged endurance cycling. *Sports medicine (Auckland, NZ)* **35,** 865-898.

Abriat A, Brosset C, Brégigeon M & Sagui E. (2014). Report of 182 cases of exertional heatstroke in the French Armed Forces. *Mil Med* **179,** 309-314.

Adams WM & Jardine JF. (2020). Overview of Exertional Heat Illness. In *Exertional Heat Illness: A Clinical and Evidence-Based Guide*, ed. Adams WM & Jardine JF, pp. 1-16. Springer International Publishing, Cham.

Armstrong LE, Casa DJ, Millard-Stafford M, Moran DS, Pyne SW & Roberts WO. (2007a). American College of Sports Medicine position stand. Exertional heat illness during training and competition. *Medicine & Science in Sports & Exercise* **39,** 556-572.

Armstrong LE, Johnson EC, Casa DJ, Ganio MS, McDermott BP, Yamamoto LM, Lopez RM & Emmanuel H. (2010). The American football uniform: uncompensable heat stress and hyperthermic exhaustion. *Journal of athletic training* **45,** 117-127.

Armstrong LE & Pandolf K. (1988). Physical training, cardiorespiratory physical fitness and exercise-heat tolerance. *Human performance physiology and environmental medicine at terrestrial extremes***,** 199-226.

ASHRAE. (2009). Thermal Comfort. In *In AHSRAE Handbook of Fundamentals*. Atlanta, GA.

AusSport. (2020). AusPlay Survey, ed. Australia S. https://www.clearinghouseforsport.gov.au/research/smi/ausplay/results/national.

Australian Football League. (2013). National Extreme Weather Policy.

Baker FC, Siboza F & Fuller A. (2020). Temperature regulation in women: Effects of the menstrual cycle. *Temperature (Austin)* **7,** 226-262.

Baker LB. (2016). Sweat testing methodology in the field: Challenges and best practices. *Sports Sci Exchange* **28,** 1-6.

Baker LB. (2017). Sweating Rate and Sweat Sodium Concentration in Athletes: A Review of Methodology and Intra/Interindividual Variability. *Sports Medicine* **47,** 111-128.

Barnes KA, Anderson ML, Stofan JR, Dalrymple KJ, Reimel AJ, Roberts TJ, Randell RK, Ungaro CT & Baker LB. (2019). Normative data for sweating rate, sweat sodium concentration, and sweat sodium loss in athletes: An update and analysis by sport. *Journal of sports sciences* **37,** 2356-2366.

Bedard C, Hanna S & Cairney J. (2020). A longitudinal study of sport participation and perceived social competence in youth. *Journal of Adolescent Health* **66,** 352-359.

Bergman BC, Horning MA, Casazza GA, Wolfel EE, Butterfield GE & Brooks GA. (2000). Endurance training increases gluconeogenesis during rest and exercise in men. *American Journal of Physiology-Endocrinology and Metabolism* **278,** E244-E251.

Bongers CCWG, Thijssen DHJ, Veltmeijer MTW, Hopman MTE & Eijsvogels TMH. (2015). Precooling and percooling (cooling during exercise) both improve performance in the heat: a meta-analytical review. *British Journal of Sports Medicine* **49,** 377-384.

Bouchama A & Knochel JP. (2002). Heat stroke. *New England journal of medicine* **346,** 1978-1988.

Bouillod A, Soto-Romero G, Grappe F, Bertucci W, Brunet E & Cassirame J. (2022). Caveats and Recommendations to Assess the Validity and Reliability of Cycling Power Meters: A Systematic Scoping Review. *Sensors* **22,** 386.

Breslow RG, Collins JE, Troyanos C, Cohen MC, D'Hemecourt P, Dyer KS & Baggish A. (2021). Exertional Heat Stroke at the Boston Marathon: Demographics and the Environment. *Med Sci Sports Exerc* **53,** 1818-1825.

Breslow RG, Shrestha S, Feroe AG, Katz JN, Troyanos C & Collins JE. (2019). Medical Tent Utilization at 10-km Road Races: Injury, Illness, and Influencing Factors. *Med Sci Sports Exerc* **51,** 2451-2457.

Bright FM, Clark B, Jay O & Périard JD. (2021). The effect of minimal differences in the skin-to-air vapor pressure gradient at various dry-bulb temperatures on self-paced exercise performance. *Journal of Applied Physiology* **131,** 1176-1185.

Bright FM, Clark B, Jay O & Périard JD. (2023). Influence of Air Velocity on Self-Paced Exercise Performance in Hot Conditions. *Med Sci Sports Exerc* **55,** 1382-1391.

Brooks GA, Arevalo JA, Osmond AD, Leija RG, Curl CC & Tovar AP. (2022). Lactate in contemporary biology: a phoenix risen. *The Journal of Physiology* **600,** 1229-1251.

Brown RD & Gillespie TJ. (1986). Estimating outdoor thermal comfort using a cylindrical radiation thermometer and an energy budget model. *International Journal of Biometeorology* **30,** 43-52.

Brown SJ. (2020). Future changes in heatwave severity, duration and frequency due to climate change for the most populous cities. *Weather and Climate Extremes* **30,** 100278.

Buller MJ, Tharion WJ, Cheuvront SN, Montain SJ, Kenefick RW, Castellani J, Latzka WA, Roberts WS, Richter M & Jenkins OC. (2013). Estimation of human core temperature from sequential heart rate observations. *Physiological measurement* **34,** 781.

Buller MJ, Tharion WJ, Duhamel CM & Yokota M. (2015). Real-time core body temperature estimation from heart rate for first responders wearing different levels of personal protective equipment. *Ergonomics* **58,** 1830-1841.

Burger F & Fuhrman FA. (1964). Evidence of injury by heat in mammalian tissues. *American Journal of Physiology-Legacy Content* **206,** 1057-1061.

Burns RD, Bai Y & Brusseau TA. (2020). Physical Activity and Sports Participation Associates With Cognitive Functioning and Academic Progression: An Analysis Using the Combined 2017–2018 National Survey of Children's Health. *Journal of Physical Activity and Health* **17,** 1197-1204.

Bynum GD, Pandolf KB, Schuette WH, Goldman RF, Lees DE, Whang-Peng J, Atkinson ER & Bull JM. (1978). Induced hyperthermia in sedated humans and the concept of critical thermal maximum. *American Journal of Physiology-Regulatory, Integrative and Comparative Physiology* **235,** R228-R236.

Campbell GS. (1977). An Introduction to Environmental Biophysics. *Heidelberg Science Library*.

Candas V, Libert J & Vogt J. (1979a). Human skin wettedness and evaporative efficiency of sweating. *Journal of Applied Physiology* **46,** 522-528.

Candas V, Libert J & Vogt J. (1979b). Influence of air velocity and heat acclimation on human skin wettedness and sweating efficiency. *Journal of applied physiology* **47,** 1194-1200.

Casa DJ, DeMartini JK, Bergeron MF, Csillan D, Eichner ER, Lopez RM, Ferrara MS, Miller KC, O'Connor F, Sawka MN & Yeargin SW. (2015). National Athletic Trainers' Association Position Statement: Exertional Heat Illnesses. *Journal of Athletic Training* **50,** 986-1000.

Casa DJ & Stearns RL. (2016). *Preventing Sudden Death in Sport & Physical Activity*. Jones & Bartlett Publishers.

Chalmers S & Jay O. (2018). Australian community sport extreme heat policies: Limitations and opportunities for improvement. *Journal of Science and Medicine in Sport* **21,** 544-548.

Chalmers S, Siegler J, Lovell R, Lynch G, Gregson W, Marshall P & Jay O. (2019). Brief in-play cooling breaks reduce thermal strain during football in hot conditions. *Journal of Science and Medicine in Sport* **22,** 912-917.

Chalmers SM. (2017). In-play cooling strategies for sport in hot and humid conditions*. *Temperature* **4,** 353-355.

Charkoudian N. (2010). Mechanisms and modifiers of reflex induced cutaneous vasodilation and vasoconstriction in humans. *Journal of Applied Physiology* **109,** 1221-1228.

Cheuvront S & Kenefick R. (2014). Dehydration: physiology, assessment, and performance effects. Comprehensive Physiology. 4: 257–285.

Cheuvront SN, Caruso EM, Heavens KR, Karis AJ, Santee WR, Troyanos C & D'Hemecourt P. (2015). Effect of WBGT Index Measurement Location on Heat Stress Category Classification. *Med Sci Sports Exerc* **47,** 1958-1964.

Clarry A, Faghih Imani A & Miller EJ. (2019). Where we ride faster? Examining cycling speed using smartphone GPS data. *Sustainable Cities and Society* **49,** 101594.

Colosio AL, Caen K, Bourgois JG, Boone J & Pogliaghi S. (2020). Bioenergetics of the VO(2) slow component between exercise intensity domains. *Pflugers Arch* **472,** 1447-1456.

Costrini AM, Pitt HA, Gustafson AB & Uddin DE. (1979). Cardiovascular and metabolic manifestations of heat stroke and severe heat exhaustion. *The American Journal of Medicine* **66,** 296-302.

Cottle RM, Lichter ZS, Vecellio DJ, Wolf ST & Kenney WL. (2022). Core temperature responses to compensable versus uncompensable heat stress in young adults (PSU HEAT Project). *Journal of Applied Physiology* **133,** 1011-1018.

Coutts AM, Beringer J & Tapper NJ. (2007). Impact of increasing urban density on local climate: Spatial and temporal variations in the surface energy balance in Melbourne, Australia. *Journal of Applied Meteorology and Climatology* **46,** 477-493.

Coyle EF. (2005). Improved muscular efficiency displayed as Tour de France champion matures. *Journal of Applied Physiology* **98,** 2191-2196.

Coyle EF, Sidossis LS, Horowitz JF & Beltz JD. (1992). Cycling efficiency is related to the percentage of type I muscle fibers. *Medicine and science in sports and exercise* **24,** 782-788.

Cramer MN, Gagnon D, Crandall CG & Jay O. (2017). Does attenuated skin blood flow lower sweat rate and the critical environmental limit for heat balance during severe heat exposure? *Exp Physiol* **102,** 202-213.

Cramer MN & Jay O. (2016). Biophysical aspects of human thermoregulation during heat stress. *Autonomic Neuroscience* **196,** 3-13.

Cramer MN & Jay O. (2019). Partitional calorimetry. *Journal of Applied Physiology* **126,** 267-277.

Crandall CG, Vongpatanasin W & Victor RG. (2002). Mechanism of cocaine-induced hyperthermia in humans. *Ann Intern Med* **136,** 785-791.

Cricket Australia. (2020). Australian Cricket Heat Policy, 3 edn.

Cunningham C, O' Sullivan R, Caserotti P & Tully MA. (2020). Consequences of physical inactivity in older adults: A systematic review of reviews and meta-analyses. *Scandinavian Journal of Medicine & Science in Sports* **30,** 816-827.

Cycling Australia. (2021). Extreme Weather Policy, 2 edn, pp. 21.

Defraeye T, Blocken B, Koninckx E, Hespel P & Carmeliet J. (2011). Computational fluid dynamics analysis of drag and convective heat transfer of individual body segments for different cyclist positions. *Journal of Biomechanics* **44,** 1695-1701.

Di Domenico I, Hoffmann SM & Collins PK. (2022). The Role of Sports Clothing in Thermoregulation, Comfort, and Performance During Exercise in the Heat: A Narrative Review. *Sports Medicine - Open* **8**.

di Prampero PE & Ferretti G. (1999). The energetics of anaerobic muscle metabolism: a reappraisal of older and recent concepts. *Respiration Physiology* **118,** 103-115.

Dickinson T & Wright J. (2021). The reliability and accuracy of the Garmin Vector 3 power pedals. *Proceedings of the Institution of Mechanical Engineers, Part P: Journal of Sports Engineering and Technology* **235,** 70-74.

Easterlin MC, Chung PJ, Leng M & Dudovitz R. (2019). Association of team sports participation with long-term mental health outcomes among individuals exposed to adverse childhood experiences. *JAMA pediatrics* **173,** 681-688.

Ettema G & Lorås HW. (2009). Efficiency in cycling: a review. *European Journal of Applied Physiology* **106,** 1-14.

Falcone T, Cordella F, Molinaro V, Zollo L & Del Ferraro S. (2021). Real-time human core temperature estimation methods and their application in the occupational field: A systematic review. *Measurement* **183,** 109776.

Foley JA, DeFries R, Asner GP, Barford C, Bonan G, Carpenter SR, Chapin FS, Coe MT, Daily GC & Gibbs HK. (2005). Global consequences of land use. *science* **309,** 570-574.

Frank SM, Raja SN, Bulcao CF & Goldstein DS. (1999). Relative contribution of core and cutaneous temperatures to thermal comfort and autonomic responses in humans. *Journal of Applied physiology* **86,** 1588-1593.

Gagge AP. (1937). A new physiological variable associated with sensible and insensible perspiration. *American Journal of Physiology-Legacy Content* **120,** 277-287.

Gagnon D, Jay O & Kenny GP. (2013). The evaporative requirement for heat balance determines whole-body sweat rate during exercise under conditions permitting full evaporation. *The Journal of Physiology* **591,** 2925-2935.

Gamage PJ, Finch CF & Fortington LV. (2020). Document analysis of exertional heat illness policies and guidelines published by sports organisations in Victoria, Australia. *BMJ open sport & exercise medicine* **6,** e000591.

Gardner JW, Kark JA, Karnei K, Sanborn JS, Gastaldo E, Burr P & Wenger CB. (1996). Risk factors predicting exertional heat illness in male Marine Corps recruits. *Medicine and science in sports and exercise* **28,** 939-944.

Gastin PB. (2001). Energy system interaction and relative contribution during maximal exercise. *Sports medicine* **31,** 725-741.

Gisolfi CV & Wenger CB. (1984). Temperature regulation during exercise: old concepts, new ideas. *Exercise and sport sciences reviews* **12,** 339-372.

Graham, C., Morris, N. B., Harwood, A. E., & Jay, O. (2020). Ad libitum water consumption off-sets the thermal and cardiovascular strain exacerbated by dehydration during a 3-h simulated heatwave. *European journal of applied physiology* **120**, 391–399. https://doi.org/10.1007/s00421-019-04283-7

Grimm NB, Faeth SH, Golubiewski NE, Redman CL, Wu J, Bai X & Briggs JM. (2008). Global change and the ecology of cities. *science* **319,** 756-760.

Grundstein A & Cooper E. (2018). Assessment of the Australian Bureau of Meteorology wet bulb globe temperature model using weather station data. *International Journal of Biometeorology* **62,** 2205-2213.

Grundstein A & Cooper E. (2020). Comparison of WBGTs over Different Surfaces within an Athletic Complex. In *Medicina*.

Grundstein AJ, Hosokawa Y & Casa DJ. (2018). Fatal exertional heat stroke and American football players: the need for regional heat-safety guidelines. *Journal of athletic training* **53,** 43-50.

Guyer H. (2021). Identifying the need for locally-observed wet bulb globe temperature across outdoor athletic venues for current and future climates in a desert environment. *Environmental Research Letters*.

Guyer H, Georgescu M, Hondula DM, Wardenaar F & Vanos J. (2021). Identifying the need for locally-observed wet bulb globe temperature across outdoor athletic venues for current and future climates in a desert environment. *Environmental Research Letters* **16,** 124042.

Hall SJ, Learned J, Ruddell B, Larson KL, Cavender-Bares J, Bettez N, Groffman PM, Grove JM, Heffernan JB, Hobbie SE, Morse JL, Neill C, Nelson KC, O'Neil-Dunne JPM, Ogden L, Pataki DE, Pearse WD, Polsky C, Chowdhury RR, Steele MK & Trammell TLE. (2016). Convergence of microclimate in residential landscapes across diverse cities in the United States. *Landscape Ecology* **31,** 101-117.

Hao L, Sun G, Huang X, Tang R, Jin K, Lai Y, Chen D, Zhang Y, Zhou D, Yang Z-L, Wang L, Dong G & Li W. (2023). Urbanization alters atmospheric dryness through land evapotranspiration. *npj Climate and Atmospheric Science* **6,** 149.

Havenith G. (2003). Interaction of Clothing and Thermoregulation. *Exogenous Dermatology* **1,** 221-230.

Havenith G, Bröde P, Hartog Ed, Kuklane K, Holmer I, Rossi RM, Richards M, Farnworth B & Wang X. (2013). Evaporative cooling: effective latent heat of evaporation in relation to evaporation distance from the skin. *Journal of Applied Physiology* **114,** 778-785.

Havenith G, Richards MG, Wang X, Brode P, Candas V, den Hartog E, Holmer I, Kuklane K, Meinander H & Nocker W. (2008). Apparent latent heat of evaporation from clothing: attenuation and "heat pipe" effects. *Journal of Applied Physiology* **104,** 142-149.

Heinemann K. (2005). Sport and the welfare state in Europe. *European journal of sport science* **5,** 181-188.

Hobson RM & Maughan RJ. (2010). Hydration status and the diuretic action of a small dose of alcohol. *Alcohol* **45,** 366-373.

Holmér I, Nilsson H, Havenith G & Parsons K. (1999). Clothing convective heat exchange--proposal for improved prediction in standards and models. *Ann Occup Hyg* **43,** 329-337.

Hopker J, Passfield L, Coleman D, Jobson S, Edwards L & Carter H. (2009). The effects of training on gross efficiency in cycling: a review. *Int J Sports Med* **30,** 845-850.

Hopker JG, Coleman DA, Gregson HC, Jobson SA, Von der Haar T, Wiles J & Passfield L. (2013). The influence of training status, age, and muscle fiber type on cycling efficiency and endurance performance. *Journal of applied physiology* **115,** 723-729.

Hopker JG, O'Grady C & Pageaux B. (2017). Prolonged constant load cycling exercise is associated with reduced gross efficiency and increased muscle oxygen uptake. *Scandinavian Journal of Medicine & Science in Sports* **27,** 408-417.

Horowitz J, Sidossis L & Coyle E. (1994). High efficiency of type I muscle fibers improves performance. *International journal of sports medicine* **15,** 152-157.

Hospers L, Cheuvront SN, Kenefick RW & Jay O. (2020). Independent Influence of Skin Temperature on Whole-Body Sweat Rate. *Medicine and science in sports and exercise* **52,** 2423-2429.

Ioannou LG, Tsoutsoubi L, Gkiata P, Brown HA, Periard JD, Mekjavic IB, Kenny GP, Nybo L & Flouris AD. (2024). Effect of sportswear on performance and physiological heat strain during prolonged running in moderately hot conditions. *Scandinavian Journal of Medicine & Science in Sports* **34,** e14520.

ISO. (7726, 1998). Ergonomics of the thermal environment — Instruments for measuring physical quantities, pp. 51. ISO.

ISO. (7933, 2004). Ergonomics of the thermal environment — Analytical determination and interpretation of heat stress using calculation of the predicted heat strain.

ISO. (9886, 2004). Ergonomics of the thermal environment — Evaluation of thermal strain by physiological measurements, pp. 21. ISO.

James LJ, Funnell MP, James RM & Mears SA. (2019). Does Hypohydration Really Impair Endurance Performance? Methodological Considerations for Interpreting Hydration Research. *Sports Medicine* **49,** 103-114.

Jay O, Broderick C & Smallcombe JW. (2021). Extreme Heat Policy, ed. Australia SM, pp. 12. Sports Medicine Australia.

Jay O, Imbeault P & Ravanelli N. (2018). The Sweating and Core Temperature Response to Compensable and Uncompensable Heat Stress Following Heat Acclimation. *The FASEB Journal* **32,** 590.516-590.516.

Jeukendrup A & Wallis G. (2005). Measurement of substrate oxidation during exercise by means of gas exchange measurements. *International journal of sports medicine* **26,** S28-S37.

Jones AM, Grassi B, Christensen PM, Krustrup P, Bangsbo J & Poole DC. (2011). Slow component of VO2 kinetics: mechanistic bases and practical applications. *Med Sci Sports Exerc* **43,** 2046-2062.

Kampmann B & Piekarski C. (2000). The evaluation of workplaces subjected to heat stress: can ISO 7933 (1989) adequately describe heat strain in industrial workplaces? *Appl Ergon* **31,** 59-71.

Kenefick RW, Cheuvront SN, Palombo LJ, Ely BR & Sawka MN. (2010). Skin temperature modifies the impact of hypohydration on aerobic performance. *Journal of Applied Physiology* **109,** 79-86.

Kerr ZY, Register-Mihalik JK, Pryor RR, Pierpoint LA, Scarneo SE, Adams WM, Kucera KL, Casa DJ & Marshall SW. (2019). The association between mandated preseason heat acclimatization guidelines and exertional heat illness during preseason high school American football practices. *Environmental health perspectives* **127,** 047003.

Kim ACH, Ryu J, Lee C, Kim KM & Heo J. (2021). Sport participation and happiness among older adults: A mediating role of social capital. *Journal of Happiness Studies* **22,** 1623-1641.

Kim ES, Yun SH, Lee DK, Kim NY, Piao ZG, Kim SH & Park S. (2023). Quantifying outdoor cooling effects of vertical greening system on mean radiant temperature. *Developments in the Built Environment* **15,** 100211.

Kosaka E, Iida A, Vanos J, Middel A, Yokohari M & Brown R. (2018). Microclimate Variation and Estimated Heat Stress of Runners in the 2020 Tokyo Olympic Marathon. *Atmosphere* **9,** 192.

Kreith F & Black WZ. (1980). Basic heat transfer.

Lane MM, Gamage E, Du S, Ashtree DN, McGuinness AJ, Gauci S, Baker P, Lawrence M, Rebholz CM, Srour B, Touvier M, Jacka FN, O'Neil A, Segasby T & Marx W. (2024). Ultra-processed food exposure and adverse health outcomes: umbrella review of epidemiological meta-analyses. *BMJ* **384,** e077310.

Lanferdini FJ, Sperb CH, Da Rocha ES, Baptista RR & Vaz MA. (2020). Power output reliability between Garmin® Vector meter and Lode Excalibur Sport® cycle ergometer. *Research on Biomedical Engineering* **36,** 333-340.

Lawn Tennis Association. (2022). Extreme Heat Policy LTA Competition Regulations.

Lei T-H, Schlader ZJ, Che Muhamed AM, Zheng H, Stannard SR, Kondo N, Cotter JD & Mündel T. (2020). Differences in dry-bulb temperature do not influence moderate-duration exercise performance in warm environments when vapor pressure is equivalent. *European Journal of Applied Physiology* **120,** 841-852.

Li D, Liao W, Rigden AJ, Liu X, Wang D, Malyshev S & Shevliakova E. (2019). Urban heat island: Aerodynamics or imperviousness? *Science Advances* **5,** eaau4299.

Liguori G, Feito Y, Fountaine C & Roy B. (2022). *ACSM's guidelines for exercise testing and prescription*. Wolters Kluwer, Philadelphia.

Liu W, Lian Z, Deng Q & Liu Y. (2011). Evaluation of calculation methods of mean skin temperature for use in thermal comfort study. *Building and Environment* **46,** 478-488.

Livingstone SD, Nolan RW, Frim J, Reed LD & Limmer RE. (1987). A thermographic study of the effect of body composition and ambient temperature on the accuracy of mean skin temperature calculations. *Europ J Appl Physiol* **56,** 120-125.

Lotens W & Havenith G. (1991). Calculation of clothing insulation and vapour resistance. *Ergonomics* **34,** 233-254.

Lucía A, Hoyos J & Chicharro JL. (2000). The slow component of $\dot{V}O_2$ in professional cyclists. *British Journal of Sports Medicine* **34,** 367-374.

Lynch GP, Périard JD, Pluim BM, Brotherhood JR & Jay O. (2018). Optimal cooling strategies for players in Australian Tennis Open conditions. *Journal of Science and Medicine in Sport* **21,** 232-237.

Mairiaux P, Malchaire J & Candas V. (1987). Prediction of mean skin temperature in warm environments. *Eur J Appl Physiol Occup Physiol* **56,** 686-692.

Makarieva AM, Gorshkov VG, Sheil D, Nobre AD & Li BL. (2013). Where do winds come from? A new theory on how water vapor condensation influences atmospheric pressure and dynamics. *Atmospheric Chemistry and Physics* **13,** 1039-1056.

Malchaire J, Kampmann B, Havenith G, Mehnert P & Gebhardt HJ. (2000). Criteria for estimating acceptable exposure times in hot working environments: a review. *Int Arch Occup Environ Health* **73,** 215-220.

Margaria R, Edwards H & Dill DB. (1933). The possible mechanisms of contracting and paying the oxygen debt and the role of lactic acid in muscular contraction. *American Journal of Physiology-Legacy Content* **106,** 689-715.

Maron MB, Wagner JA & Horvath SM. (1977). Thermoregulatory responses during competitive marathon running. *Journal of Applied Physiology* **42,** 909-914.

Marsh SA & Jenkins DG. (2002). Physiological Responses to the Menstrual Cycle. *Sports Medicine* **32,** 601-614.

Marshall J. (1968). A FIELD TRIAL OF THE BASAL-BODY-TEMPERATURE METHOD OF REGULATING BIRTHS. *The Lancet* **292,** 8-10.

Martin DT, Quod MJ & Gore CJ. (2005). Has Armstrong's cycle efficiency improved? *Journal of Applied Physiology* **99,** 1628-1629.

Maughan RJ & Leiper JB. (1983). Aerobic capacity and fractional utilisation of aerobic capacity in elite and non-elite male and female marathon runners. *Europ J Appl Physiol* **52,** 80-87.

Mazrooei A, Reitz M, Wang D & Sankarasubramanian A. (2021). Urbanization impacts on evapotranspiration across various spatio-temporal scales. *Earth's Future* **9,** e2021EF002045.

McCullough EA, Jones BW & Huck J. (1985). A comprehensive data base for estimating clothing insulation. *Ashrae Trans* **91,** 29-47.

McDermott BP, Anderson SA, Armstrong LE, Casa DJ, Cheuvront SN, Cooper L, Kenney WL, O'Connor FG & Roberts WO. (2017). National athletic trainers' association position statement: fluid replacement for the physically active. *Journal of athletic training* **52,** 877-895.

Meehl GA & Tebaldi C. (2004). More intense, more frequent, and longer lasting heat waves in the 21st century. *Science* **305,** 994-997.

Mehnert P, Malchaire J, Kampmann B, Piette A, Griefahn B & Gebhardt H. (2000). Prediction of the average skin temperature in warm and hot environments. *Eur J Appl Physiol* **82,** 52-60.

Mokha M, Kicklighter TH, Edsall JR & Martin M. (2011). Effect of Moisture-Wicking Garments on Temperature Regulation During Exercise. *International Journal of Athletic Therapy and Training* **16,** 9-13.

Montain SJ, Sawka MN, Cadarette BS, Quigley MD & McKay JM. (1994). Physiological tolerance to uncompensable heat stress: effects of exercise intensity, protective clothing, and climate. *Journal of applied physiology* **77,** 216-222.

Monteith J. (1972). Latent heat of vaporization in thermal physiology. *Nature New Biology* **236,** 96-96.

Montoye AH, Vondrasek JD & JAMES B HANCOCK I. (2020). Validity and reliability of the VO2 master pro for oxygen consumption and ventilation assessment. *International Journal of Exercise Science* **13,** 1382.

Moseley L, Achten J, Martin JC & Jeukendrup AE. (2004). No Differences in Cycling Efficiency Between World-Class and Recreational Cyclists. *International Journal of Sports Medicine* **25,** 374-379.

Myny D, Waele JD, Defloor T, Blot S & Colardyn F. (2005). Temporal scanner thermometry: a new method of core temperature estimation in ICU patients. *Scottish Medical Journal* **50,** 15-18.

Nadel ER, Mitchell JW, Saltin B & Stolwijk JA. (1971). Peripheral modifications to the central drive for sweating. *J Appl Physiol* **31,** 828-833.

United Nations (UN). (2018). World Urbanization Prospects. United Nations.

Neff LM, Hoffmann ME, Zeiss DM, Lowry K, Edwards M, Rodriguez SM, Wachsberg KN, Kushner R & Landsberg L. (2016). Core body temperature is lower in postmenopausal women than premenopausal women: potential implications for energy metabolism and midlife weight gain. *Cardiovasc Endocrinol* **5,** 151-154.

Nielsen M. (1938). Die Regulation der Körpertemperatur bei Muskelarbeit1. *Skandinavisches Archiv Für Physiologie* **79,** 193-230.

Nishi Y. (1981). Chapter 2 Measurement of Thermal Balance of Man. In *Studies in Environmental Science,* ed. Cena K & Clark JA, pp. 29-39. Elsevier.

Nishi Y & Gagge AP. (1970). Direct evaluation of convective heat transfer coefficient by naphthalene sublimation. *Journal of Applied Physiology* **29,** 830-838.

Oliveira AVM, Gaspar AR, Francisco SC & Quintela DA. (2014). Analysis of natural and forced convection heat losses from a thermal manikin: Comparative assessment of the static and dynamic postures. *Journal of Wind Engineering and Industrial Aerodynamics* **132,** 66-76.

Osborne NS & Meyers CH. (1934). A formula and tables for the pressure of saturated water vapor in the range 0 to 374 C. *Journal of research of the National Bureau of Standards* **13,** 1.

Outdoor Foundation. (2022). Outdoor Participation Trends Report. Outdoor Foundation.

Ouyang Y, Wang K, Zhang T, Peng L, Song G & Luo J. (2020). The influence of sports participation on body image, self-efficacy, and self-esteem in college students. *Frontiers in psychology* **10,** 3039.

Parsons K. (2014). *Human thermal environments: the effects of hot, moderate, and cold environments on human health, comfort, and performance*. CRC press.

Parsons KC. (2003). *Human Thermal Environments*. Taylor & Francis, London.

Pascoe DD, Shanley LA & Smith EW. (1994). Clothing and Exercise. *Sports Medicine* **18,** 38-54.

Périard JD, Racinais S & Sawka MN. (2015). Adaptations and mechanisms of human heat acclimation: Applications for competitive athletes and sports. *Scandinavian Journal of Medicine & Science in Sports* **25,** 20-38.

Perkins S, Alexander L & Nairn J. (2012). Increasing frequency, intensity and duration of observed global heatwaves and warm spells. *Geophysical Research Letters* **39**.

Peronnet F & Massicotte D. (1991). Table of nonprotein respiratory quotient: an update. *Can J Sport Sci* **16,** 23-29.

Poole DC & Jones AM. (2012). Oxygen uptake kinetics. *Compr Physiol* **2,** 933-996.

Poole DC, Kindig CA, Behnke BJ & Jones AM. (2005). Oxygen uptake (VO2) kinetics in different species: a brief review. *Equine and Comparative Exercise Physiology* **2,** 1-15.

Poole DC, Schaffartzik W, Knight DR, Derion T, Kennedy B, Guy HJ, Prediletto R & Wagner PD. (1991). Contribution of excising legs to the slow component of oxygen uptake kinetics in humans. *Journal of Applied Physiology* **71,** 1245-1260.

Pryor JL, Pryor RR, Grundstein A & Casa DJ. (2017). The Heat Strain of Various Athletic Surfaces: A Comparison Between Observed and Modeled Wet-Bulb Globe Temperatures. *Journal of Athletic Training* **52,** 1056-1064.

PW G & Charmchi M. (1997). Coupled heat and mass transfer through hygroscopic porous materials-application to clothing layers. *Sen'i Gakkaishi* **53,** 183-194.

Rabinowitz JD & Enerbäck S. (2020). Lactate: the ugly duckling of energy metabolism. *Nature Metabolism*, **7**, 566–571. https://doi.org/10.1038/s42255-020-0243-4

Racinais S, Hosokawa Y, Akama T, Bermon S, Bigard X, Casa DJ, Grundstein A, Jay O, Massey A, Migliorini S, Mountjoy M, Nikolic N, Pitsiladis YP, Schobersberger W, Steinacker JM, Yamasawa F, Zideman DA, Engebretsen L & Budgett R. (2023). IOC consensus statement on recommendations and regulations for sport events in the heat. *British Journal of Sports Medicine* **57,** 8-25.

Racinais S, Moussay S, Nichols D, Travers G, Belfekih T, Schumacher YO & Periard JD. (2019). Core temperature up to 41.5ºC during the UCI Road Cycling World Championships in the heat. *Br J Sports Med* **53,** 426-429.

Ravanelli N, Bongers CCWG & Jay O. (2019a). The Biophysics of Human Heat Exchange. In *Heat Stress in Sport and Exercise: Thermophysiology of Health and Performance*, ed. Périard JD & Racinais S, pp. 29-43. Springer International Publishing, Cham.

Ravanelli N, Coombs G, Imbeault P & Jay O. (2019b). Thermoregulatory adaptations with progressive heat acclimation are predominantly evident in uncompensable, but not compensable, conditions. *Journal of Applied Physiology* **127,** 1095-1106.

Ravanelli N, Coombs GB, Imbeault P & Jay O. (2018). Maximum Skin Wettedness after Aerobic Training with and without Heat Acclimation. *Medicine & Science in Sports & Exercise* **50,** 299-307.

Ravanelli N, Imbeault P & Jay O. (2020). Steady-state sweating during exercise is determined by the evaporative requirement for heat balance independently of absolute core and skin temperatures. *J Physiol* **598,** 2607-2619.

Ravussin E, Lillioja S, Anderson TE, Christin L & Bogardus C. (1986). Determinants of 24-hour energy expenditure in man. Methods and results using a respiratory chamber. *J Clin Invest* **78,** 1568-1578.

Rico-Campà A, Martínez-González MA, Alvarez-Alvarez I, Mendonça RdD, Fuente-Arrillaga Cdl, Gómez-Donoso C & Bes-Rastrollo M. (2019). Association between consumption of ultra-processed foods and all cause mortality: SUN prospective cohort study. *BMJ* **365,** l1949.

Riddervold S, Haug E & Kristensen SM. (2023). Sports participation, body appreciation and life satisfaction in Norwegian adolescents: A moderated mediation analysis. *Scandinavian Journal of Public Health* **0,** 14034948231184525.

Rodríguez-Monforte M, Sánchez E & Barrio F. (2017). Metabolic syndrome and dietary patterns: A systematic review and meta-analysis of observational studies. *Eur J Nutr* **56,** 925-947.

Rodríguez-Rielves V, Lillo-Beviá JR, Buendía-Romero Á, Martínez-Cava A, Hernández-Belmonte A, Courel-Ibáñez J & Pallarés JG. (2021). Are the Assioma Favero Power Meter Pedals a Reliable Tool for Monitoring Cycling Power Output? *Sensors* **21,** 2789.

Roy S, Mishra DP, Bhattacharjee RM & Agrawal H. (2022). Heat Stress in Underground Mines and its Control Measures: A Systematic Literature Review and Retrospective Analysis. *Mining, Metallurgy & Exploration* **39,** 357-383.

Salier Eriksson J, Rosdahl H & Schantz P. (2012). Validity of the Oxycon Mobile metabolic system under field measuring conditions. *European Journal of Applied Physiology* **112,** 345-355.

Sallet P, Mathieu R, Fenech G & Baverel G. (2006). Physiological differences of elite and professional road cyclists related to competition level and rider specialization. *Journal of Sports Medicine and Physical Fitness* **46,** 361-365.

Saltin B & Hermansen L. (1966). Esophageal, rectal, and muscle temperature during exercise. *Journal of Applied Physiology* **21,** 1757-1762.

Sandford GN & Stellingwerff T. (2019). “Question Your Categories”: the Misunderstood Complexity of Middle-Distance Running Profiles With Implications for Research Methods and Application. *Frontiers in Sports and Active Living* **1**.

Sawka MN, Burke LM, Eichner ER, Maughan RJ, Montain SJ & Stachenfeld NS. (2007). American College of Sports Medicine position stand. Exercise and fluid replacement. *Medicine and science in sports and exercise* **39,** 377-390.

Schnabel L, Kesse-Guyot E, Allès B, Touvier M, Srour B, Hercberg S, Buscail C & Julia C. (2019). Association Between Ultraprocessed Food Consumption and Risk of Mortality Among Middle-aged Adults in France. *JAMA Internal Medicine* **179,** 490-498.

Scott CB. (2005). Contribution of anaerobic energy expenditure to whole body thermogenesis. *Nutr Metab (Lond)* **2,** 14.

Simon E, Pierau F-K & Taylor D. (1986). Central and peripheral thermal control of effectors in homeothermic temperature regulation. *Physiological reviews* **66,** 235-300.

Smith L, Gardner B, Aggio D & Hamer M. (2015). Association between participation in outdoor play and sport at 10years old with physical activity in adulthood. *Preventive Medicine* **74,** 31-35.

Softball Australia. (2022). Softball Australia Adverse Weather Guidelines,.

Sparks SA, Dove B, Bridge CA, Midgely AW & McNaughton LR. (2015). Validity and reliability of the look Keo power pedal system for measuring power output during incremental and repeated sprint cycling. *Int J Sports Physiol Perform* **10,** 39-45.

Stacey MJ, Parsons IT, Woods DR, Taylor PN, Ross D & Brett SJ. (2015). Susceptibility to exertional heat illness and hospitalisation risk in UK military personnel. *BMJ open sport & exercise medicine* **1,** e000055.

Stearns RL, Hosokawa Y, Adams WM, Belval LN, Huggins RA, Jardine JF, Katch RK, Davis RJ & Casa DJ. (2020). Incidence of Recurrent Exertional Heat Stroke in a Warm-Weather Road Race. *Medicina (Kaunas)* **56**.

Stevens CJ, Mauger AR, Hassmèn P & Taylor L. (2018). Endurance Performance is Influenced by Perceptions of Pain and Temperature: Theory, Applications and Safety Considerations. *Sports Medicine* **48,** 525-537.

Stevens CJ, Ross ML, Périard JD, Vallance BS & Burke LM. (2020). Core Temperature Responses to Elite Racewalking Competition. *Int J Sports Physiol Perform* **15,** 892-895.

Tan CL, Wong NH & Jusuf SK. (2014). Effects of vertical greenery on mean radiant temperature in the tropical urban environment. *Landscape and Urban Planning* **127,** 52-64.

Toulouse A, Joubert D, Oden G & Davis PR. (2022). Comparison of the VO2 Master Pro and Cosmed K5 During Walking, Jogging, and Running. *Journal of Science in Sport and Exercise* **4,** 119-127.

Tripp B, Vincent HK, Bruner M & Smith MS. (2020). Comparison of wet bulb globe temperature measured on-site vs estimated and the impact on activity modification in high school football. *International Journal of Biometeorology* **64,** 593-600.

Union Cycliste Internationale. (2024). UCI CYCLING REGULATIONS - Part 2 Road Races. UCI.

VAN Erp T, Hoozemans M, Foster C & JJ DEK. (2020). Case Report: Load, Intensity, and Performance Characteristics in Multiple Grand Tours. *Med Sci Sports Exerc* **52,** 868-875.

Vanos JK, Warland JS, Gillespie TJ & Kenny NA. (2012). Thermal comfort modelling of body temperature and psychological variations of a human exercising in an outdoor environment. *International Journal of Biometeorology* **56,** 21-32.

Vogt JJ, Candas V, Libert JP & Daull F. (1981). Chapter 6 Required Sweat Rate as an Index of Thermal Strain in Industry. In *Studies in Environmental Science*, ed. Cena K & Clark JA, pp. 99-110. Elsevier.

Wallace RF, Kriebel D, Punnett L, Wegman DH, Wenger CB, Gardner JW & Kark JA. (2006). Risk factors for recruit exertional heat illness by gender and training period. *Aviation, space, and environmental medicine* **77,** 415-421.

Wang Y, Beydoun MA, Min J, Xue H, Kaminsky LA & Cheskin LJ. (2020). Has the prevalence of overweight, obesity and central obesity levelled off in the United States? Trends, patterns, disparities, and future projections for the obesity epidemic. *International Journal of Epidemiology* **49,** 810-823.

Waterhouse J, Drust B, Weinert D, Edwards B, Gregson W, Atkinson G, & Reilly T. (2005). The circadian rhythm of core temperature: origin and some implications for exercise performance. *Chronobiology International*, **22**, 207-225.

Westwood CS, Fallowfield JL, Delves SK, Nunns M, Ogden HB & Layden JD. (2021). Individual risk factors associated with exertional heat illness: A systematic review. *Exp Physiol* **106,** 191-199.

Xu F & Rhodes EC. (1999). Oxygen uptake kinetics during exercise. *Sports medicine (Auckland, NZ)* **27,** 313-327.

Xu J, Psikuta A, Li J, Annaheim S & Rossi RM. (2021a). Evaluation of the convective heat transfer coefficient of human body and its effect on the human thermoregulation predictions. *Building and Environment* **196,** 107778.

Xu J, Psikuta A, Li J, Annaheim S & Rossi RM. (2021b). A numerical investigation of the influence of wind on convective heat transfer from the human body in a ventilated room. *Building and Environment* **188,** 107427.

Y. S. Touloukian PEL, S. C. Saxena. (1970). *Thermophysical Properties of Matter, Vol. 3: Thermal Conductivity*.

Zhao L, Lee X, Smith RB & Oleson K. (2014). Strong contributions of local background climate to urban heat islands. *Nature* **511,** 216-219.

Zuo J & McCullough EA. (2004). Heat transfer characteristics of sports apparel. *Journal of ASTM International* **1,** JAI12143.

CHAPTER III

Comparing meteorological data with on-field environmental conditions when assessing heat stress risk at Australian professional and community oval sporting venues.

Lindsey Hunt[1,3], James W Smallcombe[1,3], Anna Saw[2], John Orchard[2], Michelle Court[2], Alex Kountouris[2], and Ollie Jay[1,3]
[1]Heat and Health Research Centre,
The University of Sydney, Sydney, Australia
[2]Cricket Australia, Melbourne, Australia
[3]Thermal Ergonomics Laboratory,
The University of Sydney, Sydney, Australia

Author Contributions: L. Hunt, J.W Smallcombe, M. Court, A. Kountouris, J Orchard, A. Saw and O. Jay designed the research, L. Hunt conducted data collection, O. Jay provided access to materials and equipment, L. Hunt analysed the data, L. Hunt wrote the manuscript, J.W Smallcombe, and O. Jay assisted with data interpretation and all authors assisted with reviewing the manuscript and O. Jay had primary responsibility for the final content of the paper. All authors read and approved the final manuscript.

Running head: Agreement in environmental conditions between BoM sites and playing surfaces

Address for correspondence:
Professor Ollie Jay ✉
Heat and Health Research Centre
Sydney School of Health Sciences,
Faculty of Medicine and Health,
University of Sydney, NSW 2006 Australia
+ 61 (2) 935-19328
e-mail: ollie.jay@sydney.edu.au

3.0 Abstract

Purpose: This study sought to assess how well nearby Bureau of Meteorology (BoM) station heat stress data agrees with environmental parameters measured on field using the Cricket Australia (CA) Heat Stress Risk Index (HSRI) at cricket venues across Australia. Secondly, aimed to assess whether sporting venue type (Major/professional vs. Minor/community) affected the agreement and accuracy between BoM station and the playing field.

Methods: On-site environmental conditions (dry-bulb temperature, relative humidity and air velocity) were measured with two custom built Environmental Monitoring Units (EMUs) during moderate to extreme heat stress environmental conditions. 161 hours and 28 minutes of data were collected across 29 days, at 5 Major venues and 11 Minor venues. Nearby BoM data were collected retrospectively from the nearest two weather stations.

Results: BoM sites more frequently overestimated (26.5% of data collected) the HSRI by at least one category at Major venues. For Minor venues, BoM sites more commonly underestimated (15.8%) the HSRI by at least one category. Differences in the HSRI at Major venues were predominately driven by higher dry-bulb temperatures reported at BoM sites compared to venues (+1.3 ℃, 95% CI [0.9, 1.5 ℃]) (i.e., on-field conditions were cooler than reported by the BoM). Small differences in the HSRI at Minor venues were driven by lower dry-bulb temperatures and higher wind speeds reported at BoM sites compared with venues (-0.7 ℃ 95% CI[-1.5, 1.8 ℃], +1.6 $m{\cdot}s^{-1}$ 95% CI[0.6, 3.0 $m{\cdot}s^{-1}$]).

Conclusion: BoM sites more commonly overestimated the HSRI at Major venues but more commonly underestimated the HSRI at Minor venues. During our sample of days, the ground truth measures were often substantially different from the BoM to the extent that incorrect HSRI classifications would have been made (i.e., not stopping play when conditions on field were unsafe, or disrupting play when conditions were in fact safe for play). On-site monitoring at all venues is therefore recommended during matchdays when warm conditions are present

to help mitigate potential losses in playing time and risk of heat illness due to misclassifying the heat stress risk.

Keywords: Extreme Heat Stress, Outdoor Sport, Thermal Environment, Extreme Heat Policies

3.1 Introduction

During outdoor sporting events, there is a need to protect participants from environmental stressors such as extreme heat, which is predominantly achieved through the development and implementation of Extreme Heat Policies (EHPs) (Larsen *et al.*, 2007; Nichols, 2014; Chalmers & Jay, 2018; Jay, Broderick & Smallcombe, 2021). EHPs typically rely on nearby meteorological site data, or in rare but best-case scenarios, local environmental measures at the site of play (Racinais *et al.*, 2023). Evidence indicates that considerable variation may exist between environmental data derived from local meteorological stations and those measured on-site, even across small distances (Cheuvront *et al.*, 2015; Kosaka *et al.*, 2018; Hosokawa *et al*., 2018). Such differences between on-field conditions and nearby meteorological sites may be due to factors including, the local geography/topography of the measurement sites, disparate surface types (grass/natural vs. concrete/synthetic) and potential differences in the surrounding structures (e.g. buildings, grandstands etc.) (Grundstein & Cooper, 2020; Liu & Jim, 2021). To optimally prevent heat-related injuries, sporting officials must have accurate data representing the environmental conditions on the playing field (Hughson, Staudt & Mackie, 1983; ACSM, 1984).

Cricket is a popular professional and community sport in Australia, with over 790,000 adults and children participating in matches throughout 2022 (AusPlay, 2023), and participation in cricket is associated with health across the lifespan (Luies *et al.*, 2023). The matches are often long in duration (>3 hours) and played during periods of hot weather across the Australian summer. Playing cricket is associated with a higher risk of heat-related hospitalisations (7% of all sport related hospitalisations between 2000-2004) in New South Wales (NSW) (Finch & Boufous, 2008) and across Australia (10% all sport related hospitalisations between 2002-2004) (Driscoll, Cripps & Brotherhood, 2008). Similar to other sports, the precise incidence of exertional heat illnesses (EHIs) arising from cricket participation is likely underestimated due to the ambiguity in classifying EHIs appropriately within our healthcare system (Garcia *et al.*, 2022). Popular participation in outdoor physical activity/sports combined with increasingly extreme heat stress conditions (Perkins-Kirkpatrick & Gibson, 2017; Bureau of Meteorology, 2021) compounds the risk to individuals playing sports at a professional and community level (Orr *et al.*, 2022). Heat-related hospitalisations resulting from cricket participation are likely related to a combination of playing during peak weather conditions (i.e., mid-afternoon), long match durations (2-6 hrs), regular intense, intermittent exercise bouts, and requirements to wear protective clothing and equipment, which limits convective and evaporative heat loss.

Cricket matches across Australia are mostly played at two types of sporting venues: Major/professional venues with large grandstands that enclose a large proportion of the playing field and Minor/community venues with small grandstands and few buildings surrounding the playing field. Each stadium around Australia has distinct built and natural environmental characteristics surrounding it and each Bureau of Meteorology (BoM) station will also have its own unique characteristics in terms of its location (e.g., surrounding built and natural environment/structures). Therefore, it is possible, especially when the microclimates surrounding each venue (playing surface vs. BoM station) are disparate, that the environmental conditions reported by the BoM may not always match the environmental conditions observed on-field. Representative environmental data is critical to any EHP when implementing heat stress prevention recommendations (e.g., when to introduce additional breaks in play, when to use active cooling, when to suspend play) (Chalmers, Anderson & Jay, 2020). Overestimating the heat stress risk at a playing venue could result in needless cancelling of matches, revenue losses, frustration for spectators, and reduced physical activity opportunities for the community (Chalmers *et al.*, 2020). Perhaps more importantly, underpredicting the heat stress risk could result in suspending play too late or not at all, thereby exposing players to undue risk of EHIs.

This study firstly aimed to assess how well nearby meteorological (BoM) station data agreed with heat stress conditions measured at the site of play using the Cricket Australia (CA) Heat Stress Risk Index (HSRI) at cricket venues across Australia. Secondly, we aimed to assess whether sporting venue type (Major/professional vs. Minor/community) affected the agreement and accuracy between BoM station and playing surface.

We hypothesised firstly that the on-site heat stress risk will be higher within sporting stadia due to lower ambient air velocities compared to the BoM measurement locations and secondly that dry-bulb temperatures at Major venues may be higher than observed at nearby BoM measurement locations, possibly due to reduced air turnover due the enclosing grandstands.

3.2 Methods

Data collection

Data were collected between the 4th of February 2020 and the 16th of March 2023 at 16 cricket venues across Australia. Data were collected on 1 to 2 days at each venue, for a total of 161 hours and 28 minutes, across 29 days (see **Table 1**). Onsite data were collected using two identical environmental measuring units (EMUs), custom-built, and extensively tested by engineers at The University of Sydney to meet the specifications outlined by the International Organisation for Standardization (ISO 7726, 2001). The following environmental conditions were measured: shaded aspirated dry-bulb temperature [T_{db}] (°C), shaded aspirated wet-bulb temperature [T_{wb}] (ºC), and wind speed [WS] ($m \cdot s^{-1}$), with relative humidity [RH] (%) calculated using T_{db} and T_{wb} [Eq. 1] (Abbott & Tabony, 1985):

$$RH = \frac{100\left[EXP\left[1.8096+\left(\frac{1.8096T_{wb}}{237.3+T_{wb}}\right)\right]-7.866\times10^{-4}P(T_{db}-T_{wb})\left(1+\frac{T_{wb}}{610}\right)\right]}{EXP\left[1.8096+\left(\frac{17.2694T_{db}}{237.3+T_{db}}\right)\right]} \quad [1]$$

Where: RH - relative humidity (%), T_{db} is dry-bulb temperature (°C), T_{wb} is aspirated wet-bulb temperature (°C), P = station level pressure (hPa), set at 998.3 hPa for all venues and EXP is the exponent.

The shaded aspirated dry-bulb and aspirated wet-bulb temperature thermometers used were perforated and immersion type 50 mm Class A platinum resistance thermometers, respectively (Temperature Controls, Sefton, NSW, Australia). The aspirated wet-bulb thermometer was draped in a wetted-cotton fabric connected to a reservoir of distilled water that kept the thermometer and cotton fabric fully saturated throughout data collection. Both thermometers were continuously aspirated at ~3.0 $m \cdot s^{-1}$ with a 40 mm by 40 mm x 20 mm Sunon fan (Sunonwealth Electric Machine Industry Company Ltd., Kaohsiung City, Taiwan).

Agreement in environmental conditions between BoM sites and playing surfaces

Wind Speed [WS] was measured with a Windsonic ultrasonic Anemometer (Gill Instruments Ltd., Lymington, Hampshire, UK), which the following specifications, range: 0.0 to 60 $m \cdot s^{-1}$, accuracy of ±2% at 12 $m \cdot s^{-1}$, resolution: 0.1 $m \cdot s^{-1}$ and response time: 0.01 $m \cdot s^{-1}$). Each EMU was mounted to a Rollei tripod (Digitec Audio, Zurich, Switzerland) at a height of 1.2 m. One EMU was placed on the southern edge of the playing field, ~2 m inwards from the boundary rope and the second EMU was placed ~2 m south of the southern edge of the wickets (see **Fig. 1**). The southern edge of the ground and wickets were chosen to ensure the EMUs were positioned to receive sunlight unobstructed by grandstands throughout the day. Both EMUs were placed in position for 30 minutes prior to the start of data collection to equilibrate to the environment. EMUs were placed in full sun, where only cloud cover (when present) provided shade. Data were collected and viewed with Grafana (Grafana Labs, New York City, NY, USA) and downloaded as required for analysis.

Cricket Australia Heat Stress Risk Index

The CA HSRI is a custom, evidence-based biophysical model to determine the heat stress risk when participating in cricket matches during warm weather and forms part of CA's Extreme Heat Policy (EHP) (available here: https://cms.auscricket.com.au/documents/AC-Heat-Policy-20-21-1.pdf?v=1680663603 or here: https://resources.playcommunity.pulselive.com/playcommunity/document/2023/10/30/0eae0316-0dd6-4f24-9a07-0ce13a46b14e/Mitigating-Risk-Train-or-Play-A3.pdf). The HSRI is a 10-point scale (0.0-<4.0 is 'low risk', manage heat as usual; 4.0-<8.0 is 'moderate risk', consider extra or more regular drinks breaks; 8.0-<10.0 is 'high risk', have longer drinks breaks to allow players to come off the field to cool down and apply cooling strategies; and >10 is 'extreme risk', consider suspending play until conditions have improved, e.g., <10). Currently, the algorithms within the HSRI tool are proprietary and are used by CA for elite, junior and community cricket within Australia. However, the tool considers all four environmental parameters (T_{db}, RH, WS and mean radiant temperature (T_r)) and the two personal factors (clothing insulation [clo], and metabolic heat production [H_{prod}]) that govern human heat balance (Cramer & Jay, 2019; Parsons, 2019). The user of the HSRI inputs three environmental conditions associated with heat stress risk assessment which are reported by nearby meteorological sites (T_{db}, RH, and WS) and two user inputs that estimate the effective added solar load (Havenith & Fiala, 2015). An indication of actual solar load via solar radiation data or black globe temperature (T_g) experienced outdoors is not reported by BoM sites. Therefore, the effective solar load must be estimated when measuring heat stress risk outdoors, unless appropriate on-site measures are available (e.g., an EMU or similar device).

Bureau of Meteorology Data

For every stadium from which data were collected, the nearest 1-2 BoM stations (see **Table 2**) were selected as the best-case weather stations. For every minute of data collected by the EMUs, T_a (°C), WS ($m{\cdot}s^{-1}$) and RH (%) the corresponding data from the nearest 1 to 2 BoM sites were obtained in 1-minute intervals. To account for differences in measurement height of WS data, wind velocity data acquired from the BoM (recorded at 10 m above ground) were normalised to 2 m height with the following equation (Allen *et al.*, 1998):

$$WS_2 = WS_z \frac{4.87}{\ln(67.8z - 5.42)} \quad [2]$$

Where: WS_2 is air velocity at 2 m above ground surface ($m{\cdot}s^{-1}$), WS_z is measured air velocity at z m above ground surface ($m{\cdot}s^{-1}$), and z is height of measurement above ground surface (m), in this case, 10 m. An approximation of WS at 2 m height using [**Eq. 2**] can be achieved in practice by multiplying the measured WS by the BoM (at 10 m above ground) by 0.75 (Allen *et al.*, 1998).

HSRI categorical agreement (ΔHSRI) was defined and calculated as $HSRI_{EMU} - HSRI_{BoM}$ (where: ΔHSRI = 0). BoM site accuracy was determined by the total time spent in HSRI categorical agreement divided by the total amount of data collected in at each venue. The proportion of time spent in HSRI categorical disagreement for each HSRI category ('low', 'moderate', 'high', 'suspend play') was determined by dividing by the total time spent in categorical disagreement (ΔHSRI ≠0). HSRI categories between sites could disagree by -1 to -3, which means off-site measures (BoM) overestimate the on-site (EMU) conditions and by +1 to +3, which means off-site measures underestimate the on-site heat stress risk conditions.

Stadium classification

Cricket is played at a variety of sporting venues across Australia, from large venues such as the Sydney Cricket Ground [SCG] (Sydney, NSW) and Optus Stadium (Perth, WA) to small venues such as Great Barrier Reef Arena (Mackay, QLD) and Drummoyne Oval (Sydney, NSW). To characterise any potential differences in heat stress risk classification for between venue types, each venue was stratified as a Major or Minor venue (see **Table 1**). Major venues had a seating capacity ≥20,000 and the playing surface was surrounded by large, built-up grandstands. Minor venues had a capacity of ≤10,000 and the playing surface typically had one small grandstand which covered a small section of the boundary. At the larger venues the playing surface is "enclosed" by a ring of tall grandstands that provide no protection from solar radiation throughout the middle parts of the day, yet likely reduce air flow. Major grounds are also typically located in closer proximity to artificial environments like the central business districts of major cities. Minor grounds across Australia are typically situated in natural environments and surrounded by local green space, which may impact the prevailing environmental conditions.

Experimental Design

This study employed an observational design that compared the heat stress risk measured on the playing surface at each venue (EMU) with the nearest BoM weather station/s. The 3 environmental parameters (dry-bulb temperature [T_{db}, ºC] and the associated relative humidity [RH, %] and wind velocity [WS, $m \cdot s^{-1}$]) which affect heat stress risk that are reported by BoM and other meteorological stations were compared and used to calculate the CA HSRI at each site (EMU vs BoM) for every 1-minute of data collected.
All data collection was conducted during the warmest parts of the day and when cricket matches are played (typically between 0930-1630 local time). Data collection days were selected by the research team when high heat stress conditions were forecast and the HSRI was predicted to exceed 4.0 on the scale (0.0-10.0 scale). Data collection days were chosen across the summertime period in Australia (when cricket is usually played) on warm days when the heat stress risk was its highest, and therefore when it is most important to be confident in the data that underpin official's decisions, as the public health-related and economic consequences are the greatest.

Statistical Analyses

All stadia were compared with the two geographically closest BoM weather stations except for Traeger Park (Alice Springs, NT), Great Barrier Reef Arena (Mackay QLD), and Allan Border Oval (Brisbane, QLD), where only one appropriate BoM station was identified. Differences in the HSRI category of ≥1 category were considered meaningful (*a priori*) and were calculated and expressed as a percentage of the total data collection time to quantify the level of agreement between on-site measurements and the BoM (i.e., BoM accuracy). A HSRI category difference of 1 or more was classified as meaningful given the significant change in recommendation that would take place when a categorical difference was observed (i.e., stop play, introduce lengthy breaks to apply cooling strategies). For the relatively small number of data points (30 BoM accuracy scores), determining the distribution of the BoM accuracy variable was important prior to choosing an appropriate statistical method. The Shapiro-Wilk test was selected to assess normality and BoM station accuracy (%) data showed evidence of non-normality ($W = 0.891$, $P = 0.05$). Further skewness and kurtosis analysis showed more evidence of non-normality (skewness -2.32, kurtosis 0.85). All data were analysed with Python 3.9 (PyCharm IDE, Version 2023.2). Numpy (https://numpy.org/) and Pandas (https://pypi.org/project/haversine/) were used to process and transform the data. Haversine (https://pypi.org/project/haversine/) was used to compute distances between BoM stations and venues using longitude and latitude for each venue and BoM station. Seaborn (https://seaborn.pydata.org/index.html) and matplotlib (https://matplotlib.org/)were used to visualize the data. All data and source code for data preparation, analysis and visualisation are available on request.

3.3 Results

Table 1 contains the stadium and BoM site characteristics for the data collection venues (location, capacity, time, and venue type). Data were collected at 8 venues across New South Wales, 1 in the Northern Territory, 3 across Queensland, 2 in South Australia, and 2 in Western Australia (see **Fig. 1**). Off-site environmental data were collected from the 1 to 2 nearest BoM sites. BoM sites for Minor venues were an average of 8.80 km away [range: 0.35-20.04 km]. BoM sites for Major venues were an average of 6.09 km away [1.18-11.28 km].

Differences in the Cricket Australia Heat Stress Risk Index (HSRI) and the factors that underpin the HSRI (dry-bulb temperature, relative humidity, and air velocity) between on-site and off-site measures were examined at each venue by plotting data with a line of identity (**Fig. 3** with all individual venues in the *supplemental figures*). Across all venues, 11% of data fell into the ‘low risk’ category, 26% fell into the ‘moderate risk’ category, 9% fell into the ‘high risk’ category and 54% fell into the ‘suspend play’ category. This indicates that we were successful in capturing stressful environmental conditions that are representative of conditions relevant to when extreme heat policies are in effect.

The accuracy for each BoM site across each of the HSRI categories for each venue is reported in **Table 2**. Minor venues spent a greater amount of time in categorical agreement than Major venues, with the BoM more likely to underestimate the HSRI experienced on the field at Minor venues and overestimate the HSRI at Major venues (**Fig. 5**, left). Irrespective of the level of heat stress (i.e., accuracy across all 4 HSRI categories), the BoM station accuracy was higher (80% [range: 42-100%]) for Minor venues compared with for Major venues (58% [range: 7-96%]) (**Fig. 5**, middle). The highest BoM site accuracies were observed at venues with the lowest variability in environmental conditions across the day, where most of the day (e.g., Townsville Aero) was spent in the ‘consider suspending play' >10 HSRI category. The most accurate venue and BoM site combination was at Traeger Park and the Alice Springs Airport Station, where the BoM and EMU HSRI categories agreed 100% of the day, while the HSRI was in the High and Extreme categories for 8% and 96% of the day, respectively (see **Table 2**). At the SCG and Sydney Airport Station however, on-site and off-site measures agreed 7% of the time, with the off-site measures overestimating the HSRI by one category for 93% of the time. Across two days at Adelaide Oval, most of the time was spent in the 'extreme' HSRI category (96% at West Terrace, 93% at Adelaide Airport). For the 6% of data in the -2 and -1 ΔHSRI category at the Adelaide Oval (see **Table 2**), the Adelaide Airport station observed a drop in dry-bulb temperature prior to the Adelaide Oval (see *supplemental figures*), which caused the acute categorical disagreement. A moderate negative relation was observed between BoM site accuracy and distance from the stadium for Major (r = -0.43) venues and a weak negative relation was observed for Minor venues (r = -0.22) (**Fig. 5**, right).

Across all Minor venues, the mean HSRI scores reported by the BoM were 9.7 [95% CIs: 2.0-15.9] (AU) compared with 11.2 [3.0-17.4] (AU) when measured on the playing surface, which indicates using local meteorological weather data may lead to underestimation of the heat stress risk on-field (see **Fig. 4**). Across all Major venues, the mean HSRI scores reported by the BoM were 10.9 [3.7-20.8] (AU), compared with 10.4 [2.5-21.8] (AU) when measured on the playing surface. Dry-bulb temperatures for Minor venues reported by the BoM were 31.1 [26.0-35.7] (°C) compared with 31.8 [27.5-37.5] (°C) as recorded on-site. Dry-bulb temperatures for Major venues reported by the BoM were 32.4 [27.2-40.3] (°C) compared with 31.1 [26.2-38.8] (°C) as recorded on-site. The mean relative humidity across all Minor venues as reported by the BoM was 45 [19-77] (%) compared with 44 [16-72] (%) as measured on-site by the EMUs. The mean relative humidity across all Major venues as reported by the BoM was 39 [13-63] (%) compared with 49 [20-71] (%) recorded on-site.

Agreement in environmental conditions between BoM sites and playing surfaces

The mean absolute humidity across all Minor venues as reported by the BoM was 0.0139 [0.0076-0.0222] ($g{\cdot}m^{-3}$) compared with 0.0142 [0.0071-0.0225] ($g{\cdot}m^{-3}$) when recorded at the playing surface. The mean absolute humidity across all Major venues as reported by the BoM was lower - 0.0125 [0.0069-0.0172] ($g{\cdot}m^{-3}$) compared with 0.0146 [0.0087-0.0204] ($g{\cdot}m^{-3}$) recorded on-site. Despite transforming air velocities reported by the BoM to an anthropomorphic height (see *methods)*, wind velocities remained substantially higher at the BoM sites across both Minor (BoM: 3.4 [1.3-6.4], EMU: 1.8 [0.8-3.4] ($m{\cdot}s^{-1}$)) and Major (BoM: 4.2 [1.9-7.5], EMU: 1.7 [1.2-2.5] ($m{\cdot}s^{-1}$)) venues when compared to the playing surfaces (see **Fig. 4**, bottom row).

3.4 Discussion

This study aimed to compare the agreement in the heat stress risk index (HSRI) between nearby Bureau of Meteorology (BoM) stations and ground truth on-site measurements with purpose-built Environmental Monitoring Units (EMUs) in oval sporting venues across Australia and secondly to assess whether the type of sporting venue (Major vs. Minor) affected the agreement and accuracy of each BoM station.

The first major finding of this study is that BoM station data are more likely to overestimate the HSRI category at Major venues (26.5% of data ΔHSRI ≥+1) and underestimate the HSRI category at Minor venues (15.8% of data ΔHSRI ≤-1) (**Fig. 5**, Left). Overestimates of the HSRI at Major venues were driven by higher observed air temperatures at nearby weather stations (+1.3 °C, 95% CI [0.9, 1.5 ºC]) compared with on-field measures (**Fig. 4**). Underestimates of the HSRI at Minor venues were driven by lower observed air temperatures at the nearby weather stations (-0.7 °C 95% CI[-1.5, 1.8 ºC],) compared with on-field measures (31.8 ºC), with the same absolute humidity between sites (BoM 0.0139 vs. EMU 0.0142, $g \cdot m^{-3}$). During this study, we aimed to collect data in stressful environmental conditions as it is in more oppressive environments that activity modification is most important under any extreme heat policy to ensure safety. Targeting data at these extreme conditions meant that 63% of the data collected resulted in a modification to play, whether that be moderate risk, high risk and extreme risk.

Previous research observed that meteorological station data consistently underestimates the heat stress risk when Wet-Bulb Globe Temperature (WBGT) is measured with a commercially available Kestrel Heat Stress meter (Cheuvront *et al.*, 2015; Guyer *et al.*, 2021) across multiple types of sporting fields and surfaces (grass baseball fields, asphalt tennis courts, artificial turf surfaces, and rubber athletics tracks). However, in contrast, Tripp *et al*, observed higher WBGT values using the BoM method of estimating WBGT (which has two inputs: T_{db} and RH) compared with on-site measures with a WBGT device which takes direct measurements of dry-bulb temperature, natural wet-bulb temperature and black globe temperature which are measures that underpin the WBGT index and its calculation (General Tools WBGT 8758) (Tripp *et al.*, 2020). Further, the BoM method of estimating WBGT has been reported to systematically overestimate on-site WBGT (BoM: +1.6 ºC) compared to the 'Liljegren method' (Liljegren *et al.*, 2008), particularly at times when solar radiation and air velocity are substantially different than the BoM WBGT model assumptions ('moderately high radiation level' and low air velocity) (Grundstein & Cooper, 2018). However, the underestimation of WBGT using meteorological data compared to local measures remained, despite the use of the more robust Liljegren method (Liljegren *et al.*, 2008) for estimating WBGT from the complete suite of meteorological data (T_{db}, WS, RH and solar radiation) (Guyer *et al.*, 2021). However, solar radiation data are not typically available from meteorological stations, which makes estimating WBGT appropriately from meteorological stations potentially problematic (Havenith & Fiala, 2015). Additionally, any data that uses the Kestrel heat stress meter (or similar) should be interpreted with caution due to its design limitations. The Kestrel device has been shown to overestimate WBGT compared to a reference WBGT unit (Cooper *et al.*, 2017) in outdoor environments. The overestimation of WBGT with the Kestrel meter (or similar) may increase with reductions in air velocity and increases in T_r/solar radiation (Anderson, 2023), likely due to a lack of forced convection across the dry-bulb temperature thermometer, and a black globe substantially smaller than the standard size (25.4 vs 150 mm) (Havenith & Fiala, 2015).

The second major finding is that using nearby BoM station data results in a less common rate of HSRI categorisation in Major venues (58%) than in Minor venues (80%). Major venues have large, encompassing grandstands typically situated in dense, urban environments. Minor venues are often located further away from city centres in less dense urban environments with smaller and less surrounding built infrastructure, with fewer and smaller grandstands. The lower accuracy of nearby BoM stations observed at Major venues (58%) may be a result of the unique characteristics of Major venues (e.g., grandstands, regular irrigation of the field) and the built and natural environment that surrounds the venue and the respective BoM station that affects the homogeneity of the environment between the venue and BoM station (Cheuvront *et al.*, 2015). The authors described the environment across the Boston Marathon route as homogenous, with similar built and natural environments surrounding all parts of the course and meteorological station. While the average accuracy for all Major venues was lower, the accuracy for each venue and BoM station combination may be unique to each case. For example, the highest two accuracies (96%, 93%) observed for Major venues were at Adelaide Oval and the West Terrace 'Ngayidapira' (1.60 km away) and Adelaide Airport (8.07 km away) BoM stations, respectively. Factors such as the distance between sites (distance from BoM station to playing surface) (**Fig. 5**, right), variability of environmental conditions across the day, and the built and natural environments surrounding each BoM site and sporting venue and wind direction on the day could result in a unique agreement in the HSRI between a nearby meteorological station and sporting venue.

A third important finding of this research is the air velocity experienced at a playing surface in both Major and Minor venues is lower than the air velocities reported by BoM stations (**Fig. 4**). This observation is despite using standard transformations in air velocity reported by BoM stations at 10 m above ground level to anthropomorphic heights (~1.5-2 m) (Allen *et al.*, 1998). The direct effect of the large grandstands that enclose the playing surface likely contributed to the lower air velocity within Major venues, compared with nearby BoM stations. Any reduction in airflow through and across the venue would reduce air turnover, reduce local potential evapotranspiration (Valipour, 2015; Liuzzo, Viola & Noto, 2016) and allow a microclimate to develop differently to a nearby meteorological station.

Across all Major venues, we observed a higher absolute humidity on-site 0.0146 [0.0087-0.0204] (g·m^{-3}) versus nearby BoM stations 0.0125 [0.0069-0.0172] (g·m^{-3}). Combining the higher absolute humidity with the lower observed air temperatures on-site (31.1 ºC) versus the nearby BoM station (32.4ºC) resulted in a similar HSRI at each venue. This observation could be explained by the unique characteristics of Major sporting venues described above. We assessed the environmental conditions at Major sporting venues during summer across Australia on high heat stress days and ground staff reported overnight irrigation at the playing surface. The exogenous irrigation at Major compared to Minor venues likely impacted the environmental conditions locally by increasing the available water to convert from sensible to latent heat through evapotranspiration (Mishra *et al.*, 2020), potentially cooling the local environment, and increasing absolute humidity at the field-of-play (**Fig. 4**). This phenomenon is problematic when assessing heat stress risk in sporting venues as ultimately it is the limitation placed on evaporative heat exchange by increases in absolute humidity and associated reductions in the maximum evaporative capacity of the environment (E_{max}) that drives increases in heat stress risk, rather than relative humidity (Gagge, 1937).

Across both Major and Minor venues using BoM station data, the HSRI category was overestimated for 11.4% of the time by 1 or more HSRI categories and underestimated the HSRI category for 13.2% of the time by 1 or more heat stress risk categories. The practical outcome of these differences is that when sporting officials use off-site meteorological station data to inform their EHP (e.g., when to allow additional/extra breaks in play, recommend additional cooling interventions, and suspend or indeed resume play) there is an increased risk of misclassifying the HSRI category. Overestimating the HSRI could result in economic losses (from needlessly postponed/cancelled matches) and reduced physical activity opportunities for the community due to an overly conservative modification to play. Conversely, underestimating the HSRI on the field of play could result in an increased risk of heat stress cases (Chalmers *et al.*, 2020; Racinais *et al.*, 2023). Therefore, to adequately assess heat stress risk in a particular venue, a device that measures the four environmental parameters that affect human heat balance (dry-bulb temperature and its associated relative humidity, wind velocity and mean radiant temperature) must be used to monitor the environmental conditions in real-time and must be positioned nearby to and on the same type of surface to the field of play (ideally *on* the field of play) (Racinais *et al.*, 2023; Pryor *et al.*, 2017).

The generalisability of the average agreement between each venue and the respective BoM station/s to other venues and indeed these venues on other days may be limited, although a similar pattern was observed across multiple major venues across multiple locations and days (i.e., large differences in ambient wind velocity). We observed environmental conditions across 1 or 2 days, often on back-to-back hot days. Given the variable nature of environmental conditions, our data cannot be used to develop correction factors for the observed venues, as this volume of data is insufficient for that purpose. Data collection occurred across three cool and high rainfall summers across Australia throughout the La Niña events of 2020/21, 2021/22, and 2022/23 (Bureau of Meteorology, 2022), which reduced the availability of thermally stressful days of summer. Despite those challenges, the majority (89%) of environmental data collected HSRI exceeded 4.0 on the HSRI (0-10 scale), which met our target for thermally stressful environmental conditions, relevant to when player health and welfare could be impacted. The four environmental factors measured by the EMU independently affect heat stress and as such, a heat index that combines some or all these parameters is often selected to compare environmental conditions across locations. We selected the HSRI as an index that takes continuous data and creates stepped categories ("buckets") to determine the heat stress risk and associated heat stress risk management actions within those heat stress risk buckets. With any categorical index, small fluctuations in any of the underpinning components (e.g., ± 0.5 ºC) could result in changes in the heat stress risk category (e.g., from 9.9 'high risk, extended drinks breaks' to 10.0 'extreme risk, consider suspending play'). Such a small absolute change in the HSRI results in a large change in heat stress risk management recommendations.

Previous research suggests nearby meteorological stations underestimate the prevailing heat stress within smaller sporting venues across multiple types of built and natural surfaces (Cheuvront *et al.*, 2015; Grundstein & Cooper, 2020; Tripp *et al.*, 2020). Here we have found similar results where nearby meteorological stations typically underestimate the heat stress risk for Minor venues, however for Major venues, nearby meteorological stations typically overestimate the prevailing heat stress risk. Although not directly compared in this study, one of the many reasons weather stations may never accurately reflect the correct environmental conditions in which outdoor is played, is because they do not measure black globe temperature (T_g), which is a critical component of human heat balance. Black globe temperature can be estimated however, without solar radiation data the accuracy of any estimation is currently limited and is impractical to use in the field without expensive, specialised equipment or meteorological formulae (Liljegren *et al*., 2008), when simpler and actual measurement devices are cheaper, more accurate and easier to use. Future research should evaluate the local environment of nearby meteorological stations and the venue to determine the built and natural environmental factors, which have an impact on the agreement of environmental conditions. Future research should evaluate additional venues for a longer timeframe (i.e. across an entire summer) where physical activity occurs within cities, to ensure EHP's can be implemented with data that is representative of the conditions in which activity is occurring.

Conclusion

The present study observed substantial differences in the HSRI category between meteorological stations and the field of play across a range of Major and Minor oval sporting venues across Australia. Our results suggest that as the distance between the meteorological site and the playing venue increases, the accuracy of the meteorological site decreases. The reduction in observed accuracy is more substantial for Major sporting venues, compared with Minor venues. On-site environmental monitoring reduces the chances of misclassifying the heat stress risk, particularly at Major sporting venues where the inaccurate assessment of heat stress risk with meteorological station data is more common. Therefore, on-site environmental measures may reduce the risk of heat stress cases and costly (economic and population health) reductions in safe playing time.

3.5 References

Abbott PF & Tabony RC. (1985). The estimation of humidity parameters. *Meteorological Magazine* **114,** 49-56.

ACSM. (1984). Prevention of thermal injuries during distance running. Position stand. American College of Sports Medicine. *Med J Aust* **141,** 876-879.

Allen RG, Pereira LS, Raes D & Smith M. (1998). Guidelines for computing crop water requirements. *Irrigation and drainage paper* **56,** 300.

Anderson G. (2023) Monitoring and Managing Heat Stress Risk for Summer Sports. [Doctoral dissertation, University of Sydney] https://ses.library.usyd.edu.au/handle/2123/32228

AusPlay. (2023). The Australian sport and physical activity participation survey: 2022-2023.

Bureau of Meteorology. (2021). Annual climate statement 2021.

Bureau of Meteorology. (2022). Annual climate statement 2022, ed. Meteorology Bo.

Chalmers S, Anderson G & Jay O. (2020). Considerations for the development of extreme heat policies in sport and exercise. *BMJ Open Sport & Exercise Medicine* **6,** e000774.

Chalmers S & Jay O. (2018). Australian community sport extreme heat policies: Limitations and opportunities for improvement. *Journal of Science and Medicine in Sport* **21,** 544-548.

Cheuvront SN, Caruso EM, Heavens KR, Karis AJ, Santee WR, Troyanos C & D'Hemecourt P. (2015). Effect of WBGT Index Measurement Location on Heat Stress Category Classification. *Med Sci Sports Exerc* **47,** 1958-1964.

Cooper E, Grundstein A, Rosen A, Miles J, Ko J & Curry P. (2017). An Evaluation of Portable Wet Bulb Globe Temperature Monitor Accuracy. *Journal of Athletic Training* **52,** 1161-1167.

Cramer MN & Jay O. (2019). Partitional calorimetry. *Journal of Applied Physiology* **126,** 267-277.

Driscoll TR, Cripps R & Brotherhood JR. (2008). Heat-related injuries resulting in hospitalisation in Australian sport. *Journal of Science and Medicine in Sport* **11,** 40-47.

Finch CF & Boufous S. (2008). The descriptive epidemiology of sports/leisure-related heat illness hospitalisations in New South Wales, Australia. *Journal of Science and Medicine in Sport* **11,** 48-51.

Gagge AP. (1937). A new physiological variable associated with sensible and insensible perspiration. *American Journal of Physiology-Legacy Content* **120,** 277-287.

Garcia CK, Renteria LI, Leite-Santos G, Leon LR & Laitano O. (2022). Exertional heat stroke: pathophysiology and risk factors. *BMJ Medicine* **1,** e000239.

Grundstein A & Cooper E. (2018). Assessment of the Australian Bureau of Meteorology wet bulb globe temperature model using weather station data. *International Journal of Biometeorology* **62,** 2205-2213.

Grundstein A & Cooper E. (2020). Comparison of WBGTs over Different Surfaces within an Athletic Complex. In *Medicina*.

Guyer H, Georgescu M, Hondula DM, Wardenaar F & Vanos J. (2021). Identifying the need for locally-observed wet bulb globe temperature across outdoor athletic venues for current and future climates in a desert environment. *Environmental Research Letters* **16,** 124042.

Havenith G & Fiala D. (2015). Thermal Indices and Thermophysiological Modeling for Heat Stress. In *Comprehensive Physiology*, pp. 255-302.

Hobson RM & Maughan RJ. (2010). Hydration status and the diuretic action of a small dose of alcohol. *Alcohol* **45,** 366-373.

Hosokawa, Y., Grundstein, A. J., & Casa, D. J. (2018). Extreme Heat Considerations in International Football Venues: The Utility of Climatologic Data in Decision Making. *Journal of athletic training*, *53*(9), 860–865. https://doi.org/10.4085/1062-6050-361-17

Hughson RL, Staudt LA & Mackie JM. (1983). Monitoring Road Racing in the Heat. *Phys Sportsmed* **11,** 94-105.

Jay O, Broderick C & Smallcombe JW. (2021). Extreme Heat Policy, ed. Australia SM, pp. 12. Sports Medicine Australia.

Kosaka E, Iida A, Vanos J, Middel A, Yokohari M & Brown R. (2018). Microclimate Variation and Estimated Heat Stress of Runners in the 2020 Tokyo Olympic Marathon. *Atmosphere* **9,** 192.

Larsen T, Kumar S, Grimmer K, Potter A, Farquharson T & Sharpe P. (2007). A systematic review of guidelines for the prevention of heat illness in community-based sports participants and officials. *Journal of Science and Medicine in Sport* **10,** 11-26.

Liljegren JC, Carhart RA, Lawday P, Tschopp S & Sharp R. (2008). Modeling the Wet Bulb Globe Temperature Using Standard Meteorological Measurements. *Journal of Occupational and Environmental Hygiene* **5,** 645-655.

Liu Z & Jim CY. (2021). Playing on natural or artificial turf sports field? Assessing heat stress of children, young athletes, and adults in Hong Kong. *Sustainable Cities and Society* **75,** 103271.

Liuzzo L, Viola F & Noto LV. (2016). Wind speed and temperature trends impacts on reference evapotranspiration in Southern Italy. *Theoretical and Applied Climatology* **123,** 43-62.

Luies N, Orchard JJ, Driscoll T, Sahdra SK, Cheng J, Davis AJ & Orchard JW. (2023). Sheffield Shield Cricketers Live Longer than the Age-Matched General Australian Male Population. *Indian Journal of Orthopaedics* **57,** 1613-1618.

Mishra V, Ambika AK, Asoka A, Aadhar S, Buzan J, Kumar R & Huber M. (2020). Moist heat stress extremes in India enhanced by irrigation. *Nature Geoscience* **13,** 722-728.

Nichols AW. (2014). Heat-related illness in sports and exercise. *Current Reviews in Musculoskeletal Medicine* **7,** 355-365.

Orr M, Inoue Y, Seymour R & Dingle G. (2022). Impacts of climate change on organized sport: A scoping review. *WIREs Climate Change* **13,** e760.

Parsons K. (2019). *Human heat stress*. CRC press.

Perkins-Kirkpatrick S & Gibson P. (2017). Changes in regional heatwave characteristics as a function of increasing global temperature. *Scientific Reports* **7,** 1-12.

Pryor, J. L., Pryor, R. R., Grundstein, A., & Casa, D. J. (2017). The Heat Strain of Various Athletic Surfaces: A Comparison Between Observed and Modeled Wet-Bulb Globe Temperatures. *Journal of athletic training*, *52*(11), 1056–1064. https://doi.org/10.4085/1062-6050-52.11.15

Racinais S, Hosokawa Y, Akama T, Bermon S, Bigard X, Casa DJ, Grundstein A, Jay O, Massey A, Migliorini S, Mountjoy M, Nikolic N, Pitsiladis YP, Schobersberger W, Steinacker JM, Yamasawa F, Zideman DA, Engebretsen L & Budgett R. (2023). IOC consensus statement on recommendations and regulations for sport events in the heat. *British Journal of Sports Medicine* **57,** 8-25.

Tripp B, Vincent HK, Bruner M & Smith MS. (2020). Comparison of wet bulb globe temperature measured on-site vs estimated and the impact on activity modification in high school football. *International Journal of Biometeorology* **64,** 593-600.

Valipour M. (2015). Importance of solar radiation, temperature, relative humidity, and wind speed for calculation of reference evapotranspiration. *Archives of Agronomy and Soil Science* **61,** 239-255.

Table 1. Table of data collection venues and BoM site characteristics.

Days collected = 29, totalling 161 hours 28 minutes of data

Stadium	**City, State**	**Data volume (hh:mm)**	**BoM station #1**	**Site ID**	**BoM station #2**	**Site ID**	**Seating capacity**	**Venue type**
Bankstown Oval	Sydney, NSW	11:54	Bankstown	066137	Canterbury	066194	8,000	Minor
Blacktown ISP	Sydney, NSW	12:12	Horsley Park	067119	Bankstown	066137	10,000	Minor
Drummoyne Oval	Sydney, NSW	6:00	Sydney Olympic Park	066212	Observatory Hill	066214	5,500	Minor
Howell Oval	Sydney, NSW	11:22	Penrith Lakes	067113	Badgery's Creek	061708	-	Minor
Sydney University Oval	Sydney, NSW	10:50	Sydney Airport	066037	Canterbury	066194	2,000	Minor
Hurstville Oval	Sydney, NSW	6:00	Bankstown	066137	Sydney Airport	066037	5,000	Minor
Spotless Stadium	Sydney, NSW	2:30	Sydney Olympic Park	066212	Canterbury	066194	23,600	Major
SCG	Sydney, NSW	12:20	Observatory Hill	066214	Sydney Airport	066037	48,000	Major
Traeger Park	Alice Springs, NT	12:42	Alice Springs Airport	023034	n/a	n/a	7,200	Minor
Allan Border Field	Brisbane, QLD	12:20	Brisbane	040193	n/a	n/a	6,500	Minor
Great Barrier Reef Arena	Mackay, QLD	12:51	Mackay Airport	033045	n/a	n/a	10,000	Minor
Riverway Stadium	Townsville QLD	12:04	Townsville Aerodrome	032040	Mt Stuart	032195	10,000	Minor
Adelaide Oval	Adelaide, SA	12:25	West Terrace (Ngayidapira)	023000	Adelaide Airport	023034	53,500	Major
Karen Rolton Oval	Adelaide, SA	12:21	West Terrace (Ngayidapira)	023000	Adelaide Airport	023034	5,000	Minor
Optus Stadium	Perth, WA	11:57	Perth Metro	09225	Perth Airport	09021	60,000	Major
WACA Ground	Perth, WA	12:00	Perth Metro	09225	Perth Airport	09021	24,500	Major

New South Wales = NSW, Northern Territory = NT, South Australia = SA, Western Australia = WA, Queensland = QLD, WACA = Western Australia Cricket Association, SCG = Sydney Cricket Ground, "-" = unreported, N/a indicates no appropriate secondary BoM site was available

Table 2. The percentage of time the Cricket Australia (CA) Heat Stress Risk Index (HSRI) categories differ on-site (EMU) compared to off-site (BoM) for all venues.

	Heat Stress Risk Index	**Low (0.0-3.9) 'proceed as normal'**			**Moderate (4.0-7.9) 'extended breaks'**				**High (8.0-9.9) 'extended extra breaks**			**Extreme (>10.0) 'consider suspending play'**			**ΔHSRI across all HSRI categories**				
Stadium	**ΔHSRI (BoM- EMU)**	-2	-1	0	-2	-1	0	1	-1	0	1	0	1	2	-2	-1	0	1	2
Adelaide Oval (SA)	**West Terrace**								4			96				4	96		
	Adelaide Airport				5				1			93			5	1	93		
AB Field (QLD)	**Brisbane**		11	19			45	25								11	64	25	
Bankstown Oval (NSW)	**Bankstown**		18	6	18	1	1		13			35			18	40	42		
	Canterbury			9			17	3		6	6	54	6				86	14	
	Sydney Olympic Park		5			8	11		14			62				27	73		
Blacktown ISP (NSW)	**Bankstown**	6	1	12	5	3	22	3	2	11		16		1	11	24	61	3	
	Horsley Park	6	8	15		7	15		5	7		36		1	5	20	73		
Drummoyne Oval (NSW)	**Observatory Hill**		11	17	6	31	34								6	43	51		
	Sydney Olympic Park			11	3	9	37	6	3	23	9				3	11	71	14	
GBRA (QLD)	**Mackay Aerodrome**				2	5	8		14	2		7			2	19	79		
Howell Oval (NSW)	**Badgery's Creek**		14		6	9	6		17			49			6	40	54		
	Penrith Lakes		6		1	4	22		7	3	1	46	9		1	18	71	10	
Hurstville Oval (NSW)	**Bankstown**									6		91	3				97	3	
	Sydney Airport									3		91	6				94	6	
Karen Rolton Oval (SA)	**West Terrace**					1	16			13	1	67	1			1	96	3	
	Adelaide Airport						13			8		63	16				84	16	
Optus Stadium (WA)	**Perth Airport**			7			17	44			24			8			24	68	8
	Perth Metro		1	17			44	34			4					1	61	38	
Riverway Stadium (QLD)	**Townsville Aero**								3			97					100		
	Mt Stuart											10				3	97		
SCG (NSW)	**Observatory Hill**			31	2	2	2	38			5	3			2	2	54	43	
	Sydney Airport			7				93									7	93	
Spotless Stadium (NSW)	**Bankstown**				21	14			43			21			21	57	21		
	Sydney Olympic Park								21	7		64	7			21	71	7	
University of Sydney Oval (NSW)	**Sydney Airport**		5	2			23		2	3		48					97	3	
	Observatory Hill		2	2	6		26		2	3		23			6	22	72		
	Canterbury			18			28	2		2		49	2			6	94		
Tragear Park (NT)	**Alice Springs Airport**									8		92					100		
WACA (WA)	**Perth Airport**											89	10	1			89	10	1
	Perth Metro				7	6			15	1	1	67	3		7	21	68	4	

Agreement in environmental conditions between BoM sites and playing surfaces

Where: AB Field is Allan Border Field, GBRA is Great Barrier Reef Arena, SCG is Sydney Cricket Ground, and WACA is Western Australia Cricket Ground. -3, -2, -1 represent the BoM underestimating the HSRI by 1-3 categories, and +1 and +2 represent the BoM overestimating the CA HSRI by 1-2 categories. The 0 columns represent the categorical agreement between EMU and BoM measures of heat stress risk. Note that some rows may not add to 100% due to rounding. New South Wales = NSW, Northern Territory = NT, South Australia = SA, Western Australia = WA, Queensland = QLD, WACA = Western Australia Cricket Association, SCG = Sydney Cricket Ground.

Figure 1. Schematic of approximate data collection locations across Australia. 1 = Sydney, NSW, 2 = Mackay, QLD, 3 = Perth, WA, 4 = Alice Springs, NT, 5 = Brisbane, QLD 6 =. Adelaide, SA, 7 = Townsville, QLD.

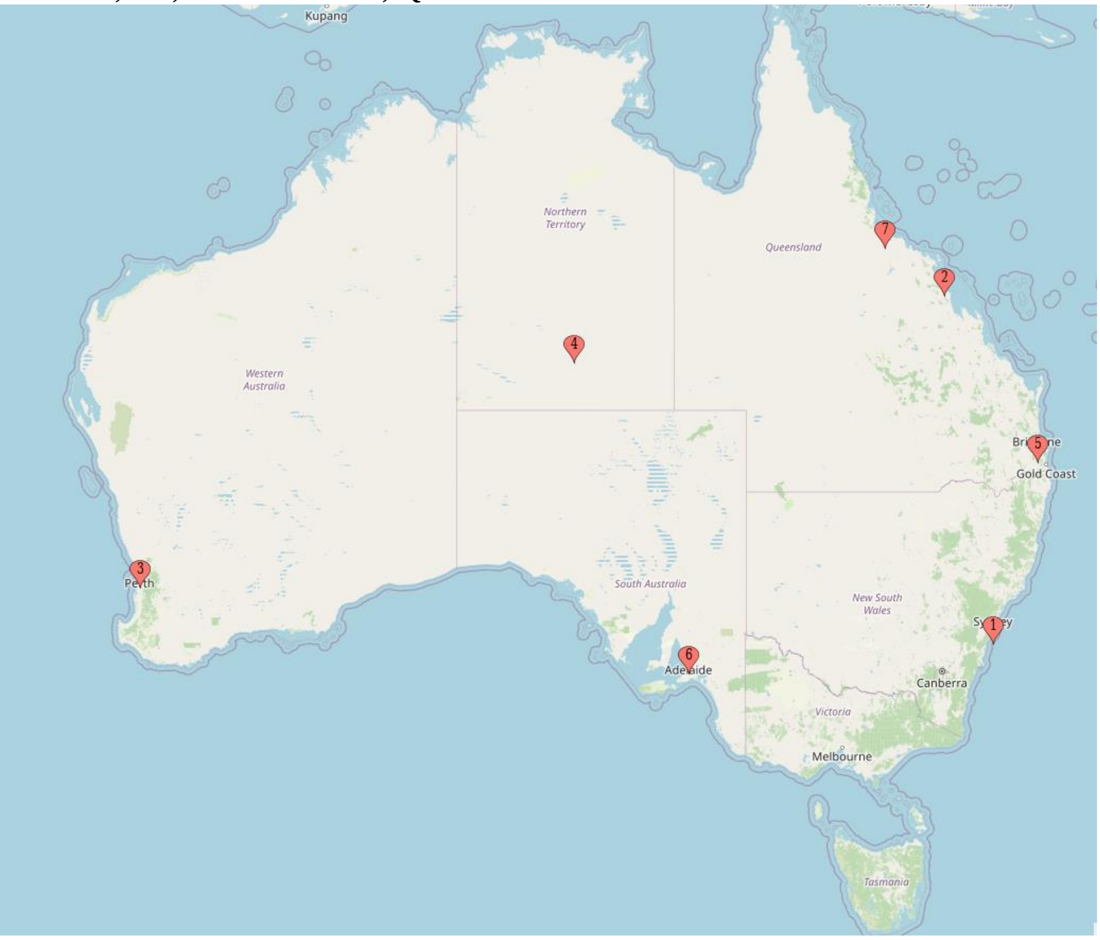

Figure 2. Schematic of EMU locations on the playing surface. One EMU was located behind the wickets area, and the second was placed inside from the boundary rope. Note – image is not to scale.

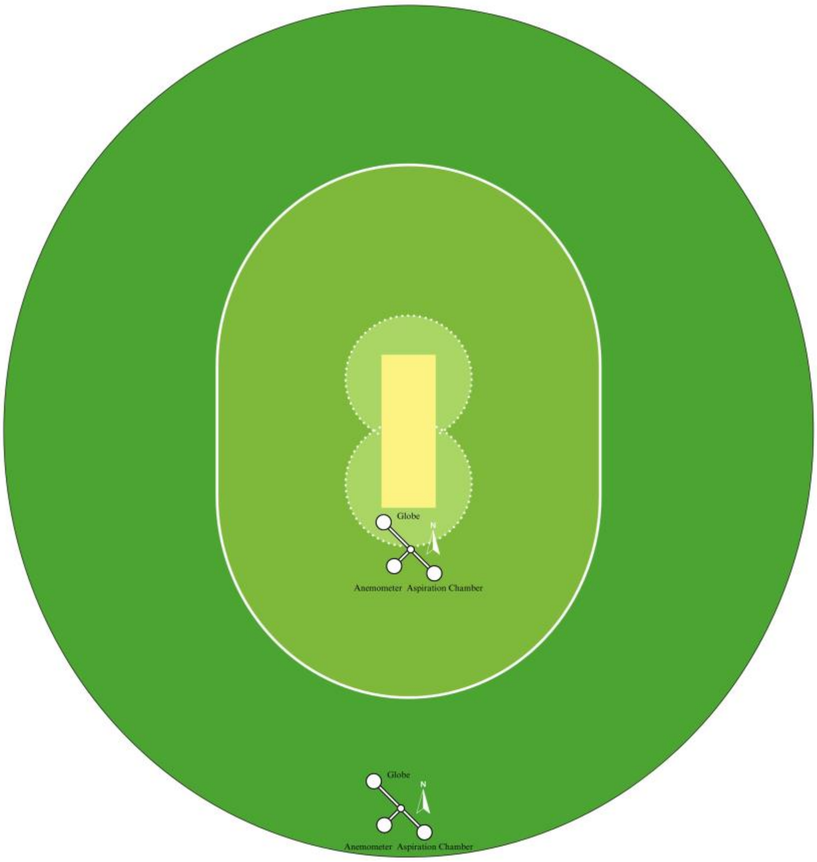

Figure 3. A summary of the environmental conditions encountered across all venues over all days. Top left – playing surface HSRI versus BoM site HSRI comparison. Top right– playing surface versus BoM station T_a comparison, bottom left – playing surface versus BoM site WS comparison, bottom right – playing surface versus BoM site RH comparison. Each hexbin and the corresponding colour code on the colour bar represents the total count of 10 minutes of data, where the darker the colour, the more data that falls within the hexbin.

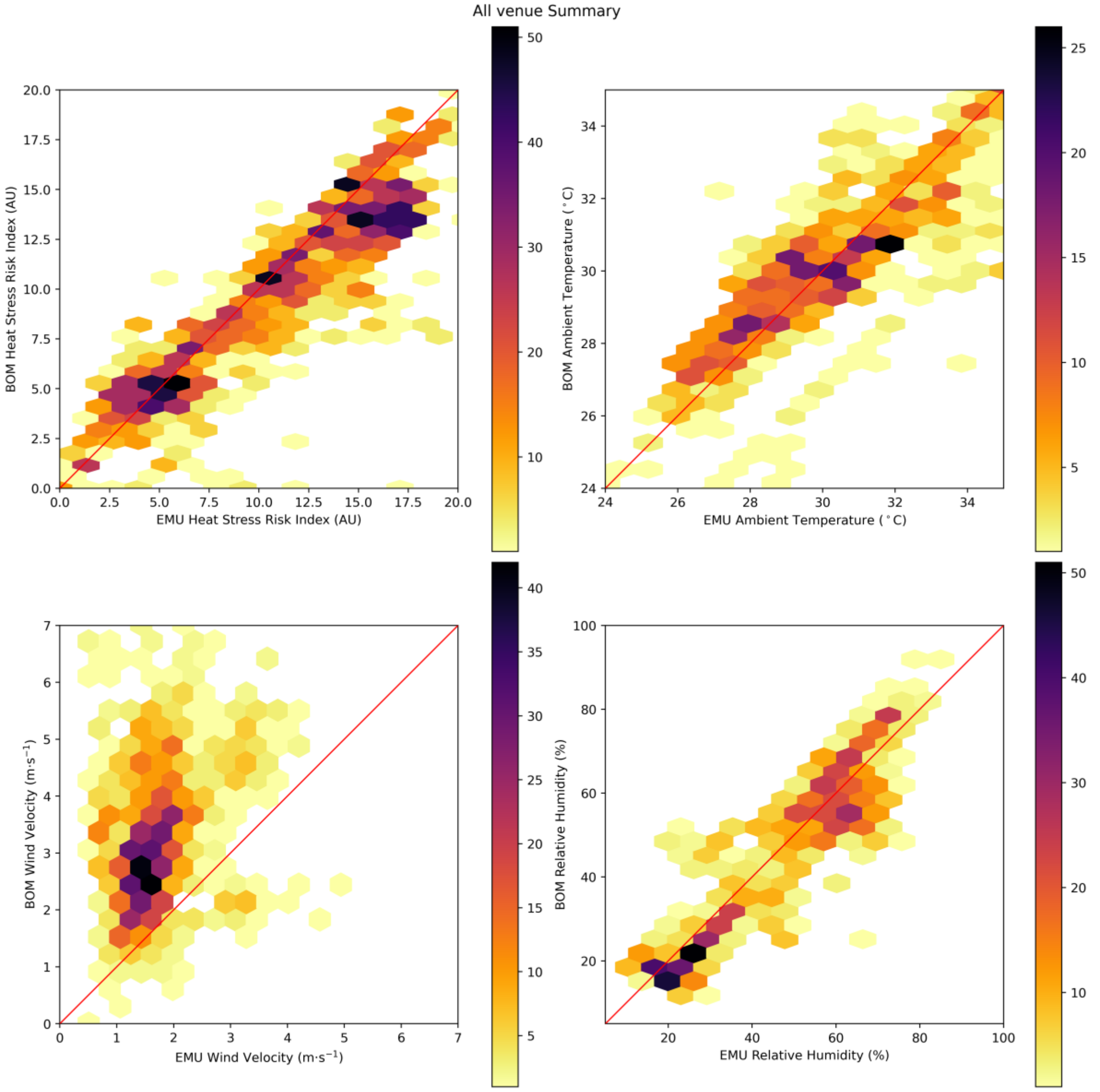

Figure 4. Mean HSRI and environmental conditions across all Major and Minor stadia. First row – time series average of the HSRI for Major and Minor Stadia. Second row – time series average of dry-bulb temperature for Major and Minor stadia. Third row – time series average of relative humidity for Major and Minor Stadia. Fourth row - time series average of air velocity for Major and Minor Stadia. Data are 10-min averages and are expressed in the figures as mean and 95% confidence intervals.

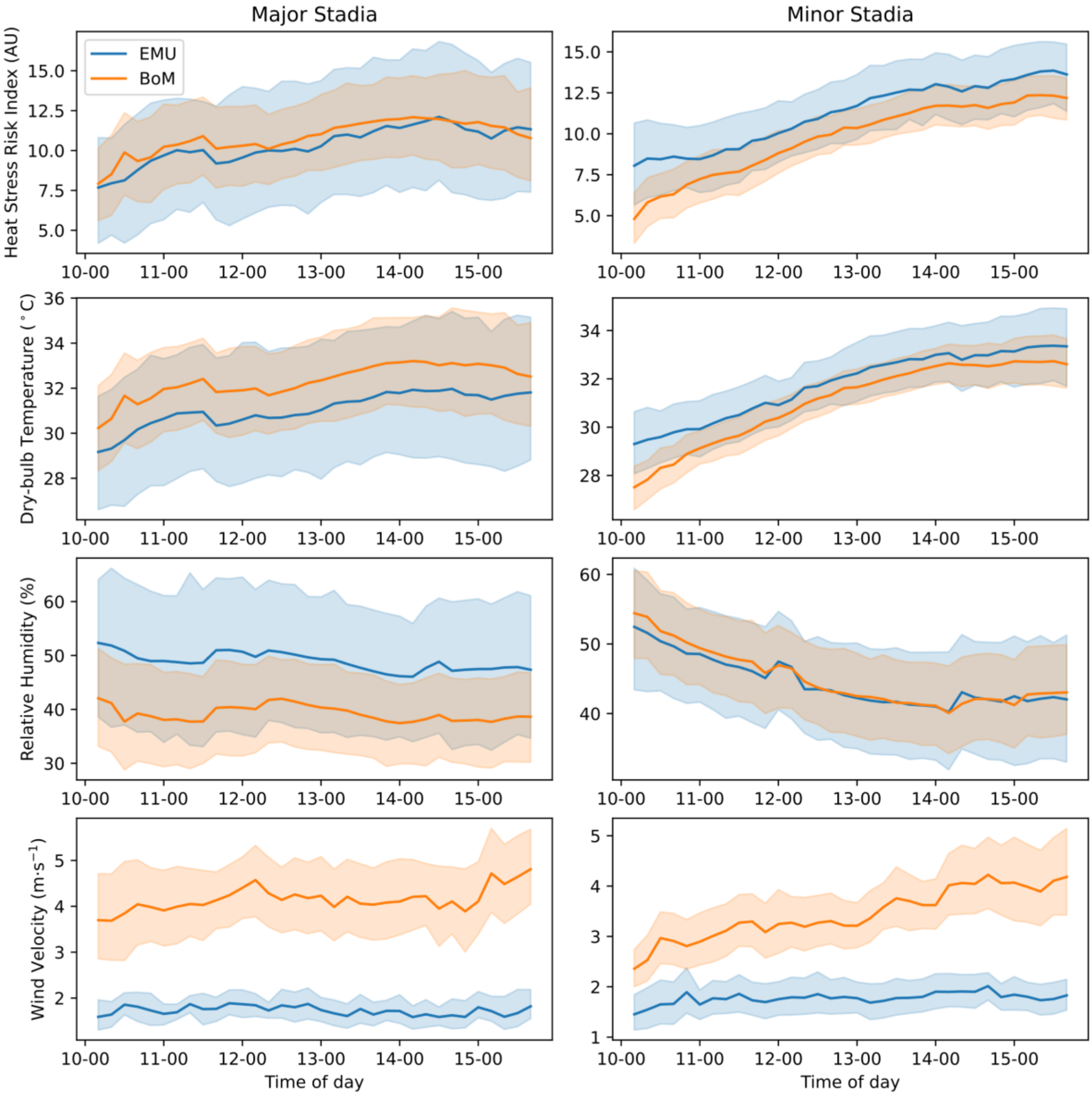

Figure 5. BoM accuracy scores for Major and Minor stadia. Left – the percentage of time spent when playing surface (EMU) categories agree with BoM sites, 0 = categorical agreement regardless of HSRI category. For example, if the EMU reports a 7 and the BOM reports a 6 then the categories agree, however, if the EMU reports a 5 and the BoM reports a 3 then the categories are mismatched by -1 and the BoM is underpredicting the heat stress experienced on field. HSRI category thresholds are: low risk = 0.0-3.9, moderate risk = 4.0-7.9, high risk = 8.0-9.9 and extreme risk is ≥10. Right – accuracy (%) of nearest BoM sites for Major and Minor stadia. Top right – accuracy (%) of nearest BoM site, plotted by the distance, for Major and Minor venues.

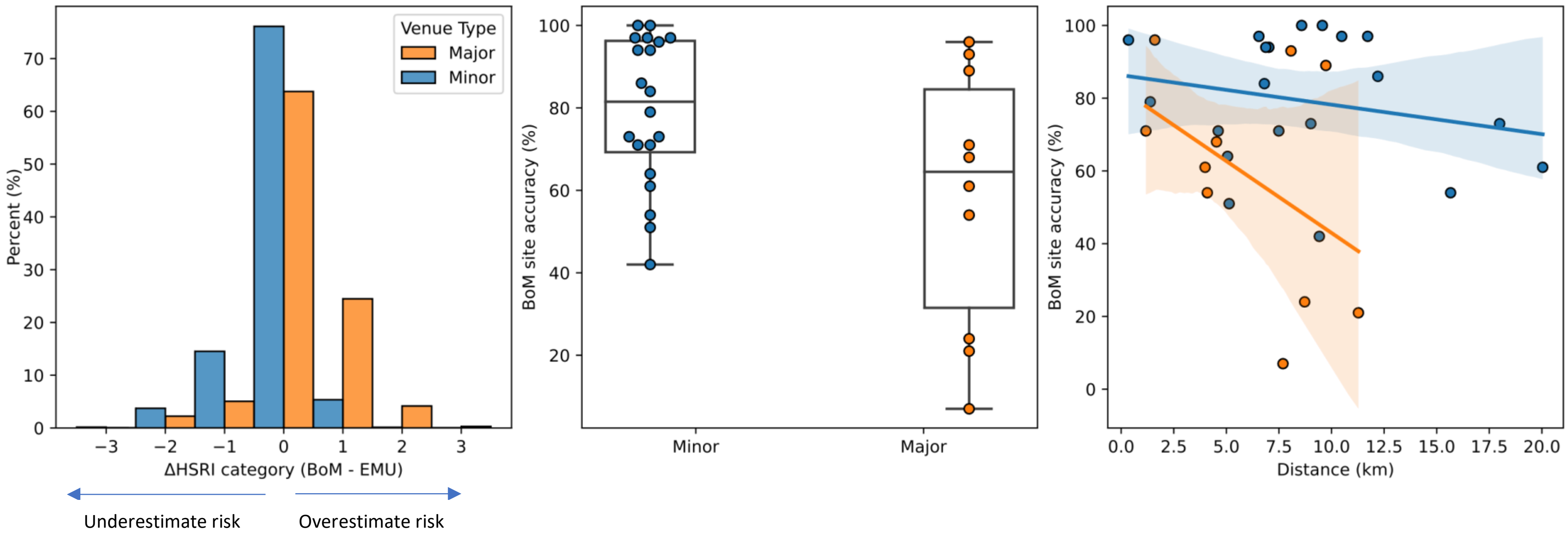

Supplementary individual figures. The following figures are a summary of the environmental conditions encountered across each venue over all days. Top left – playing surface HSRI versus BoM site HSRI comparison. Top right– playing surface versus BoM station T_a comparison, bottom left – playing surface versus BoM site WS comparison, bottom right – playing surface versus BoM site RH comparison. Each dot and the corresponding colour code represents the day and BoM site which data were compared to and is an average of 10 minutes of data.

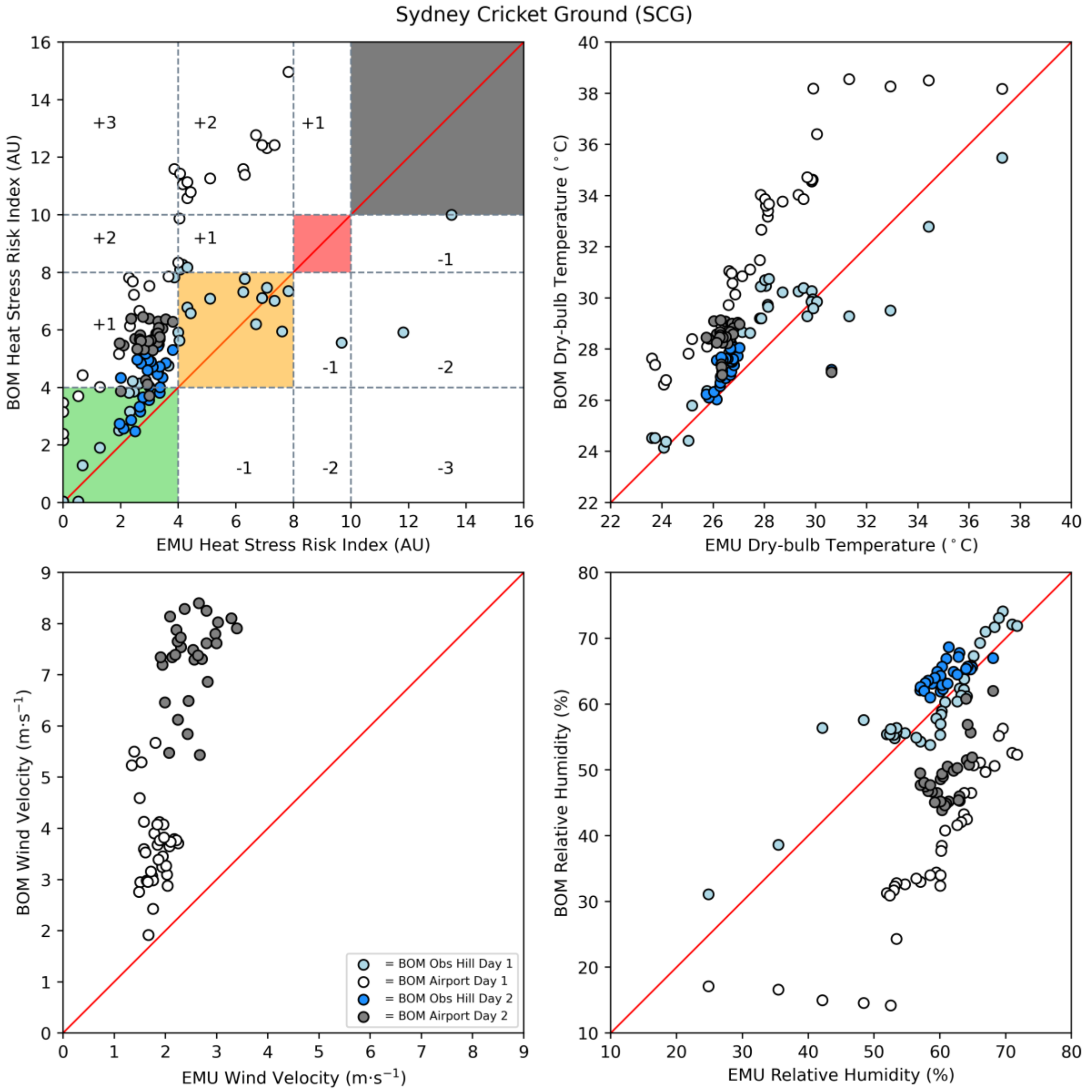

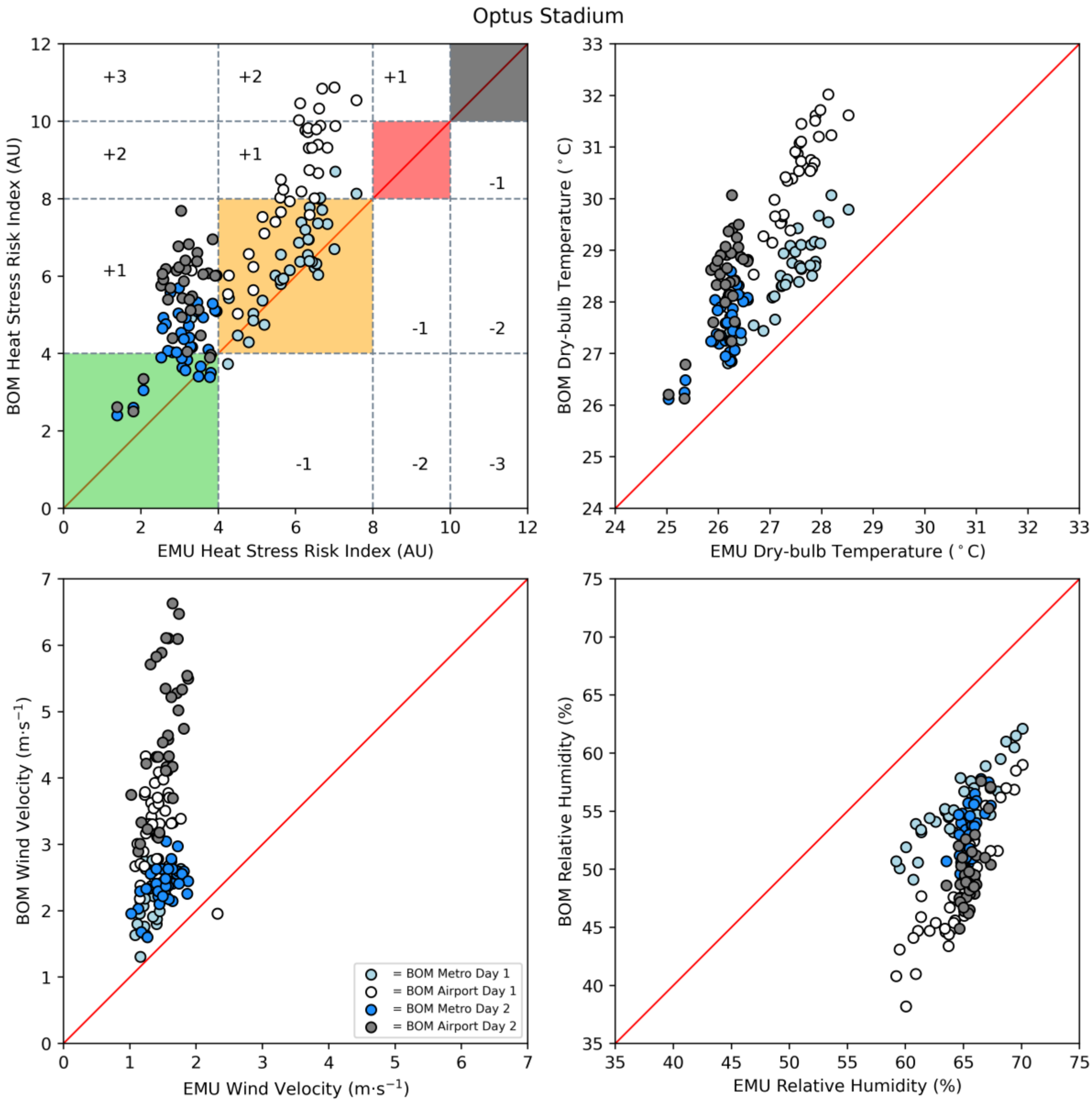
Optus Stadium
BOM Heat Stress Risk Index (AU)
EMU Heat Stress Risk Index (AU)
+3
+2
+1
-1
-2
-3
BOM Dry-bulb Temperature (°C)
EMU Dry-bulb Temperature (°C)
BOM Wind Velocity (m·s⁻¹)
EMU Wind Velocity (m·s⁻¹)
= BOM Metro Day 1
= BOM Airport Day 1
= BOM Metro Day 2
= BOM Airport Day 2
BOM Relative Humidity (%)
EMU Relative Humidity (%)

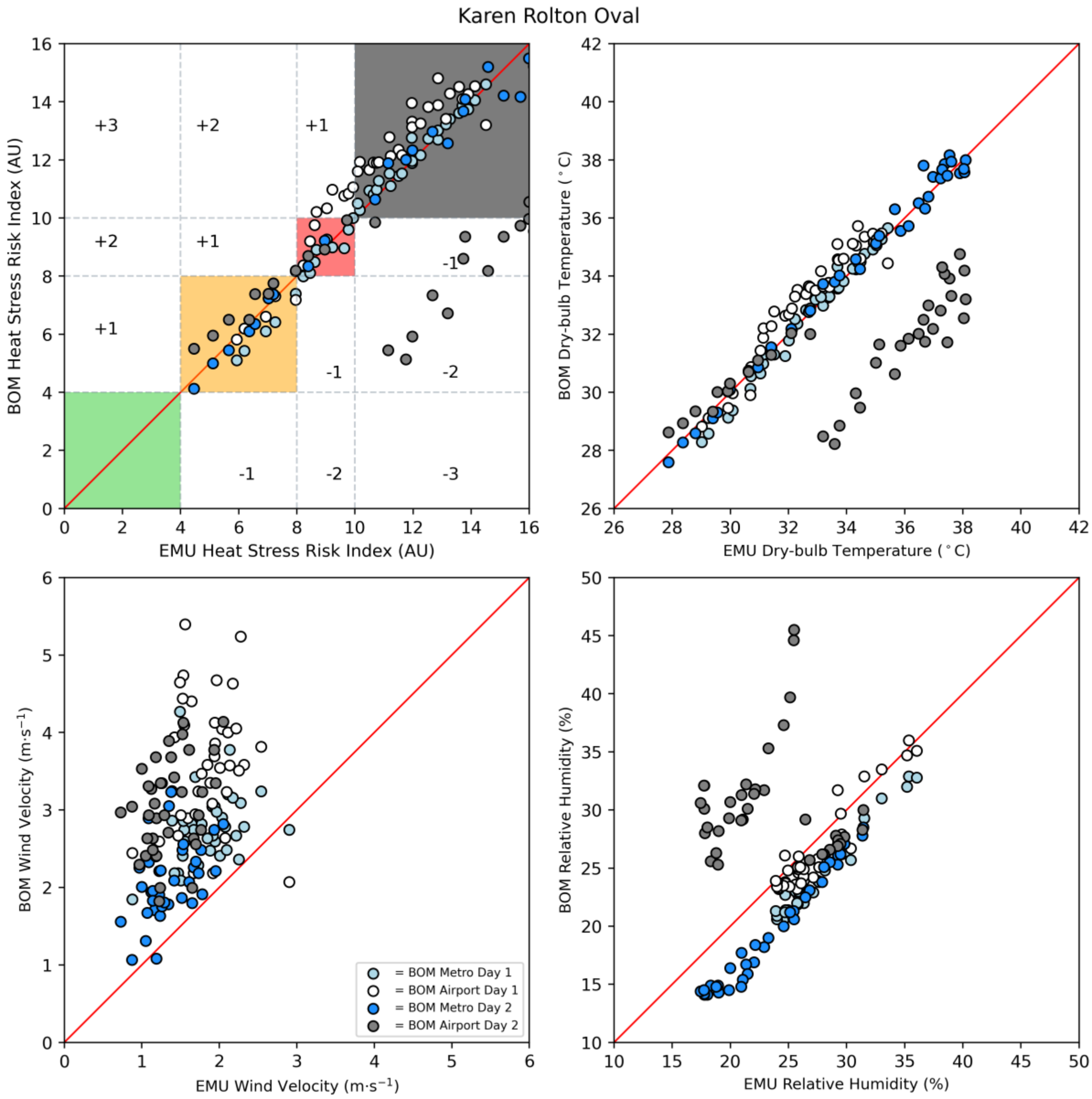
Karen Rolton Oval
BOM Heat Stress Risk Index (AU)
EMU Heat Stress Risk Index (AU)
+3
+2
+1
-1
-2
-3
BOM Dry-bulb Temperature (°C)
EMU Dry-bulb Temperature (°C)
BOM Wind Velocity (m·s⁻¹)
EMU Wind Velocity (m·s⁻¹)
= BOM Metro Day 1
= BOM Airport Day 1
= BOM Metro Day 2
= BOM Airport Day 2
BOM Relative Humidity (%)
EMU Relative Humidity (%)

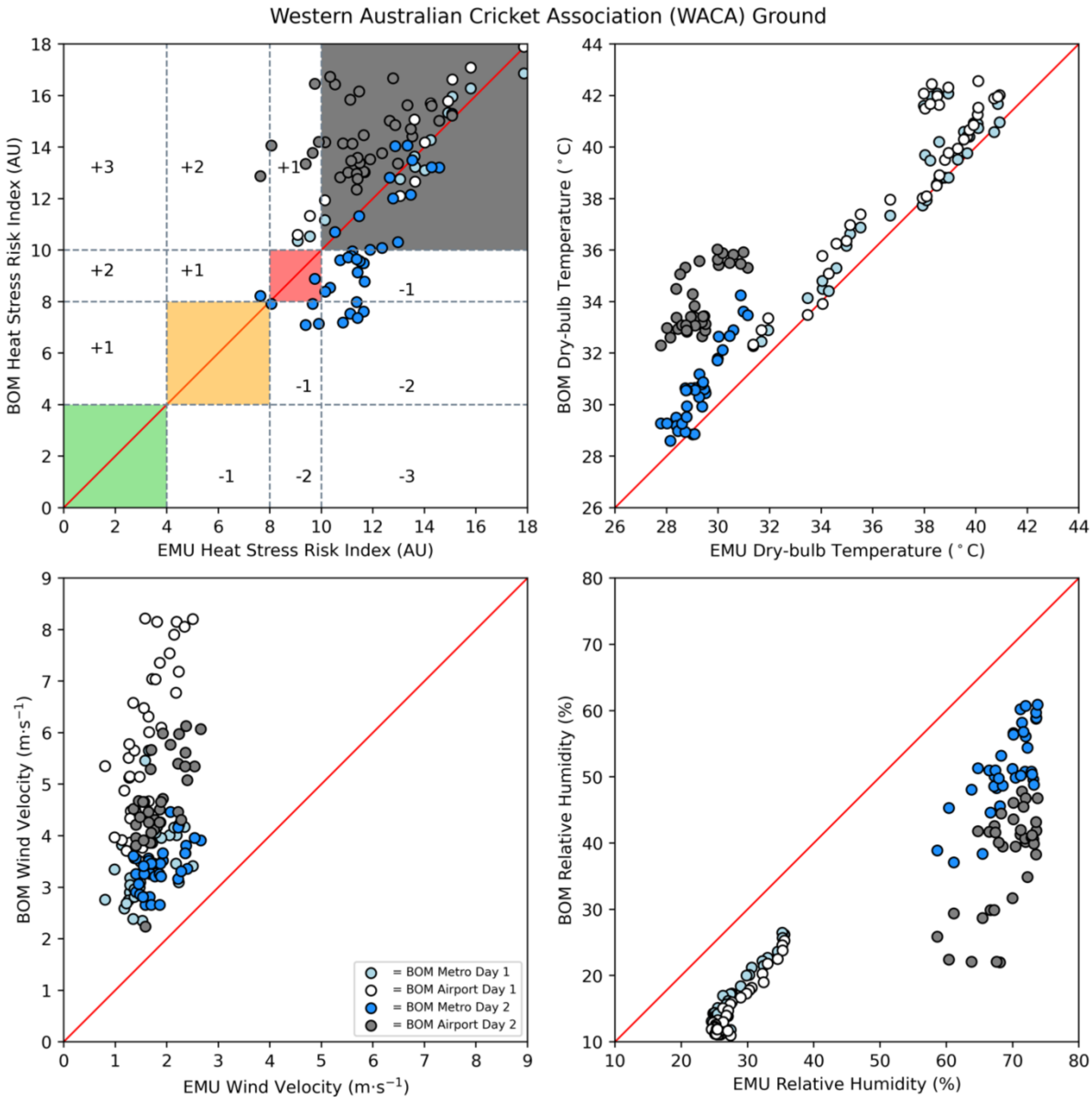

Western Australian Cricket Association (WACA) Ground
BOM Heat Stress Risk Index (AU)
EMU Heat Stress Risk Index (AU)
+3
+2
+1
-1
-2
-3
BOM Dry-bulb Temperature (°C)
EMU Dry-bulb Temperature (°C)
BOM Wind Velocity (m·s⁻¹)
EMU Wind Velocity (m·s⁻¹)
= BOM Metro Day 1
= BOM Airport Day 1
= BOM Metro Day 2
= BOM Airport Day 2
BOM Relative Humidity (%)
EMU Relative Humidity (%)

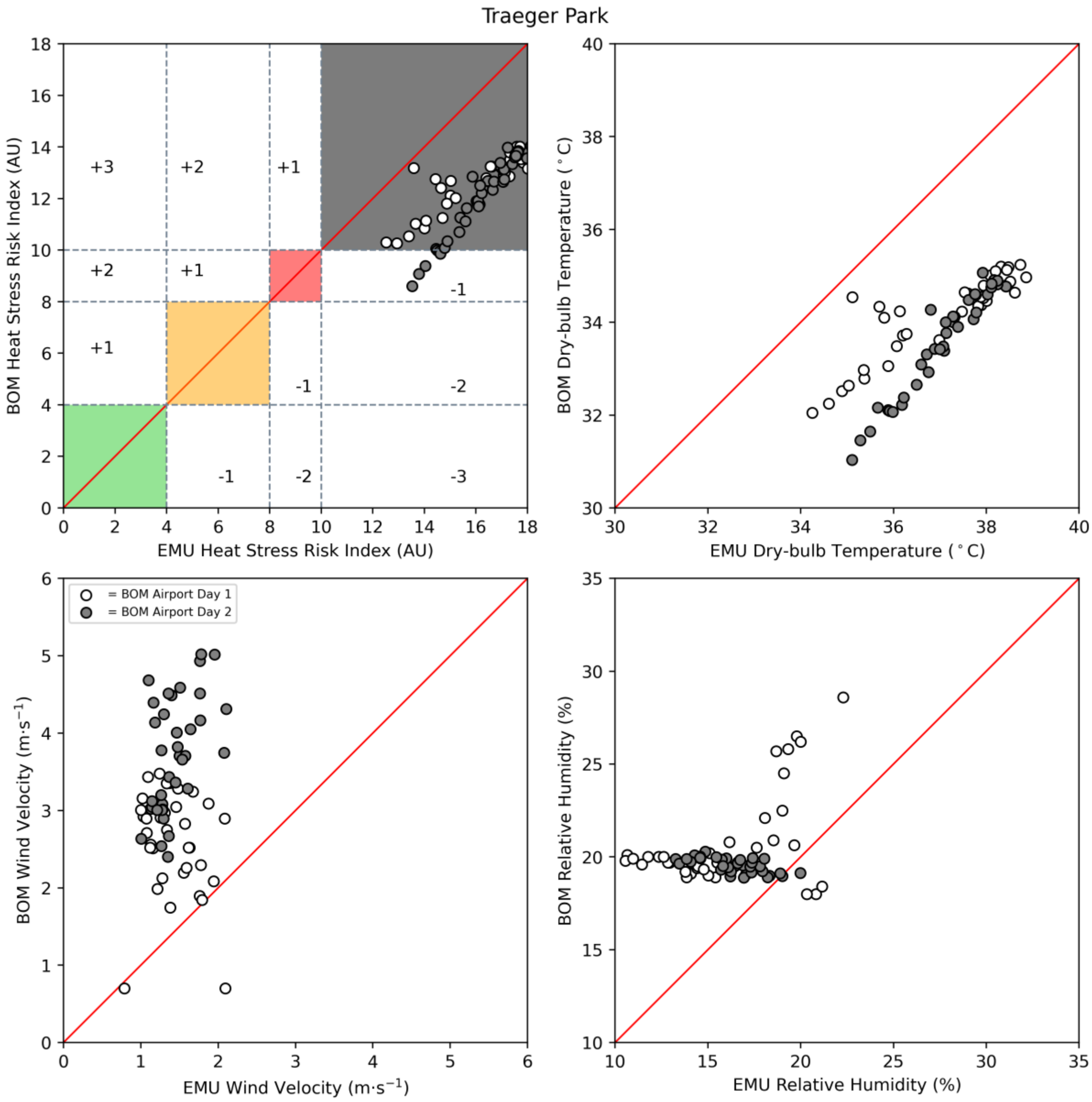
Traeger Park
BOM Heat Stress Risk Index (AU)
EMU Heat Stress Risk Index (AU)
+3
+2
+1
+2
+1
+1
-1
-1
-2
-1
-2
-3
BOM Dry-bulb Temperature (°C)
EMU Dry-bulb Temperature (°C)
= BOM Airport Day 1
= BOM Airport Day 2
BOM Wind Velocity (m·s⁻¹)
EMU Wind Velocity (m·s⁻¹)
BOM Relative Humidity (%)
EMU Relative Humidity (%)

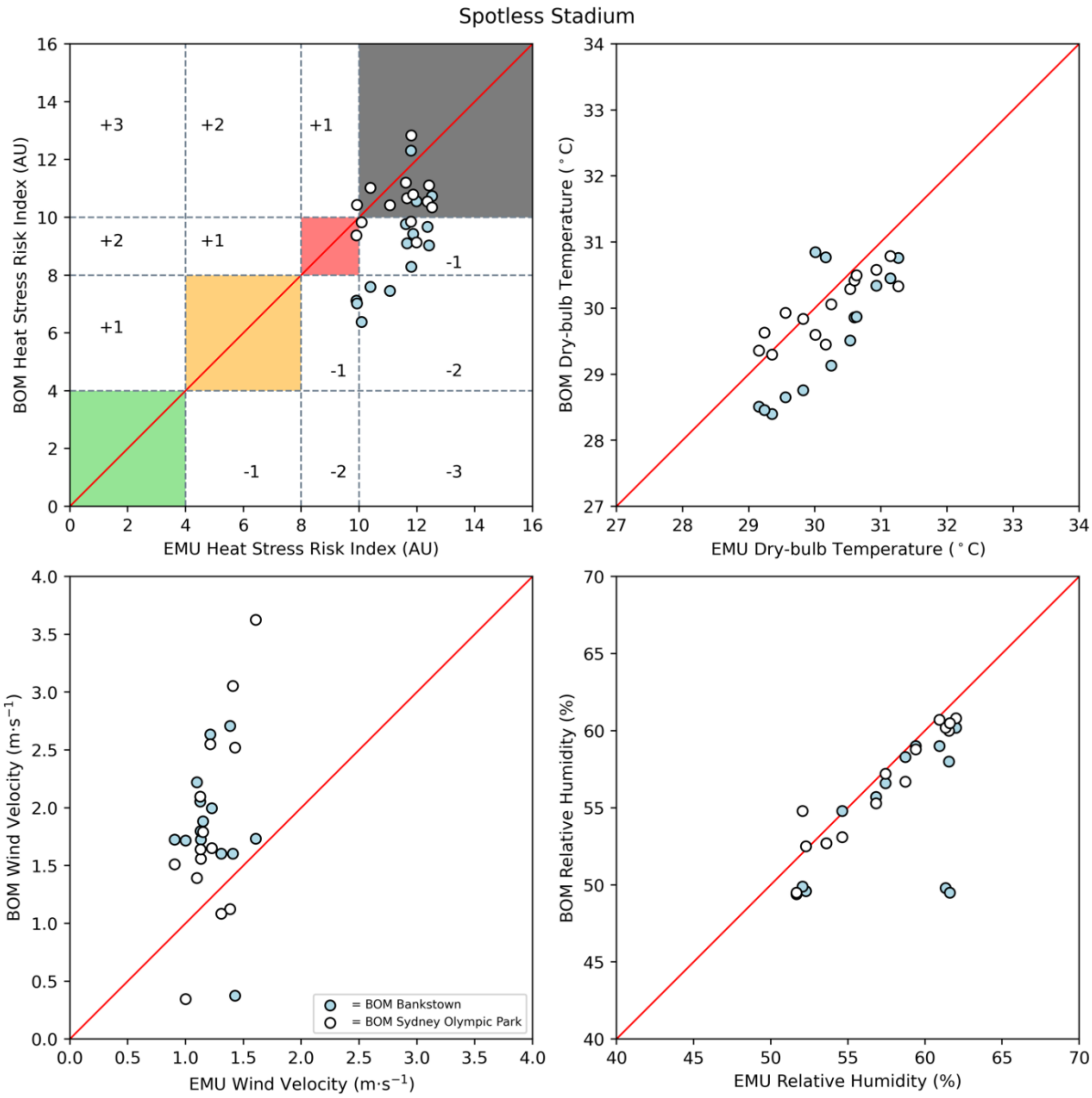
Spotless Stadium
BOM Heat Stress Risk Index (AU)
EMU Heat Stress Risk Index (AU)
+3
+2
+1
+2
+1
+1
-1
-1
-2
-1
-2
-3
BOM Dry-bulb Temperature (°C)
EMU Dry-bulb Temperature (°C)
BOM Wind Velocity (m·s⁻¹)
EMU Wind Velocity (m·s⁻¹)
= BOM Bankstown
= BOM Sydney Olympic Park
BOM Relative Humidity (%)
EMU Relative Humidity (%)

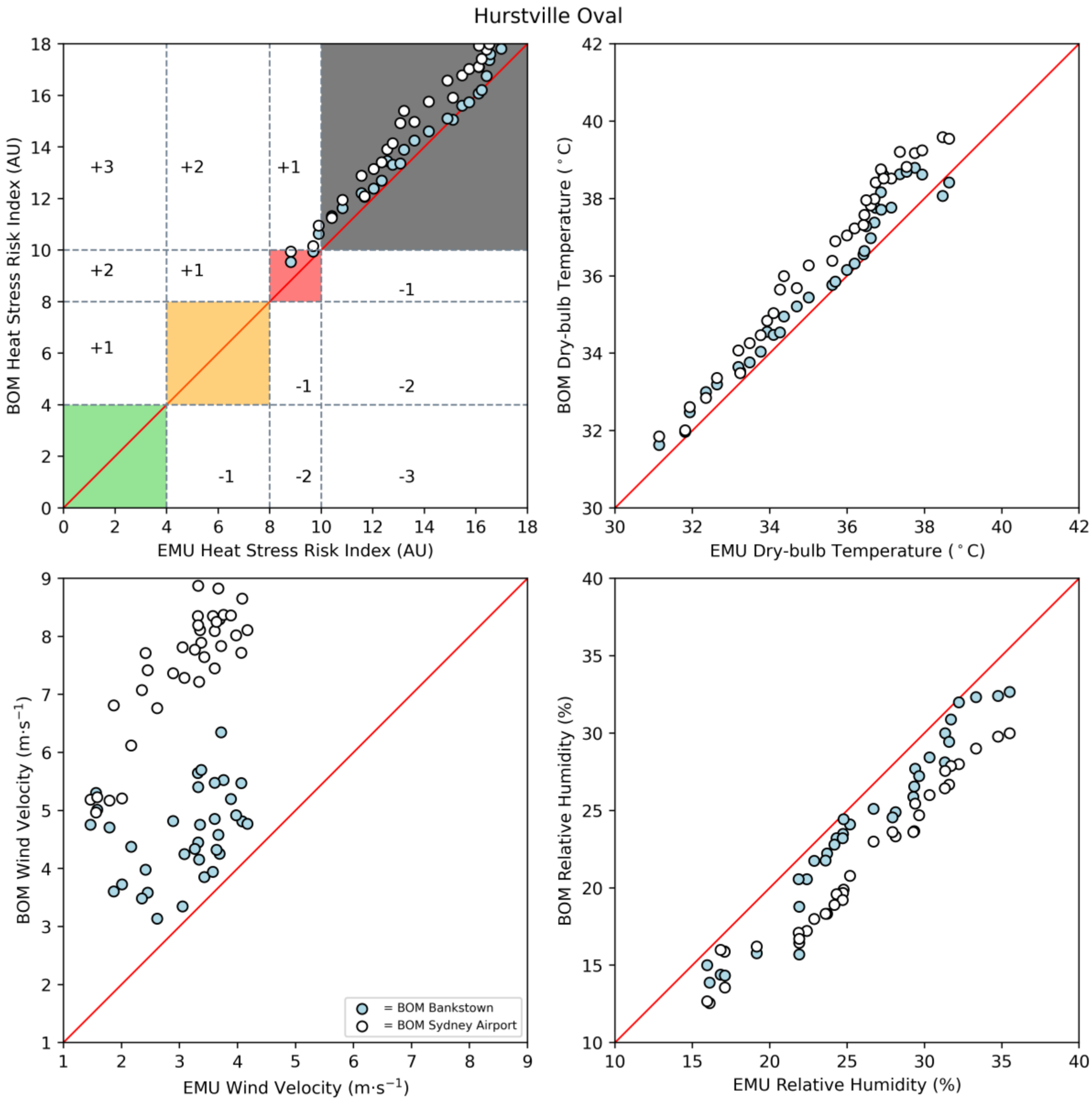
Hurstville Oval
+3
+2
+1
+2
+1
+1
-1
-1
-2
-1
-2
-3
BOM Heat Stress Risk Index (AU)
EMU Heat Stress Risk Index (AU)
BOM Dry-bulb Temperature (°C)
EMU Dry-bulb Temperature (°C)
BOM Wind Velocity (m·s⁻¹)
EMU Wind Velocity (m·s⁻¹)
= BOM Bankstown
= BOM Sydney Airport
BOM Relative Humidity (%)
EMU Relative Humidity (%)

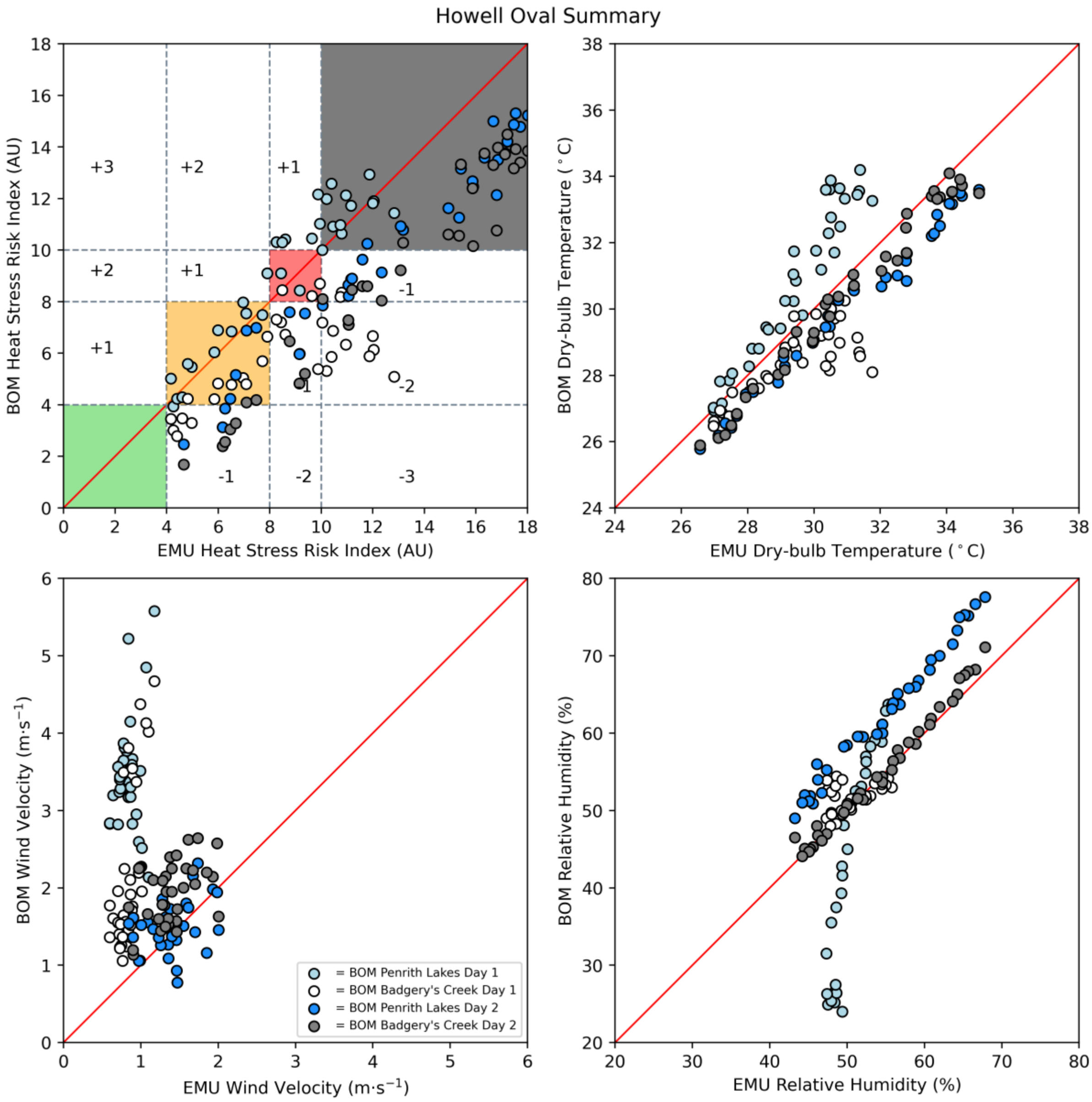
Howell Oval Summary
BOM Heat Stress Risk Index (AU)
EMU Heat Stress Risk Index (AU)
+3
+2
+1
+2
+1
+1
-1
-2
-1
-2
-3
BOM Dry-bulb Temperature (°C)
EMU Dry-bulb Temperature (°C)
BOM Wind Velocity (m·s⁻¹)
EMU Wind Velocity (m·s⁻¹)
= BOM Penrith Lakes Day 1
= BOM Badgery's Creek Day 1
= BOM Penrith Lakes Day 2
= BOM Badgery's Creek Day 2
BOM Relative Humidity (%)
EMU Relative Humidity (%)

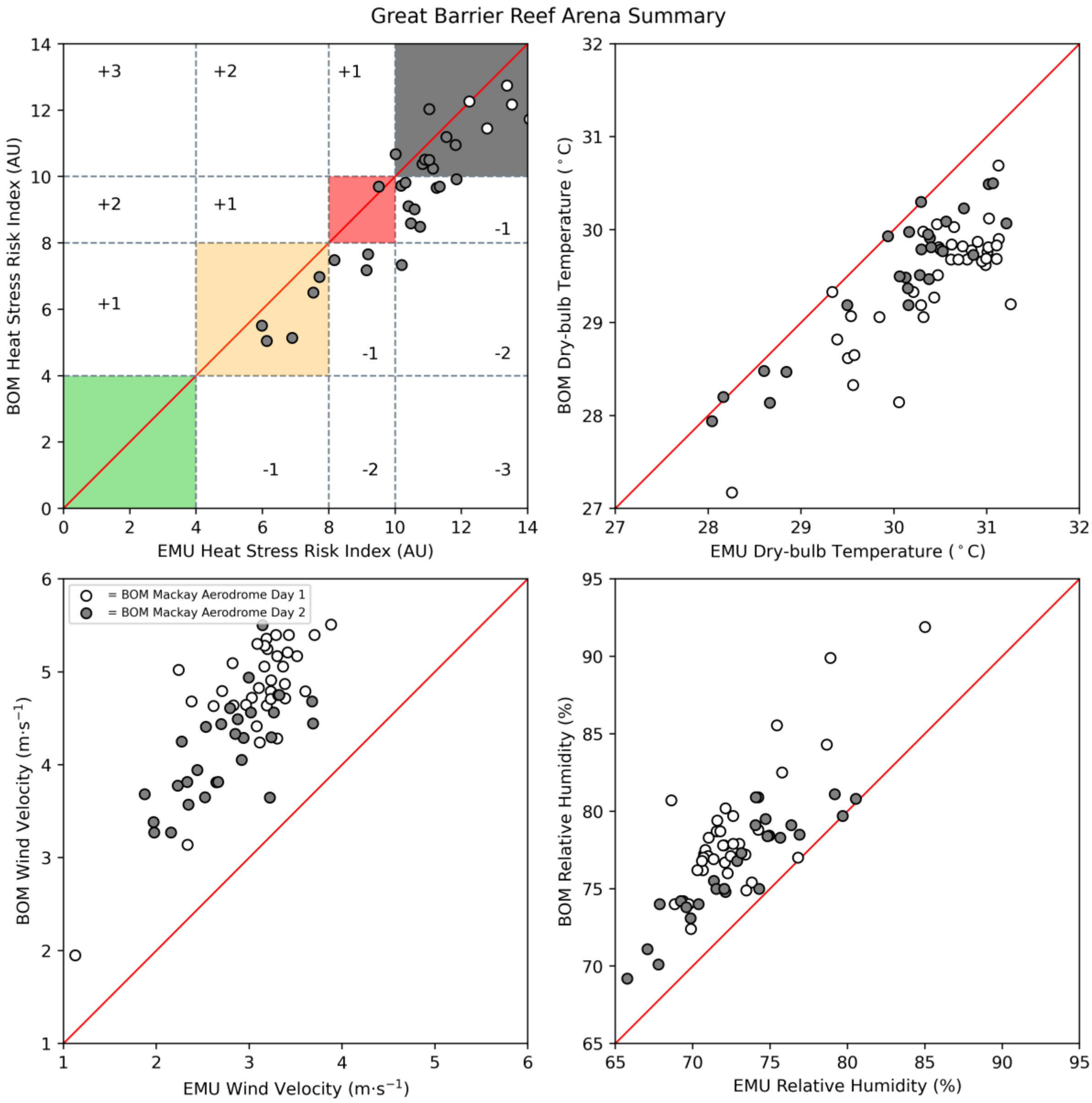

Great Barrier Reef Arena Summary
BOM Heat Stress Risk Index (AU)
EMU Heat Stress Risk Index (AU)
+3
+2
+1
-1
-2
-3
BOM Dry-bulb Temperature (°C)
EMU Dry-bulb Temperature (°C)
BOM Wind Velocity (m·s⁻¹)
EMU Wind Velocity (m·s⁻¹)
= BOM Mackay Aerodrome Day 1
= BOM Mackay Aerodrome Day 2
BOM Relative Humidity (%)
EMU Relative Humidity (%)

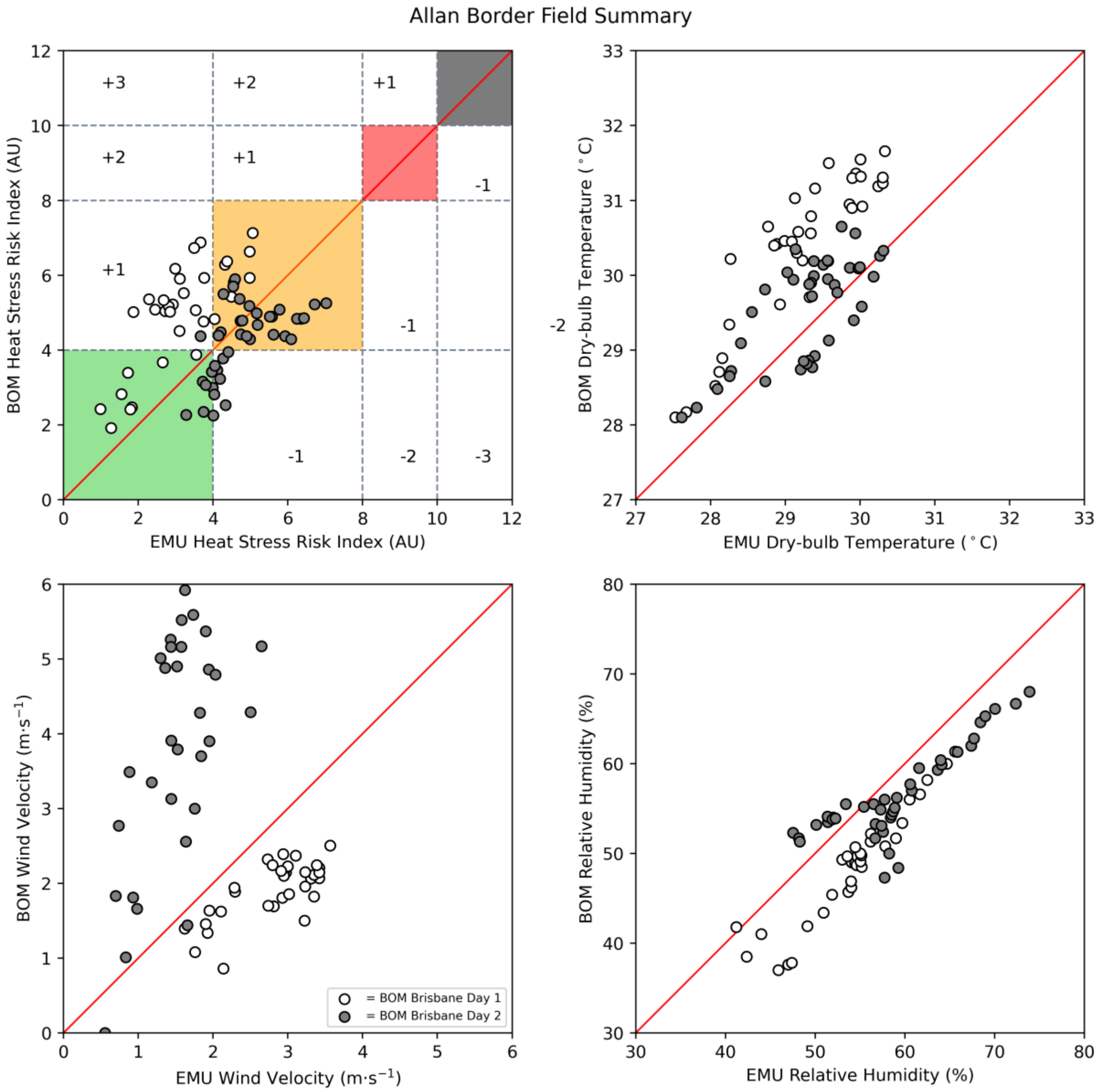
Allan Border Field Summary
BOM Heat Stress Risk Index (AU)
EMU Heat Stress Risk Index (AU)
+3
+2
+1
+2
+1
+1
-1
-1
-2
-1
-2
-3
BOM Dry-bulb Temperature (°C)
EMU Dry-bulb Temperature (°C)
BOM Wind Velocity (m·s⁻¹)
EMU Wind Velocity (m·s⁻¹)
= BOM Brisbane Day 1
= BOM Brisbane Day 2
BOM Relative Humidity (%)
EMU Relative Humidity (%)

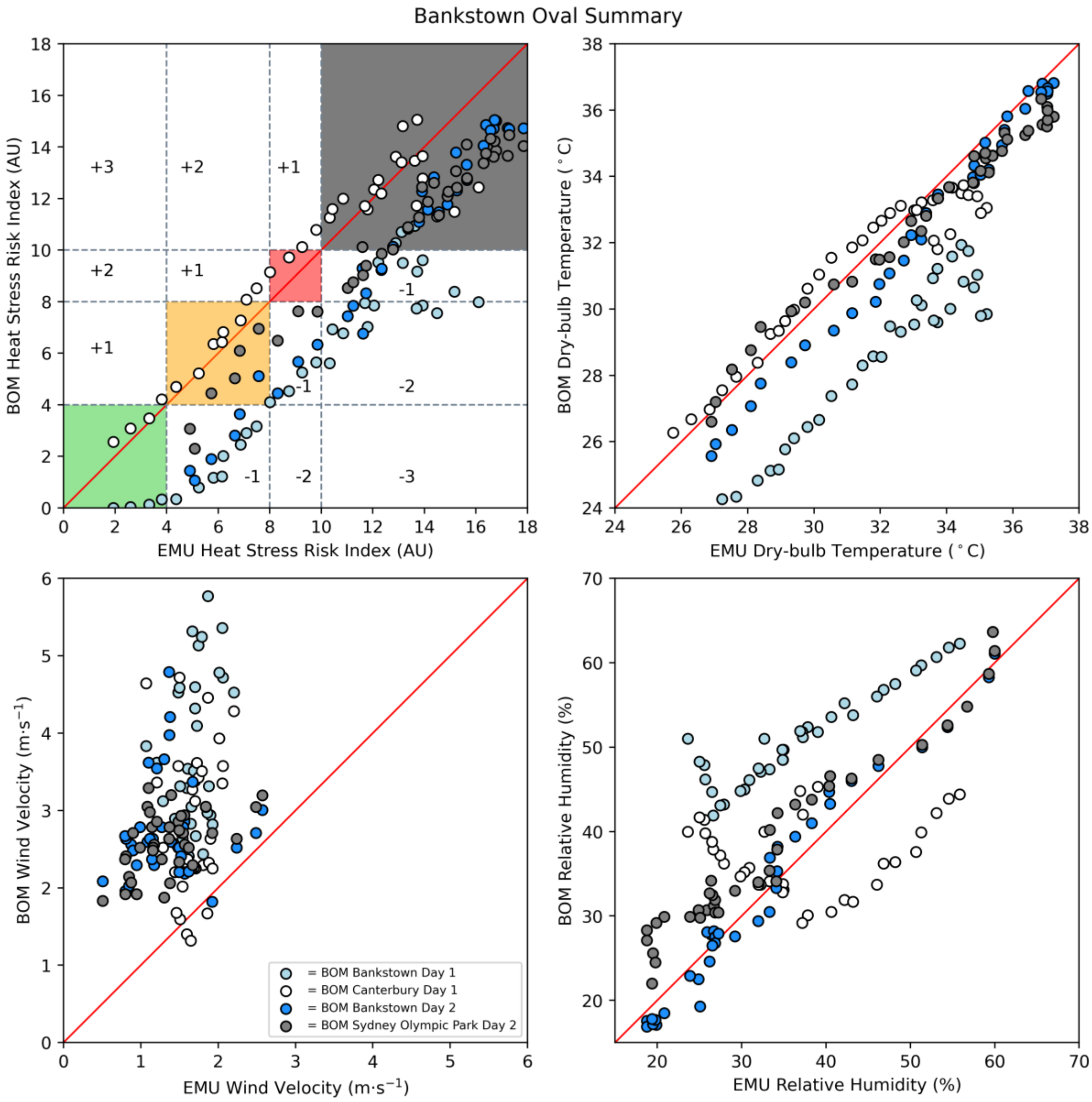
Bankstown Oval Summary
BOM Heat Stress Risk Index (AU)
EMU Heat Stress Risk Index (AU)
+3
+2
+1
-1
-2
-3
BOM Dry-bulb Temperature (°C)
EMU Dry-bulb Temperature (°C)
BOM Wind Velocity (m·s⁻¹)
EMU Wind Velocity (m·s⁻¹)
= BOM Bankstown Day 1
= BOM Canterbury Day 1
= BOM Bankstown Day 2
= BOM Sydney Olympic Park Day 2
BOM Relative Humidity (%)
EMU Relative Humidity (%)

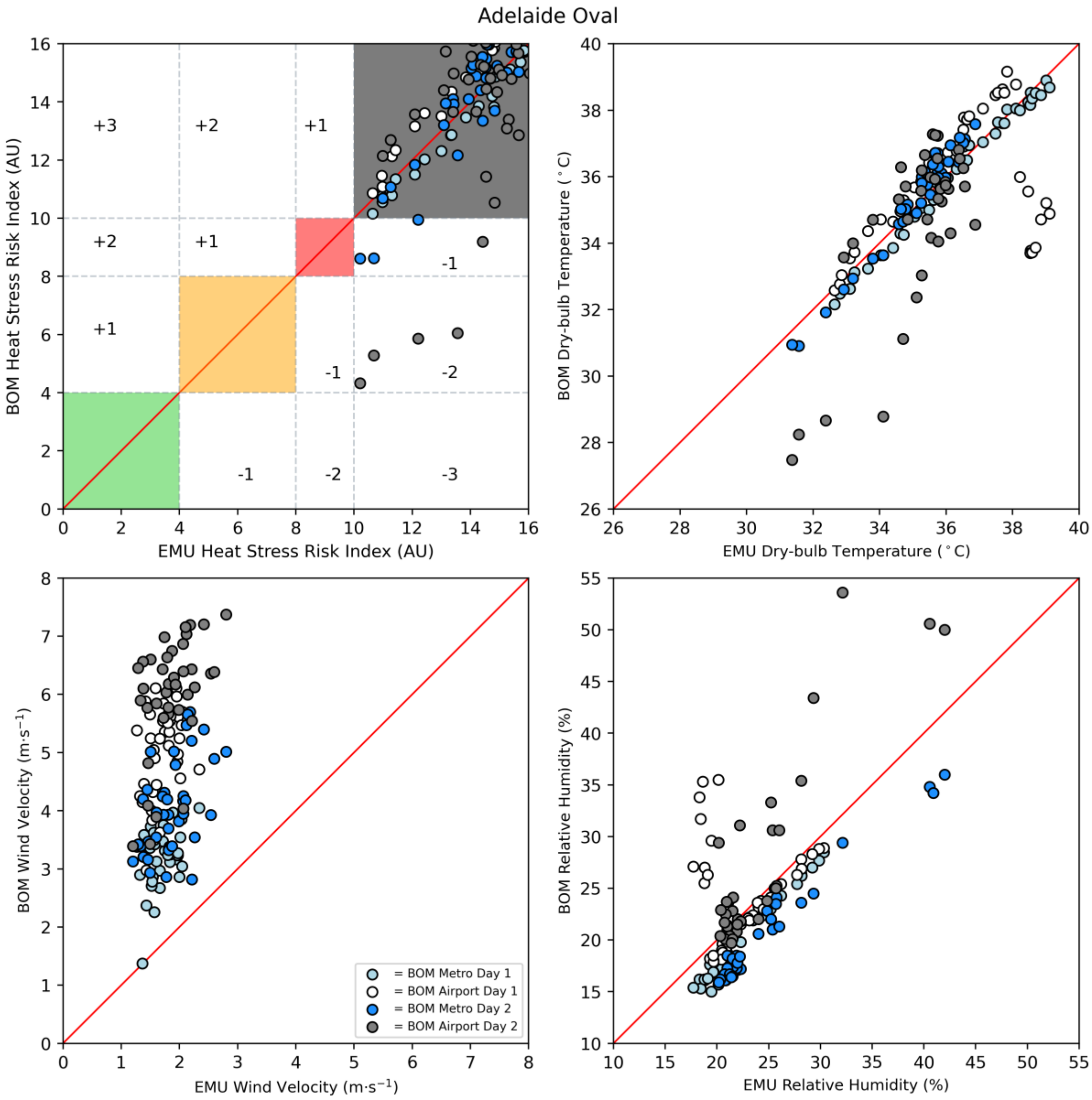
Adelaide Oval
BOM Heat Stress Risk Index (AU)
EMU Heat Stress Risk Index (AU)
+3
+2
+1
-1
-2
-3
BOM Dry-bulb Temperature (°C)
EMU Dry-bulb Temperature (°C)
BOM Wind Velocity (m·s⁻¹)
EMU Wind Velocity (m·s⁻¹)
= BOM Metro Day 1
= BOM Airport Day 1
= BOM Metro Day 2
= BOM Airport Day 2
BOM Relative Humidity (%)
EMU Relative Humidity (%)

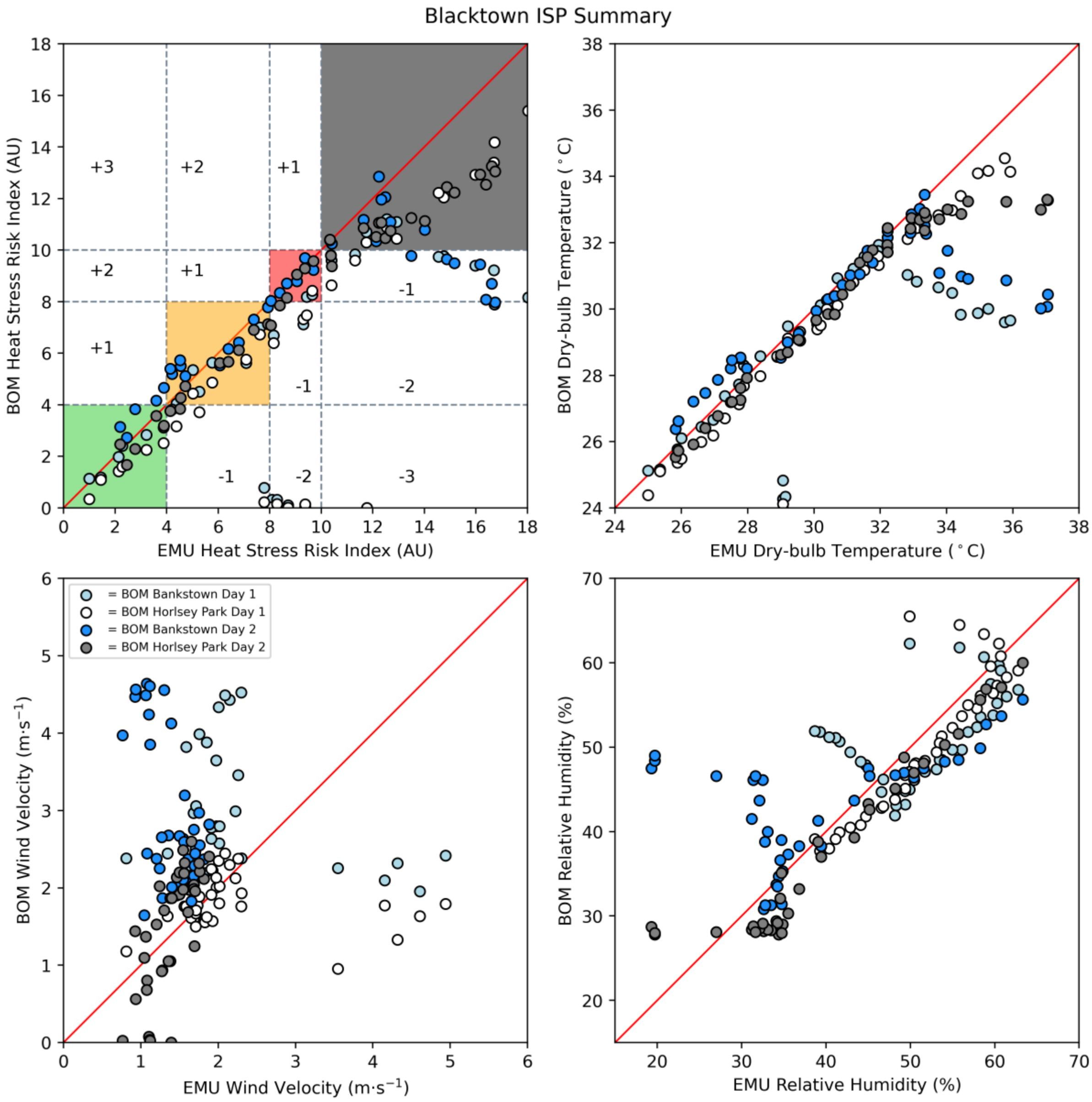
Blacktown ISP Summary
BOM Heat Stress Risk Index (AU)
EMU Heat Stress Risk Index (AU)
+3
+2
+1
+2
+1
+1
-1
-1
-2
-1
-2
-3
BOM Dry-bulb Temperature (°C)
EMU Dry-bulb Temperature (°C)
= BOM Bankstown Day 1
= BOM Horlsey Park Day 1
= BOM Bankstown Day 2
= BOM Horlsey Park Day 2
BOM Wind Velocity (m·s⁻¹)
EMU Wind Velocity (m·s⁻¹)
BOM Relative Humidity (%)
EMU Relative Humidity (%)

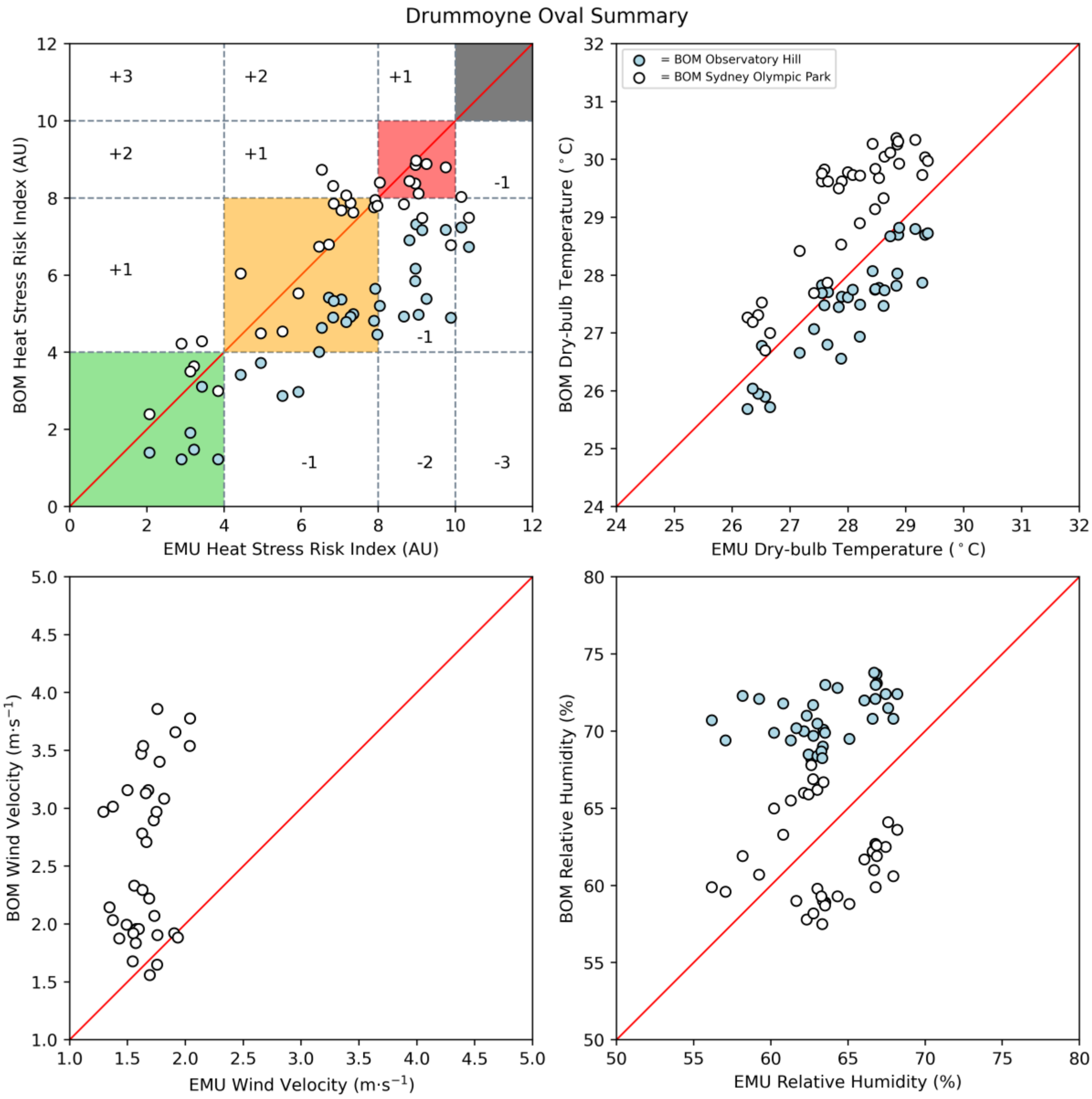

Drummoyne Oval Summary
BOM Heat Stress Risk Index (AU)
EMU Heat Stress Risk Index (AU)
+3
+2
+1
-1
-2
-3
= BOM Observatory Hill
= BOM Sydney Olympic Park
BOM Dry-bulb Temperature (°C)
EMU Dry-bulb Temperature (°C)
BOM Wind Velocity (m·s⁻¹)
EMU Wind Velocity (m·s⁻¹)
BOM Relative Humidity (%)
EMU Relative Humidity (%)

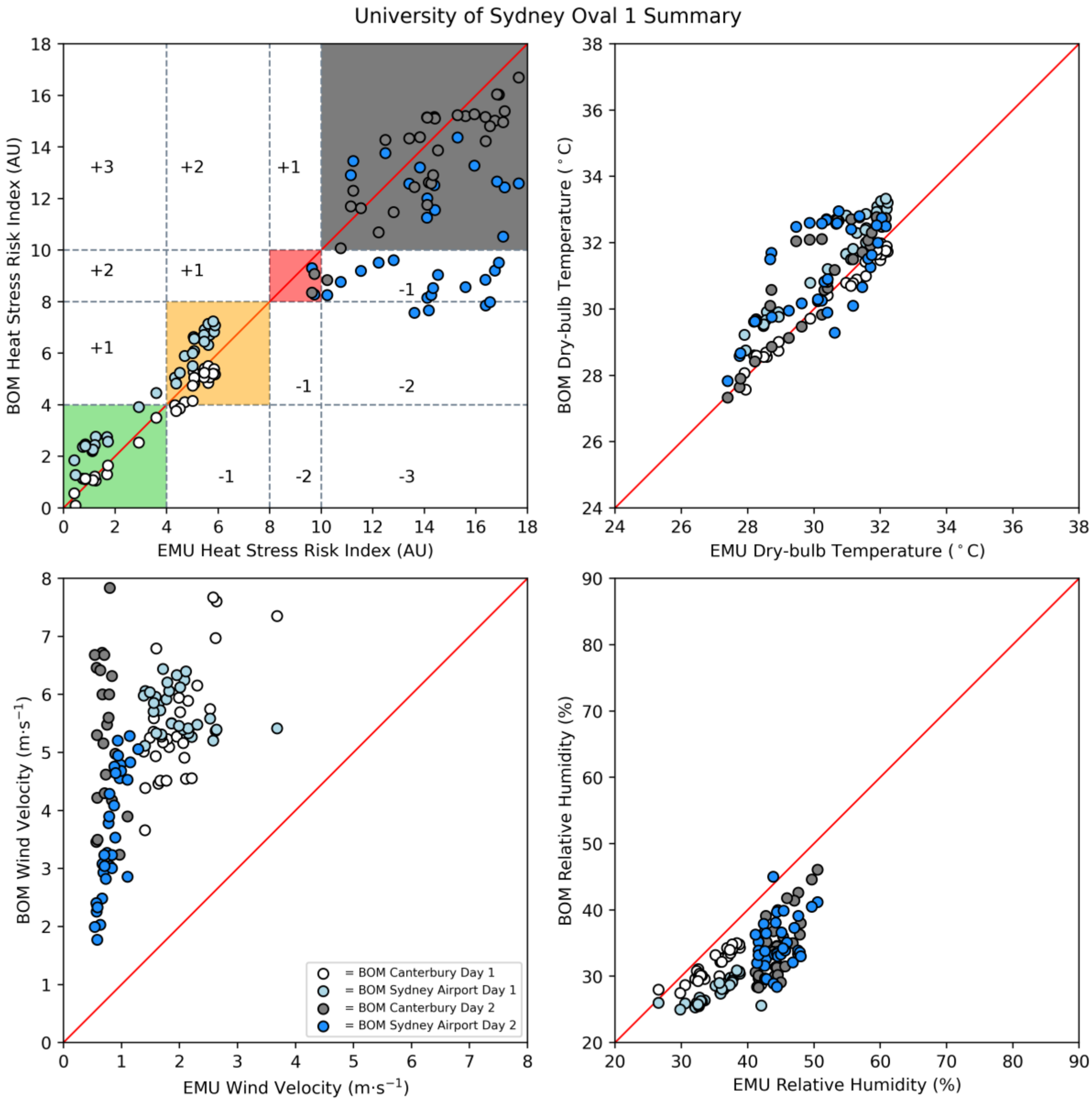
University of Sydney Oval 1 Summary
BOM Heat Stress Risk Index (AU)
EMU Heat Stress Risk Index (AU)
+3
+2
+1
+2
+1
+1
-1
-1
-2
-1
-2
-3
BOM Dry-bulb Temperature (°C)
EMU Dry-bulb Temperature (°C)
BOM Wind Velocity (m·s^{-1})
EMU Wind Velocity (m·s^{-1})
= BOM Canterbury Day 1
= BOM Sydney Airport Day 1
= BOM Canterbury Day 2
= BOM Sydney Airport Day 2
BOM Relative Humidity (%)
EMU Relative Humidity (%)

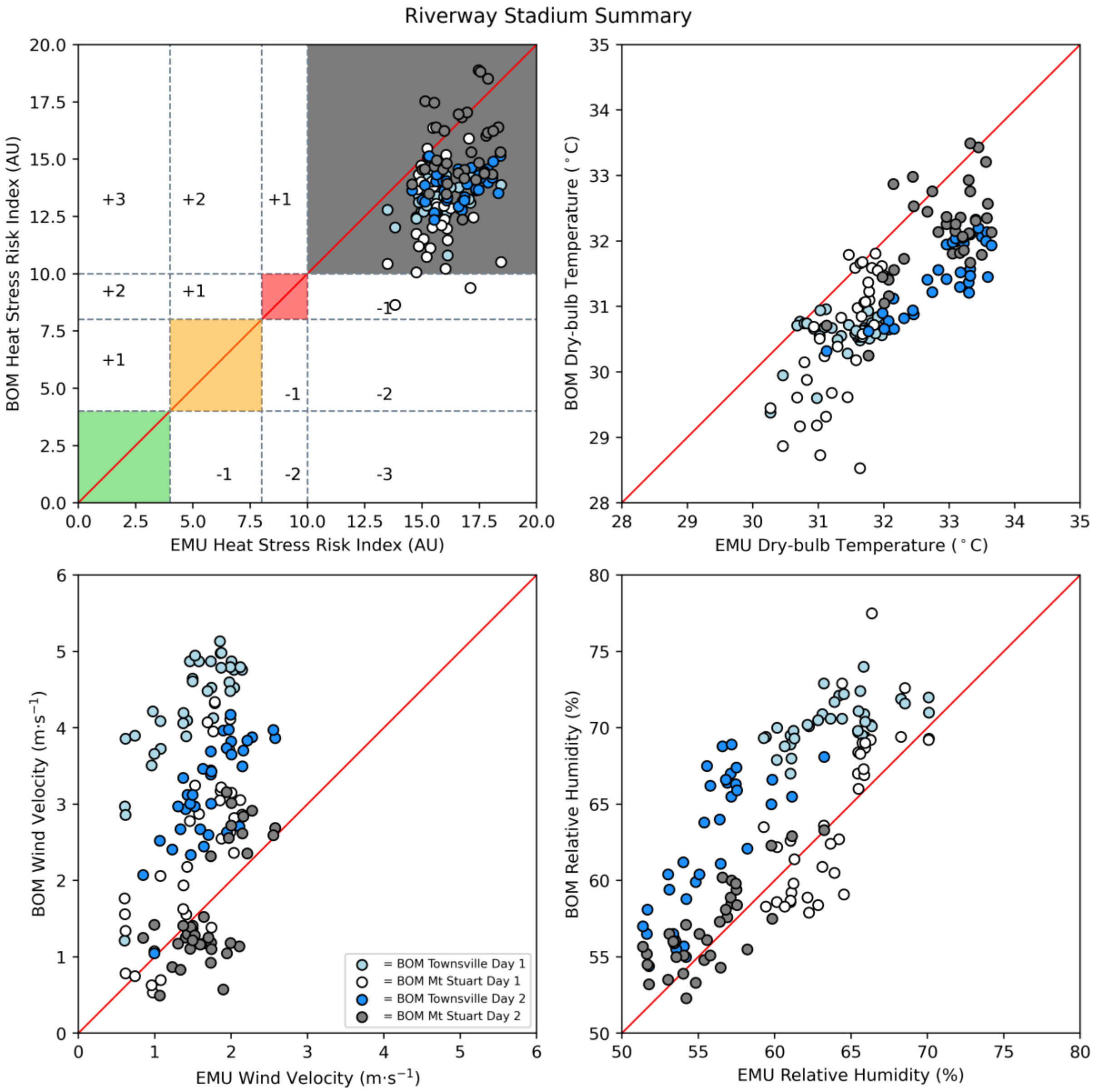

Riverway Stadium Summary
BOM Heat Stress Risk Index (AU)
EMU Heat Stress Risk Index (AU)
+3
+2
+1
-1
-2
-3
BOM Dry-bulb Temperature (°C)
EMU Dry-bulb Temperature (°C)
BOM Wind Velocity (m·s⁻¹)
EMU Wind Velocity (m·s⁻¹)
= BOM Townsville Day 1
= BOM Mt Stuart Day 1
= BOM Townsville Day 2
= BOM Mt Stuart Day 2
BOM Relative Humidity (%)
EMU Relative Humidity (%)

Bridging Statement

The first experimental chapter assessed the local thermal environment in which competitive sports are played within major and minor sporting venues across Australia. By doing so, it demonstrated the importance of local environmental monitoring in outdoor sports, given the significant differences in the local thermal environment within our cities and at Major and Minor sporting venues across Australia. This evidence is important for developing and implementing future extreme heat policies across many outdoor sports. Ensuring that the environmental conditions used within any heat stress risk assessment are accurate and readily available to support staff will ensure that the appropriate decision on when and whether to continue competition in the face of extreme heat, can be made accurately and with confidence.

The next two experimental chapters in this thesis focus on the individual factors that heat balance while exercising in an outdoor heat stress context. Heat balance modelling is an important step in the development of appropriate biophysical models for heat stress risk assessments that are embedded within extreme heat policies. Without a detailed, contextual understanding of the factors that affect heat balance in specific scenarios, such as while playing Cricket, or participating in Road Cycling, large errors in these biophysical models may be present and result in an undue risk of heat stress or being overly cautious when play or the race could safely begin or continue. The next experimental chapter will evaluate the best available methods for estimating human heat balance while participating in outdoor road cycling to help inform future extreme heat policy development and facilitate the maintenance of safe participation in sport under high heat stress conditions.

CHAPTER IV

The evaporative requirement for heat balance primarily determines whole-body sweat rate during steady-state outdoor road cycling.

Lindsey Hunt[1,3], James W Smallcombe[1,3], and Ollie Jay[1-3]
[1]The University of Sydney, Thermal Ergonomics Laboratory, Sydney School of Health Sciences, Faculty of Medicine and Health, Camperdown, Australia
[2]The University of Sydney, Charles Perkins Centre, Camperdown, Australia
[3]Heat and Health Research Centre, Faculty of Medicine and Health, Camperdown, Australia

Author Contributions: L. Hunt, J.W Smallcombe and O. Jay designed the research, L. Hunt conducted data collection, O. Jay provided access to materials and equipment, L. Hunt analysed the data, L. Hunt wrote the manuscript, J.W Smallcombe, and O. Jay assisted with data interpretation and all authors assisted with reviewing the manuscript and O. Jay had primary responsibility for the final content of the paper. All authors read and approved the final manuscript.

Running head: E_{req} and WBSR during outdoor cycling

Address for correspondence:
Prof. Ollie Jay ✉
Thermal Ergonomics Laboratory,
Heat and Health Research Centre
Sydney School of Health Sciences,
Faculty of Medicine and Health,
The University of Sydney, NSW 2006.
Australia
+ 61 (2) 9036 4102
e-mail: ollie.jay@sydney.edu.au

4.0 Abstract

Purpose: The evaporative requirement for heat balance (E_{req}) is closely associated with whole-body sweat rate (WBSR) in indoor, laboratory-based environments. We aimed to assess 1) the association between E_{req} (W) and WBSR ($L \cdot h^{-1}$) during outdoor cycling and how this association changes when using different methods for estimating metabolic rate ($\dot{M}$), mean skin temperature (T_{sk}) and the convective heat transfer coefficient (h_c) as inputs into the E_{req} model; and 2) the agreement between estimated power output from the Strava physical activity social media application and how the association between E_{req} and WBSR changes when using estimated external workload over measured external workload.

Methods: 59 participants (16 women); cycled at a self-selected intensity (external workload: 81-331 Watts) in a range of environmental conditions (T_{db}; 12.4-30.4 ºC, P_a; 0.7-2.23 kPa, T_r; 13.6-72.8 ºC, Wind Velocity; 0.34-2.90 $m \cdot s^{-1}$) for ~60 minutes at Centennial Park in Sydney, Australia on up to 9 occasions in a randomised order, totalling 236 trials.

Results: Across a large range of E_{req} (284-889 W) and WBSR values (0.28-2.31, $L \cdot h^{-1}$) the strongest association between E_{req} and WBSR in an outdoor environment (R^2=0.72) was lower than previously reported indoors (R^2>0.90). Using Strava's external workload estimate tended to underestimate external workload (-14 W [-67-40]) and further weakened the association between E_{req} and WBSR (R^2=0.65).

Conclusion: Our findings indicate that in an outdoor environment, the strength of association between E_{req} and WBSR is weaker than indoors. Standard equations for estimating dry heat exchange in a highly convective outdoor environment are likely limited. The calculation of E_{req} outside the laboratory requires the development of appropriate calculations for metabolic rate (particularly at higher metabolic rates (>750 W), and dry heat exchange (mean skin temperature, and the convective heat transfer coefficient) in high airflow environments.

Keywords: Thermoregulation, Heat Balance, Outdoor Cycling, Whole-Body Sweat Rate.

4.1 Introduction

Since the 1930s, it has been known that the evaporative requirement for heat balance (E_{req}) determines whole-body sweat rate (WBSR) in controlled laboratory settings (Nielsen, 1938). The robust associations (R^2>0.8-0.9) between E_{req} and WBSR in well-controlled indoor environments have been consistently documented in laboratory-based research (Gagnon, Jay & Kenny, 2013; Cramer & Jay, 2019; Hospers *et al.*, 2020). Indoor models that characterise the relation between E_{req} and WBSR show a high correlation across multiple physical activity modalities including walking (Hospers *et al.*, 2020) and cycling (Gagnon *et al.*, 2013) and that E_{req} closely determines WBSR independent of differences in metabolic heat production (H_{prod}), esophageal temperature (T_{es}), mean skin temperature (T_{sk}) (Hospers *et al.*, 2020) and the environmental conditions (Ravanelli, Imbeault & Jay, 2020). However, the translation of these findings to outdoor settings poses challenges due to the limitations associated with measuring specific components of the E_{req} model, such as mean skin temperature (T_{sk}, ºC), metabolic rate (M, Watts), and increased variability in environmental conditions (e.g. dry-bulb temperature [T_{db}], mean radiant temperature [T_r], relative air velocity [v_{self}] (i.e., cycling speed), and ambient vapour pressure [P_a]). Defining the relation between E_{req} and WBSR in an outdoor environment would facilitate the translation of the E_{req} model to outdoor sporting, physical activity, and occupational settings, aiding thermo-physiological modelling and heat safety policy development.

During steady-state exercise, such as cycling, humans secrete sweat to facilitate evaporative heat loss, prevent excessive core temperature elevations, and maintain core temperature homeostasis. In the absence of adequate fluid replacement, dehydration ensues, leading to negative effects on health and performance, such as increased thermal and cardiovascular strain and diminished performance (Sawka *et al.*, 1985; Watanabe *et al.*, 2020). Previous investigations into the association between E_{req} and WBSR have primarily occurred in situations where the variables required to calculate E_{req} are readily available (skin temperature, metabolic rate, environmental conditions) and where there is low variability in environmental conditions (e.g., turbulent air flow, ambient temperatures). However, recreational cycling can commonly elicit much higher steady-state metabolic heat productions ranging from 500-1,200W and race in dynamic scenarios where environmental conditions, cycling velocities, natural air velocities, metabolic rates and even the airflows experienced by each rider within the peloton due to drafting are in flux. For instance, a well-trained recreational cyclist (at ~70 kg) can readily achieve external workloads of ~300W for extended durations (15-30 minutes), while elite cyclists can sustain workloads of ~420W (Muriel *et al.*, 2022) at the same durations. For the recreational cyclist, assuming a 20% gross mechanical efficiency (η), this equates to a metabolic energy expenditure (M) of 1500W [**Eq. 8**], resulting in 1200W of metabolic heat production (H_{prod} = M – Wk, [**Eq. 9**]) (Cramer & Jay, 2019). Importantly, at times when metabolic heat production is high, E_{req} can approach and surpass the maximum ambient potential for evaporation (E_{max}), even in temperate environments, thereby reducing sweating efficiency (Vogt *et al.*, 1981) and leading to uncompensable environmental conditions ($E_{req} > E_{max}$), resulting in rapid rises in body core temperature and without adequate hydration, marked levels of dehydration which further aggravates rises in body temperature and reductions in performance (Cheuvront, 2010). However, road cycling at high air velocities (> 4 $m \cdot s^{-1}$) results in a cascade of increased convective and evaporative heat exchange, particularly as latent heat is liberated through the phase change of water to gas from the skin at the onset of sweating, from evaporation and natural convection (Parsons, 2003; Oliveira *et al.*, 2014) which allows for sustained high metabolic rates without extreme rises in core temperature.

In recent years, there has been an influx of cycling power meters entering the market. This has allowed for the reliable and accurate measurement of external workload (Dickinson

& Wright, 2021), which has led to a proliferation of external work data for researchers and recreational athletes alike, which has typically been restricted to the laboratory. The release of estimated outdoor power output for cycling activities from Strava (a popular physical activity social media platform) (Strava, 2023) means even wider access to potentially useful power output data for field-based research. The maturation and proliferation of tools for measuring (power meters) and predicting (software) external workload may facilitate accurate and accessible estimates of H_{prod} in outdoor environments. In combination with metabolic prediction equations (Liguori *et al.*, 2022) accurate and accessible methods for determining H_{prod}, may allow the quantification of E_{req} in dynamic, outdoor environments.

The current study aimed to assess our ability to estimate E_{req} accurately and how it may change the relation between E_{req} and WBSR during outdoor cycling and further determine the optimal methods for calculating E_{req} using different methods for estimating metabolic energy expenditure, the convective heat transfer coefficient, and skin temperature. Secondly, we aimed to assess the agreement between estimated external workload (Strava) and measured external workload (Garmin) while cycling outdoors and how the use of estimated external workload affects the relation between E_{req} and WBSR using the best available method for calculating E_{req}.

We hypothesised that (1) E_{req} would remain a strong predictor of WBSR in an outdoor environment, however, the strength of the relation would be lower in an outdoor environment, compared to previous indoor laboratory-based studies because of reduced ability to accurately characterise convection, skin temperature and metabolic rate, and (2) using a software-based estimate of external workload (Strava) compared with measured external workload (Garmin) would reduce the relation between E_{req} and WBSR.

4.2 Methods

Experimental design

All data were collected at a reasonably flat (19 m elevation gain per lap), outdoor cycling circuit (3.72 km) at Centennial Parklands in Sydney, Australia (Latitude: 33°53'59"S, Longitude: 151°14'01"E) across warm months (November-April), between November 2020 and December 2023. The range of environmental conditions experienced are presented in Table 1. Participants completed as few as 1 trial and as many as 10 trials. The number of trials participants were required to complete was not standardised to allow for recruiting the largest possible range of participants. Requiring participants on sign up to complete minimum number of trials would have reduced the number of individuals we recruited due to availability. The exercise intensity was self-selected by each participant for every visit to acquire a large range of intensities. To enable the collection of a range of exercise intensities, we guided participants to complete the sessions at varying intensities for each visit (easy ride [55-65% of functional threshold power (FTP)], moderate ride [65-75% of FTP], and hard ride, [75%+ of FTP]). Participants were instructed to maintain a constant effort throughout the ~60-minute ride and to keep their external workload as consistent as possible throughout.

Participants

Approval for the study was obtained from the Human Research Ethics Committee (HREC no. 2020/736). A total of 59 participants (16 females) were recruited (**Table 1**) completed 236 trials. All participants met the predetermined eligibility criteria: 18-40 years of age (inclusive), regularly participated in outdoor road cycling ($\geq$ 2 times per week for at least 6 months prior to participating), owned their equipment (road bike, shoes, helmet and clothing etc). Participants acclimatisation status may have changed across the data collection period (spring and autumn in Sydney, Australia (November-April)) due to the potential for seasonal acclimatisation (Brown et al., 2022), however, all participants were considered to be trained but not acclimatised or acclimated, as no individuals participated in any dedicated acclimation or acclimatisation protocols throughout their study participation. All participants were non-smokers and were free from respiratory, metabolic, and cardiovascular diseases. All participants were instructed to abstain from consuming caffeine in any form (liquid or solid), or alcohol, and from engaging in strenuous physical activity for 24 hours prior to participating (Hunt et al., 2021) and were instructed to keep their bike set-up (e.g. saddle height etc) consistent between trials.

Protocol

Experimental sessions: Participants were asked to consume a light meal and 500 mL of water ~2 hours prior to arriving at Centennial Park for the experimental trials. On arrival at the park, participants entered the portable change room and were provided with a Polar H10 chest strap. Nude baseline body mass measurements were taken in triplicate inside the portable changing room immediately before the commencement of the trial. Participants' bikes were then fitted with a set of cycling power meter pedals to quantify external workload. All clothing and/or equipment that could absorb sweat (helmet, clip-in shoes, socks, bibs and jersey [with the addition of a sports bra for women]) was weighed pre- and post-exercise to record sweat losses trapped within. Participant clothing thermal insulation (I_{cl}), evaporative resistance of clothing ($R_{e,cl}$), and clothing area (f_{cl}) for the cycling ensemble were estimated to be 0.3 [0.31 for women] [clo], 0.0107 [$m^2 \cdot kPa/W$], and 1.119 [n.d.] respectively (McCullough, Jones & Huck, 1985; Gonzalez, 2019; Smallcombe et al., 2021).

Participants then cycled for ~60 minutes on their road bike around the continuous cycling-friendly loop at an exercise intensity of their choosing (187 [80-331] W) (see *protocol* for further details). Participants were free to return after 56 minutes due to the circular cycling track. Participants were also instructed to continue cycling at their pace until they returned to the data collection location after at least 56 minutes (each lap of the circuit takes approximately 5-7 minutes). Participant clothing was not standardised between participants; however, individuals were asked to wear typical summer cycling clothing (cycling jersey, bibs and socks) and completed all subsequent trials in the same clothing. Upon completion of the exercise, participants entered the portable change room to measure body mass in triplicate and clothing/equipment mass. Participants towelled off any unevaporated sweat with a microfibre towel before being weighed in triplicate again inside the portable change room. Upon exiting the changeroom participants were asked for a subjective rating for a session Rating of Perceived Exertion (RPE) on a scale from 0-10 and subjective estimates of environmental conditions (see *subjective measures*). Throughout each session, participants were not able to consume food or water and they were instructed to not draft other cyclists, vehicles or anything that could obstruct airflow in front of them.

Measurements

Power output: External workload (Watts) while cycling was determined via two methods. The first, using cycling power meter pedals (Garmin Vector 3s or Garmin Rally RS200, Garmin, USA - reported error ±2%, ±1% respectively) fixed to participants' bikes and the second using an estimation of external workload from a popular physical activity social media platform (Strava, San Francisco, USA). Garmin power pedals were set up on participant bikes according to the manufacturer's instructions. Briefly, the set-up process involved setting the crank length (from 165-177.5mm) and performing a standard calibration using either a cycling computer (Garmin Edge 530, Garmin, USA) or a smartphone (iPhone 12, Cupertino, USA) with the Garmin Connect App (Garmin, 2021). The power pedals were kept in a location where they were out of the sun so they would be equilibrated to the appropriate environmental conditions and were calibrated before each test as the power output reading is affected by dry-bulb temperature (Garmin, 2023). Strava's underlying algorithm for estimating external workload ("power estimator") is proprietary, however, they detail the following requirements to provide an external workload for an activity. 1) A bike profile that includes bike type (road, mountain, triathlon/time-trial) and bike weight (kg) 2) rider weight (including equipment such as clothing, water, and equipment) and 3) elevation data from an in-device barometric altimeter or GPS data such as Strava's base map (Strava, 2023). To capture an appropriate power output estimate for each test in the Strava application, 1) a standardised bike type was selected (e.g., road bike), which included the bike weight of 10 kg (inclusive of equipment weight; helmet, shoes, jersey, etc.) and 2) participants' body mass (kg, as measured on site before exercise for each visit) and 3) accurate GPS data from an iPhone 12 which served as the data recording device using the Strava and Cyclemeter (Abvio, San Francisco, USA) applications. This phone was then placed in the participant's jersey pocket to continuously record data as the trial started. The phone recorded cycling speed, distance, time, measured power output, and cadence using the Cyclemeter application in 1-sec intervals. Data were then exported and saved as a .csv file for later processing. The estimated external workload given by Strava's estimator was calculated by Strava and then recorded at the end of the activity.

Dry heat exchange and the evaporative requirements for heat balance (E_{req}) were estimated using partitional calorimetry from (Cramer & Jay, 2019) and adjusted for our purposes (see calculations). Body surface area (BSA) was determined using the DuBois & DuBois method (Du Bois & DuBois, 1916).

<u>Whole body sweat loss:</u> Nude body mass measurements were taken in triplicate immediately pre- and post-exercise using a portable platform scale (KW-4050 Industrial Platform Scale: High Precision, Weigh, Australia ± 5 g). Whole-body sweat loss (WBSL, kg) was defined as the change (Δ) in nude body mass measured pre- and post-exercise minus

estimated respiratory and metabolic mass losses (Cheuvront & Kenefick, 2017). Whole-body sweat rate ($L.h^{-1}$) was then calculated as:

$$WBSR = \left(\frac{WBSL}{t}\right) \cdot 60 \qquad [L.h^{-1}]\,[1]$$

Where: t is the exercise duration (minutes).

Environmental conditions: Outdoor environmental conditions were measured on-site using a custom environmental monitoring unit (EMU) built and extensively tested by engineers at The University of Sydney to meet the specifications outlined by the International Organisation for Standardization (ISO) 7726 (ISO 7726, 2001). Data for shaded aspirated dry bulb temperature (T_{db}, °C), air velocity (ν, $m \cdot s^{-1}$), black globe temperature (T_g, ºC) relative humidity (RH, %) were recorded in 5-second intervals and averaged over 1-min and then averaged across each trial's total length. The aspirated dry-bulb and aspirated wet-bulb temperature thermometers used were a perforated and an immersion type 50 mm Class A platinum resistance thermometer, respectively (Temperature Controls, Sefton, NSW, Australia). The aspirated wet-bulb thermometer was draped in a cotton shroud connected to a reservoir of distilled water that kept the thermometer and cotton shroud fully saturated throughout data collection. The thermometers for T_{db} and T_{wb} were continuously aspirated at ~3.0 $m \cdot s^{-1}$ with a 40 mm by 40 mm x 20 mm Sunon fan (Sunonwealth Electric Machine Industry Company Ltd., Kaohsiung City, Taiwan). Black globe temperature (T_g) was measured with an immersion type 100 mm Class A platinum resistance thermometer (Temperature Controls, Sefton, NSW, Australia) inserted in a 150 mm copper globe painted matt black. Wind velocity was measured with a Windsonic ultrasonic Anemometer (Gill Instruments Ltd., Lymington, Hampshire, UK), with the following specifications, range: 0.0 to 60 $m \cdot s^{-1}$, accuracy of ± 2% at 12 $m \cdot s^{-1}$, resolution: 0.1 $m \cdot s^{-1}$ and response time: 0.01 $m \cdot s^{-1}$). The EMU was mounted to a Rollei tripod (Digitec Audio, Zurich, Switzerland) at a height of 1.2 m and was placed in position at least 30 minutes before the start of data collection to equilibrate to the environment. Mean radiant temperature (T_r, ºC) was calculated with **Eq. 1** (ISO, 7726, 1998) and RH was calculated with psychrometric equations using T_a and aspirated wet-bulb temperature (T_{wb}, ºC) with equation [2].

$$T_r = \left[\left(T_g + 273.15\right)^4 + \frac{\left(1.1 \times 10^8 \times v^{0.6}\right)}{\varepsilon \times d^{0.4}}\left(T_g - T_a\right)\right]^{0.25} - 273.15 \qquad [ºC]\ [2]$$

Where ν is air velocity in $m{\cdot}s^{-1}$, ε is the emissivity of the black copper globe, assumed to be 0.97 (Parsons, 2003), and d is the diameter of the globe in meters (0.15 m).

Relative humidity was calculated using psychrometry with T_{db} and T_{wb} with the following equation:

$$RH = \frac{100\left[\mathrm{EXP}\left[1.8096 + \left(\frac{17.2694T_{wb}}{237.3+T_{wb}}\right)\right] - 7.866 \times 10{-}4P(T_{db}-T_{wb})\left(1+\frac{T_{wb}}{610}\right)\right]}{\mathrm{EXP}\ [1.8096+[(\frac{17.2694T_{db}}{237.3+db})\ ]} \qquad [\%]\ [3]$$

Where: RH is relative humidity (%); T_{db} is aspirated dry-bulb temperature (°C); T_{wb} is aspirated wet bulb temperature (°C); EXP is the exponent; P is Station level pressure (hPa), assumed to be 998.3 hPa from the standard table of pressures (Abbott & Tabony, 1985). Data were collected in full sun, where only cloud cover (when present) provided shade, viewed with Grafana (Grafana Labs, New York City, NY, USA) and downloaded as required for analysis.

Calculations

The rate of heat storage was assumed to be zero (S = 0), as a steady state was assumed for all the heat transfer variables. E_{req} is therefore given by the following conceptual human heat balance equation (in Watts, W):

$$E_{req} = H_{prod} - (\pm C \pm K \pm R) - (\pm C_{res} \pm E_{res}) \qquad [W]\ [4]$$

Where: metabolic heat production (H_{prod}) is equal to M-Wk, which is given by subtracting external work (Wk) from metabolic energy expenditure (M), and dry heat exchange (convection (C), conduction (K), and radiation (R)) from the skin surface and heat exchange avenues from the respiratory tract (through convection [C_{res}] and evaporation [E_{res}]). During outdoor cycling, there are 3 parts of the body (which make up a small proportion of the body's total BSA) in contact with external surfaces (on the saddle, feet in shoes and hands on the handlebars). The minor contact and heat transfer with these solid surfaces is further insulated by the bibs short's chamois, socks and bar tape and is therefore considered to be negligible and would be consistent across and between participants. Therefore, dry heat loss is assumed to be equal to the sum of convection and radiation (Cramer & Jay, 2019).

The E_{req} model is a biophysical calculation which requires inputs of metabolic heat production (H_{prod}), and dry heat loss through convection and radiation. Accurate calculation of the E_{req} model outside the laboratory is challenged by increased measurement uncertainty (e.g., metabolic rate, mean skin temperature) and uncontrolled or environmental conditions. These components of E_{req} can typically be measured via established methods within a laboratory via indirect calorimetry, mean skin temperature, and an empirically derived convective heat transfer coefficient for the human body. We have attempted to overcome those challenges by selecting and comparing three available methods each for estimating metabolic rate from external workload, mean skin temperature (ºC), and the convective heat transfer coefficient (h_c).

Three methods for estimating metabolic energy expenditure rate from external workload were used. The first estimate of metabolic energy expenditure (M_{acsm}): assumes rates of oxygen consumption calculated using the ACSM recommended prediction equation for oxygen consumption curing cycle exercise [3] (Liguori et al., 2022) then converted to an estimated metabolic energy expenditure using **Eq. 4** assuming a metabolic energy equivalent (MEE) of 20.7 for low-moderate intensity sessions (session RPE <4) and 21.1 for high intensity sessions (session RPE >4) (in kj·LO_2^{-1}) (Peronnet & Massicotte, 1991): Oxygen consumption is given by:

$$\dot{V}O_2 = \left[\frac{(10.8 \times \mathrm{Wk})}{m_b}\right] + 7 \qquad [\mathrm{mL \cdot kg^{-1} \cdot min^{-1}}]\ [5]$$

Where: $\dot{V}O_2$ is the rate of oxygen consumption (mL·kg^{-1}·min^{-1}), Wk is external workload and m_b is total body mass (kg). Metabolic energy expenditure (M_{acsm}) is then given by:

$$M_{acsm} = \frac{(\dot{V}O_2 \times m_b) \cdot \mathrm{MEE} \cdot 1000}{60} \qquad [\mathrm{W}]\ [6]$$

Where: $\dot{V}O_2$ is the rate of oxygen consumption (mL·kg^{-1}·min^{-1}), m_b is total body mass (kg) and MEE is the relevant metabolic energy equivalent for each session, given above (e.g., high: 21.1; low: 20.7, kj·LO_2^{-1}).

The second method ($\dot{M}_{ett}$) for estimating metabolic rate from external workload used external workload and average cycling cadence to estimate metabolic rate based on previous data (Ettema & Lorås, 2009) using the following equation:

$$\dot{M}_{ett} = 39.7 + (28.4 \times f_{ped}) + (3.73 \times \mathrm{Wk}) \qquad [\mathrm{W}]\ [7]$$

Where: f_{ped} is average cycling cadence (revolutions·min^{-1}) and Wk is external workload (W). As Strava does not estimate cycling cadence, for Strava estimated metabolic rate, an assumed cycling cadence was used – 80 revolutions·min^{-1}.

The third estimate for metabolic energy expenditure ($\dot{M}_{ge}$) uses previous data to estimate gross mechanical efficiency, η, [%] for each trial using a second-order polynomial [**Eq. 8**] created from previous work that has described a relation between Wk and η (Moseley et al., 2004).

$$\eta = \frac{-0.0001 \cdot \mathrm{Wk}^2 + 0.0579 \cdot \mathrm{Wk} + 11.605}{100} \qquad [\%]\ [8]$$

Where: Wk is external workload (W) and η is gross mechanical efficiency (%). Therefore, M_{ge} is given by:

$$M_{ge} = \frac{Wk}{\eta} \quad \text{[W] [9]}$$

Convective and radiative heat exchange at the skin surface was estimated with equations 10 and 11 respectively (Parsons, 2003):

$$C = h_c \cdot f_{cl} \cdot (T_{sk} - T_{db}) \quad [\mathrm{W \cdot m^{-2}}]\ [10]$$

$$R = h_r \cdot f_{cl} \cdot (T_{sk} - T_{db}) \quad [\mathrm{W \cdot m^{-2}}]\ [11]$$

Where: T_{db} is dry-bulb temperature (in ˚C); h_c is the convective heat transfer coefficient; h_r is the radiative heat transfer coefficient and f_{cl} is clothing area factor. The radiative heat transfer coefficient (h_r) is given by (Parsons, 2014):

$$h_r = 4 \cdot \varepsilon \cdot \sigma \cdot f_{eff} \cdot \left[273.15 + \frac{T_{sk} + T_r}{2}\right]^3 \quad [\mathrm{W \cdot m^{-2} \cdot K}]\ [12]$$

Where: ε is the emissivity of clothed human (assumed to be 0.97), σ is the Stefan-Boltzmann constant (5.67×10^{-8} $\mathrm{W/m^{-2} \cdot K^{-4}}$), f_{eff} is effective radiation area factor (assumed to be 0.7 for cycling), T_{sk} is estimated using equations [T_{sk1}, T_{sk2}, T_{sk3}]; T_r was calculated using **Eq. 2** from measured black globe temperature (T_g, ºC) and wind velocity (v, $\mathrm{m \cdot s^{-1}}$) data by the on-site EMU.

Most methods for estimating the convective heat transfer coefficient have been derived for use indoors with minimal clothing and low forced convection except for Lotens and Havenith (1991) who describe the first method (h_{c1}) as potentially appropriate for high air velocities (0-10 $\mathrm{m \cdot s^{-1}}$) (Lotens & Havenith, 1991).

$$h_{c1} = 8.3 \cdot \left(0.07 + 0.0043 \cdot f_{ped} + v_{self}\right)^{0.86} \quad [\mathrm{W \cdot m^{-2} \cdot {^\circ}C^{-1}}]\ [13]$$

Where: f_{ped} is average cycling cadence ($\mathrm{revolutions \cdot min^{-1}}$) and v_{self} is cycling velocity ($\mathrm{m \cdot s^{-1}}$). The second and third methods for estimating h_c were developed for individuals seated indoors (Hardy, Du Bois & Soderstrom, 1938) or cycling indoors (Nishi & Gagge, 1970; Gagge & Gonzalez, 2010) in low-moderate airflows (0.2-4.0 $\mathrm{m \cdot s^{-1}}$). These methods are given by equations [14] and [15].

$$h_{c2} = 8.3 \cdot \left(v_{self}\right)^{0.86} \qquad [\mathrm{W \cdot m^{-2} \cdot {}^{\circ}C^{-1}}]\ [14]$$

$$h_{c3} = 5.5 + 1.96 \cdot \left(v_{self}\right)^{0.86} \qquad [\mathrm{W \cdot m^{-2} \cdot {}^{\circ}C^{-1}}]\ [15]$$

Where: v_{self} is self-generated air velocity (i.e., average cycling velocity) in $m \cdot s^{-1}$. Self-generated air velocity has been solely used here rather than a combination of self-generated air velocity and natural wind velocity as participants cycled around the Centennial Park circuit, which results in a net zero effect of natural wind velocity, assuming consistent air velocities throughout each lap.

Mean skin temperature was estimated using three methods: T_{sk1} (Mehnert et al., 2000), T_{sk2} (ISO, 7933, 2004) and T_{sk3} (Brown & Gillespie, 1986; Vanos et al., 2012):

$$T_{sk1} = 12.17 + 0.02T_a + 0.044T_r - 0.253v_{self} + 0.194P_a + 0.0029M + 0.51346T_{c_{eq}}\ [^{\circ}C]$$

[16]

The ISO standard (7933) gives two equations for scenarios where clothing is > 0.6 clo (T_{sk1}, **Eq. 16),** and < 0.2 clo (T_{sk_nu}, **Eq. 17**). For situations where clothing falls between 0.2-0.6 clo, the equation T_{sk2} is given which is a combination of T_{sk1} and T_{sk_nu}.

$$T_{sk\_nu} = 7.19 + 0.064T_a + 0.061T_r - 0.348v_{self} + 0.198P_a + 0.616T_{c_{eq}} \qquad [^{\circ}C]\ [17]$$

$$T_{sk2} = T_{sk\_nu} + 2.5\left(T_{sk\_1} - T_{sk\_nu}\right) \times (I_{cl} - 0.2) \qquad [^{\circ}C]\ [18]$$

$$T_{sk3} = \left(\frac{T_{c_{eq}} - T_{db}}{r_t + r_c + r_a}\right)(r_a + r_c) + T_{db} \qquad [^{\circ}C]\ [19]$$

Where: T_{db} is dry bulb temperature (in ˚C), T_r is mean radiant temperature (in ˚C), P_a is absolute humidity (in kPa); $\dot{M}$ is metabolic rate from the respective estimates [$\dot{M}_{acsm}$, $\dot{M}_{ett}$, $\dot{M}_{ge}$] (in W), and $T_{c_{eq}}$ is steady state body core temperature [estimated with **Eq. 19**]. Tissue (r_t), dynamic clothing (r_c) and aerodynamic (r_a) resistances ($s \cdot m^{-1}$) were calculated according to Brown and Gillespie (1986) (Brown & Gillespie, 1986). I_{cl} is the insulative resistance of the clothing ensemble given in clo. Clo is an arbitrary unit of clothing insulation (1 clo =

186.6, s·m^{-1} = 0.1555 m^2·°C^{-1}·W^{-1}). Steady state body core temperature ($T_{c_{eq}}$) was estimated using **Eq. 19** (Malchaire et al., 2000).

$$T_{c_{eq}} = 36.6 + 0.002 \cdot M \qquad [^\circ C]\ [19]$$

Body tissue thermal resistance (r_t) decreases with metabolic rate (W·m^{-2}) and was calculated as (Brown & Gillespie, 1986):

$$r_t = (-0.1\ \dot{M}) + 65 \qquad [W \cdot m^{-2}]\ [20]$$

Static and dynamic clothing thermal resistance (r_{co}, r_c) were calculated respectively as (Brown & Gillespie, 1986):

$$r_{co} = clo\ \times\ 186.6\ 1 \qquad [s \cdot m^{-1}]\ [21]$$

$$r_c = r_{co}\ \times \left(-0.37\ \left(1 - exp^{\frac{-v_{self}}{0.72}}\right) + 1\right) \qquad [s \cdot m^{-1}]\ [22]$$

Boundary layer thermal resistance (r_a) was calculated as (Brown & Gillespie, 1986):

$$r_a = \frac{(0.17)}{(ARe^n Pr^{0.33} k)} \qquad [s \cdot m^{-1}]\ [23]$$

Where: Re is the Reynolds number $\left(\frac{0.17 v_{self}}{v}\right)$, where v_{self} is free stream air velocity (cycling velocity, m·s^{-1}), v is the kinematic viscosity of air (~1.5 × 10^{-5} m^{-2}·s^{-1}). A and *n* are empirical constants. When Re is > 40,000, A=0.0266, *n*=0.805 (Kreith & Black, 1980). In our case the Re number always exceeds 40,000. Pr is the Prandtl number assumed to be 0.7296 (Kreith & Black, 1980), k is the thermal diffusivity of air assumed to be 2.14 × 10^{-5} m^2·s^{-1} at 25 °C (Y. S. Touloukian, 1970).

Respiratory heat loss (H_{res}) was calculated by combining estimated respiratory heat loss via convection (C_{res}) and evaporation (E_{res}) from the respiratory tract (Parsons, 2003):

$$C_{res} = 0.001516 \cdot \dot{M}(28.56 + 0.641 \cdot P_a - 0.641\ \cdot T_{db}) \qquad [W]\ [24]$$

$$E_{res} = 0.00127 \cdot \dot{M}(59.34 + 0.53 \cdot T_{db} - 11.63 -\ P_a) \qquad [W]\ [25]$$

$$H_{res} = C_{res} + E_{res} \qquad [W]\ [26]$$

Where: $\dot{M}$ is metabolic rate [W], T_{db} is the temperature of the inspired air [ºC], assumed to be equal to the dry-bulb temperature, and P_a is the ambient vapour pressure [kPa].

Finally, a method to estimate E_{req} described first by Givoni and Goldman (1972) and then by utilised in one of the first sweat rate prediction models by Shapiro et al. (1982) was used to further examine the association between E_{req} and WBSR. This method is given by (Givoni & Goldman, 1972):

$$E_{req\_givoni} = H_{prod} + \left(\frac{11.6}{I_{cl}}\right) \times \left(T_{db} - 36\right) \qquad \text{[W] [27]}$$

Where: T_{db} is dry-bulb temperature (in ˚C), H_{prod} is metabolic heat production (in W) and I_{cl} is the insulative resistance of the clothing ensemble (in clo).

Subjective measures: After completing the exercise and exiting the portable change room for the second time, participants were asked about their session Rating of Perceived Exertion (RPE) on a 0-10 scale (Foster *et al*, 2001; Fusco *et al.*, 2019).

Statistical Analyses

Data were assessed for normality using the Shapiro Wilk normality test and were assumed normal when $p \geq 0.05$, with visual inspections of the q-q plots of the residuals and histograms to confirm normality or otherwise. A series of simple linear regressions were used for each method used to calculate E_{req} vs WBSR. To assess the association between E_{req} and WBSR, the Pearson correlation coefficient (r) was used and to assess the goodness of fit relative to the line of identity (i.e., y=x), the coefficient of determination (R^2) was used. The Breusch-Pagan test was used to assess the heteroskedasticity of residuals for independent variables for the highest performing model of E_{req}. This data set includes up to 9 trials per participant, however, trials were conducted on different days with different environmental conditions, and external workloads and as such were considered as independent data points with our analyses. A Durbin-Watson test was employed to assess autocorrelation. With a result of 1.8, it was assumed there were no issues of autocorrelation. Bland–Altman plots were used to assess the accuracy of the Strava method for estimating external workload by calculating mean bias and limits of agreement (Bland & Altman, 2007). All analyses were performed with Python using the PyCharm IDE (version 2023.2.3) and the following packages Seaborn (https://seaborn.pydata.org/index.html), Scipy (https://scipy.org/), Matplotlib (https://matplotlib.org/), Pandas (https://pypi.org/project/haversine/), Numpy (https://numpy.org/), Statsmodels (https://www.statsmodels.org/), and Scikit-learn (https://scikit-learn.org/stable/) (Pedregosa et al., 2011).

4.3 Results

Table 1 provides descriptive information regarding the physical characteristics of the participants. Collectively, 236 trials were conducted for an average trial duration of 61.5 ± 2.4 minutes with an average external workload of 199 ± 45W (2.50 ± 0.56W·kg^{-1}) and cadence of 82 ± 9 revolutions·min^{-1} for men and external workload of 157 ± 31W (2.43 ± 0.45 W·kg^{-1}) and cadence of 77 ± 9 revolutions·min^{-1} for women. Participants self-selected more high intensity trials compared with low-moderate intensity trials (144H vs 92L-M) (**Table 1**).

Table 2 contains descriptive data for dependent (WBSR, L·h^{-1}) and independent variables. Across all trials, the range of combined exercise intensity and environmental conditions resulted in a wide range of E_{req} [284-889W] and WBSR values [0.28-2.31 L·h^{-1}]. Predicted mean skin temperatures for each prediction method were, T_{sk1} 34.6 ± 0.8 [32.7-36.1 ºC], T_{sk2} 33.2 ± 0.9 [31.0-34.7 ºC], T_{sk3} 34.8 ± 1.3 [30.7-38.5 ºC]. Body mass loss as a percentage across all trials was 1.50 ± 0.51 [0.44-3.60%].

Simple linear regression analyses

The highest association between E_{req} and WBSR was observed using the $\dot{M}_{acsm}$, method for estimating metabolic rate ($R^2 > 0.71$; r > 0.84; $p < 0.01$, **Fig. 1).** All methods for estimating mean skin temperature and the convective heat transfer coefficient resulted in similar explained variance and association (**Figures 1, 2 and 3**). The lowest associations between E_{req} and WBSR were observed using $\dot{M}_{ge}$ (R^2 = 0.67-0.68; r = 0.82-0.83; $p < 0.01$, **Fig. 3**). Subsequent analysis for heteroscedasticity on the residuals for the highest performing E_{req} model ($\dot{M}_{acsm}$, h_{c2}, T_{sk3}) revealed that the variability in the residuals is not consistent for external workload ($p < 0.001$). As absolute external workload increases, the variability in the residuals increases both in the positive and negative direction (**Fig. 6D)**. However, residual variability for the environmental variables [T_{db}, T_r] was consistent across the range of environmental conditions (**Fig. 6A-C**, $p > 0.05$).

The variance in WBSR was significantly associated with external workload, with over half of the variance in WBSR described by external workload alone ($R^2 = 0.53$; $p < 0.01$, **Fig. 4A**). Using external workload data to estimate H_{prod} (using M_{acsm}, see **Eq. 5**) only explained an additional 1% of variance compared to external workload alone ($R^2 = 0.53$; $p < 0.01$, (**Fig. 4E**). T_{db} described 14% of the variance in WBSR ($R^2 = 0.14$; $p < 0.01$), while T_r described marginally less variance (12%) in WBSR compared to T_{db} ($R^2 = 0.11$; $p < 0.01$). Increases in ambient vapour pressure had no impact on WBSR ($R^2 = 0.01$, r=0.10, p>0.05, **Fig. 4F**) Cycling velocity described 29% of the variance in WBSR ($R^2 = 0.31$; $p < 0.01$, **Fig. 4G**). Cycling velocity was strongly correlated with external workload (r=0.72, $p < 0.01$). When deriving an estimated E_{req} with the Givoni and Goldman (1972) equation which uses only three input variables: H_{prod}, clo, and T_{db} (see methods: *calculations*), we observed an explained variance in WBSR by E_{req} of 72% ($R^2 = 0.72$; r=0.85, $p < 0.001$, **Fig. 4H**).

Estimated or measured external workload

The external workload estimates from Strava associated highly with measured external workloads measured from Garmin power meter pedals ($R^2 = 0.87$; r=0.80; $p < 0.01$, **Fig. 5A**). A Bland-Altman analysis revealed that the estimated external workload from Strava tended to underestimate measured external workload (mean bias: -14W, LOA [-67 to 40], **Fig. 5B**). Using estimated external workload from Strava rather than measured external workload as an input to calculate E_{req} reduced the association between E_{req} and WBSR ($R^2 = 0.66$; r=0.81; $p <$ 0.01, **Fig. 5C**). Expressing E_{req} relative to body surface area ($W\cdot m^{-2}$) rather than in absolute terms (W), reduced the explained variability in WBSR by E_{req} ($R^2 = 0.57$; r=0.76; $p < 0.01$, **Fig. 5D**).

4.4 Discussion

The main finding of this study was that the evaporative requirement for heat balance (E_{req}) was strongly associated (peak R^2=0.72, peak r=0.85, **Fig 1 A, C-H**) with whole-body sweat rate (WBSR) during outdoor recreational road cycling. Notably, this association, though robust, exhibited a lower peak R^2 compared with previous observations in controlled laboratory environments (up to R^2=0.93) (Gagnon *et al.*, 2013). Although the outdoor association of E_{req} and WBSR was lower than indoors, changing the way metabolic heat production impacted this association the most (compared with changes to skin temperature and the convective heat transfer coefficients). The reduced association was more pronounced when employing estimated external workload data from Strava to the E_{req} model (R^2=0.65), as opposed to measured external workload data from Garmin power meter pedals (**Fig. 5C**). The reduced association when using estimated external workload to estimate H_{prod} could be explained by compounded error in the metabolic rate calculation for the purposes of calculating E_{req}. These findings build upon earlier laboratory studies (Gagnon *et al.*, 2013; Cramer & Jay, 2015; Hospers *et al.*, 2020) which supports the notion that E_{req} predominantly determines WBSR during steady-state exercise and suggests that the E_{req} model can be applied in high airflow outdoor environments such as middle-long distance triathlon and road cycling.

The lower explained variance in our study (~73%) is due to increased measurement error in the field (i.e., measurements of external workload), and the reliance on prediction equations for key input variables into the E_{req} model. For example, estimating metabolic rate from external workload includes inherent measurement uncertainty with commercial power meters (e.g., ± 1-2% error) and then translating that external workload to metabolic rate without knowing mechanical efficiency then relies on impersonal prediction equations. Mean skin temperature must also be estimated rather than measured and finally ,there is uncertainty around how natural convection and turbulent air flows affect the convective heat transfer coefficient and the follow-on effects on dry and evaporative heat exchange. Previous laboratory-based research has observed high associations between E_{req} and WBSR during rest and steady-state exercise at low-moderate metabolic heat productions (200-500W), inside a calorimeter with high airflow and by design, complete sweat evaporation (100% sweating efficiency) (Gagnon *et al.*, 2013). Gagnon and colleagues (2013) observed that as H_{prod} increased at a given air temperature (30 ºC), the variance in WBSR explained by E_{req}, reduced (from ~97% at 500W [H_{prod}] to ~82% at 200W [H_{prod}]). In our data (**Fig. 6D)** it appears that the absolute variability increases beyond external workload data > 250W, however, this could be explained by amplified measurement error from the Garmin power pedals as absolute external workloads increase (reported accuracy is ± 1-2% for the Vector 3s and RS200, respectively). Therefore, as absolute external workload increases, measurement errors may occur with a greater magnitude, which is then amplified by any error in the metabolic rate prediction equation. Subsequent analysis of the residuals for the highest performing E_{req} model aligns with this theory, whereby the residual variability for external workload increased with higher absolute external workloads (**Fig 6D**), but not for any environmental variables (T_{db}, T_r, Pa, **Fig. 6A-C**). Indicating that the main source of error in the model used to E_{req} is likely a result of measurement error at a higher absolute workload, amplified by subsequent metabolic rate estimations.

We observed differences in the explained variance in WBSR by E_{req} when moving from $\dot{M}_{acsm}$ (Liguori *et al.*, 2022), to $\dot{M}_{ett}$ (Ettema & Lorås, 2009) to M_{ge} (Moseley *et al.*, 2004) (highest R^2: 0.72, 0.69, 0.67, lowest R^2: 0.71, 0.68, 0.65 respectively). The higher explained variance with $\dot{M}_{acsm}$ is observed despite the use of the equation outside its recommended parameters (i.e., external work > 200W (Liguori *et al.*, 2022)) for 84 trials. Given the high correlation of estimated H_{prod} and external workload with WBSR (r=0.74, 0.73 respectively)

(**Fig. 5 A, E**), estimating metabolic rate from external workload is crucial to the calculation of E_{req} in an outdoor environment, when gas exchange data is unavailable. The main driver for metabolic rate is oxygen consumption whereby the final rate is augmented by the fuel used during oxidative phosphorylation (typically carbohydrates and fats) to produce ATP (i.e., respiratory exchange ratio [RER]). Assuming a modest steady-state oxygen consumption of 2.0 L $O_2 \cdot min^{-1}$ and an RER of 1, the resultant metabolic rate is 604W, yet with an RER of 0.85 (50:50 carbohydrates:fats ratio) at the same 1.5 L $O_2 \cdot min^{-1}$ the resultant metabolic rate is 579 (-25W difference) (Cramer & Jay, 2019). Predicting metabolic rate from only external workload data is therefore problematic, however, the quality of the prediction may be improved with an assessment or estimation of the individual's physiological state (i.e., RER or %$\dot{V}O_{2max}$) or mechanical efficiency. Additionally, since O_2 consumption primarily occurs in skeletal muscle mass and not fat mass, using the $\dot{M}_{acsm}$ method, absolute O_2 consumption and therefore metabolic heat production may be over and underestimated for individuals with above and below-average body fat percentages, respectively.

Current methods for estimating mean skin temperature (Mehnert *et al.*, 2000; Vanos *et al.*, 2012; ISO, 7933, 2004) were developed predominantly inside laboratories (i.e., walking or running on a treadmill, cycling on an ergometer with air velocities between 0.1-2.2 ($m \cdot s^{-1}$) via forced convection [e.g., fans]), across comparatively low metabolic rates (102-620W versus our observed rates 468-1481W, **Table 2**) and low (≤0.2, clo) or moderate-high clothing (0.6-1.0, clo). One more recent study observed individuals in an outdoor environment (while cycling on a stationary ergometer) in cool to temperate conditions (8.9-24.4 ºC) with regular athletic clothing (cotton t-shirt, athletic shorts and shoes) and natural airflow (1.9-2.8 $m \cdot s^{-1}$) (Vanos *et al.*, 2012). How well these indoor models, which have been validated on low ambient/forced wind velocity data, translate to scenarios with much higher self-generated convection is uncertain. In our data, we observed no real influence of the method used to estimate mean skin temperature [T_{sk1}, T_{sk2}, T_{sk3}] on explained variance in WBSR by E_{req}: (highest R^2: 0.72, 0.72, 0.72, lowest R^2: 0.65, 0.66, 0.66 respectively, **Fig. 1-3**). Given the significant effect of airflow on skin temperature (from increased convection and the cooling effect of the evaporation of sweat from the skin surface (Parsons, 2014)) current available models may be limited in these high airflow environments. In low airflow environments, the impact of differences in skin temperature on convective and radiative heat exchange are relatively minimal (compared to metabolic heat production and the evaporative heat loss). However, in a high airflow environment such as cycling, small differences in skin temperature could inflate differences in E_{req}. For example, a difference between skin and the air of 2 ºC would result in a difference in dry heat loss of 44 W at 9 m·s^{-1} but at 0.5 m·s^{-1} would result in a difference in dry heat loss of 9 W would be observed (when using h_{c2}). Another significant challenge when evaluating skin temperature prediction models is access to invasive data required as an input (namely core body temperature) and indeed a true metabolic rate value in an environment outside the laboratory, without gas exchange measures.

Much of the existing literature on the h_c at high air velocities (>4.0 m·s^{-1}) is limited to computational fluid dynamics modelling (CFD) (Defraeye *et al.*, 2011), however recent work has observed the h_c through CFD analysis and validation studies in wind tunnels (Li & Ito, 2014; Xu *et al.*, 2021b, a). According to seminal work that first evaluated h_c, it appears the relationship between air velocity and h_c follows a logarithmic curve, where between 0-2 m·s^{-1} (Nishi & Gagge, 1970) for every unit increase in air velocity, there is a sharp increase in h_c. Beyond ~2 m·s^{-1} however, the rise in h_c for every unit of air velocity increase reduces according to Nishi& Gagge (1970). In our results, the method for estimating h_c had little effect on the explained variance in WBSR by E_{req} (the largest difference in explained variance was 2% across h_c methods, **Fig. 1-3**). Prior research in high airflow environments (including cycling position-specific work) indicates that the h_{c1} method may be the most applicable method for estimating h_c in high airflow scenarios (Defraeye *et al.*, 2011; Li & Ito, 2014). In the context of our data, it is unclear which method for estimating h_c is the most appropriate, as the explained variance between each method was 0-2%, however, h_{c2} and h_{c3} were on average the highest performing methods across metabolic rate and mean skin temperature estimates (**Fig. 1-3**). Therefore, in these data we may be overestimating the skin-to-air temperature gradient, where the convective heat transfer coefficients with the lower estimated values (h_{c2} and h_{c3}) then compensate for the overestimated mean skin temperature, resulting in higher explained variance in WBSR with h_{c2} and h_{c3} than the theoretically more appropriate convective heat transfer coefficient (h_{c1}).

Perspectives

Our study and associated findings are strengthened by the range of combined environmental conditions and metabolic rates achieved throughout data collection, resulting in a wide range of E_{req} [289-889W] and WBSR [0.28-2.31 $L \cdot h^{-1}$] values (**Table 2**). However, undescribed variability in WBSR remains in our data, which may be partially explained by our use of estimation models outside the original model domain (e.g., higher self-generated air velocity associated with outdoor cycling than mean skin temperature, convective heat transfer models, and higher external workloads >200W). However, observing the strength of the relation between E_{req} and WBSR in a challenging outdoor environment, with natural fluctuations in exercise intensity and environmental conditions should be considered an important step in validating the E_{req} model for use during outdoor cycling and other high airflow scenarios. Translating this modelling into real-world practice to inform hydration strategies requires the implementing this type of model into integrated technology like Garmin devices where data such as power, height, weight and environmental conditions can be measured to estimate E_{req}. Any of these implementations must then be tested with rigour to inform real-world practice.

Limitations

Our study would have been strengthened with indirect calorimetry measures to confirm metabolic rate rather than relying on prediction equations using external workload data. However, we sought to estimate E_{req} with the freely accessible equipment in a field setting. Future work may be necessary to further improve metabolic rate estimations while cycling at high external workloads where sweat losses will be higher. Despite having no confirmatory gas exchange data, the current study shows that E_{req} explains a high amount of variance in WBSR in an outdoor environment, even when using estimated metabolic heat production, and mean skin temperature data. We relied on prediction equations for measures of mean skin temperature that are used here at much higher air velocities than experienced during the development of the original skin temperature models. Therefore, the skin temperature values predicted by each of the models could be higher than those experienced by the participants in this study, particularly at lower dry-bulb temperatures and higher cycling velocities. We assumed wind speed and direction was the same within each trial and thus the relative contribution of ambient wind speed was zero. With real time, on bike wind speed and direction sensors which are coming on to the market now, these assumptions could be improved in future work. Our participants were not able to consume fluid throughout this study, and as such experienced a range of levels of dehydration from 0.44 - 3.60% of body mass loss. As such, they experienced different levels of dehydration which could have affected their cycling efficiency and resulted in errors in metabolic rate estimates. Future work should consider providing individualised fluid intakes to account for differing rates of fluid loss between individuals and trials during similar studies.

Future research

Future research should focus on refining current or developing new methods for calculating or predicting metabolic rate, mean skin temperature and the convective heat transfer coefficient in an outdoor, high airflow environment. Measures of skin temperature could be utilised to examine the factors that influence skin temperature during outdoor road cycling and address the gap in current skin temperature prediction equations. The apparent lack of metabolic rate estimation models at high external workloads and cadences for recreational-elite cyclists calls for further research to establish such appropriate models. Furthermore, riding in the pro peloton results in marked reductions in relative wind velocity but also metabolic rate due to the significantly reduced aerodynamic drag compared to riding solo at equivalent ground speeds. Further research should be conducted into how well this type of modelling works in the pro peloton under different riding conditions.

Conclusion

In this study, we investigated the association between the evaporative requirement for heat balance and whole-body sweat rate during *quasi*-steady-state outdoor road cycling. We observed that E_{req} remained highly associated with WBSR in an outdoor environment, despite estimating key variables for calculating the E_{req} model. We observed the highest explained variance in WBSR by E_{req} when calculating E_{req} with $\dot{M}_{acsm}$, T_{sk3}, and h_{c3}, however, differences between the methods used to predict mean skin temperature and convective heat transfer coefficient were marginal. Using estimated external workload data (from Strava) to calculate metabolic rate and subsequently $E_{req,}$ explained a reduced but still moderate amount of variability in WBSR. Current prediction models for estimating mean skin temperature and the convective heat transfer coefficient should be improved by evaluating them in high airflow specific research.

4.5 References

Abbott PF & Tabony RC. (1985). The estimation of humidity parameters. *Meteorological Magazine* **114,** 49-56.

Bland JM & Altman DG. (2007). Agreement Between Methods of Measurement with Multiple Observations Per Individual. *Journal of Biopharmaceutical Statistics* **17,** 571-582.

Brown HA, Topham TH, Clark B, Smallcombe JW, Flouris AD, Ioannou LG, Telford RD, Jay O & Périard JD. (2022). Seasonal Heat Acclimatisation in Healthy Adults: A Systematic Review. *Sports medicine (Auckland, NZ)* **52,** 2111-2128.

Brown RD & Gillespie TJ. (1986). Estimating outdoor thermal comfort using a cylindrical radiation thermometer and an energy budget model. *International Journal of Biometeorology* **30,** 43-52.

Cheuvront SN & Kenefick RW. (2017). CORP: Improving the status quo for measuring whole body sweat losses. *Journal of Applied Physiology* **123,** 632-636.

Cheuvront, SN, Kenefick, RW, Montain, SJ, & Sawka, MN. (2010). Mechanisms of aerobic performance impairment with heat stress and dehydration. *Journal of applied physiology,* **109**, 1989-1995.

Cramer MN & Jay O. (2015). Explained variance in the thermoregulatory responses to exercise: the independent roles of biophysical and fitness/fatness-related factors. *Journal of Applied Physiology* **119,** 982-989.

Cramer MN & Jay O. (2019). Partitional calorimetry. *Journal of Applied Physiology* **126,** 267-277.

Defraeye T, Blocken B, Koninckx E, Hespel P & Carmeliet J. (2011). Computational fluid dynamics analysis of drag and convective heat transfer of individual body segments for different cyclist positions. *Journal of Biomechanics* **44,** 1695-1701.

Dickinson T & Wright J. (2021). The reliability and accuracy of the Garmin Vector 3 power pedals. *Proceedings of the Institution of Mechanical Engineers, Part P: Journal of Sports Engineering and Technology* **235,** 70-74.

Du Bois D & Du Bois. (1916). Clinical Calorimetry. *Archives of Internal Medicine* **XVII,** 863-871.

Ettema G & Lorås HW. (2009). Efficiency in cycling: a review. *European Journal of Applied Physiology* **106,** 1-14.

Foster, Carl; Florhaug, Jessica A.; Franklin, Jodi; Gottschall, Lori; HROVATIN, LAURI A.; Parker, Suzanne; Doleshal L, Pamela; Dodge, Christopher. A New Approach to Monitoring Exercise Training. Journal of Strength and Conditioning Research 15(1):p 109-115, February 2001.

Fusco, A., Knutson, C., King, C., Mikat, R. P., Porcari, J. P., Cortis, C., & Foster, C. (2020). Session RPE During Prolonged Exercise Training. *International Journal of Sports Physiology and Performance*, **15**, 292-294. https://doi.org/10.1123/ijspp.2019-0137.

Gagge AP & Gonzalez RR. (2010). Mechanisms of Heat Exchange: Biophysics and Physiology. In *Comprehensive Physiology*, pp. 45-84.

Gagnon D, Jay O & Kenny GP. (2013). The evaporative requirement for heat balance determines whole-body sweat rate during exercise under conditions permitting full evaporation. *The Journal of Physiology* **591,** 2925-2935.

Garmin. (2021). Garmin Rally RS, RK, XC Owner's Manual.

Garmin. (2023). Temperature Change Effects on the Vector Power Meter Pedals.

Givoni B & Goldman RF. (1972). Predicting rectal temperature response to work, environment, and clothing. *Journal of Applied Physiology* **32,** 812-822.

Gonzalez R. (2019). Biophysics of Heat Exchange and Clothing: Applications to Sports Physiology.

Hardy JD, Du Bois EF & Soderstrom GF. (1938). Basal Metabolism, Radiation, Convection and Vaporization at Temperatures of 22 to 35°C.: Six Figures. *The Journal of Nutrition* **15,** 477-497.

Hospers L, Cheuvront SN, Kenefick RW & Jay O. (2020). Independent Influence of Skin Temperature on Whole-Body Sweat Rate. *Medicine and science in sports and exercise* **52,** 2423-2429.

Hunt LA, Hospers L, Smallcombe JW, Mavros Y & Jay O. (2021). Caffeine alters thermoregulatory responses to exercise in the heat only in caffeine-habituated individuals: a double-blind placebo-controlled trial. *Journal of Applied Physiology* **131,** 1300-1310.

ISO. (7726, 1998). Ergonomics of the thermal environment — Instruments for measuring physical quantities. International Organization for Standardization, Geneva.

ISO. (7933, 2004). Ergonomics of the thermal environment — Analytical determination and interpretation of heat stress using calculation of the predicted heat strain.

Kreith F & Black WZ. (1980). Basic heat transfer.

Li C & Ito K. (2014). Numerical and experimental estimation of convective heat transfer coefficient of human body under strong forced convective flow. *Journal of Wind Engineering and Industrial Aerodynamics* **126,** 107-117.

Liguori G, Feito Y, Fountaine C & Roy B. (2022). *ACSM's guidelines for exercise testing and prescription*. Wolters Kluwer, Philadelphia.

Lotens W & Havenith G. (1991). Calculation of clothing insulation and vapour resistance. *Ergonomics* **34,** 233-254.

Malchaire J, Kampmann B, Havenith G, Mehnert P & Gebhardt HJ. (2000). Criteria for estimating acceptable exposure times in hot working environments: a review. *Int Arch Occup Environ Health* **73,** 215-220.

McCullough EA, Jones BW & Huck J. (1985). A comprehensive data base for estimating clothing insulation. *Ashrae Trans* **91,** 29-47.

Meade RD & Kenny GP. (2017). Are All Heat Loads Created Equal? *Medicine and science in sports and exercise* **49,** 1796-1804.

Mehnert P, Malchaire J, Kampmann B, Piette A, Griefahn B & Gebhardt H. (2000). Prediction of the average skin temperature in warm and hot environments. *Eur J Appl Physiol* **82,** 52-60.

Moseley L, Achten J, Martin JC & Jeukendrup AE. (2004). No Differences in Cycling Efficiency Between World-Class and Recreational Cyclists. *International Journal of Sports Medicine* **25,** 374-379.

Muriel X, Valenzuela PL, Mateo-March M, Pallarés JG, Lucia A & Barranco-Gil D. (2022). Physical Demands and Performance Indicators in Male Professional Cyclists During a Grand Tour: WorldTour Versus ProTeam Category. *International journal of sports physiology and performance* **17,** 22-30.

Nielsen M. (1938). Die Regulation der Körpertemperatur bei Muskelarbeit1. *Skandinavisches Archiv Für Physiologie* **79,** 193-230.

Nishi Y & Gagge AP. (1970). Direct evaluation of convective heat transfer coefficient by naphthalene sublimation. *Journal of Applied Physiology* **29,** 830-838.

Oliveira AVM, Gaspar AR, Francisco SC & Quintela DA. (2014). Analysis of natural and forced convection heat losses from a thermal manikin: Comparative assessment of the static and dynamic postures. *Journal of Wind Engineering and Industrial Aerodynamics* **132,** 66-76.

Parsons K. (2014). *Human thermal environments: the effects of hot, moderate, and cold environments on human health, comfort, and performance*. CRC press.

Parsons KC. (2003). *Human Thermal Environments*. Taylor & Francis, London.

Pedregosa F, Varoquaux G, Gramfort A, Michel V, Thirion B, Grisel O, Blondel M, Prettenhofer P, Weiss R & Dubourg V. (2011). Scikit-learn: Machine learning in Python. *the Journal of machine Learning research* **12,** 2825-2830.

Peronnet F & Massicotte D. (1991). Table of nonprotein respiratory quotient: an update. *Can J Sport Sci* **16,** 23-29.

Ravanelli N, Imbeault P & Jay O. (2020). Steady-state sweating during exercise is determined by the evaporative requirement for heat balance independently of absolute core and skin temperatures. *J Physiol* **598,** 2607-2619.

Sawka MN, Young AJ, Francesconi RP, Muza SR & Pandolf KB. (1985). Thermoregulatory and blood responses during exercise at graded hypohydration levels. *Journal of Applied Physiology* **59,** 1394-1401.

Smallcombe J, Hodder S, Kuklane K, Młynarczyk M, Loveday D, Eggeling J, Halder A & Havenith G. (2021). Updated Database of Clothing Thermal Insulation and Vapor

Permeability Values of Western Ensembles for Use in ASHRAE Standard 55, ISO 7730, and ISO 9920. **VC-21-011**.

Strava. (2023). How to Get Power for Your Rides.

Vanos JK, Warland JS, Gillespie TJ & Kenny NA. (2012). Thermal comfort modelling of body temperature and psychological variations of a human exercising in an outdoor environment. *International Journal of Biometeorology* **56,** 21-32.

Vogt JJ, Candas V, Libert JP & Daull F. (1981). Chapter 6 Required Sweat Rate as an Index of Thermal Strain in Industry. In *Studies in Environmental Science*, ed. Cena K & Clark JA, pp. 99-110. Elsevier.

Watanabe K, Stöhr EJ, Akiyama K, Watanabe S & González-Alonso J. (2020). Dehydration reduces stroke volume and cardiac output during exercise because of impaired cardiac filling and venous return, not left ventricular function. *Physiol Rep* **8,** e14433.

Xu J, Psikuta A, Li J, Annaheim S & Rossi RM. (2021a). Evaluation of the convective heat transfer coefficient of human body and its effect on the human thermoregulation predictions. *Building and Environment* **196,** 107778.

Xu J, Psikuta A, Li J, Annaheim S & Rossi RM. (2021b). A numerical investigation of the influence of wind on convective heat transfer from the human body in a ventilated room. *Building and Environment* **188,** 107427.

Y. S. Touloukian PEL, S. C. Saxena. (1970). *Thermophysical Properties of Matter, Vol. 3: Thermal Conductivity*.

Table 1. Descriptive information (mean, standard deviation and range) during outdoor cycling.

Group	n	Age, y	Height, cm	Body mass, kg	A_D, m^2	Trial intensity, AU	External workload, W "best effort"	Session RPE for each "best effort", AU	Session RPE (0 to 10)
Men	43	29 ± 4 [19-39]	181.9 ± 7.6 [165.2-196.4]	80.25 ± 9.69 [61.07-103.36]	2.01 ± 0.14 [1.71-2.31]	100H, 68L-M	233 ± 37 [158-331]	7.0 ± 2.1 [2-10]	5.3 ± 2.7 [2-10]
Women	16	29 ± 4 [25-39]	171.5 ± 6.1 [162.3-182.9]	64.93 ± 7.5 [53.14-83.97]	1.76 ± 0.12 [1.58-2.04]	44H, 24L-M	173 ± 34 [124-254]	5.6 ± 2.3 [1-9]	5.1 ± 2.3 [1-9]
All	59	29 ± 4 [19-39]	178.9 ± 8.6 [162.3-196.4]	75.83 ± 11.45 [53.14-103.36]	1.94 ± 0.18 [1.58-2.31]	144H, 92L-M	217 ± 45 [124-331]	6.6 ± 2.2 [5-10]	5.2 ± 2.6 [1-10]

Where: A_D, is body surface area, RPE is Rating of Perceived Exertion, best effort refers to each participant's highest average external workload achieved across all trials, and H=high, L-M=low-moderate intensity. Mean ± SD [Range]

Table 2: Descriptive data for dependent and independent variables from 236 trials.

Group	T_{db}, ºC	P_a, kPa	T_r, ºC	v, m·s^{-1}	$\dot{M}_{acsm}$, W	E_{req}, W	Duration, min	WBSR, L·h^{-1}	External workload, W, Garmin	External workload, W, Strava
Men	23.4 ±3.8 [12.4-30.4]	1.54 ± 0.32 [0.70-2.23]	47.8 ± 14.7 [13.6-72.8]	1.09 ± 0.45 [0.38-2.90]	947 ± 183 [468-1481]	617 ± 133 [284-889]	61.3 ± 2.5 [43.0-70.0]	1.09 ± 0.37 [0.28-2.31]	199 ± 45 [81-331]	186 ± 44 [94-343]
Women	24.4 ± 3.2 [12.5-29.0]	1.61 ± 0.32 [0.79-2.17]	50.4 ± 13.3 [14.7-71.7]	1.11 ± 0.49 [0.34-2.61]	751 ± 129 [513-1153]	499 ± 95 [284-761]	61.9 ± 2.1 [55.4-68.0]	0.77 ± 0.25 [0.28-1.49]	157 ± 31 [97-254]	153 ± 25 [103-212]
All	23.7 ± 3.6 [12.4-30.4]	1.56 ± 0.32 [0.70-2.23]	48.5 ± 13.6 [13.6-72.8]	1.09 ± 0.46 [0.34-2.90]	890 ± 191 [468-1481]	583 ± 134 [284-889]	61.5 ± 2.4 [43.0-70.0]	1.00 ± 0.37 [0.28-2.31]	187 ± 46 [81-331]	177 ± 42 [94-343]

Where, WBSR, whole-body sweat rate; T_{db}, dry-bulb temperature, P_a, ambient vapour pressure, T_r mean radiant temperature, v, wind velocity, $\dot{M}_{acsm}$, estimated metabolic rate, and E_{req}, rate of evaporation required for heat balance – best case (using $\dot{M}_{acsm}$, T_{sk3}, h_{c2}). Fewer trials with Strava estimated external workload data available were conducted: Men: n=125, Women: n=48, All: n=173. Mean ± SD [Range].

Figure 1. A series of simple linear regressions of whole-body sweat rate (WBSR) described by the required rate of evaporation to attain heat balance (E_{req}) which has been calculated using three methods of estimating mean skin temperature (T_{sk}) and three methods of estimating the convective heat transfer coefficient (h_c) (see methods: *calculations*), n = 236, *p < 0.001.

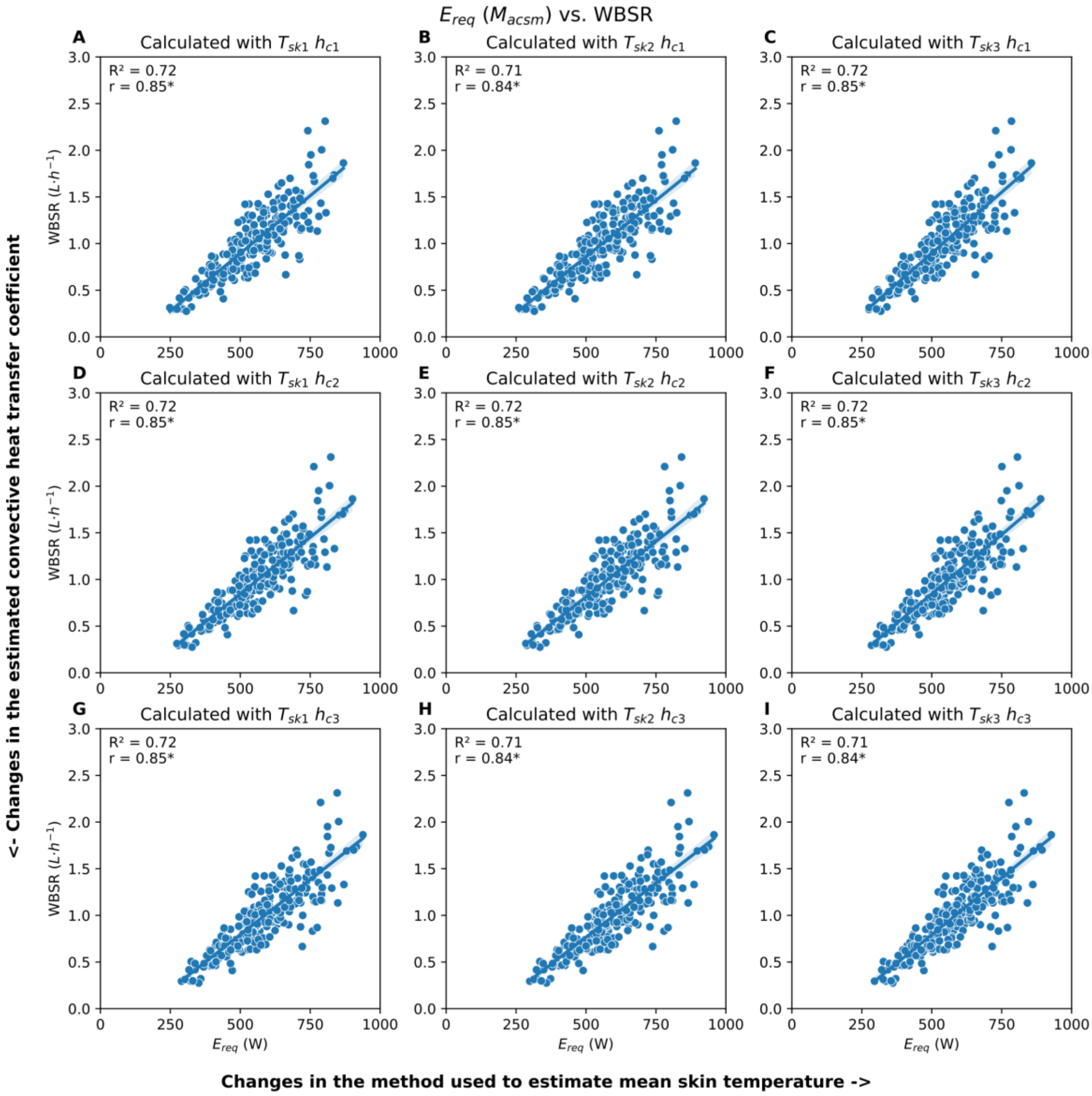

Figure 2. A series of simple linear regressions of whole-body sweat rate (WBSR) described by the required rate of evaporation to attain heat balance (E_{req}) where metabolic energy expenditure has been calculated using $\dot{M}_{ett}$ for all plots, dry heat loss (C + R) has been calculated with three methods of estimating mean skin temperature (T_{sk}) and three methods of estimating the convective heat transfer coefficient (h_c) (see methods: *calculations*) resulting in the 9 plots, n = 236, *p < 0.001.

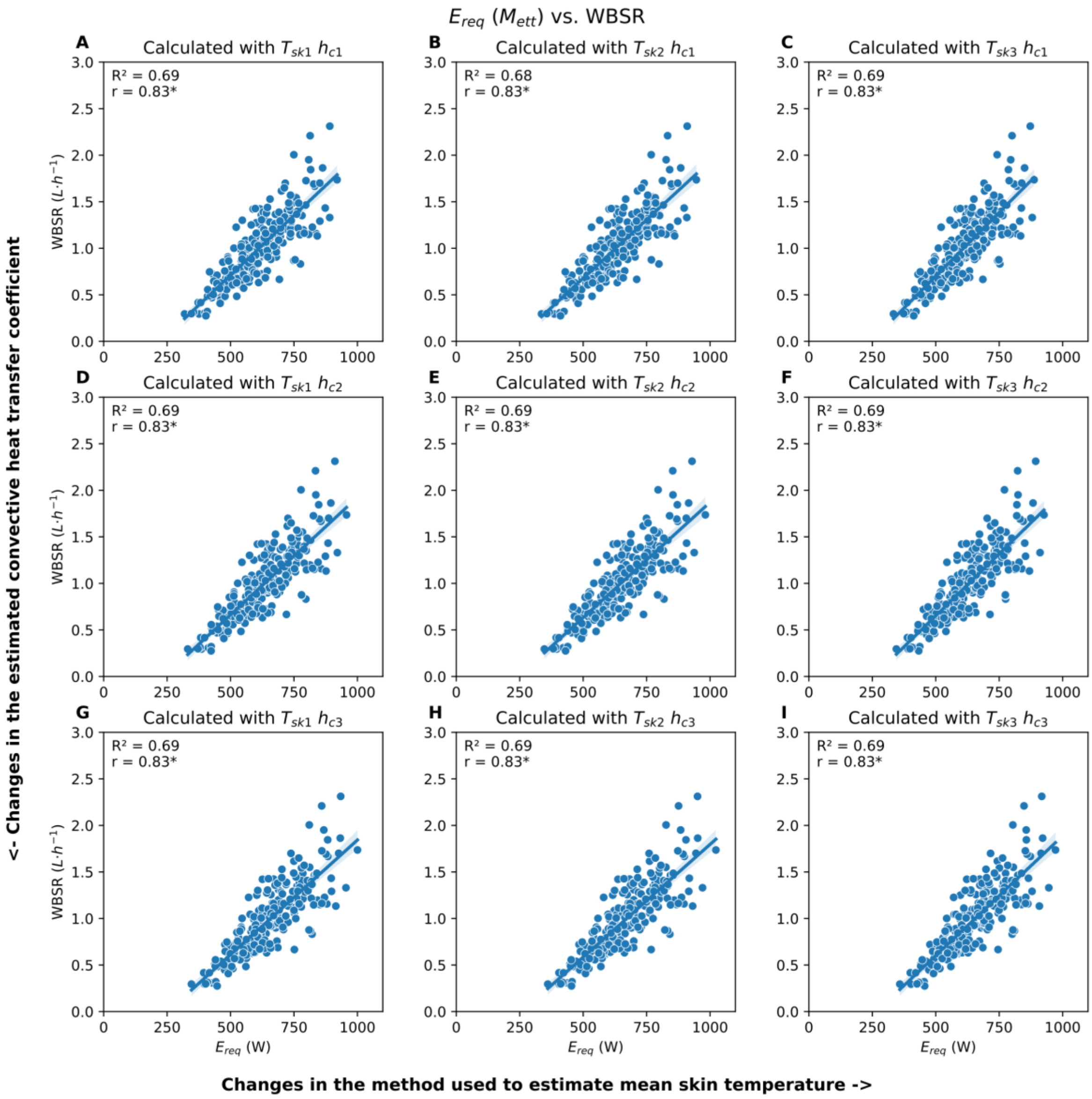

Figure 3. A series of simple linear regressions of whole-body sweat rate (WBSR) described by the required rate of evaporation to attain heat balance (E_{req}) where metabolic energy expenditure has been calculated using $\dot{M}_{ge}$ for all plots, dry heat loss (C + R) has been calculated with three methods of estimating mean skin temperature (T_{sk}) and three methods of estimating the convective heat transfer coefficient (h_c) (see [methods: *calculations*]) resulting in the 9 plots, n = 236, *p < 0.001.

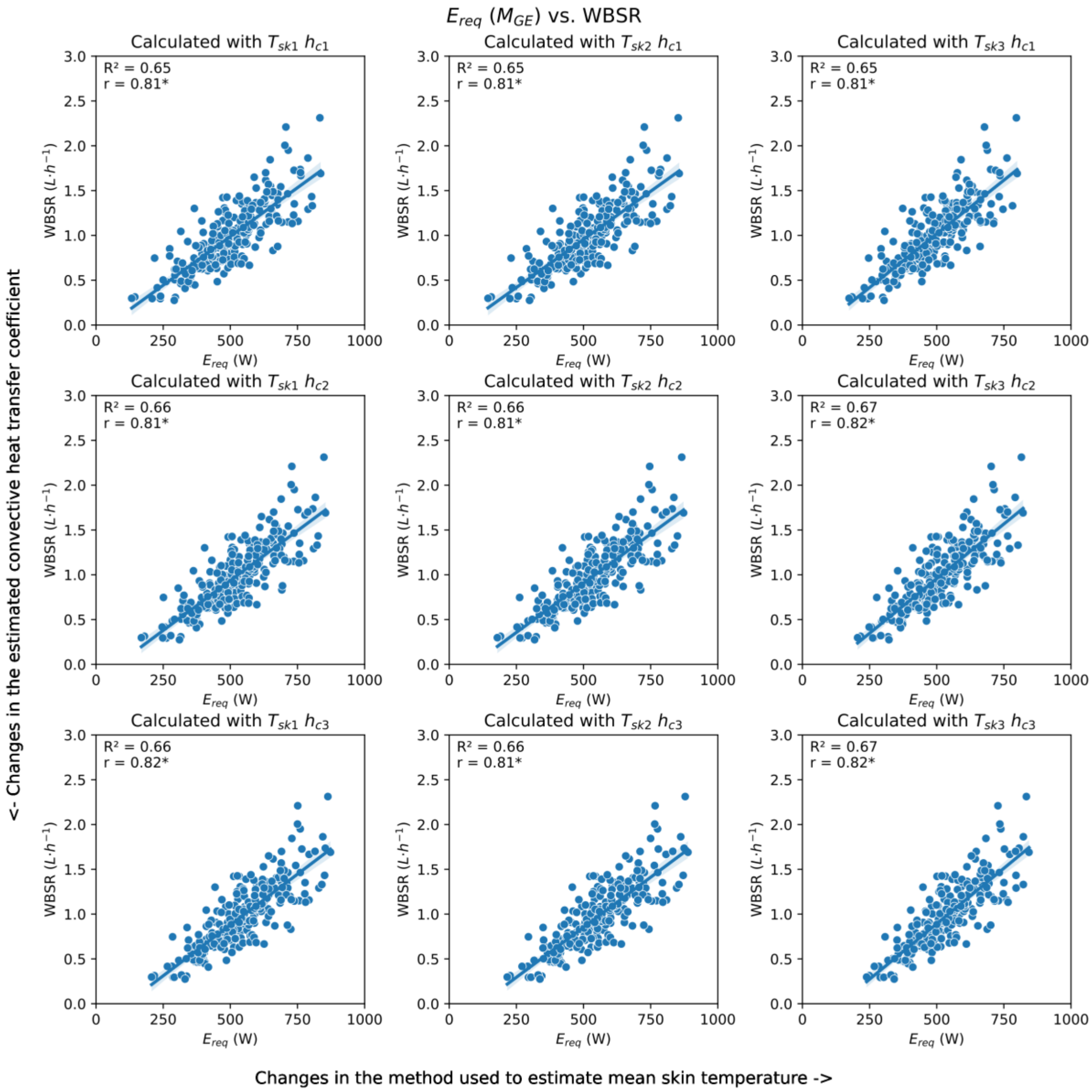

Figure 4. A series of simple linear regressions of whole-body sweat rate (WBSR) described by external workload (W), dry-bulb temperature [T_{db}] (ºC), ambient vapour pressure [P_a] (kPa), cycling velocity [v_{self}] (m·s^{-1}), mean radiant temperature [T_r] (ºC), metabolic heat production [H_{prod}] (W), and the evaporative requirement for heat balance [E_{req}] (W) calculated with the best method of estimating E_{req} calculated with $\dot{M}_{acsm}$, T_{sk3} and h_{c2} and an additional calculation of $E_{req\_givoni+goldman}$ (see [methods: *calculations*]), n=236, *p < 0.001.

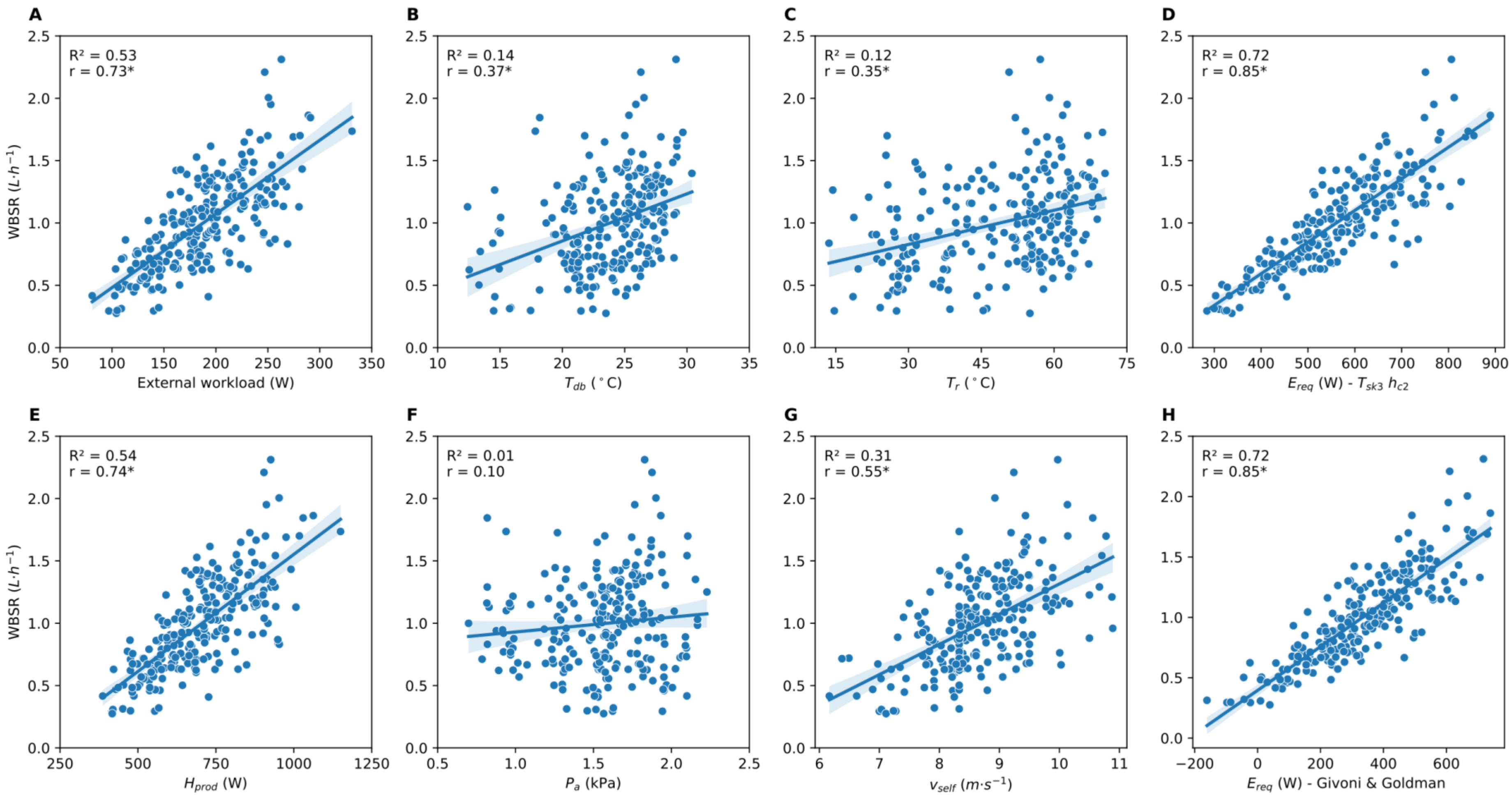

Figure 5A: scatter plot comparison of measured external workload (via Garmin power pedals) versus estimated external workload (via the Strava power estimator). **B:** Bland Altmann analysis of the mean difference of estimated vs measured external work. **C and D**: simple linear regressions of whole-body sweat rate (WBSR) described by the evaporative requirement for heat balance (E_{req}, W and E_{req}, W·m^{-2} respectively) - calculated with estimated power - using the best method for calculating E_{req} ($\dot{M}_{acsm}$ for metabolic rate, T_{sk2} for mean skin temperature and h_{c2}), n=173, *p < 0.001.

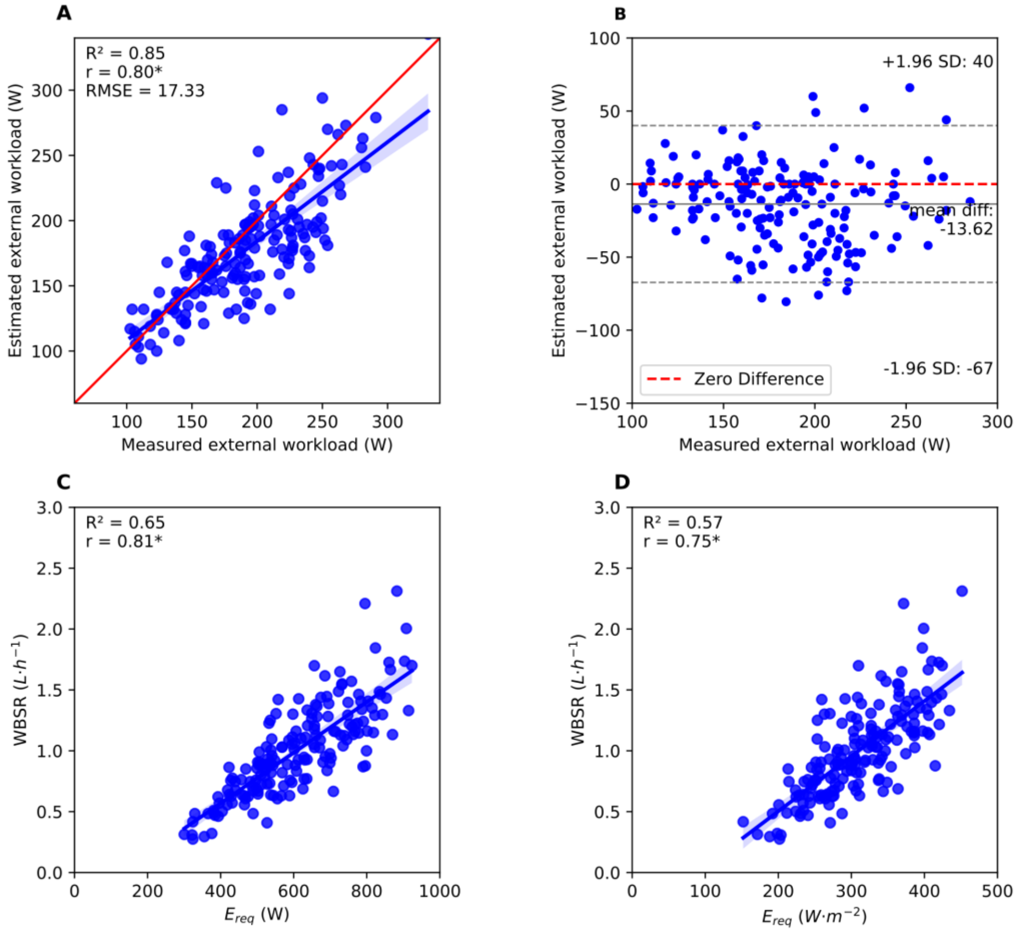

Figure 6. Residual plots for the regression plotted with E_{req} as the predictor of WBSR for input variables [T_{db}: **A**: P_a: **B**, T_r: **C,** external workload: **D**] into the E_{req} model to assess heteroskedasticity of residuals. n=236, * denotes $p < 0.05$.

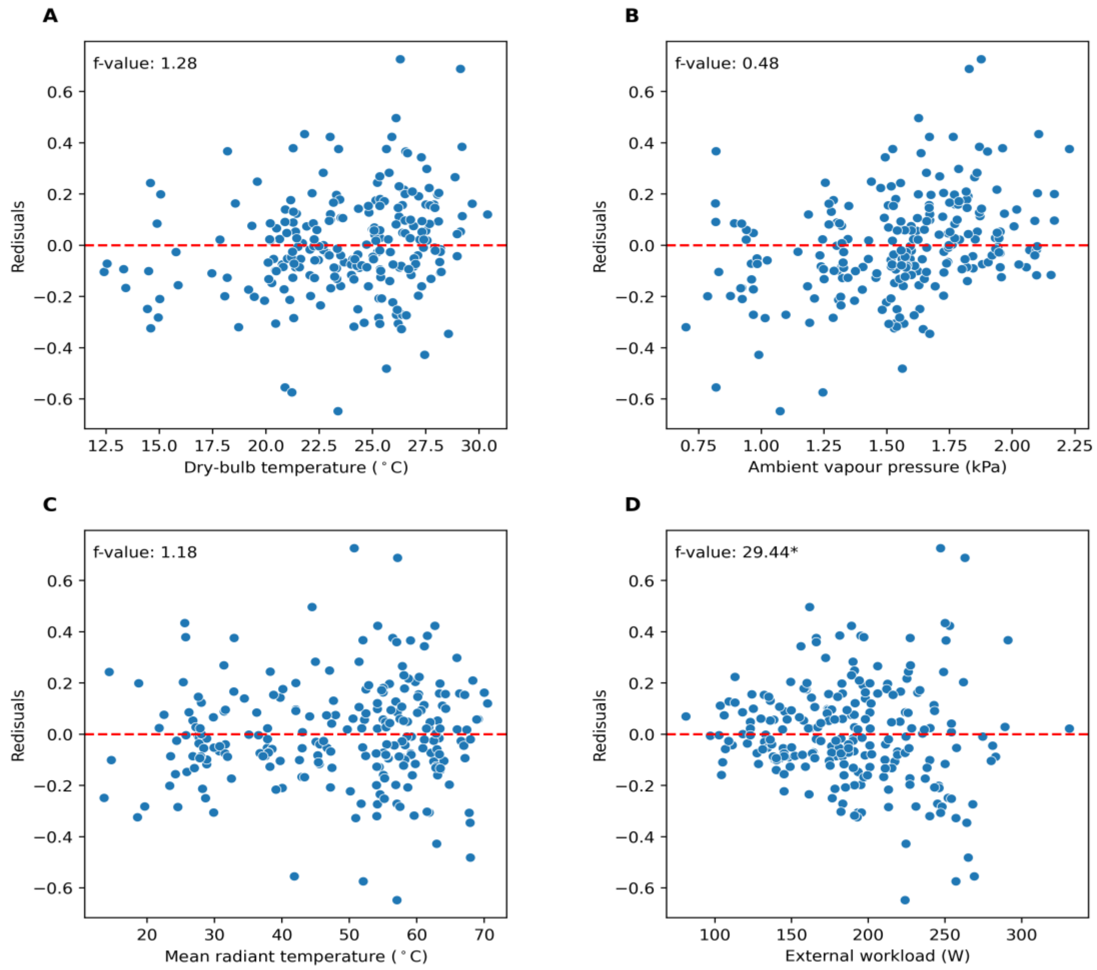

CHAPTER V

Prediction of the mean skin temperature from readily available data while outdoor road cycling

Lindsey Hunt[1], James W Smallcombe[1], and Ollie Jay[1,2]
[1]The University of Sydney, Thermal Ergonomics Laboratory, Sydney School of Health Sciences, Faculty of Medicine and Health, Australia
[2]The University of Sydney, Charles Perkins Centre, Camperdown, Australia

Author Contributions: L. Hunt, J. Smallcombe and O. Jay designed the research, L. Hunt, and J. Smallcombe conducted the research, O. Jay provided access to materials and equipment, L. Hunt analysed the data, L. Hunt drafted the first manuscript, J.W Smallcombe, and O. Jay assisted with data interpretation and reviewing the draft manuscript and O. Jay had primary responsibility for the final content of the paper. All authors read and approved the final manuscript.

Running head: Skin temperature during outdoor road cycling

Address for correspondence:
Prof. Ollie Jay ✉
Thermal Ergonomics Laboratory,
Sydney School of Health Sciences,
Faculty of Medicine and Health,
The University of Sydney, NSW 2006.
Australia
+ 61 (2) 9036 4102
e-mail: ollie.jay@sydney.edu.au

5.0 Abstract

Purpose: Mean skin temperature (T_{sk}) is critical to human heat balance models as the skin-to-air temperature gradient, coupled with the convective heat transfer coefficient, dictates dry heat exchange with the environment. Current models for estimating skin temperature have mostly been developed for use in laboratory environments, with low to moderate metabolic heat productions (100-620 W), low airflow (< 4.0 m·s^{-1}) and across a range of clothing levels (0.1-1.5 clo). We aimed to 1) assess the agreement of available skin temperature models ($T_{sk\_mehnert}$ T_{sk_ISO} T_{sk_COMFA}) with empirical data, and 2) develop a new model for estimating mean skin temperature during outdoor cycling.

Methods: 23 participants (7 women); cycled at a self-selected intensity (External Workload: 118-267 W) in a range of environmental conditions (T_{db}; 21.1-30.3 ºC, P_a; 0.96-1.82 kPa, T_r; 23.3-72.1 ºC, Wind Velocity; 0.5-2.9 m·s^{-1}) for ~60 minutes outdoors at Centennial Park in Sydney, Australia on average for 2 [range:1 to 9] occasions, to a total of 51 trials. Data were randomly allocated into separate modelling and validation groups.

Results: All available skin temperature prediction models overestimated T_{sk} when compared with measured T_{sk} (Mean differences and 95% CI: $T_{sk\_mehnert}$: + 3.3 ºC [3.1, 3.4],T_{sk_ISO}: + 1.5 ºC [1.3, 1.7], T_{sk_COMFA}: + 3.3 ºC [3.1, 3.5]). The agreement between available estimation methods and measured T_{sk} reduced with lowering dry-bulb temperature. The following expression was obtained: $T_{sk\_pred} = 16.6585 + 0.4235 \cdot T_{db} + 1.1449 \cdot P_a + 0.007 \cdot H_{prod}$. Our skin temperature prediction method resulted in an RMSE of ± 0.94 ºC in the validation group and a mean difference of -0.03 ºC and 95% CI [-1.9, 1.9 ºC] which results in a mean underprediction of fluid losses compared to measured T_{sk} of -74 (g.h^{-1}).

Conclusion: This study observed that the currently available methods for predicting skin temperature during activities with high air velocities during outdoor cycling exercise overestimated mean skin temperature. Here, we report a newly developed skin temperature prediction equation, which is specific to high airflow physical activity, such as road cycling that demonstrated a higher agreement to measured mean skin temperature data and more accurately predicted estimated fluid losses.

Keywords: Mean Skin Temperature, Heat Balance, Road Cycling, Fluid Requirements, Biophysical Modelling.

5.1 Introduction

Outdoor road cycling can be a physically demanding outdoor activity that places a significant burden on the thermoregulatory system due to the internal metabolic heat generated. A considerable amount of metabolic heat can be produced by recreational and top-performing World Tour male (~4.0-6.6 $W \cdot kg^{-1}$) and female (~3.0-4.6 $W \cdot kg^{-1}$) athletes for extended durations (~20 minutes) (Menaspà *et al.*, 2017; VAN Erp *et al.*, 2020; Gallo *et al.*, 2022). Assuming a 21% gross mechanical efficiency, at 5.5 $W \cdot kg^{-1}$ of external work would result in a metabolic heat production (H_{prod}) of ~1448 W. Such high rates of metabolic heat production while cycling must be offset primarily via convective and evaporative heat exchange pathways, which are driven by skin-to-air thermal and vapour pressure gradients and their respective convective, radiative, and evaporative heat transfer coefficients (h_c, h_r, h_e) (Parsons, 2014). Physiological modification of T_{sk} and saturated vapour pressure at the skin surface ($P_{sk,\ sat}$) occurs through thermoeffector responses (e.g., increases in skin blood flow and the onset of sweating) (Gagge & Gonzalez, 2010). When T_{sk} is above the operative temperature (T_o), convective and radiative (dry) heat loss to the environment occurs, and as T_{sk} approaches T_o more metabolic heat must be lost via sweat evaporation until all heat must be lost via evaporation, as T_o exceeds T_{sk}. T_o is a mathematical average of the surrounding mean radiant temperature (T_r) and dry-bulb temperature (T_{db}) which is weighted by their convective and radiative heat transfer coefficients (Parsons, 2003). Thus, mean skin temperature during recreational road cycling influences dry and evaporative heat exchange and, is crucial to the precise estimation of heat strain and fluid requirements, particularly while exposed to warm environmental conditions and/or high rates of metabolic heat production.

Existing models for the prediction of mean skin temperature (T_{sk}) (Mehnert *et al.*, 2000; Vanos *et al.*, 2012; ISO, 7933, 2004) have proposed both regression and empirical models using available personal and environmental factors (dry-bulb temperature, metabolic rate, clothing, ambient vapour pressure, body core temperature, and local environmental wind speed). Currently, available prediction equations for mean skin temperature yield good results in both indoor laboratory (Mehnert *et al.*, 2000; ISO, 7933, 2004) and outdoor environments (although on stationary ergometers) (Vanos *et al.*, 2012) as they have been validated for use in environments with a wide range of ambient humidities (0.2-5.3, kPa) and mean radiant temperatures (up to 145 ºC). Early models for the prediction of mean skin temperature in warm and hot environments (Mairiaux, Malchaire & Candas, 1987; Mehnert *et al.*, 2000) include a range of metabolic rates and thermal environmental conditions, however, lacked high metabolic rates (>620 W) and air velocities (>2.0 $m \cdot s^{-1}$) which can be readily achieved by recreational and World Tour level male and female cyclists (Thompson *et al.*, 1997; Clarry, Faghih Imani & Miller, 2019; VAN Erp *et al.*, 2020; Sanders & van Erp, 2021; Sitko, Cirer-Sastre & López-Laval, 2022). With outdoor cycling presenting much higher ambient air velocities it is likely that current skin temperature prediction models may not adequately account for the high rates of convection that are present at high air speeds. Predicting mean skin temperature using these models outside their validated conditions may lead to inaccuracies, particularly in the context of outdoor road cycling as the conditions (namely wind velocity and metabolic rate) can be so different.

Therefore, we aimed to 1) examine the agreement between available skin temperature models with measured mean skin temperature data during outdoor road cycling, and 2) develop a new model for estimating mean skin temperature across a range of high airflow, high metabolic rate and temperate-warm outdoor environmental conditions.

We hypothesised that (1) current prediction methods would overestimate mean skin temperature given the high front-facing self-generated air velocities which increase convection and evaporation at the skin surface and (2) the new model developed on outdoor cycling data will perform better than previous low airflow skin temperature estimation models.

5.2 Methods

Experimental design

All data were collected at a ~flat (19m elevation gain per lap), outdoor circuit (3.72 km) at Centennial Parklands in Sydney, Australia (Latitude: 33°53'59"S, Longitude: 151°14'01"E) across the warmer months (November-April), between November 2022 and January 2024. The range of environmental conditions experienced is presented in **Table 1**. Exercise intensity was self-selected by each participant for every visit to observe a range of metabolic heat productions. To enable the collection of a range of exercise intensities we guided participants to complete each session at varying intensities for each visit with the following descriptors (e.g., easy ride [55-65% of functional threshold power (FTP)], moderate ride [65-75% of FTP], and hard ride, [75%+ of FTP]). As performance (power output) was not an outcome variable for this study, we only required a range of power outputs across a range of absolute and relative intensities to develop and test any models. Participants were instructed to maintain a steady-state cycling effort throughout the ~60-minute ride and to keep their external workload as consistent as possible throughout.

Participants

Approval for the study was obtained from the Human Research Ethics Committee (HREC no. 2020/736), and each participant was provided with complete information about the study before completing a health screen and informed consent form. A total of 23 participants (7 females) were recruited. The descriptive characteristics of the participants are in **Table 1**. All participants met the predetermined eligibility criteria: 18-40 years of age (inclusive), regularly participated in outdoor road cycling (≥ 2 times per week for at least 6 months before participating), owned their equipment (road bike, shoes, helmet, and clothing etc). All participants were not current smokers and were free from respiratory, metabolic, and cardiovascular diseases. Participants' acclimatisation status may have changed across the data collection period due to the potential for seasonal acclimatisation (Brown et al., 2022), however, all participants were trained but not acclimatised or acclimated, as no individuals participated in any dedicated acclimation or acclimatisation protocols throughout their study participation. All participants were instructed to abstain from consuming caffeine in any form (liquid or solid) (Hunt et al., 2021), or alcohol, and from engaging in strenuous physical activity for 24 hours before participating and were instructed to maintain their position on the bike between trials (i.e., not adjust saddle height, fore, aft) which may affect exercise efficiency between trials.

Protocol

Experimental sessions: Participants were asked to consume a light meal and 500 mL of water ~2 hours before arriving at Centennial Park for the experimental trials. On arrival at the data collection site, participants' bikes were fitted with a set of cycling power meter pedals to quantify external workload. Additionally, participants were fitted with 8 iButton sensors to measure mean skin temperature (see *Measurements*). Participant clothing thermal insulation (I_{cl}), evaporative resistance of clothing ($R_{e,cl}$), and clothing area (f_{cl}) for the cycling ensemble were estimated to be 0.3 [0.31 for women] [clo], 0.0107 [$m^2 \cdot kPa/W$], and 1.119 [n.d.] respectively (McCullough, Jones & Huck, 1985; Gonzalez, 2019; Smallcombe et al., 2021). The estimation of clothing was standardised across all participants, and it was assumed all participants cycling clothing had the same insulative and evaporative properties aside from accounting for the addition of a sports bra for women.

Participants then cycled for ~60 minutes on their road bike around the continuous cycling-friendly loop at an exercise intensity of their choosing (mean external workload 193 ± 44 [84-267] W). Participants were also instructed to continue cycling at their steady-state pace until they returned to the data collection location after at least 56 minutes (each lap of the circuit takes approximately 5-7 minutes). Participant clothing was not standardised between participants; however, individuals were asked to wear typical summer cycling clothing (cycling jersey, bibs and socks [with the addition of a sports bra for women]) and completed all subsequent trials in the same clothing. Upon returning to the data collection site after completing the exercise trial, were asked for a subjective rating for the session Rating of Perceived Exertion (RPE) on a scale from 0-10, had the iButtons removed and the power meter pedals removed from their bike. Throughout each trial, participants did not consume food or water and they were instructed to avoid drafting other cyclists, vehicles or anything that could obstruct airflow in front of them.

Measurements

Skin temperature: Skin temperature (T_{sk}) was measured using wireless temperature sensors (iButtons DS1921H-F5, Embedded Data Systems, Lawrenceburg, KY, USA) (Smith et al., 2009) secured to the skin using surgical tape at 8 sites (ISO, 9886, 2004). Mean skin temperature (T_{sk}) was then estimated using a weighted average at the recorded 8 sites (chest, shoulder, thigh, calf, elbow, forehead, hand and upper back) fixed to the left side of the body. Dry heat exchange, the evaporative requirements for heat balance (E_{req}), the maximum evaporative capacity of the environment (E_{max}), and the rate of sweating to achieve heat balance (S_{req}) were estimated using partitional calorimetry (Cramer & Jay, 2019) and adjusted for our purposes (see calculations). Body surface area (BSA) was determined using the DuBois & DuBois method (Du Bois & Du Bois, 1916).

Power output: External workload (Watts) while cycling was determined using cycling power meter pedals (Garmin Rally RS200, Garmin, USA - reported error ±1%) fixed to participants' bikes. Garmin power pedals were set up on participant bikes according to the manufacturer's instructions. Briefly, the set-up process involved setting the crank length (from 165-177.5 mm) and performing a standard calibration using either a cycling computer (Edge 530, Garmin, Olathe, USA) or a smartphone (iPhone 12, Apple, Cupertino, USA) with the Garmin Connect App (Garmin, 2021). The power pedals were kept in a location out of the sun so they would be equilibrated to the environmental conditions and were calibrated before each test as the reported power output is affected by temperature (Garmin, 2023). Cycling data were recorded (including GPS data) with an iPhone 12 using the Cyclemeter (Abvio, San Francisco, USA) application. This phone was then placed in the participant's jersey pocket to continuously record data as the trial started. The phone recorded cycling speed, cycling time, cycling distance, and external workload using the Cyclemeter application in 1-sec intervals. Data were then exported and saved as a .csv file for later processing into 1-min intervals using Python (pandas.resample).

Environmental conditions: Outdoor environmental conditions were measured on-site using a custom environmental monitoring unit (EMU) built and extensively tested by engineers at The University of Sydney to meet the specifications outlined by the International Organisation for Standardization (ISO 7726, 2001). Data for shaded aspirated dry-bulb temperature (T_{db}, °C), air velocity (ν, $m \cdot s^{-1}$), black globe temperature (T_g, ºC) relative humidity (RH, %) were recorded in 5-second increments and averaged every 1-min. Finally, the data was resampled into 15-minute buckets from minute 15-30, 30-45, and 45-60 to obtain three data points per trial. Data from 15-minute onwards was used to allow participants to reach a relative steady state with their environment. The T_{db} and aspirated wet-bulb (T_{awb}) thermometers used were a perforated and an immersion type 50 mm Class A platinum resistance thermometer, respectively (Temperature Controls, Sefton, NSW, Australia). The T_{awb} thermometer was draped in a cotton shroud connected to a reservoir of distilled water that kept the thermometer and cotton shroud fully saturated throughout data collection. The thermometers for T_{db} and T_{awb} were continuously aspirated at ~3.0 $m \cdot s^{-1}$ with a 40 mm by 40 mm x 20 mm Sunon fan (Sunonwealth Electric Machine Industry Company Ltd., Kaohsiung City, Taiwan). Black globe temperature (T_g) was measured with an immersion type 100 mm Class A platinum resistance thermometer (Temperature Controls, Sefton, NSW, Australia) inserted in a 115 mm copper globe painted matt black. Wind velocity was measured with a Windsonic ultrasonic Anemometer (Gill Instruments Ltd., Lymington, Hampshire, UK), with the following specifications, range: 0.0 to 60 $m \cdot s^{-1}$, accuracy of ±2 % at 12 $m \cdot s^{-1}$, resolution: 0.1 $m \cdot s^{-1}$ and response time: 0.01 $m \cdot s^{-1}$). The EMU was mounted to a Rollei tripod (Digitec Audio, Zurich, Switzerland) at a height of 1.2 m and was placed in position at least 30 minutes before the start of data collection to equilibrate to the environment. Data were collected in full sun, where only cloud cover (when present) provided shade, viewed with Grafana (Grafana Labs, New York City, NY, USA) and downloaded as required for analysis. Mean radiant temperature (T_r, ºC) was calculated with equation [1] (ISO, 7726, 1998).

$$T_r = \left[\left(T_g + 273.15\right)^4 + \frac{\left(1.1 \times 10^8 \times v^{0.6}\right)}{\varepsilon \times d^{0.4}}\left(T_g - T_a\right)\right]^{0.25} - 273.15 \qquad [^\circ C]\ [1]$$

Where ν is air velocity in $m \cdot s^{-1}$, ε is the emissivity of the black copper globe, assumed to be 0.97 (Parsons, 2003), T_a is aspirated dry-bulb temperature (°C), T_g is black globe temperature (ºC), and d is the diameter of the globe in meters (0.115 m). Relative humidity was calculated using psychrometry with T_{db} and T_{wb} with the following equation:

$$\mathrm{RH} = \frac{100\left[\mathrm{EXP}\left[1.8096 + \left(\frac{17.2694T_{wb}}{237.3+T_{wb}}\right)\right] - 7.866 \times 10{-}4P(T_{db}-T_{wb})\left(1+\frac{T_{wb}}{610}\right)\right]}{\mathrm{EXP}\ [1.8096+[(\frac{17.2694T_{db}}{237.3+T_{db}})\ ]} \qquad [\%]\ [2]$$

Where: RH is relative humidity (%); T_a is aspirated dry-bulb temperature (°C); T_{wb} is aspirated wet bulb temperature (°C); EXP is the exponent; P is Station level pressure (hPa), assumed to be 998.3 hPa, from the standard table of pressures (Abbott & Tabony, 1985).

Calculations

Mean skin temperature was estimated using three methods, $T_{sk\_mehnert}$ (Mehnert et al., 2000), T_{sk_ISO} (ISO, 7933, 2004) and T_{sk_COMFA} (Brown & Gillespie, 1986; Vanos et al., 2012):

$$\mathrm{T}_{sk\_menhert} = 12.17 + 0.02\mathrm{T}_a + 0.044\mathrm{T}_r - 0.253v_{self} + 0.194\mathrm{P}_a + 0.0029\mathrm{M} + 0.51346T_{c_{eq}} \quad [^\circ\mathrm{C}][3]$$

The ISO standard (7933) gives an equation for scenarios where clothing is > 0.6 clo (T_{sk_cl}), and < 0.2 clo clothing (T_{sk_nu}) and a third equation for situations where clothing falls between 0.2-0.6 clo. The resultant third equation T_{sk_ISO} is given which is a combination of T_{sk_cl} and T_{sk_nu}. T_{sk_cl} is equal to $T_{sk\_mehnert}$ (ISO, 7933, 2004).

$$\mathrm{T}_{sk\_nu} = 7.19 + 0.064\mathrm{T}_a + 0.061\mathrm{T}_r - 0.348v_{self} + 0.198\mathrm{P}_a + 0.616T_{c_{eq}} \quad [^\circ\mathrm{C}]\ [4]$$

$$\mathrm{T}_{sk\_ISO} = \mathrm{T}_{sk\_nu} + 2.5\left(\mathrm{T}_{sk\_menhert} - \mathrm{T}_{sk\_nu}\right) \times (I_{cl} - 0.2) \quad [^\circ\mathrm{C}]\ [5]$$

$$\mathrm{T}_{sk\_COMFA} = \left(\frac{T_{c_{eq}} - \mathrm{T}_a}{r_t + r_c + r_a}\right)(r_a + r_c) + T_a \quad [^\circ\mathrm{C}]\ [6]$$

Where: T_{db} is dry-bulb temperature (in ˚C), T_r is mean radiant temperature (in ˚C), P_a is absolute humidity (in kPa); M is metabolic rate (in W·m^{-2}), and $T_{c_{eq}}$ is steady state body core temperature [estimated with **Eq. 7**]. Tissue (r_t), clothing (r_c) and aerodynamic (r_a) resistances (s·m^{-1}) were calculated according to Brown and Gillespie (1986) (Brown & Gillespie, 1986). I_{cl} is the insulative resistance of the clothing ensemble. Clo is an arbitrary unit of clothing insulation (1 clo = 186.6, s·m^{-1} = 0.1555 m^2·°C^{-1}·W^{-1}).

$$T_{c_{eq}} = 36.6 + 0.002 \cdot M \quad [^\circ\mathrm{C}]\ [7]$$

Body tissue thermal resistance (r_t) decreases with metabolic rate (W·m^{-2}) and was calculated as (Brown & Gillespie, 1986):

$$r_t = (-0.1\ \dot{\mathrm{M}}) + 65 \quad [\mathrm{s \cdot m^{-1}}]\ [8]$$

Static and dynamic clothing thermal resistance (r_{co}, r_c) were calculated respectively as: (Brown & Gillespie, 1986)

$$r_{co} = clo \times 186.61 \quad [\mathrm{s \cdot m^{-1}}]\ [9]$$

$$r_c = r_{co} \times \left(-0.37\left(1 - exp^{\frac{-v_{self}}{0.72}}\right) + 1\right) \quad [\mathrm{s \cdot m^{-1}}]\ [10]$$

Where: v_{self} is cycling velocity ($m \cdot s^{-1}$), clo is equal to I_{cl} and r_{co} is static clothing thermal resistance given by **Eq. 9**.

Boundary layer thermal resistance (r_a) was calculated as(Brown & Gillespie, 1986):

$$r_a = \frac{(0.17)}{(ARe^n Pr^{0.33} k)} \qquad [s \cdot m^{-1}]\ [11]$$

Where: Re is the Reynolds number $\left(\frac{0.17 v_{self}}{v}\right)$, where v_{self} is free stream air velocity (cycling velocity, $m \cdot s^{-1}$), v is the kinematic viscosity of air ($\sim 1.5 \times 10^{-5}\ m^{-2} \cdot s^{-1}$). A and n are empirical constants. In our case, Re always exceeds 40,000. When Re is > 40,000, A=0.0266, and n=0.805 (Kreith & Black, 1980). Pr is the Prandtl number assumed to be 0.7296(Kreith & Black, 1980), and k is the thermal diffusivity of air assumed to be $2.14 \times 10^{-5}\ m^2 \cdot s^{-1}$ at 25 °C (Y. S. Touloukian, 1970).

The rate of oxygen consumption ($\dot{V}O_2$) was estimated using the ACSM standard equation for during cycle ergometry [**Eq. 12**] (Liguori et al., 2022). This predicts $\dot{V}O_2$ which can be converted to an estimated metabolic energy expenditure using equation [12]. To calculate metabolic rate, we assumed a metabolic energy equivalent (MEE) of 20.7 for low-moderate intensity sessions (session RPE <4) and 21.1 for high-intensity sessions (session RPE >4) (in $kj \cdot LO_2^{-1}$) (Peronnet & Massicotte, 1991): Oxygen consumption ($\dot{V}O_2$) is given by:

$$\dot{V}O_2 = \left[\frac{(10.8 \times \text{Wk})}{m_b}\right] + 7 \qquad [mL \cdot kg^{-1} \cdot min^{-1}]\ [12]$$

Where: $\dot{V}O_2$ is the rate of oxygen consumption ($mL \cdot kg^{-1} \cdot min^{-1}$), Wk is external workload and m_b is total body mass (kg). Metabolic energy expenditure (M) is then given by:

$$\text{M} = \frac{(\dot{V}O_2 \times m_b) \cdot \text{MEE} \cdot 1000}{60} \qquad [W]\ [13]$$

Where: $\dot{V}O_2$ is the rate of oxygen consumption ($mL \cdot kg^{-1} \cdot min^{-1}$), m_b is total body mass (kg) and MEE is the relevant metabolic energy equivalent given above for each session (e.g., high: 21.1; low-moderate: 20.7, $kj \cdot LO_2^{-1}$).

Metabolic heat production (H_{prod}) is given by:

$$\mathrm{H}_{prod} = \mathrm{M} - \mathrm{W} \qquad [\mathrm{W}]\ [14]$$

Where: M is metabolic energy expenditure in Watts as calculated by Eq. 13, and W is external workload given in Watts.

Convective and radiative heat exchange at the skin surface was estimated with equations 5 and 16 respectively (Parsons, 2003):

$$C = h_c \cdot f_{cl} \cdot (T_{sk} - T_{db}) \qquad [\mathrm{W \cdot m^{-2}}]\ [15]$$

$$R = h_r \cdot f_{cl} \cdot (T_{sk} - T_r) \qquad [\mathrm{W \cdot m^{-2}}]\ [16]$$

Where: T_{db} is dry-bulb temperature (in ˚C); h_c is the convective heat transfer coefficient; h_r is the radiative heat transfer coefficient and f_{cl} is clothing area factor. The radiative heat transfer coefficient (h_r) is given by (Parsons, 2014):

$$h_r = 4 \cdot \varepsilon \cdot \sigma \cdot f_{eff} \cdot \left[273.15 + \frac{T_{sk} + T_r}{2}\right]^3 \qquad [\mathrm{W \cdot m^{-2} \cdot K}]\ [17]$$

Where: ε is the emissivity of clothed human (assumed to be 0.97), σ is the Stefan-Boltzmann constant (5.67×10^{-8} $\mathrm{W/m^{-2} \cdot K^{-4}}$), f_{eff} is effective radiation area factor (assumed to be 0.7 for cycling), T_{sk} is estimated using measured, and predictive equations [T_{sk_mes}, $T_{sk\_mehnert}$, T_{sk_ISO}, T_{sk_COMFA} and T_{sk_pred}]; T_r was calculated using equation [2] from measured black globe temperature (T_g, ºC) and wind velocity (v, $\mathrm{m \cdot s^{-1}}$) data by the on-site EMU.

The most appropriate method for estimating the convective heat transfer coefficient is given by Lotens and Havenith (1991) who describe the first method as potentially appropriate for high air velocities (0-10 $\mathrm{m \cdot s^{-1}}$) (Lotens & Havenith, 1991).

$$h_{c1} = 8.3 \cdot \left(0.07 + 0.0043 \cdot f_{ped} + v_{self}\right)^{0.86} \qquad [\mathrm{W \cdot m^{-2} \cdot {}^\circ C^{-1}}]\ [18]$$

Where: f_{ped} is average cycling cadence ($\mathrm{revolutions \cdot min^{-1}}$) and v_{self} is cycling velocity ($\mathrm{m \cdot s^{-1}}$).

Statistical Analyses

Data were assessed for normality using the Shapiro-Wilk normality test and were assumed normal when $p \geq 0.05$, with visual inspections of the q-q plots of the residuals and histograms to confirm normality or otherwise. Exploratory data analyses were conducted with a series of simple linear regressions were used to assess the association between dependent variables and mean skin temperature, the Pearson correlation coefficient (*r*) was also used to assess bivariate relationships and collinearities between variables. A modelling and validation group were randomly allocated (but not shuffled) using the test_train_split function within Statsmodels and a test group size of 0.40 which resulted in a modelling group of 91 and a validation group of 62 data points respectively. A multiple linear regression analysis was performed for the development of the model. Data were averaged over three 15-minute intervals (15-30 minutes, 30-45 minutes and 45-60 minutes) to allow for the steady state to be achieved after the outset of exercise from 0-15 minutes. The coefficient of determination (R^2) mean bias, root mean squared error (RMSE), Lin's Concordance Correlation Coefficient (Lin's CCC) and mean absolute error (MAE), were used to assess the model fit for the skin temperature prediction model. Some participants completed multiple trials, on different days, at different exercise intensities and with different environmental conditions. All analyses were performed with Python using the Pycharm IDE (version 2023.3) and the following packages Seaborn (https://seaborn.pydata.org/index.html), Scipy (https://scipy.org/), Matplotlib (https://matplotlib.org/), Pandas (https://pandas.pydata.org/), Numpy (https://numpy.org/), Statsmodels (https://www.statsmodels.org/stable/index.html), and Scikit-learn (https://scikit-learn.org/stable/) (Pedregosa et al., 2011).

5.3 Results

Descriptive characteristics

Table 1 gives the descriptive features of the participants from the study. This population is representative of a wide range of body shapes and sizes however, it is also representative of relatively young and regularly recreationally active cyclists. The mean skin temperature, cycling speed and metabolic heat production for all trials across are presented with cycling distance in **Figure 2**, which characterises the natural rise and fall in gradient across the cycling circuit. **Figure 3** shows the distribution and range plotted with mean skin temperature for each potential primary variable to determine mean skin temperature. These data include a wide range and combination of conditions (20.2-31.1 ºC [T_{db}], 16.5-83.3 ºC [T_r], and 0.77-1.84 kPa, [P_a]) and metabolic rates (102-946 W·m^{-2}, [$\dot{M}$]) across trials. End exercise body mass loss was 1.43 ± 0.37 [0.60-2.15 %]

Agreement of mean skin temperature estimation models

The difference in estimated skin temperature between prediction models was small (**Table 2**) however all prediction models overestimated skin temperature compared to measured mean skin temperature (Mean differences and 95% CI: $T_{sk\_mehnert}$: + 3.3 ºC [3.1, 3.4],T_{sk_ISO}: + 1.5 ºC [1.3, 1.7], T_{sk_COMFA}: + 3.3 ºC [3.1, 3.5]) (**Fig. 1A**). Using the existing methods to predict mean skin temperature resulted in an overestimation of the air-to-skin temperature gradient and subsequent inflation of dry heat exchange for all skin temperature prediction methods (**Fig. 1B, Table 2**). The differences between predicted and measured mean skin temperatures increased with reductions in dry-bulb temperature (**Fig. 1C**). Ultimately, differences of 1-4 ºC between currently available T_{sk} prediction methods and measured T_{sk} result in an overestimation of dry heat loss and E_{max}, resulting in meaningful underestimations of S_{req} ($T_{sk\_mehnert:}$ -272 ± 139, T_{sk_ISO}: -161 ± 160, T_{sk_COMFA}: -323 ± 158 g.h^{-1}) (**Table 4**).

Exploratory data analysis

Figure 2 plots dependent variables with measured mean skin temperature as exploratory analysis to examine the bivariate relations (including frequency and distribution) between potential predictor variables and any multi-collinearities between dependent variables. **Table 2** contains summary results for the bivariate relations between potential predictor variables and measured mean skin temperature. Dry-bulb temperature had the highest correlation with measured T_{sk} (r=0.72, p<0.001), followed closest by mean radiant temperature (r=0.49, p<0.001) and ambient vapour pressure (r=0.29, p<0.001). Utilising mean radiant temperature and dry-bulb temperature in the predictive linear regression is not possible due to the high collinearity between variables (r=0.51, p<0.001, **Fig.3**). Based on the exploratory data analysis (**Table 2**, **Fig. 3**), the following predictor variables were selected (T_a, H_{prod}, and P_a) which had the strongest correlations with the dependent variable (T_{sk}) and the ones that had the lowest potential issues with collinearity with other variables. For example, While T_r has been shown to affect skin temperature at rest, given the high convective airflow over the skin and the significant collinearity with dry-bulb temperature (r=0.51), T_r was excluded. Similarly, wind velocity or in this case, cycling velocity has been shown to reduce T_{sk}, given the relationship between metabolic heat production and v_{self} velocity and the collinearity observed between v_{self} and H_{prod}, v_{self} was excluded.

Prediction of mean skin temperature

The regression coefficients and standard errors from the multiple linear regression on the modelling data set (n=91) are found in **Table 2**. Model performance was assessed on a validation data set (n=62) with an RMSE error of ± 0.94 ºC and a Bland-Altman analysis revealing no mean bias with a mean difference of -0.03 ºC (**Fig. 5B**), which is improved compared with existing models on the same validation data set ($T_{sk\_mehnert}$: +3.3 ºC, T_{sk_ISO}: +1.5 ºC, T_{sk_COMFA}: +3.3 ºC) (**Fig. 4A-C)**.

$T_{sk\_pred} = 16.6585 + 0.4603 \cdot T_{db} + 1.1449 \cdot P_a + 0.007 \cdot H_{prod}$ [Eq. 12]

Where T_{sk_pred} is the predicted mean skin temperature in ºC, T_{db} is dry-bulb temperature in ºC, H_{prod} is metabolic heat production in $W \cdot m^{-2}$ and P_a is ambient vapour pressure in kPa.

Table 4 contains descriptive data for outcomes variables in the S_{req} model which are affected by T_{sk}. Data other than measured and estimated T_{sk} are reported as differences between predicted and measured T_{sk}. The differences between estimated dry heat loss (W), E_{req} (in W) and S_{req} ($g \cdot h^{-1}$) between measured T_{sk}, and the three available prediction models [$T_{sk\_mehnert}$, T_{sk_ISO} T_{sk_COMFA}] was reduced with our model [**Eq. 12**] when predicting T_{sk} in the validation group (**Table 4**).

5.4 Discussion

The main finding of this study is that existing methods for estimating mean skin temperature (T_{sk}) consistently overestimate mean T_{sk} during road cycling and thus are unsuitable for use in applications where high air velocities frequently occur (via natural air movement or self-generated). Our data demonstrate that the currently available T_{sk} prediction models fail to account for the increased convective and evaporative heat transfer during outdoor road cycling at recreational speeds (**Fig 1A-D**). Furthermore, the differences between measured and predicted T_{sk} increased with decreasing dry-bulb temperatures (**Fig. 1D**), indicating that dry-bulb temperature and skin temperature may have a stronger relationship than previously established (Mehnert *et al.*, 2000; Vanos *et al.*, 2012), or the relationship may be non-linear (as airspeed increases, the rate at which air temperature reduces skin temperature in a temperate environment increases). Overpredicting mean skin temperature leads to an overestimation of dry heat loss (through estimating a greater skin-air-temperature gradient [when T_o/T_{db} is < T_{sk}]) and the maximum evaporative capacity of the environment (E_{max}). Together, using existing T_{sk} estimation methods results in a potential underestimation of sweat losses compared with measured T_{sk} (**Table 4**). The major follow-on impact of underestimating fluid losses is notably the risk of dehydration, which has well-described negative impacts on health and performance, particularly beyond 2% of body mass loss (James *et al.*, 2017) and where the effects of dehydration are usually exacerbated in hot conditions (Kenefick *et al.*, 2010).

The secondary aim of this paper was to detail the development and validation of a novel mean skin temperature prediction equation that is suitable for use during recreational road cycling and other high air velocity applications in warm environmental conditions with moderate to high metabolic rates (i.e., where sweat rates were high, and the prediction of sweat rates would therefore be relevant from performance and heat stress risk management perspectives) (Jay, Broderick & Smallcombe, 2021). Our skin temperature prediction model, which is specific to road cycling, has improved performance when tested against our independent validation group (RMSE ± 0.9 ºC (mean difference and 95% CI: -0.03ºC [-1.4, 1.4 ºC] [**Fig. 5A-B**]) and when compared to existing models (**Table 5.** RMSE ± 3.6 ºC (Vanos *et al.*, 2012), ± 3.4 ºC (Mehnert *et al.*, 2000) and 1.8 ºC (ISO, 7933, 2004).

Skin temperature has consistently been shown to be augmented by metabolic rate in low airflow environments (Mairiaux *et al.*, 1987; Mehnert *et al.*, 2000; Vanos *et al.*, 2012), however, we did not observe cycling velocity to reduce mean skin temperature which may be explained by the interaction of cycling power output which increases metabolic rate (and is typically associated with increases in mean skin temperature) and increases to cycling velocity which would typically reduce skin temperature due to increased convection. More dynamic cycling conditions might be required to elucidate the rise and fall of skin mean skin temperature across varying cycling speeds and exercise intensities. One prior study that has developed prediction equations for mean skin temperature has collected data with similarly high metabolic rates (912 ± 194 W [459-1303]) estimated within this study, however, data were collected on stationary ergometers (Vanos *et al.*, 2012) and there was subsequently substantially less convective and evaporative cooling (natural wind velocities: 1.9-2.8 $m \cdot s^{-1}$) compared with on the road bikes in this study. We observed a range of mean skin temperatures [29.1-34.4 ºC] which represents similar observed skin temperature values to Vanos *et al* (2012), which had dry-bulb temperatures from 8.9-24.4 ºC, which were lower than during this study (20.2-31.1 ºC) however, had substantially less convective and evaporative cooling over participants due to cycling on stationary ergometers.

Predicted skin temperatures from our model had a mean bias of -0.03 ºC 95% CI [-1.8, 1.8 ºC] compared with measured skin temperature (**Fig. 5B**). This provides acceptable agreement when extrapolating this skin temperature prediction model into sweat rate prediction models across extended exercise durations where maintaining a relative state of euhydration becomes increasingly important (Von Duvillard *et al.*, 2004; Grego *et al.*, 2005; Murray, 2007). Over or under-predicting the skin temperature by large amounts would result in unfavourable accuracy over longer exercise durations where over or under-hydration can equally lead to undesired outcomes (e.g., hyponatremia and dehydration) (ACSM, 2007; James *et al.*, 2017). For example, when using the $T_{sk\_menhert}$ model, a difference of ~3.2 ºC in mean T_{sk} was observed, using the average value to estimate S_{req} in those conditions would result in an underestimation of the sweat losses by 272 $g{\cdot}h^{-1}$ [95%CI: -333 to -97 $g{\cdot}h^{-1}$]. For a 75 kg individual, this would result in a 0.73% error in body mass loss after 2 hours which could tip an individual further into dehydration than necessary. Being 0.73% down in body mass due to dehydration will not impact performance over 2 hours, however, this level of error could mean the differences of exercising at ~1.5% and not having any performance impacts, compared with being at ~2.2% have suffering the consequences. These errors would only be amplified in events with increasing duration such as Ironman® distance triathlon and Ultra-distance running events.

When measured T_{sk} is expressed alongside predicted T_{sk} data as 1-minute data across cycling distance, (**Fig. 1A)**, we observe different patterns of predictions. All three skin temperature prediction equations display a distinct rise and fall in skin temperature with an amplitude of around ±1 ºC, however, this is not observed with the measured skin temperature data. The cycling course was slightly uphill (0-2% grade) for half of the circuit and slightly downhill (-2-0%) for the other half of the circuit. While minute-by-minute estimations of skin temperature may have limited utility, having some degree of resolution to estimate skin temperature in dynamic scenarios (as gradients, metabolic heat production and environmental conditions change) will be more useful than steady-state predictions. Despite requesting participants to maintain a steady power output across each trial, this profile change naturally resulted in a rise and fall in metabolic rate (through increases in power output up the 'hill' and concomitant reductions in power output which correspond with the gradient of the course, **Fig. 2A-B**), along with increases in cycling velocity down the hill and concomitant decrease in cycling speed up the hill (despite the increased power output) (**Fig. 2A-B**). Compared to predicted T_{sk} values, we did not observe a rise in fall in T_{sk} with changes in speed and metabolic rates (**Fig. 2A-B**), which, is in contrast to previously observed research in low airflow scenarios (Mehnert *et al.*, 2000; Vanos *et al.*, 2012), indicates that increases in metabolic rate do not increase skin temperature dramatically when there is sufficient convective and evaporative cooling from airflow and evaporation of sweat/water while cycling.

Perspectives

We observed that for trials with higher dry-bulb temperatures, there was increased agreement between skin temperature estimation models and measured mean skin temperatures. As skin temperature is an interface temperature between the internal body tissues and the external environment, it follows that air temperature should and indeed has been consistently observed to augment skin temperature across cool and hot conditions, at rest and during exercise (Ramanathan, 1964; Livingstone *et al.*, 1987; Kenefick *et al.*, 2010; Hospers *et al.*, 2020). The error in previous skin temperature estimation models may partly be due to the research being conducted with air velocities limited to < 4.0 $m \cdot s^{-1}$, which means that the prior models may not adequately account for increases in convective heat losses in cool environments with such high speeds. As these differences between measured and predicted T_{sk} values appeared to be greater at lower air temperatures, these models may not place a high enough weighting on air temperature ($T_{sk\_menhert}$ T_{db} coefficient = 0.2 compared with our T_{db} coefficient = 0.4235) for high air velocity applications and future models may be improved by the addition of the convective heat transfer coefficient.

Skin temperature during outdoor road cycling

During outdoor road cycling with high self-generated air velocity, rises in skin temperature are initially prevented by large amounts of convective cooling driven by the skin-air temperature gradient, and secondly, by the secretion of sweat and the subsequent evaporation of that sweat to cool the skin surface (Berglund & Gonzalez, 1977). Increases in ambient vapour pressure in the atmosphere (humidity) could reduce the rate of sweat evaporation from the skin surface, thereby independently altering (increasing) skin temperature. Our data were collected across mild ambient humidities (<1.84 kPa, equivalent to ~24 ºC and 61.6% RH). As ambient humidities increase – reducing the skin-air vapour pressure gradient – there could be an even greater influence of extreme ambient vapour pressures increasing mean skin temperature values.

Limitations

The data used to develop the current prediction model were collected across a range of cycling velocities, external workloads, and local environmental conditions, however, these data were collected while cycling along a ~flat surface with small changes in gradient across the course (-2 - + 2%) and/or speed (± 2-4 $m \cdot s^{-1}$) compared to real-world cycling. The data collected in this study was at modest dry-bulb temperatures (up to ~30 ºC) as were limited by the environmental conditions over unseasonably cool summertime conditions across Sydney, and so our predictions may be limited outside those temperatures. The prediction model presented here would be challenged during lower air velocity (< 4.0 $m \cdot s^{-1}$) such as climbing at slower speeds, where the precision between mean skin temperature from existing prediction equations at lower air velocities (< 4.0 $m \cdot s^{-1}$) may be more appropriate. It must also be stressed that the predictions made here are for relative steady-state exercise and these predictions might not be suitable for interval type workouts.

Future research

Future work should investigate the performance of the model reported here across more widely varying terrains such as on longer climbs and over longer durations. The much lower airflow and increased metabolic heat production experienced while climbing could reduce the gap between measured and predicted skin temperatures during climbing and therefore previous skin temperature estimation models may be suitable in those instances. Future work should reconcile the high airflow specific work presented here, with the prior skin temperature estimation models to streamline the usage of any prediction method across various exercise and environmental conditions to further enhance hydration recommendations from fluid loss prediction equations. To aid in translating this research to practical use within the sports sciences, research should assess how the predictive ability of this outdoor model change in different practical scenarios, such as when riding in a peloton, and when riding uphill or downhill.

Conclusion

This study observed that the existing methods for predicting skin temperature during activities with high air velocities during outdoor cycling exercise are inadequate, and consistently overestimate the skin-air temperature gradient, which resulted in substantial underpredictions of sweat fluid losses. Here, we present a novel skin temperature prediction equation, which is specific to high air flow physical activity, that demonstrated a higher agreement to measured mean skin temperature data and more accurately predicted estimated fluid losses. This skin temperature prediction method could improve fluid loss prediction methods for determining fluid requirements for cycling-based physical activity such as road cycling and triathlon.

5.5 References

Abbott PF & Tabony RC. (1985). The estimation of humidity parameters. *Meteorological Magazine* **114,** 49-56.

ACSM MNS, Louise M Burke, E Randy Eichner, Ronald J Maughan, Scott J Montain, Nina S Stachenfeld. (2007). Exercise and Fluid Replacement. *Medicine & Science in Sports & Exercise* **39,** 377-390.

Berglund LG & Gonzalez RR. (1977). Evaporation of sweat from sedentary man in humid environments. *Journal of Applied Physiology* **42,** 767-772.

Brown HA, Topham TH, Clark B, Smallcombe JW, Flouris AD, Ioannou LG, Telford RD, Jay O & Périard JD. (2022). Seasonal Heat Acclimatisation in Healthy Adults: A Systematic Review. *Sports medicine (Auckland, NZ)* **52,** 2111-2128.

Brown RD & Gillespie TJ. (1986). Estimating outdoor thermal comfort using a cylindrical radiation thermometer and an energy budget model. *International Journal of Biometeorology* **30,** 43-52.

Clarry A, Faghih Imani A & Miller EJ. (2019). Where we ride faster? Examining cycling speed using smartphone GPS data. *Sustainable Cities and Society* **49,** 101594.

Cramer MN & Jay O. (2019). Partitional calorimetry. *Journal of Applied Physiology* **126,** 267-277.

Du Bois D. (1916). Clinical Calorimetry. *Archives of Internal Medicine* **XVII,** 863-871.

Gagge AP & Gonzalez RR. (2010). Mechanisms of Heat Exchange: Biophysics and Physiology. In *Comprehensive Physiology*, pp. 45-84.

Gallo G, Mateo-March M, Gotti D, Faelli E, Ruggeri P, Codella R & Filipas L. (2022). How do world class top 5 Giro d'Italia finishers train? A qualitative multiple case study. *Scandinavian Journal of Medicine & Science in Sports* **32,** 1738-1746.

Garmin. (2021). Garmin Rally RS, RK, XC Owner’s Manual.

Garmin. (2023). Temperature Change Effects on the Vector Power Meter Pedals.

Gonzalez R. (2019). Biophysics of Heat Exchange and Clothing: Applications to Sports Physiology.

Grego F, Vallier J-M, Collardeau M, Rousseu C, Cremieux J & Brisswalter J. (2005). Influence of exercise duration and hydration status on cognitive function during prolonged cycling exercise. *International journal of sports medicine* **26,** 27-33.

Hospers L, Cheuvront SN, Kenefick RW & Jay O. (2020). Independent Influence of Skin Temperature on Whole-Body Sweat Rate. *Medicine and science in sports and exercise* **52,** 2423-2429.

Hunt LA, Hospers L, Smallcombe JW, Mavros Y & Jay O. (2021). Caffeine alters thermoregulatory responses to exercise in the heat only in caffeine-habituated individuals: a double-blind placebo-controlled trial. *Journal of Applied Physiology* **131,** 1300-1310.

ISO. (7726, 1998). Ergonomics of the thermal environment — Instruments for measuring physical quantities. International Organization for Standardization, Geneva.

ISO. (7933, 2004). Ergonomics of the thermal environment — Analytical determination and interpretation of heat stress using calculation of the predicted heat strain.

ISO. (9886, 2004). Ergonomics of the thermal environment — Evaluation of thermal strain by physiological measurements, pp. 21. ISO.

James LJ, Moss J, Henry J, Papadopoulou C & Mears SA. (2017). Hypohydration impairs endurance performance: a blinded study. *Physiological Reports* **5,** e13315.

Jay O, Broderick C & Smallcombe JW. (2021). Extreme Heat Policy, ed. Australia SM, pp. 12. Sports Medicine Australia.

Kenefick RW, Cheuvront SN, Palombo LJ, Ely BR & Sawka MN. (2010). Skin temperature modifies the impact of hypohydration on aerobic performance. *Journal of Applied Physiology* **109,** 79-86.

Kreith F & Black WZ. (1980). Basic heat transfer.

Liguori G, Feito Y, Fountaine C & Roy B. (2022). *ACSM's guidelines for exercise testing and prescription*. Wolters Kluwer, Philadelphia.

Livingstone SD, Nolan RW, Frim J, Reed LD & Limmer RE. (1987). A thermographic study of the effect of body composition and ambient temperature on the accuracy of mean skin temperature calculations. *Europ J Appl Physiol* **56,** 120-125.

Lotens W & Havenith G. (1991). Calculation of clothing insulation and vapour resistance. *Ergonomics* **34,** 233-254.

Mairiaux P, Malchaire J & Candas V. (1987). Prediction of mean skin temperature in warm environments. *Eur J Appl Physiol Occup Physiol* **56,** 686-692.

McCullough EA, Jones BW & Huck J. (1985). A comprehensive data base for estimating clothing insulation. *Ashrae Trans* **91,** 29-47.

Mehnert P, Malchaire J, Kampmann B, Piette A, Griefahn B & Gebhardt H. (2000). Prediction of the average skin temperature in warm and hot environments. *Eur J Appl Physiol* **82,** 52-60.

Menaspà P, Sias M, Bates G & La Torre A. (2017). Demands of World Cup Competitions in Elite Women's Road Cycling. *International Journal of Sports Physiology and Performance* **12,** 1293-1296.

Murray B. (2007). Hydration and physical performance. *Journal of the American College of Nutrition* **26,** 542S-548S.

Parsons K. (2014). *Human thermal environments: the effects of hot, moderate, and cold environments on human health, comfort, and performance*. CRC press.

Parsons KC. (2003). *Human Thermal Environments*. Taylor & Francis, London.

Pedregosa F, Varoquaux G, Gramfort A, Michel V, Thirion B, Grisel O, Blondel M, Prettenhofer P, Weiss R & Dubourg V. (2011). Scikit-learn: Machine learning in Python. *the Journal of machine Learning research* **12,** 2825-2830.

Peronnet F & Massicotte D. (1991). Table of nonprotein respiratory quotient: an update. *Can J Sport Sci* **16,** 23-29.

Ramanathan NL. (1964). A new weighting system for mean surface temperature of the human body. *Journal of Applied Physiology* **19,** 531-533.

Sanders D & van Erp T. (2021). The Physical Demands and Power Profile of Professional Men's Cycling Races: An Updated Review. *International journal of sports physiology and performance* **16,** 3-12.

Sitko S, Cirer-Sastre R & López-Laval I. (2022). Time to exhaustion at estimated functional threshold power in road cyclists of different performance levels. *Journal of Science and Medicine in Sport* **25,** 783-786.

Smallcombe J, Hodder S, Kuklane K, Młynarczyk M, Loveday D, Eggeling J, Halder A & Havenith G. (2021). Updated Database of Clothing Thermal Insulation and Vapor

Permeability Values of Western Ensembles for Use in ASHRAE Standard 55, ISO 7730, and ISO 9920. **VC-21-011**.

Smith AH, Crabtree D, Bilzon J & Walsh N. (2009). The validity of wireless iButtons® and thermistors for human skin temperature measurement. *Physiological measurement* **31,** 95.

Thompson DC, Rebolledo V, Thompson RS, Kaufman A & Rivara FP. (1997). Bike speed measurements in a recreational population: validity of self reported speed. *Injury Prevention* **3,** 43.

VAN Erp T, Hoozemans M, Foster C & JJ DEK. (2020). Case Report: Load, Intensity, and Performance Characteristics in Multiple Grand Tours. *Med Sci Sports Exerc* **52,** 868-875.

Vanos JK, Warland JS, Gillespie TJ & Kenny NA. (2012). Thermal comfort modelling of body temperature and psychological variations of a human exercising in an outdoor environment. *International Journal of Biometeorology* **56,** 21-32.

Von Duvillard SP, Braun WA, Markofski M, Beneke R & Leithäuser R. (2004). Fluids and hydration in prolonged endurance performance. *Nutrition* **20,** 651-656.

Y. S. Touloukian PEL, S. C. Saxena. (1970). *Thermophysical Properties of Matter, Vol. 3: Thermal Conductivity*.

Table 1. Mean physical characteristics of all participants (*n*=23) and cycling speed, power and cadence metrics. BSA Body surface area, SD standard deviation.

Factor	Mean (SD)	Range [Min-Max]
Male (*n*=16)		
Age (years)	29 ± 3	24 – 37
Height (m)	1.81 ± 0.08	1.68 – 1.96
Weight (kg)	80.41 ± 9.44	62.65 – 94.69
BSA (m^2)	2.00 ± 0.13	1.77 – 2.19
External workload (W)	210 ± 41	84 – 267
Cadence (revolutions·min^{-1})	83 ± 2.3	23 - 110
Cycling velocity (m·s^{-2})	9.1 ± 2.7	1.2 - 16.2
Female (*n*=7)		
Age (years)	27 ± 1	25 - 29
Height (m)	1.74 ± 0.05	1.63 - 1.83
Weight (kg)	63.93 ± 6.71	56.40 - 76.56
BSA (m^2)	1.77 ± 0.11	1.59 - 1.98
External workload (W)	165 ± 36	118 - 253
Cadence (revolutions·min^{-1})	73.6 ± 1.6	16 - 95
Cycling velocity (m·s^{-2})	8.6 ± 1.6	0.8 - 15.1

Table 2. Pearson correlation coefficient (*r*) evaluation of select factors with measured mean skin temperature (T_{sk}) for outdoor road cycling. T_{db} dry-bulb temperature, T_r mean radiant temperature, v_{self} cycling velocity, H_{prod} metabolic heat production, and $\dot{M}$ metabolic rate. (n=153).

Correlation (*r*) with T_{sk}

Factor	Value	*p*-value
T_{db} (ºC)	0.721	0. 001
T_r (ºC)	0.486	0. 001
v_{self} ($m{\cdot}s^{-1}$)	0.195	0. 016
P_a (kPa)	0. 294	0. 001
H_{prod} ($W{\cdot}m^{-2}$)	0. 282	0. 001
H_{prod} (W)	0. 261	0. 001
M ($W{\cdot}m^{-2}$)	0. 285	0. 001
External workload (W)	0. 288	0. 001

Table 3. Linear regression model output for the prediction of mean skin temperature during outdoor road cycling for the modelling data set (n=91). T_{db}, dry-bulb temperature, H_{prod}, metabolic heat production and P_a, partial water vapour pressure.

	Coefficient	Standard error	Significance	Explained variance (R^2)
Intercept	16.6585	13.473	$P < 0.001$	
T_{db} (ºC)	0.4235	0.046	$P < 0.001$	$T_{db} = 0.557$
H_{prod} ($m{\cdot}s^{-1}$)	1.1449	0.402	$P = 0.005$	$T_{db} + H_{prod} = 0.604$
P_a (kPa)	0.007	0.002	$P < 0.001$	$T_{db} + H_{prod} + P_a = 0.638$

n=91, $R^2 = 0.638$, adjusted $R^2 = 0.625$

Table 4. Summary of factors affected by type of skin temperature assessment (measured vs predicted).

Skin temperature method	T_{sk} (ºC)	ΔDry heat loss (W)	ΔE_{req} (W)	ΔE_{max} (W)	$\Delta \omega_{req}$ (AU)	ΔS_{req} ($g{\cdot}h^{-1}$)
Modelling group						
$T_{sk\_measured}$	31.8 ± 1.4	-	-	-	-	-
	[29.1 to 34.4]	-	-	-	-	-
$T_{sk\_mehnert}$	35.0 ± 0.8	48 ± 17	-94 ± 33	384 ± 125	-0.18 ± 0.07	-272 ± 139
	[32.9 to 36.2]	[17 to 99]	[-192 to -34]	[151 to 751]	[-0.47 to -0.06]	[-333 to -97]
T_{sk_ISO}	33.3 ± 0.9	27 ± 22	-50 ± 39	161 ± 131	-0.10 ± 0.08	-161 ± 160
	[30.1 to 34.5]	[-11 to 93]	[-182 to 22]	[64 to 540]	[-0.30 to 0.04]	[-912 to 78]
T_{sk_COMFA}	35.1 ± 1.2	62 ± 26	-140 ± 49	400 ± 181	-0.48 ± 0.08	-323 ± 158
	[32.9 to 38.7]	[17 to 187]	[-320 to -42]	[91 to 1414]	[-0.48 to -0.06]	[-1021 to -76]
Validation group						
$T_{sk\_measured}$	31.7 ± 1.1	-	-	-	-	-
	[29.3 to 34.2]	-	-	-	-	-
$T_{sk\_mehnert}$	34.9 ± 0.6	49 ± 16	-93 ± 32	378 ± 126	-0.18 ± 0.07	-268 ± 135
	[33.4 - 36.1]	[5 to 88]	[-173 to -9]	[39 to 714]	[-0.26 to -0.02]	[-755 to -20]
T_{sk_ISO}	34.3 ± 0.6	28 ± 20	-53 ± 35	163 ± 107	-0.10 ± 0.07	-162 ± 124
	[30.8 to 34.3]	[-15 to 73]	[-123 to 25]	[-82 to 382]	[-0.18 to 0.01]	[-584 to 55]
T_{sk_COMFA}	35.0 ± 1.2	62 ± 27	-119 ± 55	389 ± 185	-0.19 ± 0.09	-318 ± 180
	[32.4 - 37.3]	[-8 to 136]	[-266 to 13]	[42 to 901]	[-0.41 to 0.02]	[-945 to 26]
$T_{sk\_predicted}$	31.7 ± 0.9	-19 ± 39	-23 ± 34	9 ± 97	-0.02 ± 0.07	-74 ± 117
	[29.2 to 33.0]	[-77 to 90]	[-55 to 86]	[-220 to 189]	[-0.2 to 0.13]	[-392 to 144]

T_{sk} mean skin temperature (ºC), Dry heat loss is combined mean convective and radiative heat exchange (W), and S_{req} is the estimated difference in sweat rate between the three predicted T_{sk} models and measured mean T_{sk} ($g{\cdot}hr^{-2}$). Mean ± SD and [minimum-maximum] are reported in brackets.

Table 5. Summary of skin temperature prediction model performance.

	$T_{sk\_mehnert}$	T_{sk_ISO}	T_{sk_COMFA}	$T_{sk\_predicted}$
Mean bias, ºC	3.3 ± 1.1	1.5 ± 1.0	3.3 ± 1.4	0.3 ± 0.9
Lin's CCC	0.04	0.11	0.05	0.57
Root mean square error, ºC	3.4	1.8	3.6	0.9
Mean absolute error (%)	10.4	5.0	10.5	2.4

CCC, Concordance Correlation Coefficient

Figure 1A: Line plot displaying the relationships between predicted mean T_{sk} compared to measured mean T_{sk}. **1B**: Bar plot displaying dry heat exchange when calculated from the three T_{sk} prediction equations, plotted as a difference (Δ) from measured dry heat exchange. Mean and 95% confidence intervals. **1C**: Predicted versus mean T_{sk} across the steady state component of the trials. **1D:** The difference between measured mean T_{sk} and predicted T_{sk} plotted against dry-bulb temperature (T_{db}). Plots C and D are averaged into 15-minute blocks across the final 45 minutes of each trial (i.e., the steady-state period) and each plot represents 91 paired comparisons per T_{sk} prediction method with 3 data points per trial.

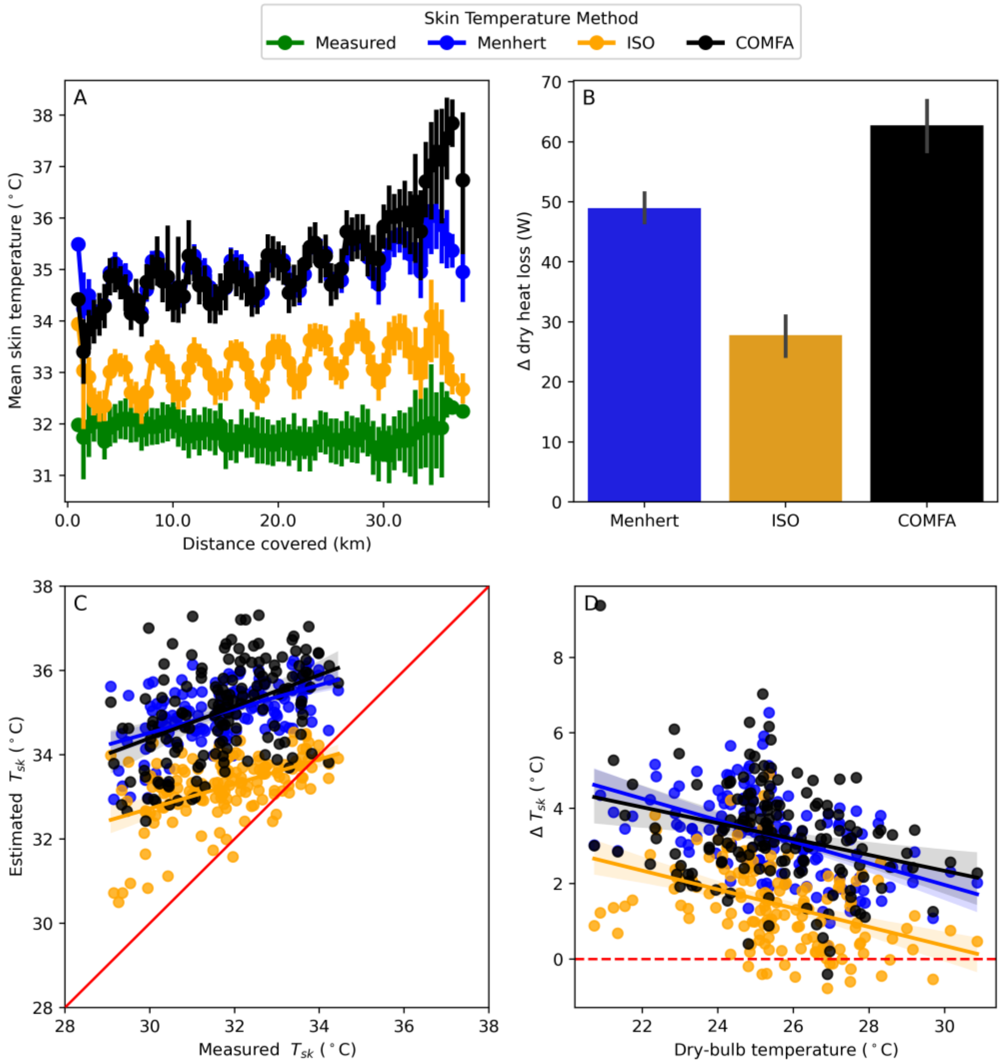

Figure 2: line plots displaying change in mean skin temperature and cycling velocity (**2A**) and metabolic heat production and cycling velocity (**2B)**: across distance cycled; mean and 95% confidence intervals.

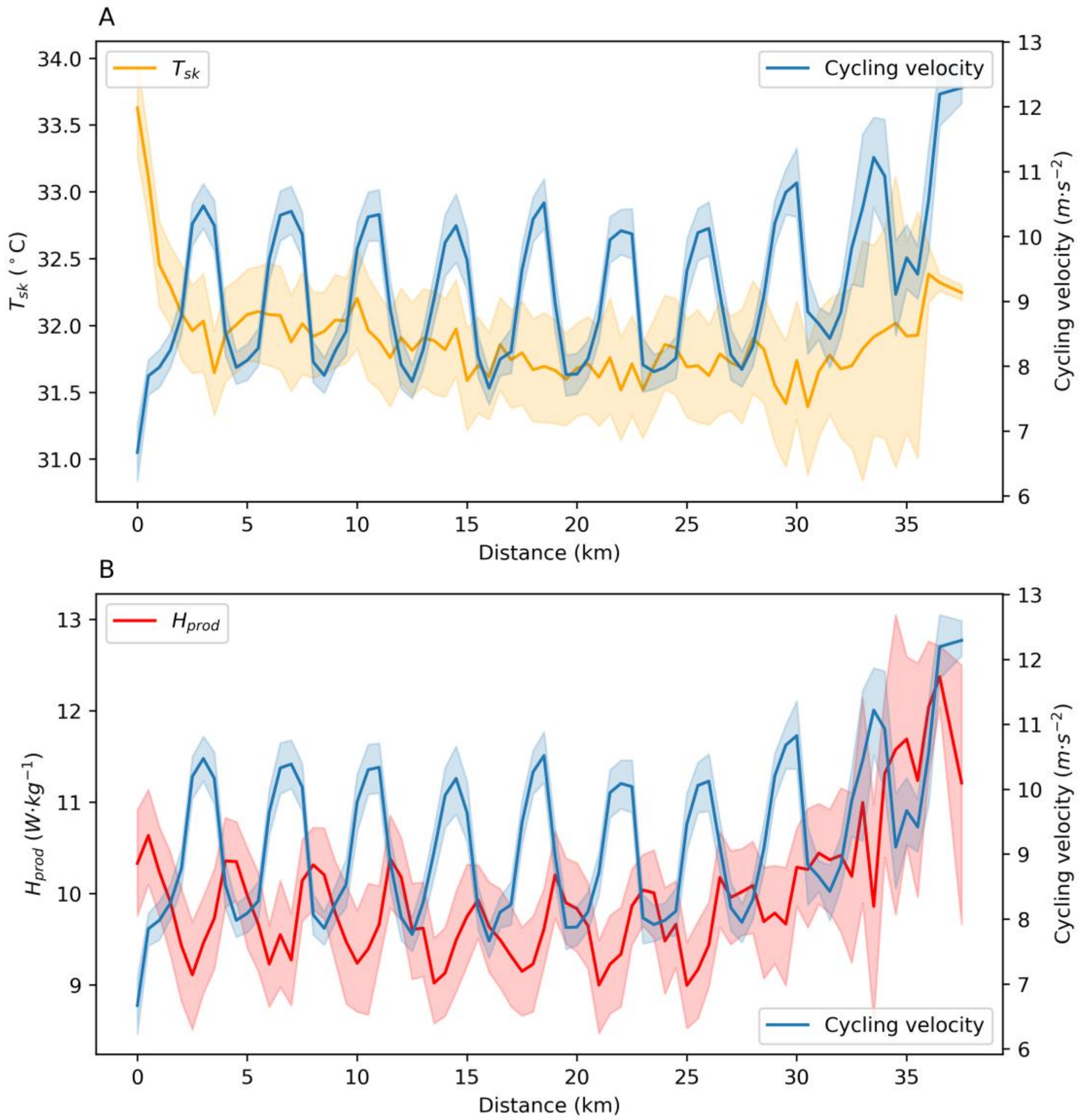

T_{sk} is measured mean skin temperature (ºC) and H_{prod} is metabolic heat production (in $W{\cdot}kg^{-1}$)

Figure 3. Dependent variables are plotted with measured mean skin temperature (ºC) to establish bivariate relationships to inform the predictive model via exploratory data analysis [T_{db}, T_r, and P_a, v_{self}, H_{prod}, Legend = Participant ID]. Asterisk (*) denotes $P < 0.05$.

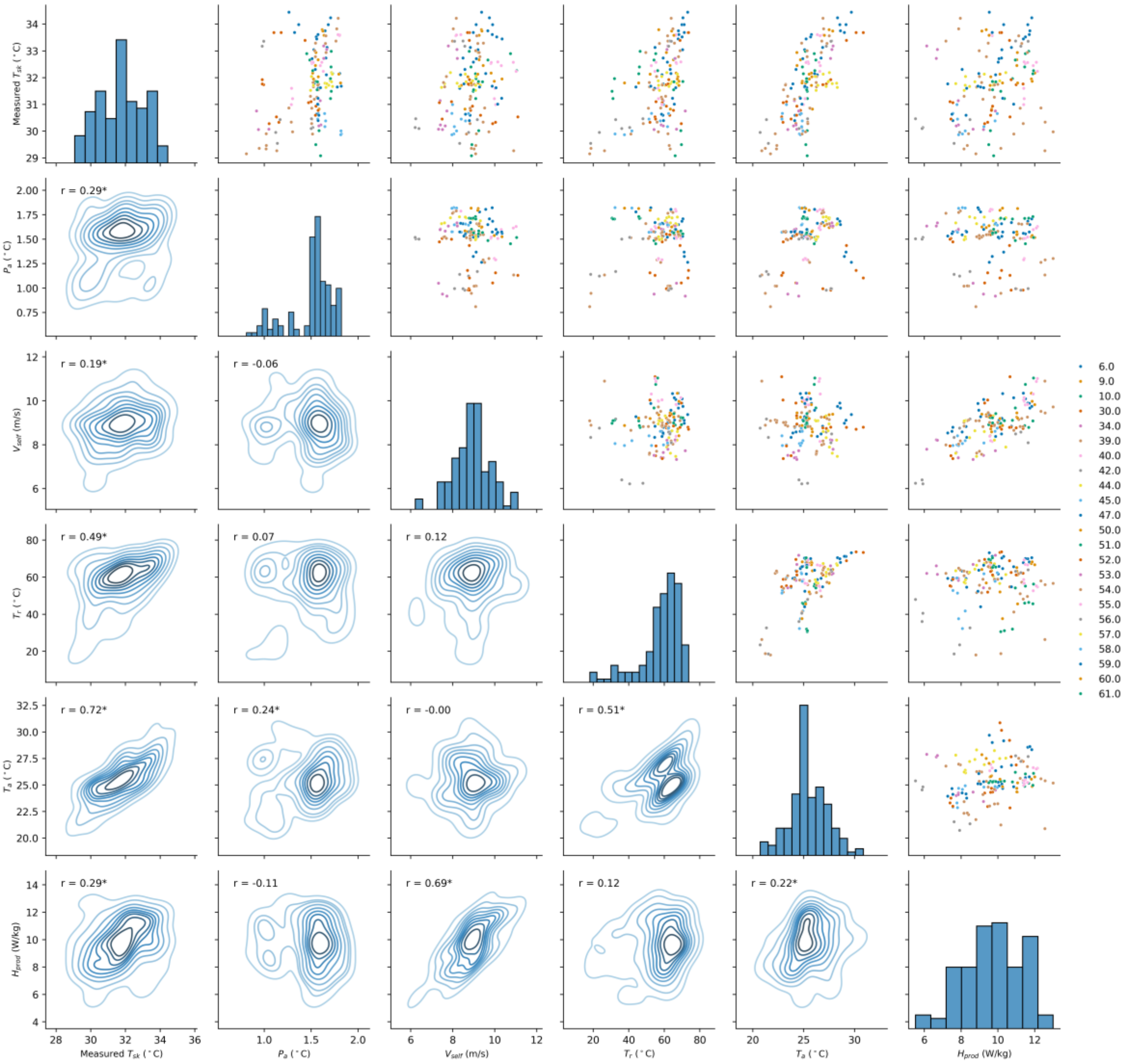

Figure 4A-C: Bland-Altman plots illustrating mean bias solid black line) and 95% confidence intervals (dotted lines) for current models (A: $T_{sk\_mehnert}$, B: T_{sk_ISO}, C: T_{sk_COMFA}) and measured mean T_{sk} in the independent validation group using measured environmental variables.

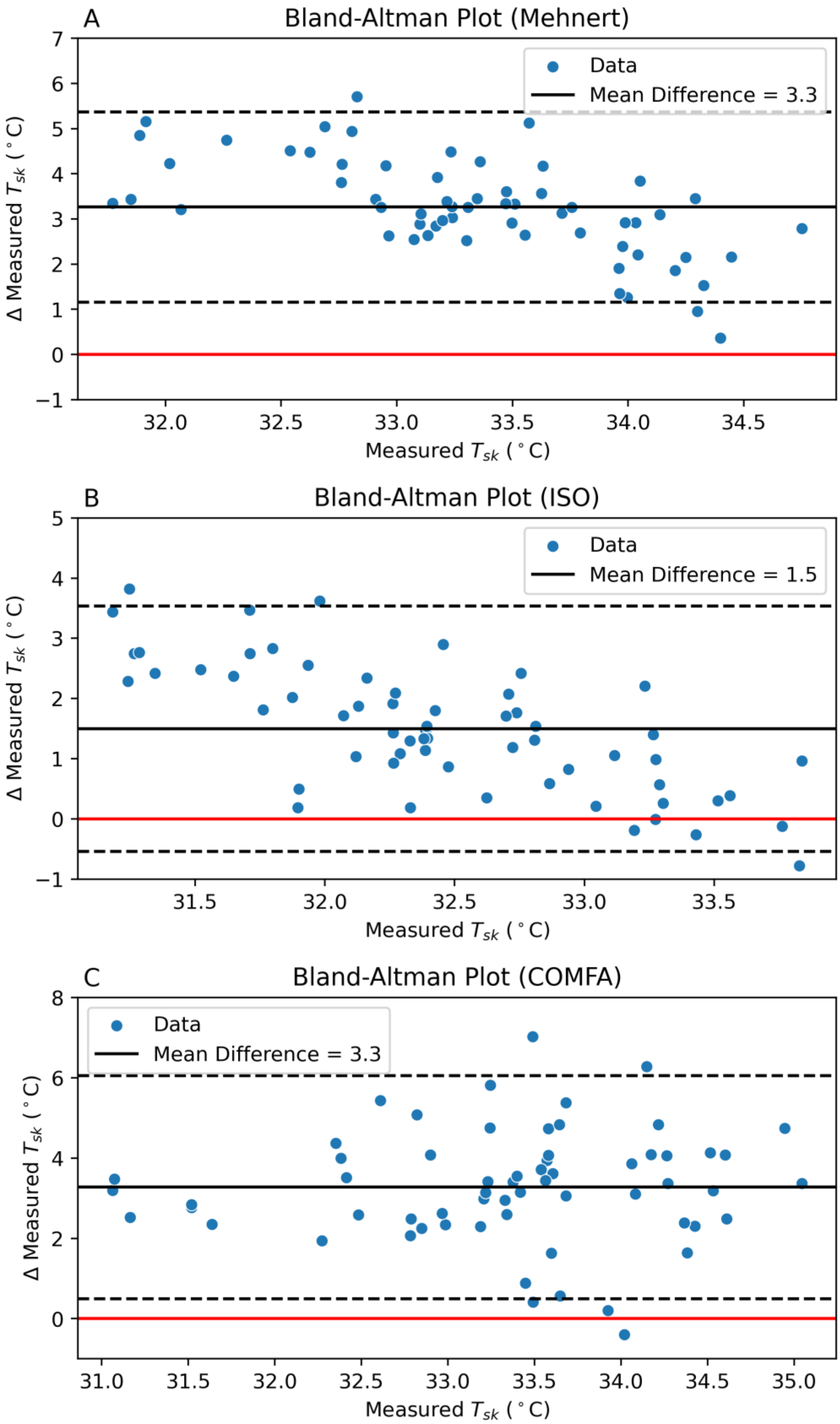

Figure 5A: Predicted vs measured mean T_{sk} values for the independent validation trials using the linear regression model to predict T_{sk}. **5B:** Bland-Altman plots illustrating mean bias solid black line) and 95% confidence intervals (dotted lines) for predicted and measured mean T_{sk} in the independent validation group using measured environmental variables.

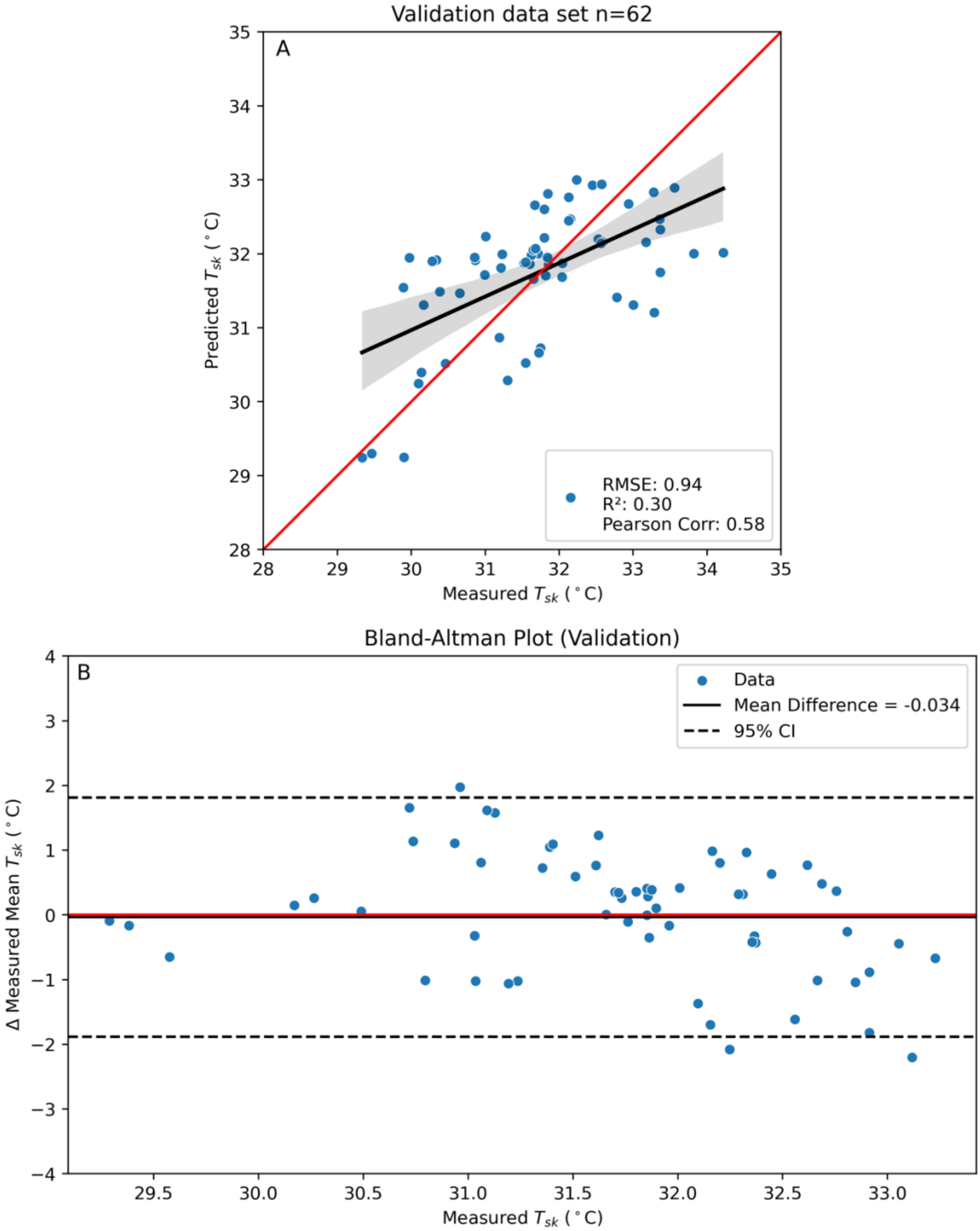

CHAPTER VI

Thesis Discussion and Conclusions

6.0 Thesis Discussion and Conclusions

The risks posed by extreme heat to human health will only increase in the coming decades as climate change continues. Vulnerable populations, such as those with pre-existing health conditions (e.g., chronic disease etc.) will be particularly at risk when exposed to heat at rest, whilst recreational and professional athletes will become increasingly exposed to extreme heat during outdoor physical activity. Therefore, maintaining safe access to outdoor physical activity/sports for the public and professional sportspersons is becoming increasingly challenging in our warming world. The current thesis provides novel data that may further inform the management of heat stress risk in a wide array of outdoor sports settings that are relevant globally, in various environmental conditions.

By accurately quantifying the level of environmental heat stress and characterising the expected level of heat strain experienced by the individual, sound biophysical modelling (in combination with laboratory-based physiological experiments) will play a crucial role in mitigating the risk of extreme heat stress to the public and professional sportspersons participating in outdoor sports or physical activity.

The key findings and practical implications presented in this thesis are:

1. In Chapter 3, it was observed that nearby BoM stations typically underestimate the heat stress risk at Major venues such as the SCG, Optus Stadium and the Adelaide Oval, while overestimating the heat stress risk at Minor sporting venues across Australia. Overestimating the heat stress risk leads to unnecessarily delaying or cancelling play while underestimating the heat stress risk increases the likelihood of athletes experiencing heat illnesses. Practically speaking, this finding means that community/minor cricket venues (without large obstructive grandstands that contribute to the development of a microclimate) may be able to safely utilise nearby BoM weather site data to inform their heat policies, with the caveat that the

on-field heat stress risk may be overestimated by the BoM, however on-site environmental monitoring is highly recommended where feasible. For Major venues, on-site monitoring of the thermal environment is recommended due to the increased likelihood of underestimating the heat stress risk during play when relying on environmental data provided by the BoM

2. In Chapter 4, it was demonstrated that the rate of sweat loss is primarily associated with the evaporative requirement for heat balance (E_{req}) during outdoor road cycling. Practically this demonstrates that even with the reduced accuracy of field equipment and increased variability in environmental conditions experienced outside the laboratory, E_{req} remains highly associated with WBSR and, therefore, can be utilised within biophysical modelling to accurately predict fluid loss during exercise.
3. In Chapter 5, currently available methods for estimating the mean skin temperature during outdoor cycling were assessed for accuracy. It was found that existing methods do not adequately capture the increased rate of convective cooling experienced in high airflow environments initially experienced during road cycling and subsequently overestimate the steady-state mean skin temperature. Our data were then used to derive a new regressive model to estimate the mean skin temperature during outdoor road cycling. These data should improve future biophysical modelling, through improved predictions of dry heat transfer, which assesses heat stress risk factors such as predicted sweat rates, in sports such as road cycling.

The main findings of this thesis have been discussed in detail within each chapter and therefore the next section looks to describe the future directions and implications for research and practice that results from the thesis more globally.

The findings from the 3 experimental chapters within this thesis may be used together by practitioners (e.g., coaches and sporting organisations) to help reduce the overall risk of adverse heat outcomes across a range of outdoor sports. Firstly, if practitioners are using nearby meteorological sites to inform decisions based on their extreme heat policy, they must be aware of the potential differences in the thermal environmental conditions between the field of play and the nearby meteorological sites. Best practice should be considered to be on-site monitoring with a high quality, purpose built environmental monitoring unit that measures al flour environmental parameters that affect human heat balance (dry-bulb temperature, relative humidity, black globe temperature and wind velocity), such as the design used in this thesis by EMU systems or similar. Secondly, many major sporting organisations around the globe still use fixed environmental cut-offs (T_{db} sometimes combined with RH and/or WBGT) to determine their thresholds within their policies including the UCI (Union Cycliste Internationale, 2024). Data gathered in Chapters 4 and 5 may be used to integrate biophysical modelling and advance extreme heat policies, which not only the environmental conditions, but importantly also consider athletes/participants' training and acclimation status (through ω_{max} estimations), clothing, and forecasted sweat rates to determine the appropriate upper tolerable limit of heat stress for that particular activity and associated environmental conditions in which the activity occurs.

Future directions and implications

The existence of microclimates across Australian sporting venues

Chapter 3 focussed on how appropriate it is to use nearby weather station data from the Australian Bureau of Meteorology (BoM) to characterise the prevailing level of heat stress within major and minor AFL/cricket venues across Australia. The use of nearby environmental measurements is what underpins the Extreme Heat Policies of not only Cricket Australia but also many other major outdoor sporting organisations across Australia (Australian Football

League, 2013; Cricket Australia, 2020; Cycling Australia, 2021; Lawn Tennis Association, 2022). Extreme Heat Policies are multifaced documents that dictate the procedures to allow as much play to occur as is considered safe by the organisers (Racinais *et al.*, 2023). This benefits the players, the spectators, and the organisers, as play is allowed to continue for as long as possible before becoming unsafe for the players. We observed that Major venues often reported lower dry-bulb temperatures, wind speeds, and higher absolute humidities than observed at nearby BoM sites. These differences may be explained by local factors related to the grounds themselves such as that the fields are typically watered overnight to maintain the grassy playing surface which releases water in the form of water vapour via increased evapotranspiration (Liuzzo, Viola & Noto, 2016; Mazrooei *et al.*, 2021; Hao *et al.*, 2023) and the large, encompassing grandstands that surround the playing surfaces substantially blocks/reduces the airflows experienced at the playing surface compared to nearby meteorological sites (Chatzidimitriou & Yannas, 2015; Grundstein & Cooper, 2020). This confirms the need for on-site environmental monitoring, particularly at major venues where the heat stress risk was typically *underestimated*, meaning that professional sportspersons may be exposed to undue risk of exertional heat illness during thermally stressful playing conditions typically due to reduced wind speeds and higher humidities experienced at the playing surface. Further research may be necessary to confirm exactly why and when these differences present themselves with longer-term, ground-specific assessment, however, certainly the most practical solution is to implement high-quality on-site environmental monitoring where possible, particularly when the thermal environment is forecasted to be stressful. Major sporting venue developers should place further emphasis on the design of the sporting venue with specific regard to how the venue influences the local thermal environment for players and spectators, to help ensure that safe outdoor sports participation can remain a staple in our society.

Agreement of E_{req} and WBSR in an outdoor environment

Chapter 4 shifted focus from accurately quantifying the physical thermal environment at sporting venues (Chapter 3) to better understanding human physiological responses to heat stress exposure during physical activity, when exertional heat illness is most likely to occur. Exercise heat stress is experienced when there is an excessive rise in body core temperature as the rate of metabolic heat produced by active musculature exceeds the rate of heat dissipation to the surrounding environment. Additionally, during prolonged exercise, if adequate fluids are not taken on board, dehydration may ensue, further exacerbate the level of heat strain (Hillman *et al.*, 2011; Akerman *et al.*, 2016) and increase the risk of severe exertional heat illness. Fluid intake recommendations are of course highly varied based on the intensity, duration and environmental conditions of any race/activity where for longer and hotter races, it's sensible to replace a higher % of fluid losses, where in cooler and shorter races, individuals can tolerate higher levels of dehydration without significant performance losses. There will be cases where fluid losses exceed the ability to consume enough fluids (either physiologically or through lack of access), and such that dehydration will progress until exercise must cease. By improving our biophysical modelling capabilities, our ability to appropriately prescribe personalised hydration regimes and prepare athletes and individuals competing in the heat will only improve (Jay *et al.*, 2024).

The current thesis first aimed to improve our biophysical modelling capabilities by adapting the E_{req} model that has been shown to explain most of the individual variability in whole-body sweat rates at rest and during exercise in indoor environments (Gagnon, Jay & Kenny, 2013; Hospers *et al.*, 2020; Ravanelli, Imbeault & Jay, 2020) to and apply it to an outdoor environment. In Chapter 4, the most appropriate methods for calculating E_{req} in outdoor settings using freely available data (e.g., dry-bulb temperature, relative humidity, power output, cycling velocity) are reported. Whilst E_{req} was found to associate highly with whole-body sweat loss during 1-hour of outdoor cycling, future research should assess the strength of these associations over longer durations and in more variable environmental conditions. For example, by experimental design, there was limited variability in the exercise intensity and cycling velocity within each trial. For conditions with greater variations in power output and speed, we would expect to see transient and significant changes in E_{req} and E_{max} which may lead to a reduction in sweating efficiency at times, which could ultimately result in a reduced association of E_{req} with whole-body sweat rate.

At the onset of exercise, there is a sharp rise in metabolic rate that is not immediately matched by heat loss mechanisms (increases in sweat output and skin blood flow) until the onset of sweating occurs and a relative steady state of heat balance is achieved. The rate at which steady state occurs is dependent on the environmental conditions and exercise intensity (longer in warmer conditions, shorter in cooler conditions, ~10-30 minutes) (Cramer & Jay, 2019; Ravanelli, Bongers & Jay, 2019). During this time a certain amount of heat is stored within the body and results in a rise in body core temperature. In our calculations of E_{req} within Chapters 4 and 5, we have assumed that heat storage was 0 and therefore for ~60 minutes of exercise, our whole-body sweat rate values may indeed be underestimating sweat losses over hours 2, 3 and onwards. Together, both the unaccounted-for time before the onset of sweating and the initial amount of heat stored within the body before steady state, may result in systematic underestimations of WBSL in our model, particularly at shorter exercise durations <60 minutes. Furthermore, as metabolic rate increases for a given external workload as fatigue sets in (particularly at high exercise intensities due to the slow component of $\dot{V}O_2$ (Poole *et al.*, 1991; Xu & Rhodes, 1999; Lucía, Hoyos & Chicharro, 2000; Jones *et al.*, 2011; Colosio *et al.*, 2020), which is unaccounted for the E_{req} model. Future research should identify the magnitude of metabolic rate increases with fatigue to improve estimations of metabolic rate during prolonged exercise bouts.

Prediction of mean skin temperature

Chapter 5 followed Chapter 4 by taking the next steps to further our understanding of mean skin temperatures (and therefore dry heat transfer and E_{max}) during outdoor road cycling. All previous research aimed at estimating mean skin temperature has been conducted either within laboratories or outdoors but with limited air velocities (0-4 $m \cdot s^{-1}$) and therefore the mean skin temperatures experienced while cycling was unknown (Mehnert *et al.*, 2000; Vanos *et al.*, 2012; ISO, 9886, 2004). This chapter identified large discrepancies between the existing methods for estimating mean skin temperature and measured mean skin temperature, particularly at lower dry-bulb temperatures. Practically, this means that existing methods for estimating mean skin temperature led to an underestimation of fluid requirements during steady state road cycling, as dry heat loss is inflated (in temperate conditions where $T_{db} < T_{sk}$). Overestimating the amount of dry heat loss in the E_{req} model reduces the value of E_{req} thereby reducing the required amount of evaporation to attain heat balance when translated into an S_{req} value. However, whether existing methods for estimating mean skin temperature perform better or worse in warmer environments where T_{db} is > T_{sk} is worthy of investigation in the future as when T_{db} increases beyond T_{sk}, all metabolic and environmental heat must be lost via evaporative mechanisms, which results in further increases in whole-body sweat rates. As sweat rates increase, so does the risk of dehydration and the development of associated exertional heat illness, especially during prolonged exercise.

The second aim of Chapter 5 was to develop a more precise method for estimating mean skin temperature during outdoor road cycling. Our method provided a better estimate of mean skin temperature and associated dry heat loss when compared with the existing methods. Within our data, metabolic rate, metabolic heat production and external workload appeared not to increase skin temperature when examining steady-state measured skin temperatures, potentially as any increases in metabolic heat production were negated by concomitant increases in cycling velocity, and therefore self-generated airspeed. All existing models integrated a form of metabolic heat production into their prediction equations, which at low air velocities, is conceptually and practically sound. When metabolic rate rises, so does skin blood flow which is mediated by both peripheral (Johnson & Kellogg Jr, 2010) and central (Kenney & Johnson, 1992) thermoregulatory pathways to transfer more (heated) blood from the core to the periphery to facilitate cooling via evaporation. Typically, an associated rise in skin temperature would be expected, however, at higher air velocities, mean skin temperature appears vastly more affected and determined by dry-bulb temperature and much less affected by rises and falls in metabolic rate or metabolic heat production. As air velocity increases, so does the convective heat transfer coefficient which leads to an increased rate of convective heat exchange between the skin and the environment. At the outset of cycling exercise, we observed a sharp drop in measured mean skin temperature with large amounts of convective heat loss until a relative steady state was experienced as mean skin temperature became closer to dry-bulb temperatures where convective heat loss was much lower due to the diminished T_{sk} to T_{db} temperature gradient. Current empirical investigations into the convective heat transfer coefficient suggest that the rise in the convective heat transfer coefficient reduces with increasing airspeed (i.e., logarithmic effect of airspeed on h_c) (Nishi & Gagge, 1970; Lotens & Havenith, 1991), however, others suggest that it is linear. To help elucidate the interaction between the ambient environment (T_{db} and T_r) on mean skin temperature and associated dry heat loss in high airflow environments, more research into the characteristics of the convective heat transfer coefficient at higher air velocities is necessary.

Thesis conclusions

The main findings resulting from each chapter of this thesis are as follows: Firstly, differences in the estimated heat stress risk using BoM sites versus playing surface data are substantial enough to result in large categorical differences in the reported heat stress risk. The on-site environmental monitoring of thermal environmental conditions (with appropriate equipment) reduces the risk of misclassifying the heat stress risk and may reduce the risk of heat illness cases and costly (from both economic and population health perspectives) reductions in safe playing time. Secondly, we observed that the association between E_{req} and WBSR remained strong (peak R^2=0.72, peak r=0.85) in an outdoor environment. Strong associations between these variables mean that the E_{req} may be utilised within sweat rate prediction models during physical activity to produce quality fluid predictions across dynamic environments. Thirdly, we observed that existing skin temperature prediction equations fail to adequately account for the high rates of convective heat loss, which occurs at such high airspeeds as experienced during recreational road cycling and therefore overestimate dry heat loss and subsequently underestimate fluid losses. We subsequently developed a novel skin temperature prediction equation, specific to high airflow physical activity, which demonstrated increased agreement to measured skin temperature and more accurate estimated fluid losses compared to existing methods for estimating skin temperature during physical activity in warm environments.

6.1 Thesis Discussion References

Akerman AP, Tipton M, Minson CT & Cotter JD. (2016). Heat stress and dehydration in adapting for performance: Good, bad, both, or neither? *Temperature* **3,** 412-436.

Australian Football League. (2013). National Extreme Weather Policy.

Chatzidimitriou A & Yannas S. (2015). Microclimate development in open urban spaces: The influence of form and materials. *Energy and Buildings* **108,** 156-174.

Colosio AL, Caen K, Bourgois JG, Boone J & Pogliaghi S. (2020). Bioenergetics of the VO(2) slow component between exercise intensity domains. *Pflugers Arch* **472,** 1447-1456.

Cramer MN & Jay O. (2019). Partitional calorimetry. *Journal of Applied Physiology* **126,** 267-277.

Cricket Australia. (2020). Australian Cricket Heat Policy, 3 edn.

Cycling Australia. (2021). Extreme Weather Policy, 2 edn, pp. 21.

Gagnon D, Jay O & Kenny GP. (2013). The evaporative requirement for heat balance determines whole-body sweat rate during exercise under conditions permitting full evaporation. *The Journal of Physiology* **591,** 2925-2935.

Grundstein A & Cooper E. (2020). Comparison of WBGTs over Different Surfaces within an Athletic Complex. In *Medicina*.

Hao L, Sun G, Huang X, Tang R, Jin K, Lai Y, Chen D, Zhang Y, Zhou D, Yang Z-L, Wang L, Dong G & Li W. (2023). Urbanization alters atmospheric dryness through land evapotranspiration. *npj Climate and Atmospheric Science* **6,** 149.

Hillman AR, Vince RV, Taylor L, McNaughton L, Mitchell N & Siegler J. (2011). Exercise-induced dehydration with and without environmental heat stress results in increased oxidative stress. *Applied Physiology, Nutrition, and Metabolism* **36,** 698-706.

Hospers L, Cheuvront SN, Kenefick RW & Jay O. (2020). Independent Influence of Skin Temperature on Whole-Body Sweat Rate. *Medicine and science in sports and exercise* **52,** 2423-2429.

ISO. (9886, 2004). Ergonomics of the thermal environment — Evaluation of thermal strain by physiological measurements, pp. 21. ISO.

Jay O, Périard JD, Clark B, Hunt L, Ren H, Suh H, Gonzalez RR & Sawka MN. (2024). Whole-Body Sweat Rate Prediction: Outdoor Running and Cycling Exercise. *Journal of Applied Physiology* **0:**.

Johnson JM & Kellogg Jr DL. (2010). Local thermal control of the human cutaneous circulation. *Journal of applied physiology* **109,** 1229-1238.

Jones AM, Grassi B, Christensen PM, Krustrup P, Bangsbo J & Poole DC. (2011). Slow component of VO2 kinetics: mechanistic bases and practical applications. *Med Sci Sports Exerc* **43,** 2046-2062.

Kenney WL & Johnson JM. (1992). Control of skin blood flow during exercise. *Medicine and science in sports and exercise* **24,** 303-312.

Lawn Tennis Association. (2022). Extreme Heat Policy LTA Competition Regulations.

Liuzzo L, Viola F & Noto LV. (2016). Wind speed and temperature trends impacts on reference evapotranspiration in Southern Italy. *Theoretical and Applied Climatology* **123,** 43-62.

Lotens W & Havenith G. (1991). Calculation of clothing insulation and vapour resistance. *Ergonomics* **34,** 233-254.

Lucía A, Hoyos J & Chicharro JL. (2000). The slow component of $\dot{V}O_2$ in professional cyclists. *British Journal of Sports Medicine* **34,** 367-374.

Mazrooei A, Reitz M, Wang D & Sankarasubramanian A. (2021). Urbanization impacts on evapotranspiration across various spatio-temporal scales. *Earth's Future* **9,** e2021EF002045.

Mehnert P, Malchaire J, Kampmann B, Piette A, Griefahn B & Gebhardt H. (2000). Prediction of the average skin temperature in warm and hot environments. *Eur J Appl Physiol* **82,** 52-60.

Nishi Y & Gagge AP. (1970). Direct evaluation of convective heat transfer coefficient by naphthalene sublimation. *Journal of Applied Physiology* **29,** 830-838.

Poole DC, Schaffartzik W, Knight DR, Derion T, Kennedy B, Guy HJ, Prediletto R & Wagner PD. (1991). Contribution of excising legs to the slow component of oxygen uptake kinetics in humans. *Journal of Applied Physiology* **71,** 1245-1260.

Racinais S, Hosokawa Y, Akama T, Bermon S, Bigard X, Casa DJ, Grundstein A, Jay O, Massey A, Migliorini S, Mountjoy M, Nikolic N, Pitsiladis YP, Schobersberger W, Steinacker JM, Yamasawa F, Zideman DA, Engebretsen L & Budgett R. (2023). IOC consensus statement on recommendations and regulations for sport events in the heat. *British Journal of Sports Medicine* **57,** 8-25.

Ravanelli N, Bongers CCWG & Jay O. (2019). The Biophysics of Human Heat Exchange. In *Heat Stress in Sport and Exercise: Thermophysiology of Health and Performance*, ed. Périard JD & Racinais S, pp. 29-43. Springer International Publishing, Cham.

Ravanelli N, Imbeault P & Jay O. (2020). Steady-state sweating during exercise is determined by the evaporative requirement for heat balance independently of absolute core and skin temperatures. *J Physiol* **598,** 2607-2619.

Union Cycliste Internationale. (2024). UCI CYCLING REGULATIONS - Part 2 Road Races. UCI.

Vanos JK, Warland JS, Gillespie TJ & Kenny NA. (2012). Thermal comfort modelling of body temperature and psychological variations of a human exercising in an outdoor environment. *International Journal of Biometeorology* **56,** 21-32.

Xu F & Rhodes EC. (1999). Oxygen uptake kinetics during exercise. *Sports medicine (Auckland, NZ)* **27,** 313-327.

Appendix I

7.0 Human Research Ethics Approvals for Chapters IV and V

THE UNIVERSITY OF SYDNEY

Research Integrity & Ethics Administration
HUMAN RESEARCH ETHICS COMMITTEE

Tuesday, 12 January 2021

Dr Ollie Jay
Exercise Health and Performance; Faculty of Medicine and Health
Email: Ollie.jay@sydney.edu.au

Dear Ollie,

The University of Sydney Human Research Ethics Committee (HREC) has considered your application.

I am pleased to inform you that after consideration of your response, your project has been approved.

Details of the approval are as follows:

Project No.:	**2020/736**
Project Title:	**Sweat responses to outdoor cycling in hot and cool conditions**
Authorised Personnel:	**Jay Ollie; Hospers Lily; Hunt Lindsey; Smallcombe James; Vargas Nicole;**
Approval Period:	**12/01/2021** to **12/01/2025**
First Annual Report Due:	**12/01/2022**

Documents Approved:

Date Uploaded	Version Number	Document Name
08/01/2021	Version 3	TCCC-online-flyer-V3-clean
08/01/2021	Version 3	Cycling Study-PIS-V3-clean
13/11/2020	Version 2	Flyer-B-V2-clean
12/10/2020	Version 1	FMH COVID-19 RTW (plan)
12/10/2020	Version 1	FMH COVID-19 RTW (supplementary material)
12/10/2020	Version 1	Heat Safety Protocol
12/10/2020	Version 1	Off-Campus Safety Protocol
12/10/2020	Version 1	Par-Q Screening Form
12/10/2020	Version 1	First Contact Email
12/10/2020	Version 1	Consent Form
12/10/2020	Version 1	AHA Screening Form
12/10/2020	Version 1	COVID-19 Risk Mitigation Plan
12/10/2020	Version 1	FMH COVID-19 RTW (checklist)

Condition/s of Approval

- Research must be conducted according to the approved proposal.
- An annual progress report must be submitted to the Ethics Office on or before the anniversary of approval and on completion of the project.

Research Integrity & Ethics Administration
Research Portfolio
Level 3, F23 Administration Building
The University of Sydney
NSW 2006 Australia

T +61 2 9036 9161
E human.ethics@sydney.edu.au
W sydney.edu.au/ethics

ABN 15 211 513 464
CRICOS 00026A

THE UNIVERSITY OF SYDNEY

- You must report as soon as practicable anything that might warrant review of ethical approval of the project including:
  - Serious or unexpected adverse events (which should be reported within 72 hours).
  - Unforeseen events that might affect continued ethical acceptability of the project.
- Any changes to the proposal must be approved prior to their implementation (except where an amendment is undertaken to eliminate *immediate* risk to participants).
- Personnel working on this project must be sufficiently qualified by education, training and experience for their role, or adequately supervised. Changes to personnel must be reported and approved.
- Personnel must disclose any actual or potential conflicts of interest, including any financial or other interest or affiliation, as relevant to this project.
- Data and primary materials must be retained and stored in accordance with the relevant legislation and University guidelines.
- Ethics approval is dependent upon ongoing compliance of the research with the *National Statement on Ethical Conduct in Human Research*, the *Australian Code for the Responsible Conduct of Research*, applicable legal requirements, and with University policies, procedures and governance requirements.
- The Ethics Office may conduct audits on approved projects.
- The Chief Investigator has ultimate responsibility for the conduct of the research and is responsible for ensuring all others involved will conduct the research in accordance with the above.

This letter constitutes ethical approval only.

Please contact the Ethics Office should you require further information or clarification.

Sincerely,

[REDACTION]

Associate Professor Mark Arnold
Chair, Human Research Ethics Committee (HREC 2)

The University of Sydney of Sydney HRECs are constituted and operate in accordance with the National Health and Medical Research Council's (NHMRC) National Statement on Ethical Conduct in Human Research (2018) and the NHMRC's Australian Code for the Responsible Conduct of Research (2018)